Elucidating Flux Regulation of the Fermentation Modes of *Lactococcus lactis*: A Multilevel Study

PhD Thesis

Siu Hung Joshua Chan

DTU Food
National Food Institute

Elucidating Flux Regulation of the Fermentation Modes of *Lactococcus lactis*: A Multilevel Study

PhD Thesis

Siu Hung Joshua Chan

November, 2014

Supervisors:

Associate Professor Christian Solem

Professor Peter Ruhdal Jensen

Systems Biotechnology and Biorefining

National Food Institute

Technical University of Denmark

Summary

The long history of application to the dairy industry has established *Lactococcus lactis* (*L. lactis*), the lactic acid bacterium, as one of the most extensively characterized low GC organisms. The relatively simple metabolism of *L. lactis* has also made it an attractive target for metabolic engineering for the production of non-food related chemicals. Moreover, the status of being the first genetically modified organism to deliver immunoproteins alive to human has brought *L. lactis* considerable fame in biomedical research.

Beside the exceptional industrial relevance of *L. lactis*, it is also an important subject for basic research in cellular metabolism because *L. lactis* exhibits an interesting metabolic shift. Under anaerobic conditions, on fast fermentable sugars, *L. lactis* produces lactate as the primary product, known as homolactic fermentation but on slowly fermentable sugars, significant amounts of formate, acetate and ethanol are formed, known as mixed-acid fermentation. This shift is termed the mixed-acid shift. This type of shift between a low-yield and a high-yield metabolism has drawn a lot of research focus and has similarly been observed in other bacteria, yeast and even tumor cells.

Efforts have been put to find out the mechanism regulating the mixed-acid shift as well as to answer questions such as why *L. lactis* prefers such a switch. Until now, some pieces of evidence have been reported and several factors and models have been proposed as the keys to regulating the shift, including the expression level of certain genes in glycolysis and fermentation pathways, the levels of the cofactors NADH, NAD^+, ATP and ADP, the balance between catabolism and anabolism, etc.

In this project, we studied the mixed-acid fermentation of *L. lactis* by (i) examining the roles of the enzymes in the mixed-acid fermentation pathway under different growth conditions; (ii) testing the predicted effect of the cofactors NADH, NAD^+ on the mixed-acid shift proposed in previous studies; (iii) looking into the connection between amino acid metabolism and the mixed-acid shift; and (iv) contrasting the difference regarding the mixed-acid shift between two widely studied laboratory strains of *L. lactis*, MG1363 that shifts significantly and IL1403 that does not shift.

We have measured the promoter activities of several mixed-acid genes which suggested that the regulatory elements governing the transcriptional regulation of the mixed-acid genes in MG1363 and IL1403 were different. This led us to performing experimental control analysis of the role of pyruvate formate-lyase (PFL) in MG1363 and IL1403. The expression of PFL in MG1363 appeared to be optimized for growth rate when growing on maltose whereas overexpressing PFL in IL1403 was probably detrimental.

The two homologous acetate kinases in MG1363 were also chacterized with respect to the transcription and enzyme activities. The isozymes were found to have complementary physiological roles that became important in acetate-producing or acetate-assimilating conditions respectively.

The proposed roles of NADH and NAD^+ on the mixed-acid shift were tested by perturbation via introducing activities of 2,3-butanediol dehydrogenase and supplying extracellular acetoin as an oxidizing agent. The additional NAD^+- regenerating activities allowed a faster growth of MG1363 on maltose by shifting ethanol production into acetate production and also stimulated formate and acetate production in IL1403.

Dependance of the mixed-acid fermentation of MG1363 on amino acid availability was observed and the impact of individual amino acids could differ significantly. Meanwhile, a computational method for combining metabolic flux analysis and elementary mode analysis was developed and applied to analyse a case of amino acid metabolism of *L. lactis*.

Dansk resumé

De mange års anvendelse af mælkesyrebakterien *Lactococcus lactis* (*L. lactis*) indenfor mejeriindustrien, har været medvirkende til at *L. lactis* er blevet en af de mest velkarakteriserede bakterier. Denne Gram positive bakterie, som har et lavt GC indhold, har en relativt simpel metabolisme og er let at modificere genetisk. Dette har gjort den til et attraktivt mål for "metabolic engineering", bl.a. med henblik på produktion af non-food relaterede kemikalier. Derudover har den status som den første genetisk modificerede organisme der i levende form er blevet anvendt til at levere immunproteiner til mennesker, og *L. lactis* er velkendt inden for biomedicinsk forskning.

Ud over de vigtige roller som er blevet nævnt ovenfor, er *L. lactis* det også vigtig for grundforskning i cellulær metabolisme, bl.a. fordi *L. lactis* udviser et interessant metabolisk skift, som bevirker en ændring i produktdannelse. Let fermenterbare sukre giver anledning til hovedsagelig laktat (homolactic), medens sukre der omsættes langsommere giver anledning til andre organiske syrer og ethanol i tillæg til laktat (mixed-acid). Denne form for skift mellem en metabolisme med et lavt og et højt udbytte er der blevet forsket meget i, ikke kun i *L. lactis* men også i andre bakterier, gær og endda cancerceller.

Indtil nu har mange beviser blevet rapporteret, og flere faktorer og modeller er blevet foreslået som nøglerne til regulering af skift, herunder udtrykket af visse gener i glycolyse og fermentering veje, niveauet for cofaktorer NADH, NAD^+, ATP og ADP, balancen mellem katabolisme og anabolisme, etc.

I dette projekt, vi studerede blandet syre fermentering af *L. lactis* ved (i) at undersøge de roller enzymer i blandet syre gæring vej under forskellige vækstbetingelser; (ii) testning af forudsagte virkning af cofaktorer NADH, NAD^+ på blandede syre skift foreslået i tidligere undersøgelser; (iii) at se på sammenhængen mellem aminosyre metabolisme og det blandede syre skift; og (iv) kontrasterende forskellen med hensyn til blandet syre skift mellem to vidt studerede laboratoriestammer, *L. lactis* subsp. *cremoris* MG1363, der skifter betydeligt og *L. lactis* subsp. *lactis* IL1403, der ikke skifter.

Vi har målt promotoraktiviteter i flere blandet syre gener, som antydede, at de regulatoriske elementen for transkriptionel regulering af det blandede syre gener i MG1363 og IL1403 var anderledes. Dette førte os til at udføre eksperimentel kontrol analyse af den rolle, pyruvat format lyase (PFL) i MG1363 og IL1403. Ekspressionen af PFL i MG1363 syntes at være optimeret til vækst, når de vokser på maltose henviser overekspression PFL i IL1403 var sandsynligvis skadelige.

De to homologe acetat kinaser i MG1363 blev også chacterized med hensyn til transkription og enzymaktiviteter. De isozymer viste sig at have komplementære fysiologiske roller, som fik betydning i acetat-producerende eller acetat-assimilere betingelser hhv.

De foreslåede roller af NADH og NAD^+ på blandet syre skift blev testet ved perturbation via indføre aktiviteter af 2,3-butandiol dehydrogenase og leverer ekstracellulære acetoin som et oxidationsmiddel. De yderligere NAD^+-regenererende aktiviteter have en hurtigere vækst i MG1363 på maltose ved at flytte ethanolproduktion i acetat produktion og også stimuleret formiat og acetat produktion i IL1403.

Afhængighed af det blandede syre gæring af MG1363 på aminosyre tilgængelighed blev observeret og virkningen af individuelle aminosyrer kan afvige væsentligt. I mellemtiden var en beregningsmetode til at kombinere metabolisk flux analyse og elementær tilstand analyse udviklet og anvendt på metabolismen af *L. lactis*.

Acknowledgements

It is impossible to complete my PhD study without the help of many people. First of all, I must express my sincerest gratitude to my supervisors, Christian Solem and Peter Ruhdal Jensen.

Christian has taught me numerous principles, skills and knowledge in practical as well as theoretical molecular biology and cellular metabolism. From the very first day he has helped me, a person without any previous experience in biological experiments, to survive in the lab. He always came up with pragmatic solutions as well as interesting ideas that led to new directions. The most important thing of all that I have learnt from him, for a skeptical person like me, is his will power and faith to find out the truth through continuous efforts, as reflected by his passionate encouragement that usually put an end to our discussion: 'Just do it!'. It has powered me to continue the journey from time to time.

Peter has also been equally important to my PhD study who taught me a lot of knowledge in bacterial metabolism and how elegent it is. More importantly, I have learnt a lot from the perspective, insights and discernment he has demonstrated as a world-leading scientist when looking into biological problems. The close guidance, support and meanwhile flexibility and freedom he has given have allowed me to gradually become independent and better in productivity. In addition, the direction, spirit, morale and working environments he has built for the whole research group has propelled every one of us to move forward in a supportive and positive manner.

I must also thank people who have been working with me and helped me. Thank Jun Chen who from the very first day of my arrival in Copenhagen has helped me to settle my life here, provided countless useful tips and advices in my experiments and shared his extensive knowledge on *Lactococcus lactis.* This greatly accelerated my progress. Thank also Xiaoying Liu for her support and care in my beginning stage when she was in the group. Thank Lasse Nørregaard and Aria Aminzadeh for the good time that we worked together in their bachelor theses. Thank all the colleagues that have once helped me, including Anders Cai Holm Hansen and Tina Suhr for their help in using lab facilities from time to time; Kia Vest Petersen who always maintained a good working environment and taught me some good practices in the lab; professor Ole Michelsen who is very humorous and has shared some of his unimaginably vast knowledge with me; and many others who have been so nice to me.

Special thanks are given to Zhihao Wang who always has a lot of scientific and insightful discussion with me. He has personally become a good friend of mine from whom I got countless heartfelt physical and mental support and from whom I learnt a lot in improving my imperfect personality.

I would also like to acknowledge the Danish Council for Independent Research in Natural Sciences for the financial support, Techical University of Denmark for the great research environment and the transnational SysMOLAB2 consortium for a fruitful discussion.

For my personal life in Denmark for these several years, I would like to thank my family and many friends in Hong Kong as well as in Denmark who show their love and care constantly which are vital for me to face the live and challenges in Denmark.

A person of paramount importance to me who I must thank most deeply is my wife, Sandy Wong, who has accompanied me to have a new life here and has always supported me and helped me in every aspect of my life. She deserves all the compliments that I receive (if any).

Finally, thank God whom I believe in. He made a way in the waste land, and rivers in the dry country.

Outline of the thesis

The thesis comprises seven chapters and three appendices.

Chapter 1 introduces the background of this study. Beginning with a general review of the industrial relevance, characteristics and available tools for research and engineering of lactic acid bacteria, the focus then turns to the metabolism of *L. lactis*, especially the regulation of the glycolytic flux and the shift from homolactic to mixed-acid fermentation. The research objectives and strategies are defined at the end of the chapter.

Chapter 2 includes the growth characterization of the two widely studied laboratory strains, MG1363 and IL1403 as well as the transcriptional activity of the enzymes in the mixed-acid fermentation pathways in the two strains.

Chapter 3 reports the findings of the modulation of the expression of pyruvate formate-lyase and the control analysis of it in MG1363.

Chapter 4 presents the characterization of two genes encoding acetate kinases in MG1363 with respect to the transcription structure, enzyme kinetics and their physiological roles.

Chapter 5 describes the study of the effect of perturbing NADH/NAD^+ for MG1363 and IL1403 growing on maltose or glucose respectively.

Chapter 6 briefly summarizes some results of a bachelor project initiated by this project regarding the effect of amino acid availability on the mixed-acid shift and at the same time reports some observations from a computational study in which a new method to analyse flux distributions by elementary modes was proposed. The derivation, validation and application of the method were presented in detail in the publication reprinted in Appendix A.

Chapter 7 concludes the results of the entire project and discusses some future directions.

Supplementary information for Chapter 4 and Chapter 5 are attached in Appendix B and Appendix C respectively.

Table of Contents

List of Figures

List of Tables

Chapter 1. Background

1.1 Lactic acid bacteria

At the beginning of the twentieth century, the concept of lactic acid bacteria (LAB) gradually emerged to describe a group of bacteria with similarities in morphology, metabolism and physiology that produces primarily lactic acid during fermentation of carbohydrates and whose first prominent role was recognized in milk fermentation [1]. LAB are generally Gram-positive, non-sporulating, non-respiring, nonmotile, low-GC, in the shape of rods or cocci [2, 3]. Mostly under the order *Lactobacillales*, LAB include genera *Aerococcus*, *Carnobacterium*, *Enterococcus*, *Lactobacillus*, *Lactococcus*, *Leuconostoc*, *Oenococcus*, *Pediococcus*, *Streptococcus*, *Tetragenococcus*, *Vagococcus*, *Weissella*, etc. [4, 5]. Figure 1.1 shows the evolutionary relationship between different genera of LAB [5].

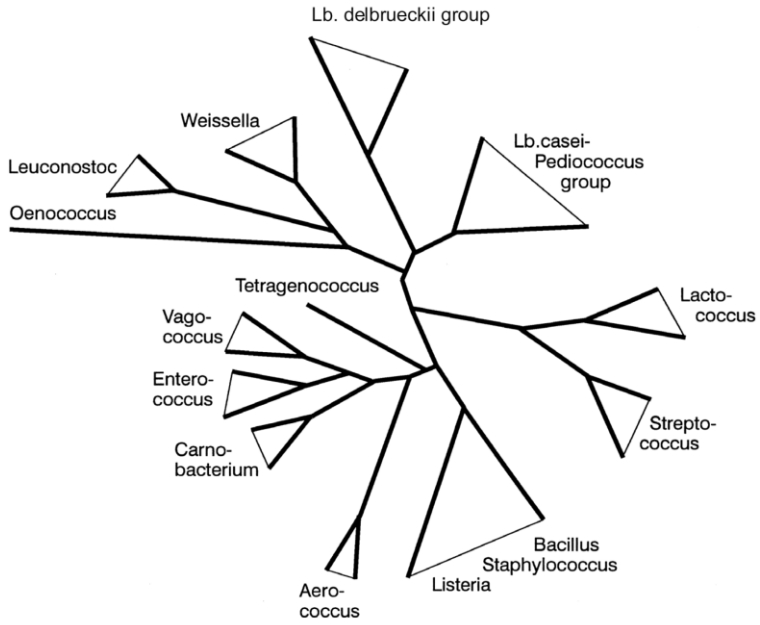

Figure 1.1. Schematic phylogenetic tree of LAB.
Reprinted from [5] with permission.

The habitats of LAB range from plants, milk, meat and other different foods, to the mammalian intestine and month [1]. LAB also have diverse relationships with human, such as starter cultures in food fermentation [6], probiotics in human gut [7] and pathogens causing fatal diseases [8]. The ubiquitous presence of well-adapted LAB in different environments which still maintain central similarity, as well as their intimate relationship with human make them an extremely important subject in both basic and applied research in microbiology.

1.2 Industrial relevance of lactic acid bacteria

1.2.1 Starter cultures

LAB have been employed in the production of a wide variety of fermented food products. The ability to affect texture, flavour and prolonging shelf-life of the fermented product in combination with many years of safe use has led to the establishment of many LAB as workhorses within food fermentation. For instance, *Lactococcus lactis* (*L. lactis*) is famous for its role in producing dairy products including cheese, butter and sour cream [9]. When producing different types of cheese, other LAB species are present in the starter cultures used, e.g. *Lactobacillus* species, *Streptococcus thermohilus, Leuconostoc mesenteroides* and they all tend to have an effect on flavour and texture [10]. Flavour compounds of exceptional importance to cheese include various aldehydes, alcohols, carboxylic acids and esters, in particular those derived from methionine phenylalanine, threonine and the branched-chain amino acids (reviewed in [10, 11]). *Lactobacillus delbrueckii* (*Lb. delbrueckii*) *subsp. bulgaricus* and *Streptococcus thermophilus* are the essential bacteria in yogurt cultures [12]. Some *Lactococcus, Lactobacillus, Pediococcus* and *Enterococcus* species can be used in the preservation of fermented meats, fish, vegetables, soy sauce, wine etc. due to their bacteriocin production in addition to the acidification of the food (reviewed in [13–15]). Both of the effects can inhibit the growth of pathogenic bacteria and help LAB to dominate the microflora of food.

1.2.2 Probiotics

In addition to their essential roles in food fermentations, some LAB including some *Lactobacillus*, *Enterococcus* and *Bifidobacterium* species can also act as probiotics which exert extra health benefits more than the inherent nutrition [16]. They are naturally present in the human gut and together with other bacterial species form the so-called ‘microbiome’. They can survive in the acidic environment of the stomach and colonize the large intestine where they produce antioxidants that scavenge free radicals, antimicrobial compounds that inhibit the growth of intestinal and gastric pathogens and in addition occupy the intestinal surface and prevent other bacteria from invading the body [7]. For instance, *Lb. acidophilus* produces compounds called lactocidin, acidolin and acidophilin with a broad spectrum activity that targets both Gram-positive and negative bacteria [1]. Reuterin produced by *Lb. reuteri* has been reported to inhibit yeast, fungi, protozoa and bacteria including *Salmonella*, *Clostridium*, *Staphylococcus*, *Listeria*, etc. [1]. A number of LAB species have even been tested as live carriers of oral vaccine because of their safe status and mimicry of natural infection [17]. For example, recombinant *L. lactis* expressing tetanus toxin fragment C has been tested to successfully induce immune response when orally administered [18].

1.2.3 Cell factories

While the GRAS status of LAB establish their important position in food industry, the relatively simple carbon metabolism of LAB further makes them attractive targets for metabolic engineering for

production of food ingredients, nutraceuticals and even as cell factories for non-food related chemicals (reviewed in [19, 20]). By all means, the most natural product of all LAB is lactic acid. About 90% of the 80 000 tonnes of lactic acid produced worldwide were by LAB in year 2000 for application to food, pharmaceutical, leather and textile industries and for producing base chemicals and polylactic acid, an important precursor of biodegradable plastic [21]. The worldwide demand for lactic acid has increased to 130 000 – 150 000 tons in 2007 and 259 000 tons in 2012 [250]. Other compounds, for example, alanine, acetaldehyde, low-calorie sugars, vitamins, certain plant metabolites and polysaccharides can be produced by *L. lactis* and some *Lactobacillus* species (reviewed in [6, 20]). *Streptococcus thermophilus*, *Lb. planetarium*, *Lb. acidophilus* and *Enterococcus faecalis* have also been applied to reduce anti-nutritional compounds such as excessive sugars and amines [6]. LAB have also become popular hosts for overproduction of recombinant proteins, and this is largely due to available food-grade controlled gene expression systems, among which the most popular is the nisin controlled gene expression system [22]. For production of biofuels, *L. lactis* has been engineered to produce ethanol with a high yield by introducing genes from *Zymomonas mobilis* [23]. Production of butanol has been achieved in *Lb. brevis* by introducing the butanol pathway in *Clostridium acetobutylicum* [24]. 2,3-butanediol widely used as feedstock can be produced concomitant with a low-calorie sugar mannitol in *L. lactis* by cofactor engineering [25]. There have been many review articles on the metabolic engineering of LAB. Interested readers are referred to [19, 20, 26, 27].

1.3 Some characteristics of lactic acid bacteria

The exceptional relevance of LAB to food industry, human health and as microbial cell factories calls forth tremendous efforts to study their genetics, molecular biology, metabolism and biochemistry in order to optimize fermentation yield, to increase the health benefits of products, to better engineer LAB for production of other chemicals, as well as to learn the interactions with other bacterial communities in gut and the host. In this section, some of the biological knowledge on LAB is reviewed.

1.3.1 Genomics

Genome sequences

The genome of a laboratory strain *L. lactis* subsp. *lactis* IL1403 was the first completely sequenced genome of LAB and was published in 2001 [28]. Since then, more and more LAB have been genome-sequenced. Until 2009, there were 31 complete genome sequences of LAB [29]. Thanks to the popularization of next generation sequencing, up to September 2014, search in the NCBI database showed that there are 232 species containing thousands of strains under the order *Lactobacillales* with complete genome sequences. Almost all of them are considered as members of LAB. It is a dramatic increase and highlights the growing attention received by LAB from the scientific community as well.

The typical size of the genome of LAB ranges from 1.7 Mbp to 3.4 Mbp with the number of genes lying between 1,500 to 3,300 and GC content between 35% and 50% [30].

Reductive genomes

From evolutionary genomic analysis, LAB shows a reductive genomic evolution [29, 30]. It has been estimated that the common ancestor of *Lactobacillales* had lost 600 to 1,200 genes but gained less than 100 genes since the divergence from class *Bacilli* [31]. The reduction in genome size was probably due to adaptation to environments with rich nutrient availability [29, 32], for instance, from plant to milk, which has recently been elegantly demonstrated by subjecting *L. lactis* isolated from plant to adaptive evolution in milk [33]. Another example is the smaller genome sizes and lower GC content of *Lactobacillus* species found in vaginal cavity among all LAB which was suggested to be a result of vaginal adaptation [30, 34].

Pseudogenes

The genomic reduction is also evidenced by the pervasive presence of pseudogenes (genes that have lost their functions during the course of evolution), which in LAB generally are more frequent than in other bacteria [4, 29]. This in general has been compensated by enrichment for genes encoding transporters for amino acids, sugars, ions, peptides, etc. to take up the nutrients required for growth from the rich enviroments instead of synthesizing them *de novo* [29, 30].

Mobile genetic elements

Plasmids and other mobile genetic elements are also important factors that have shaped the evolution of LAB [30], by facilitating horizontal gene transfer. This has enabled many LAB to utilize lactose, galactose, oligo-peptide and has also provided them with various phage resistance mechanism, etc. (reviewed in [29, 35]). For example, the megaplasmid in a *Lb. salivarius* strain contains genes for bacteriocin production and bile salt hydrolase which make the strain probiotic [36]. Plasmids responsible for traits critical for dairy fermentation were also found in a dairy *L. lactis* strain [37] but not present in plant isolates [30].

1.3.2 Metabolism

Fermentation of carbohydrates

LAB do not have an electron transport chain and thus are unable to perform oxidative phosphorylation for ATP synthesis. Instead, LAB rely on substrate-level phosphorylation to generate energy from sugars. Sugars are taken up by the phosphoenolpyruvate (PEP)-dependent phosphotransferase system (PTS), a common sugar transport system of bacteria in which extracellular sugar is directly phosphorylated to become intracellular sugar phosphate by receiving the phosphate group from PEP [38]. PTS is also the main system for carbon catabolite repression, a major way of regulating carbohydrate metabolism in bacteria, which is discussed in a later subsection. An alternative way of

sugar transport is uptake by sugar-specific permeases. The ability to utilize different sugars by different species of LAB is reviewed in [39] in great detail. Usually, over 95% of sugar is converted into lactic acid by LAB [20]. Generically, there are two fermentation pathways for this in LAB [5].

Glycolysis

The first is glycolysis which is the typical Embden-Meyerhof-Parnas (EMP) pathway in which one mole of glucose is oxidized to form two moles of pyruvate concomitant with two moles of ADP phosphorylated into two moles of ATP (Figure 1.2). Lactate dehydrogenase (LDH) then reduces the two moles of pyruvate into two moles of lactate, balancing the redox. Other sugars such as galactose can also be metabolized through glycolysis by conversion into glucose 6-phosphate (G6P) through the Leloir pathway or conversion into triosephosphate through the tagatose 6-phosphate pathway (Figure 1.2) [5]. This pathway has sometimes been called homofermentative pathway in the literature.

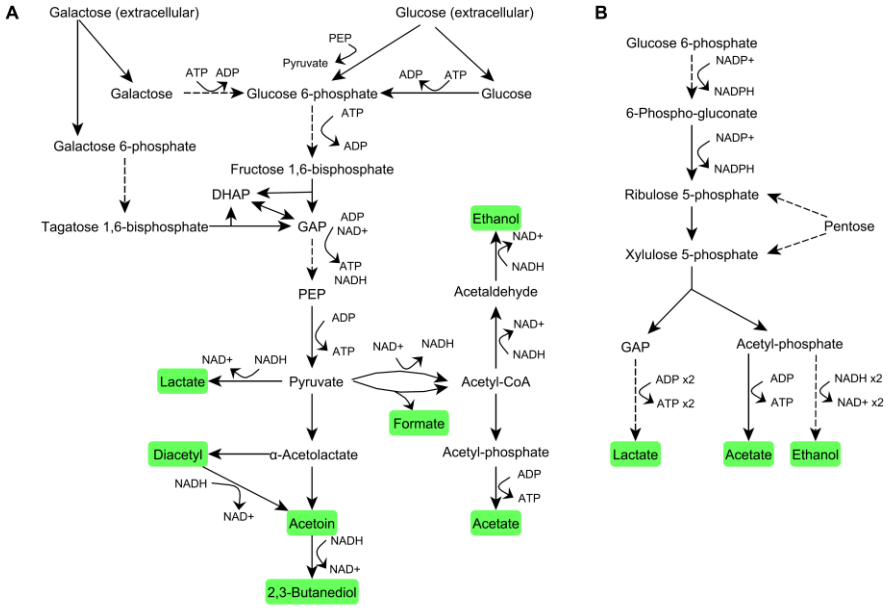

Figure 1.2. Fermentation pathways in lactic acid bacteria.

(A) Homofermentative pathway including tagatose 6-phosphate pathway and Lelior pathway for galactose uptake and mixed-acid fermentation. (B) Heterofermentative pathways. PEP, phosphoenolpyruvate; GAP, glyceraldehyde 3-phosphate; DHAP, dihydroxyacetone phosphate. Lumped reactions are in dotted lines. Fermentation end products are highlighted.

Mixed-acid fermentation and flavour compound production

Under certain environmental conditions, the pyruvate formed in the homofermentative pathway is not totally converted to lactate, but goes into the other two branches. The first branch is the formation of acetyl-CoA by pyruvate-formate lyase or pyruvate dehydrogenase, followed by acetate and ethanol production [40, 41]. When a significant amount of these end products is produced in addition to lactate during fermentation, it is called ‘mixed-acid fermentation’. This is also the main subject of study in this thesis which is discussed in section 1.5.3. The second is the conversion of pyruvate into

α-acetolactate, followed by diacetyl, acetoin and 2,3-butanediol production which are important flavour compounds in dairy industry [5].

Phosphoketolase pathway

The second fermentation pathway is the phosphoketolase pathway (Figure 1.2) [1, 5]. In this pathway, glucose 6-phosphate or pentose enters pentose phosphate pathway rather than EMP pathway. Xylulose 5-phosphate is then converted by phosphoketolase into glyceraldehyde 3-phosphate (GAP) entering glycolysis, and acetyl phosphate from which acetate or ethanol is produced [1, 5, 41]. This pathway has also been called heterofermentative/ heterolactic pathway in the literature.

The fermentation type is an important characteristic of LAB. For instance, *Leuconostoc*, *Oenococcus*, *Weissella*, *Lb. brevis*, *Lb. buchneri*, *Lb. fermentum*, and *Lb. reuteri* are obligatory heterolactic; *Lb. acidophilus*, *Lb. delbrueckii*, *Lb. helveticus* and *Lb. salivarius* cannot catabolize pentose and are obligatory homolactic; many other LAB are facultatively heterolactic [5, 42].

Carbon catabolite repression

Most of the bacteria including LAB are known to have the ability to selectively consume carbon sources for fastest immediate growth by the carbon catabolite repression (CCR) system (reviewed in [43, 44]). The most classical example must be the diauxic growth of *Escherichia coli* in the presence of both glucose and lactose discovered by Monod [45]. In Firmicutes, which consists of many low-GC Gram-positive bacteria including LAB and *Bacillus*, CCR is exerted through the concerted effort of the histidine protein (HPr), which is one of the component proteins of PTS and the global regulator called catabolite control protein (CcpA) [46].

When a sugar allowing fast growth such as glucose is present, the glycolytic flux is relatively high and so are the levels of ATP and fructose 1,6-bisphosphate (FBP). This activates the HPr kinase/phosphorylase which phosphorylates HPr at Ser46 (HPr-Ser-P). HPr-Ser-P on the one hand triggers inducer exclusion which inhibits the activities of permeases of other sugars by allosteric regulation and on the other hand forms a complex with CcpA which serves as a global transcriptional regulator binding to cre sites on DNA to exert transcriptional regulation [46]. In the absence of glucose or when the levels of glycolytic intermediates are low, HPr is mostly not Ser46-phosphorylated for catabolization of carbon sources. In particular, in *B. subtilis*, induction of specifc catabolic operons by glycerol kinase and other substrate-specific regulators containing PTS-regulatory domains (PRDs) is prevented by the low level of HPr(His-P) in the presence of glucose. The mechanism is visualized in Figure 1.3 (reprinted from [43] with permission).

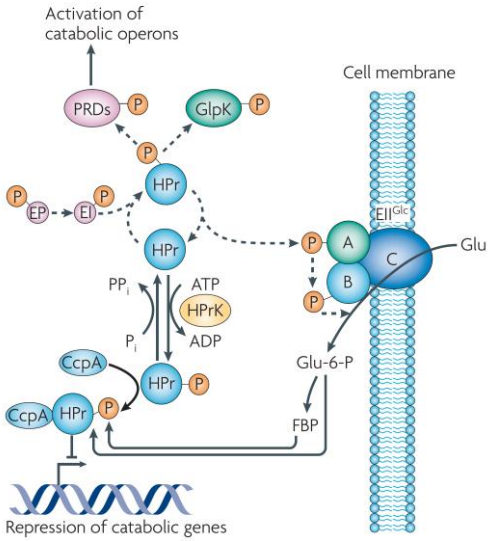

Figure 1.3. Carbon catabolite repression in Firmicutes including lactic acid bacteria.
EI, enzyme I of PTS; EII, enzyme II of PTS; HPr, histidine protein; HPrK, HPr kinase/phosphorylase; P, phosphate; CcpA, catabolite control protein; Glu, glucose; Glu-6-P, glucose 6-phosphate; FBP, fructose 1,6-bisphosphate; PRD, PTS-regulatory domain; GlpK, glycerol kinase. Reprinted from [43] with permission.

Nutritional auxotrophy

As discussed in section 1.3.1, LAB have evolved reductively to adapt to nutritionally rich environments. Many of the lost genes encode enzymes that are involved in biosynthetic pathways. LAB are thus in general auxotrophic for many nutrients such as some amino acids and vitamins. There is however not a clear pattern of the auxotrophy depending on species. Some strains of *L. lactis*, *Lb. plantarum*, *Lb. casei*, *Lb. helveticus* were tested for the amino acid requirements for growth and it was found that even different strains under the same species can have different amino acid requirements [47]. Recent results from comparative genomics have shown that, for instance, the families of Lactobacillaceae and Leuconostocaceae lost the genes for synthesizing serine and glycine; *Pediococcus pentosaceus*, *Oenococcus oeni* and some *Lb.* species lost the genes for arginine and aromatic amino acid biosynthesis; some genes for biosynthesis of fatty acid were not found in *Lb. gasseri* and *Lb. johnsonii* [4]. Most of these results, however, have not yet been confirmed by physiological characterization. A lot of effort is required to characterize the different nutritional requirements of LAB.

Proteolytic system

To adapt to nutritionally rich environments, the loss of ability to synthesize nutrients necessary for growth usually comes along with gain of ability to take up nutrients from environments quickly [29, 30]. The proteolytic ability of LAB, especially those adapted to the dairy environment, is a very important trait for LAB to prevail. LAB can express cell-envelope proteinases to break down extracellular casein, the protein of largest fraction in milk, into peptides primarily ranging from 4 to

10 residues which are then taken up by LAB with specific transport systems followed by further hydrolysis by peptidases into single amino acids [48]. The characterized proteinases, peptide transport systems and peptidases have been extensively reviewed (e.g. [48–50]).

1.3.3 Stress tolerance

LAB encounter various stressful conditions when used in food processing, and stress tolerance is important to consider if a consistent product quality is to be obtained. The quality of the final products may not be assured if the culture dies too early or produces different compounds under stress condition. There are several types of stress, including acid, oxidative, osmotic, heat, cold and starvation stress [51]. Tolerance to these stresses is also an important phenotype that distinguishes different species of LAB. Examples include: *Streptococcus* is unable to grow at 10 ˚C; *Enterococcus* is able to grow at 45 ˚C but most other species are unable; *Aerococcus*, *Enterococcus* and *Tetrageonococcus* are able to grow under significant osmotic stress (6.5% sodium chloride, and up to 18% for *Enterococcus*) or at pH as high as 9.6; *Aerococcus* and *Streptococcus* are unable to grow at pH 4.4 [5]. It should be noted that sometimes the tolerance can differ from strain to strain and exceptions can exist. The species-specific phenotypes under various stress conditions of many LAB are reviewed in [39] in great detail. The response to stress and its mechanism in LAB are extensively reviewed in [51].

1.4 Tools for studying lactic acid bacteria

The advance in science is deeply influenced by the technology available to study it. It is exceptionally conspicuous in the course of development of biological science in the last century. Since the discovery of the molecular model of DNA by Watson and Crick and the later proposed central dogma of molecular biology by Crick in the 1950s, much of the biological research has turned the focus to biomolecules and their interactions. Many molecular tools have been developed to manipulate cells. The different '–omics' techniques developed in the last two decades also gave birth to the systems biology paradigm which studies biology at a system level. A lot of bioinformatics and computational tools have thus been developed for this purpose. The study of LAB, as an important branch of microbiology, has undergone the same transformation. In this section, the molecular tools, computational models and tools for systems biology developed for or applied to LAB are briefly reviewed.

1.4.1 Molecular tools

Different genetic tools, with applications within strain optimization or basic research, have been developed for LAB. Beside the general tools designed for DNA manipulation, there are two important tools specifically for modulating gene expression, namely inducible promoters for controlled gene expression and synthetic promoter libraries. Many of the tools were first engineered for *L. lactis* and later applied to other LAB.

Controlled gene expression systems

The most influential controlled gene expression system invented for LAB must be the nisin controlled gene expression (NICE) system [22, 52]. In this system, the histidine-protein kinase NisK acts as a sensor which autophosphorylates in the presence of nisin, a broad spectrum bacteriocin, and the phosphate group is transferred to the response regulator NisR which then activates the specific promoter which is originally responsible for initiating the transcription of the gene cluster for nisin biosynthesis in the nisin-producing *L. lactis* strain NZ9700 [53]. There are a number of advantages of the NICE system. First, nisin is known to be safe so the overexpression of recombinant proteins by this system can be considered food-grade [22]. Second, it has a high sensitivity in the sense that only a tiny amount of nisin is required for induction (0.1 – 5 ng/ml) which normally does not cause growth inhibition to other microorganisms in a starter culture during fermentation [22, 54]. Third, the induced expression level is linearly correlated with the level of inducer, namely nisin, in a dynamic range which can be more than 1,000-fold [53, 55]. This property enables the study of hierarchical flux control by the inductively expressed enzyme, for instance, how the pyruvate distribution is controlled by the activity of NADH oxidase in *L. lactis* [56], the conversion of *L. lactis* from homolactic to homoalanine fermentation [57], high-level production of diacetyl [58]. The NICE system has been applied in other LAB such as *Streptococci* and *Enterococci* (reviewed in [22]).

Later another similar system using another bacteriocin sakacin as inducer was developed for *Lb. sakei* and *Lb. plantarum* [59–61]. There are other attempts to develop other expression systems, e.g. expression controlled by zinc availability in *L. lactis* [62]. The controlled gene expression systems naturally existing in or developed for LAB have been reviewed in [54, 63, 64].

Synthetic promoter libraries

A synthetic promoter library (SPL) is a set of promoters with the consensus sequences (e.g. -10 element and -35 element for bacteria) fixed and sequence of spacers in between randomized (reviewed in [65–67]). Such a library of promoters, essentially equivalent to saturation mutagenesis, has been shown to be capable of modulating gene expression in a dynamic range of up to thousand-fold [68, 69]. Traditional approaches usually either knock out a gene or overexpress a gene by a strong promoter. In comparison, SPL results in a continuous range of activity which allows the optimization of the desired metabolic phenotype as well as the estimation of flux control coefficient in the theory of metabolic control which requires only a slight perturbation from the original level of enzyme activity [65–67, 69].

Several strategies for practical construction of a collection of strains with a SPL have been proposed later [70]. One strategy is a single integration of a plasmid with a truncated part of the gene of interest following a SPL inserted into the plasmid. A marker for selection will reside in the resultant strains in this case. This approach has been applied to study glycolytic flux control in *L. lactis* [71–73]. Another

approach is to remove the marker and the rest of the plasmid by a double-crossover event but then there should be a homologous region upstream of the native promoter inserted prior to the SPL in the plasmid. These two methods are suitable for modulating the promoter strength of a natively existing gene. A third way is to make use of the site specific integration system to directly introduce a complete gene of interest following an SPL into the chromosome. For example, a site-specific integration system requiring a resolvase-like integrase derived from the temperate lactococcal bacteriophage TP901-1 [74–76] has been used together with SPLs in a number of studies on glycolytic flux control in *L. lactis* (e.g. [77, 78]). A fourth way is to express the gene of interest by a SPL on a replicating plasmid directly. It has been applied to study, e.g. the dependence of glycolytic flux on ATP/ADP level in *E. coli* and *L. lactis* [79–81]. The method of SPL has also been used in other LAB such as *Lb. plantarum* [82].

Other genetic tools

In addition to inducible controlled gene expression systems and the method of synthetic promoter libraries, other basic genetic tools for DNA manipulation are also indispensable for studying LAB.

DNA modifications by homologous recombination

In *L. lactis*, several plasmids have been created for insertion, deletion or mutation of chromosomal DNA by homologous recombination. An earlier one is pINT1 which is non-replicable and was derived from the plasmid pWV01 isolated from *L. lactis* subsp. *cremoris* Wg2 [83] by removing the *repA* gene [84]. Another plasmid system pGhost also derived from pWV01 is replication-thermosensitive [85, 86]. The property that the plasmid is replicable below 35˚C but not above eases the requirement of high transformation frequency by uncoupling the transformation step and the recombination step but the higher temperature required for selection can meanwhile pose other disadvantages to the bacteria [87]. Later the pORI series was developed to make use of the two systems [87, 88]. Another plasmid, pCS1966 derived from the pBluescript [89], was made to manipulate chromosomal DNA [90]. It makes use of the gene *oroP* encoding an orotate transporter as a counterselection tool by adding 5-fluoroorotate, a toxic analogue of orotate. pSEUDO, a derivative of pCS1966, was then designed for chromosomal integration into a pseudo gene in *L. lactis* [91]. The similar idea of adding the gene *upp* encoding uracil phosphoribosyltransferase to the pORI vector for counterselection has also been applied to *Lb. acidophilus* [92, 93]. Systems for integration by homologous recombination in other LAB include, for example, integration into a number of LAB species with the transposon Tn916 on chromosomes [94], other thermosensitive plasmids in *Streptococcus thermophilus* [95], *Lb. helveticus* [96], *Enterococcus faecalis* [97] (reviewed in [98]).

DNA insertion by site-specific integration

Site-specific integration is another popular tool for introducing a single copy of gene into the chromosome. An obvious example is the system derived from the temperate lactococcal

bacteriophage TP901-1 in *L. lactis* mentioned above [74]. Cre-*lox*-based system, which has been used in many organisms, has recently been used to develop a multiple-gene-deletion system in *Lb. plantarum* [99]. Recently, based on these two systems, a new system for repetitive, marker-free, site-specific integration has even been developed [100]. In fact, similar site-specific integration systems originating from temperate bacteriophage naturally exist in many LAB such as *Lactobacillus* [101, 102] and *Streptococcus thermophilus* [103]. Other examples include the pTRK system developed for *Lb. acidophilus* and *Lb. gasseri* adapted from the pORI system [104].

Random mutagenesis

Transposition-based mutagenesis is also an effective method for both targeted and random DNA disruption. While targeted mutagenesis aims to study the effect of disrupting a specific gene which can also be achieved by the aforementioned chromosomal integration, random mutagenesis is an elegant method to match genotype to an observed phenotype. Building a genomic library for random mutagenesis based on homologous recombination is a feasible way, e.g. [105], but transposons and insertion sequences are particular convenient tools for this purpose. For instance, an efficient system using lactococcal ISS1 concomitant with pGhost has been developed for *L. lactis* [106] and applied to discover regulators of the operon of cystathionine lyase and cysteine synthase [107], as well as to identify a gene important for protein secretion [108]. Transposase IS1223 and its target P_{junc} sequence have been used for a random mutagenic system in *Lb. casei* [109] and finding critical genes for the growth of *Lb. pentosus* in olive brine [110]. Systems for insertional mutagenesis were reviewed in [98]. Commonly used mobile and other genetic elements among LAB can be found in [35].

It should be noted that there are molecular tools for LAB other than the aforementioned, e.g. the ssDNA recombineering that has become very popular recently [111]. Some commonly used LAB strains for molecular cloning and their characteristics have been summarized in [35].

1.4.2 Tools and computation models for systems biology

Different -omics and high-throughput experimental techniques have been applied to the research on LAB. They are able to generate data which give a holistic view of cells. Several transcriptional regulatory networks, genome-scale metabolic networks of LAB have been reconstructed based on these data. Meanwhile, some refined kinetic models of LAB incorporating enzyme kinetics and enzyme assay data were also built as bottom-up approaches to study cellular metabolism.

Transcriptional regulatory networks

Transcriptional regulatory networks (TRNs) are networks that describe the interactions between genes and transcription factors (TFs). It is able to reveal changes at transcriptional level in response to a stimulus. The whole set of genes and operon regulated by a particular TF is called a regulon. The regulon of a given TF can be found experimentally by first comparing the transcriptomes of the wild-

type strain and the TF-knockout strain under a condition in which the TF is expressed. The binding of the TF to the upstream region of a differentially expressed gene can then be confirmed by other assays. Many of the known regulons in LAB were characterized by this method. A more direct but more expensive method is to combine chromatin immunoprecipitation (ChIP) and transcriptomic techniques which target DNA bound to the TF only (ChIP-chip or ChIP-seq). A general review on the construction of TRNs can be found in [112].

Many of the regulons of TFs that are common in many LAB have been characterized, such as CcpA for global catabolite repression [113, 114], CodY for amino acid metabolism [115–118], CopR for copper homeostasis [119, 120], FabT for fatty acid biosynthesis [121] and many others (e.g. [122–124]). Many evidences of genes regulated by TFs were also reviewed by transcriptomic profiling of the same strain in different growth conditions, e.g. changing growth rate [125, 126] , changing temperature [127].

Based on the huge amount of experimental data, several attempts have been made to construct regulatory networks for LAB recently. Regulatory network of a *Lb. plantarum* strain has been reconstructed based on correlation of gene expression in more than 70 experimental conditions and the binding motifs predicted from it [128]. Although it was not a TRN, it clustered genes into different transcription units that were co-expressed. A TRN for *L. lactis* growing in milk has been reconstructed by time-resolved transcriptomic analysis as well [129]. Since the proposal of the comparative genomic approach for reconstructing TRNs which is a very powerful tool to make use of genome sequences and biological knowledge of closely related species [130], it has been applied to reconstruct TRNs for 30 LAB strains with available genome sequences in a single study [131]. The results are available on RegPrecise which is a database of both manually curated and automatically propagated regulons with detailed description and interactive graphics [132]. The approach has later been applied for the reconstruction of a TRN of *Enterococcus faecalis* [120]. In this study, sub-networks of the TRN induced by varying copper levels were identified and the authors showed that the TRN of *Enterococcus faecalis* can be refigured to maintain copper homeostasis under genetic perturbation.

Genome-scale metabolic networks

Thanks to popularization of whole-genome sequencing technologies, genome-scale metabolic networks (GSMNs) of a cell containing all the metabolic reactions catalysed by genes with known functions that are present in the genome can be reconstructed. Roughly speaking, the reconstruction involves an iterative procedure, starting from a drafted list of reactions, to reconcile known experimental data with computational feasibility of the generated model. A detailed guide for a high-quality reconstruction can be found in [133]. A huge and expanding computational toolbox for GSMNs, the so-called constraint-based reconstruction and analysis (COBRA) approach, has also been

developed (reviewed in [134, 135]). It depends on the quasi-steady-state assumption of metabolism so that the kinetic details can be neglected and fluxes can be estimated by solving linear constraints. Among the many methods, flux balance analysis (FBA) is one of the most important techniques to predict optimal flux distributions [136]. GSMNs which represent the metabolic capability reflected by the genome can have several useful functions in systems biology. A very crucial one is the 'context' provided by GSMNs to understand the content of –omics data. Integrating –omics data (e.g. genome, transcriptome, proteome, metabolome) into GSMNs offers a way to link those data to the metabolic phenotype (reviewed in [137]). As the embodiment of genotype-phenotype relations, GSMNs can guide metabolic engineering by suggesting strategies of gene perturbation (reviewed in [138]) and even predict evolution (reviewed in [139]).

In LAB, the application of GSMNs is becoming more and more popular, too. Since the reconstruction of the first GSMN among LAB (*L. lactis* subsp. *lactis* IL1403) in 2005 for studying aerobic and anaerobic growth [140], models have been constructed for several species of LAB. They include *Lb. plantarum* for studying growth on complex media [141]; *Streptococcus thermophilus* for comparing the amino acid auxotrophy and the capability to produce volatiles with other LAB models [142]; *Lb. reuteri* to look into the metabolic mechanism of probiotic features [143]; an updated model of *L. lactis* IL1403 for increasing the production of recombinant proteins using dynamic FBA [144]; and *L. lactis* subsp. *cremoris* MG1363 for analysing the flavour-forming ability [145] (reviewed in [146]). As a good example to follow, the practical reconstruction of *Lb. plantarum*'s model has been described in detail [147]. It is believed that 'metagenome-scale' models of LAB would be the next step in response to metagenomics to push forward the frontiers of the study on microbial communities such as gut microbiota [146].

Kinetic models

As opposed to GSMNs, kinetic modelling is a bottom-up approach which includes only a limited number (usually dozens) of reactions of interest but the kinetics of each reaction is provided. The change in metabolite concentrations depends on fluxes of reactions which in turn depend on metabolite concentrations. This forms a dynamical system which can simulate system response to dynamic changes and well-established techniques are available for system analysis. Kinetic models however usually suffer from the lack of kinetic parameters which can sometimes be unidentifiable even through data fitting.

For LAB, many attempts have been made to model the kinetics of *L. lactis*'s glycolysis because of its intriguing regulation. Kinetics of individual enzymes, in particular those involving the conversion of global cofactors NADH/NAD^+ and ATP/ADP have been studied and modelled because of their high relevance to the regulation of glycolytic flux, including lactate dehydrogenase (LDH) [148, 149], glyceraldehyde 3-phosphate dehydrogenase (GAPDH) [149], pyruvate kinase (PYK) [150, 151],

alcohol dehydrogenase [149], acetate kinase [152] etc. The first kinetic model that gathered different enzyme kinetic data for *L. lactis*'s glycolysis was constructed to analyse the effect of different metabolic engineering strategies on acetoin and diacetyl formation [153]. It has also been used to simulate glucose run-out experiments [154] and later adapted to incorporate the effect of pH level [155]. Recently kinetic models for *L. lactis* and *Streptococcus pyogenes* taking extracellular phosphate concentration into considerations have been built and successfully described the different characteristics of the two species [156]. The model of *Streptococcus pyogenes* has later been shown to possess the characteristic of glycolytic oscillation [157].

Another type of models was constructed by assigning a generic rate equation to each reaction and obtaining parameters by fitting time-series data, such as a rational function of substrate and product concentrations [158], the generalized mass action [159] and its special case S-system [160]. They are quite capable of capturing the kinetic features but usually do not lead to mechanistic insights.

For these two types of kinetic models, many of the data of metabolite concentrations used for fitting were generated from nuclear magnatic resonance (NMR) applied to live cells consuming labelled substrates (e.g. [158, 161–163]. Detailed reviews on modelling LAB can be found in [146, 164]

Metabolic control analysis

Metabolic control analysis (MCA) aims to study how steady-state fluxes change in response to small changes in enzyme activities [165]. One application is the identification of targets for drugs [166] and metabolic engineering [167]. The flux control coefficient (FCC) is one of the central objects in MCA defined by the rate of fractional change of a steady-state flux with respect to the (infinitesimal) fractional change of an enzyme activity. It can be computed given a kinetic model by perturbing the V_{max} value of an enzyme or determined experimentally by modulating the expression level of an enzyme using methods like synthetic promoter libraries described in section 1.4.1. It has been widely employed to study the glycolysis of *L. lactis* which is reviewed and discussed later in section 1.5.1. The kinetic model mentioned previously which analysed the engineering strategies for increasing the production of acetoin and diacetyl actually used MCA for prediction [153]. A method combining MCA and kinetic modelling has also been proposed to predict flux distributions from the proteome in *L. lactis* [168].

1.5 *Lactococcus lactis*

L. lactis is a species of LAB in the family of streptococcaceae. It is in the shape of cocci and mesophilic with maximum growth rate at 30˚C and pH 7.0. *L. lactis* can be isolated from dairy environments or non-dairy environments such as plants [169].

There are two subspecies under *L. lactis*, namely subsp. *lactis* and subsp. *cremoris*. The subspecies were originally differentiated by phenotypic differences which include the ability of subsp. *lactis* to

consume arginine, to grow at higher temperatures or higher salt concentrations [170]. There is one biovar in subsp. *lactis* which can utilize citrate, namely subsp. *lactis* biovar *diacetylactis*[170, 171]. Two main genome homology groups were also found by nucleotide sequence comparison. They do, however, not perfectly match the two phenotypic subspecies [172]. An obvious example is the two most widely studied *L. lactis* laboratory strains, IL1403 and MG1363. IL1403 was derived from *L. lactis* subsp. *lactis* biovar *diacetylactis* CNRZ157 (or IL594) by curing the citrate plasmid [171]. It has a *lactis* genotype and a *lactis* phenotype. In contrast, MG1363, a plamid-free derivative of the dairy strain NCDO712 [173], was considered to have a *cremoris* genotype but a *lactis* phenotype.

As one may notice from the review of LAB in the previous sections, among all LAB, *L. lactis* is one of the most studied species and has become a model organism of the group. Much pioneering research on LAB was first conducted in *L. lactis*. One of the reasons is its extreme industrial importance. *L. lactis* is involved in the fermentation of a wide range of dairy products [170], primarily soft and hard cheeses. It can also be engineered to become a cell factory for chemicals of different categories, including recombinant protein [174], therapeutic proteins, DNA and vaccine antigens [175], flavour ingredients [19], nutraceuticals [6] etc.

Another reason for the huge curiosity aroused by *L. lactis* is its theoretical importance in cellular metabolism because it exhibits very significant metabolic shift from homolactic fermentation to mixed-acid fermentation as sugar concentration decreases, termed the mixed-acid shift or switch [40]. The control and regulation of the glycolytic flux is also a related and interesting object of study because of its intrinsic theoretical value [164] as well as the potential application to industrial production by increasing the glycolytic flux. In this section, the glycolysis and pyruvate metabolism which includes the well-known shift between fermentation modes in *L. lactis* and the regulation of fluxes in these pathways are reviewed.

1.5.1 Glycolysis

The glycolysis of *L. lactis* comprises the typical EMP pathway with different carbohydrates entering at different points. This subsection describes the uptake of glucose and maltose in *L. lactis* which are used extensively in our study. The transcriptional regulation of glycolytic enzymes is also briefly reviewed. The roles of glycolytic enzymes and metabolic regulation in determining glycolytic flux are reviewed in the next subsection.

Sugar transport

Sugars enter cells of *L. lactis* by either the PEP-dependent PTSs described in section 1.3.2 or sugar-specific permeases. For glucose uptake, there are two distinct PTSs, mannose PTS and cellobiose PTS, and a proton-motive force dependent permease in *L. lactis* and the kinetic properties of these transport systems in MG1363 have been characterized recently [176]. Mannose PTS has a much higher affinity

of micro-molar than the permease of milli-molar. PTSs should be responsible for the majority of the glucose uptake especially for cells starved for sugar for a period of time [176]. Many other monosaccharides like galactose can be transported into *L. lactis* similarly and enter glycolysis via G6P or GAP [177].

For the disaccharide maltose, the pathway for its uptake and entry into glycolysis is shown in Figure 1.4. Maltose is taken up into *L. lactis* cells by an ABC transporter ATP-binding protein [178, 179]. Intracellular maltose is split by maltose phosphorylase (MP) into one glucose and one β-glucose 1-phosphate which is then converted into glucose 6-phosphate by β-phosphoglucomutase (β-PGM) [180, 181]. Through this and the EMP pathway, one maltose is converted into four pyruvate with the formation of four ATP and four NADH from four ADP and four NAD^+. A gene, predicted to encode for an α-glucosidase (or called maltase) which hydrolyzes one unit of maltose into two units of glucose, exists in the genome of some *L. lactis* strains, such as MG1363 [182, 183]. The physiological significance of the gene product, however, has not yet been demonstrated.

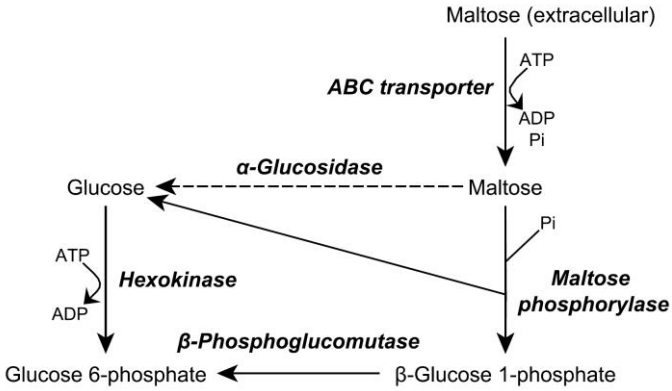

Figure 1.4. Pathway for maltose uptake in *L. lactis*.

The gene for α-glucosidase is only predicted and the function has not been confirmed.

Transcriptional regulation

Glycolytic enzymes are in general highly expressed to sustain the huge glycolytic flux in *L. lactis*. A recent study suggested that about 20% of total soluble protein is glycolytic enzymes [184]. Their genes are in general located close to the origin of replication for higher expression [177]. Transcriptional regulation of the expression of glycolytic genes in *L. lactis* primarily lies in the carbon catabolite repression (CCR) as described in 1.3.2 which has been verified experimentally in *L. lactis* [185]. The HPr protein, at high levels of FBP and ATP which reflect high glycolytic flux, is phosphorylated and then forms a complex with CcpA acting as a global regulator binding to the *cre* sites on chromosome. The consensus well-conserved in Gram-positive bacteria for *cre* binding site is TGNNANCGNTNNCA which is roughly palindromic with the central CG base always present [186]. A study on CcpA regulon in MG1363 proposed the consensus WGWAARCGYTWWMA which is specific for *L. lactis* [113].

The binding of CcpA to *cre* sites can lead to either activation or repression, depending on the position relative to promoters as in the case of *Bacillus* [187]. When a *cre* site is upstream of, inside, or downstream of the promoter of a gene, transcription is activated, repressed, or aborted accordingly [177]. Results also indicated that the interaction between CcpA and the transcription machinery may be dependent on the helix side of CcpA binding because strongest repression was observed for *cre* sites that were consecutively separated by around 10.5 bp, equal to a full helical turn of double-stranded DNA [113]. The expression of a number of glycolytic enzymes was found to be up-regulated by CcpA, including PFK, PYK and LDH (the members of the *las* operon) [188], phosphoglucose isomerase (PGI), GAPDH, enolase [186].

1.5.2 Control of the glycolytic flux

In the intracellular environment, assuming constant environmental factors, such as pH, temperature, viscosity etc., the reaction rate of an enzyme depends on concentrations of the enzyme, substrates, products and other effectors modulating the activity. Reaction rates would in turn change metabolite concentrations, forming a dynamical system. The metabolic flux of a pathway is the overall conversion rate of metabolites by the pathway resulting from the dynamical interactions between all metabolic enzymes and metabolites. The aforementioned factors controlling flux can be divided into two levels. The first level is the enzyme level, which accounts for changes in fluxes caused by changes in gene expression level. It is sometimes called hierarchical regulation in the literature. The second level is the metabolic level referring to changes in fluxes which are not caused by altered gene expression but by changes in metabolite concentrations and the inherent kinetic properties of enzymes such as maximum velocity and substrate affinity. It is called metabolic regulation. Here the distinction between ‘control’ and ‘regulation’ suggested in [164] is worth mentioned. The statement that an enzyme has ‘control’ on a flux should refer to the phenomenon that change in the enzyme level leads to change in the flux but not the direct regulatory mechanism. ‘Regulation’ should refer to the exact mechanism causing the change. These two terms have occasionally been used interchangeably though.

Control by individual enzyme levels

Control of fluxes by individual enzymes can be quantified by FCCs in MCA (which is defined by the rate of fractional change of a steady-state flux with respect to the fractional change of an enzyme activity). Finding out the so-called ‘rate-limiting’ step or an enzyme with high flux control that can lead to increase in glycolytic flux in *L. lactis* can have direct industrial relevance, e.g. speeding up the production. An earlier study trying to inhibit the activity of GAPDH by the specific inhibitor iodoacetate indicated that GAPDH had a high FCC of about 0.9 on glycolytic flux in non-growing cells of *L. lactis* subsp. *cremoris* Wg2 [189]. Similar results were obtained in another strain NCDO2118 with GAPDH having a FCC equal to 0.7 [190]. Later, the control of glycolytic flux by

glycolytic enzymes has been extensively studied by Jensen's group by experimental estimation of FCCs in the laboratory strains *L. lactis* IL1403 and MG1363. The results are summarized in Table 1.1.

Table 1.1. Summary of experimentally determined FCCs.

Enzyme	FCC at wild-type level				Min. fraction of wild-type enzyme level for maximal glycolytic flux	Definite expression level for optimality*	Ref.
	growth rate	glycolytic flux	lactate flux	formate flux			
MG1363							
LDH	≈ 0	≈ 0	≈ 0	-1.45 ~ -1.27	< 59%	No	[191]
TPI	≈ 0	≈ 0	≈ 0	≈ -0.25	< 40%	No	[72]
GAPDH	≈ 0	≈ 0	≈ 0	≈ 0	< 59%	No	[78]
PFK	≈ 0	≈ 0	≈ 0	≈ 0	≈ 100%	Slightly	[77, 192]
PYK	≈ 0	≈ 0	≈ 0	0.9 ~ 1.1	≈ 100%	Yes	[77]
IL1403							
TPI	≈ 0	≈ 0	≈ 0	≈ 0	< 75%	No	[72]
PGM	≈ 0	≈ 0	≈ 0	≈ 0	≈ 100%	Yes	[73]
ENO	≈ 0	≈ 0	≈ 0	≈ 0	≈ 100%	Yes	[71]

*'Definite expression level for optimality' refers to a unique maximum of growth rate and glycolytic flux at the wild-type enzyme level. See Figure 1.5 for illustration. LDH, lactate dehydrogenase; TPI, triosephosphate isomerase; GAPDH, glyceraldehyde 3-phosphate dehydrogenase; PFK, phosphofructokinase; PYK, pyruvate kinase; PGM, phosphoglycerate mutase; ENO, enolase.

Interestingly, usually each individual enzyme appears to have no control on growth rate and glycolytic flux at the wild-type enzyme level, including LDH [191], GAPDH [78], phosphofructokinase (PFK), PYK [77] and triosephosphate isomerase (TPI) [72] for MG1363; TPI, enolase [71] and phosphoglycerate mutase (PGM) [73] for IL1403. Among these enzymes, some are present in the wild type in significant excess for attaining maximum glycolytic flux, such as LDH, TPI and GAPDH whereas some enzymes appear to be optimally expressed in the wild type for maximum glycolytic flux, such as PFK, PYK, PGM and ENO. This means that when the level of any of the latter set of enzymes is perturbed slightly, the growth rate and glycolytic flux do decrease no matter for over- or under-expression. This property of maximum growth rate and glycolytic flux in the wild type also leads to a zero FCC at the wild-type level. Figure 1.5 illustrates the two different scenarios leading to zero FCCs in the wild type encountered in the experimental studies of glycolytic flux control by glycolytic enzymes. In the literature, nonetheless, the possible consequence and interpretation of this observation have not been discussed thoroughly.

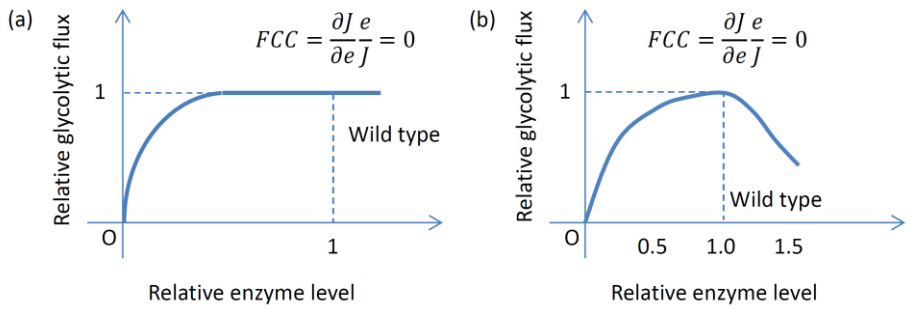

Figure 1.5. Two different scenarios leading to a zero FCC.

(a) An enzyme is present in excess and perturbing its level slightly does not change the flux. (b) The level of an enzyme allows maximum flux and perturbing the level slightly always decreases the flux.

The reason for the zero flux control for these several enzymes also remains elusive. One possible explanation is that glycolysis is already running at its maximum possible rate or the control is distributed over many enzymes [193]. Another conjecture is that the glycolysis is so optimized throughout evolution that the true FCCs were not measured due to optimal regulation of protein expression which somehow counteracted the effect of modulating an enzyme by reallocating the protein expression profile [164]. If this is true, the calculated rate is not the defined partial derivative because the concentrations of other enzymes are also functions of the concentration of the perturbed enzyme.

The conflicting results on the role of GAPDH from different studies also highlight the difficulty of studying flux control. In an earlier study, nearly full control of glycolytic flux by GAPDH in *L. lactis* Wg2 and NCDO2118 was found [189, 190] but zero control was found in *L. lactis* MG1363 [78]. One possible explanation is the intrinsic difference between the two strains as the GAPDH level was found to be two-fold higher in MG1363 compared to Wg2 [78]. Another possibility is the difference in experimental methods. GAPDH's activity in Wg2 was only inhibited but not increased whereas both under- and over-expression of GAPDH were included in the study of MG1363. This can lead to contradictory estimation of FCCs.

Hierarchical regulation under different growth conditions

Another approach used to distinguish between hierarchical regulation and metabolic regulation was proposed by Ter Kuile and Westerhoff [194] by estimating coefficients for the two types of regulation. This approach is to a certain extent working in a reverse sense to the aforementioned approach which estimates the FCC of an enzyme by growing strains with different activities of the enzyme under the same condition and then measuring the changes in activities and fluxes. In contrast, the same strain is cultured under different growth conditions, for example, in chemostat at different dilution rates [194], or different starvation conditions [195]. Then the relative change in enzyme level, measured by enzyme assay, is divided by the relative change in fluxes to define the 'hierarchical regulation

coefficient' (HRC). It is equal to one in the ideal case of pure hierarchical regulation. The 'metabolic regulation coefficient' (MRC) can then be computed by 1 – HRC to account for the change in fluxes not accountable by hierarchical regulation.

In *L. lactis*, several studies have been conducted using this approach. For instance, MG1363 has been grown in chemostat at a dilution rate of 0.1 h^{-1} at different pH, from 4.7 to 6.6 [196]. It was found that when taking the inhibitory effect of pH on enzyme activities into account, metabolic regulation was the dominant force controlling glycolytic flux. Also among the hierarchical regulation, post-transcriptional regulation of gene expression was found to be more prominent than transcriptional regulation by comparing change in mRNA transcript level with change in enzyme activity. Recently, MG1363 has been grown in chemostat at different dilution rates from 0.15 to 0.6 h^{-1} and transcriptomes, proteomes, enzyme activities have been quantified simultaneously [184]. Similar conclusions were reached. For dilution rates between 0.15 to 0.5 h^{-1}, the changes in flux through most enzymes were predominantly caused by metabolic regulation instead of hierarchical regulation except for alcohol dehydrogenase (ADH) and possible pyruvate formate lyase (PFL) whose concentrations decreased as the dilution rate increased and the flux through mixed-acid fermentation pathway decreased. So these two enzymes probably controlled the switch between fermentation modes but not the glycolytic flux. Significant hierarchical regulation only occurred during transition from 0.5 to 0.6 h^{-1} in which the expression of several enzymes were found to have changed, probably due to the effect of carbon catabolite repression by the regulatory protein CcpA. Indeed, similar results of the lack of significant change in expression of glycolytic enzymes have also been observed in an accelerostat study on IL1403 in which the dilution rate increased very slowly from 0.1 to 0.6 h^{-1} to obtain different steady states [126]. Only PGM was found to show changes in expression.

Metabolic regulation

Metabolic regulation is not easy to discover because it usually involves interactions between an enzyme and metabolites other than substrates and products of that enzyme. Extensive *in vitro* enzyme characterization is required to identify possible effector metabolites and experiments for confirmation of *in vivo* regulatory roles can even be more difficult to design. As mentioned above some studies indicated that metabolic regulation was the main driving force for flux regulation and meanwhile many pieces of knowledge on particular regulatory relationships are available, nonetheless, a clear and integrative picture of how different types of metabolic regulation work together to explain most of the known experimental results still remains elusive.

<u>Negative feedback on PTS by FBP and inorganic phosphate</u>

One example of the metabolic regulation of glycolysis is the regulation of the phosphorylation of HPr protein (HPr/HPr-Ser-P) by FBP, ATP and inorganic phosphate (Pi) mentioned previously. Since HPr helps sugar uptake through PTS but HPr-Ser-P does not, high level of FBP due to high rate of sugar

uptake causing more HPr phosphorylated into HPr-Ser-P eventually slow down the sugar uptake, forming a negative feedback loop. This loop may help to stabilize the glycolytic flux, especially against sudden change in sugar availability [164]. The question of whether this negative feedback loop poses a bottleneck on maximum glycolytic flux, nevertheless, remains unanswered.

Feedforward on PYK by FBP

Beside the role in PTS, FBP has also been known to be an activator for PYK [197]. A kinetic study of glycolytic intermediates in glucose-pulse experiments using NMR found that FBP level rose to the peak during glucose uptake and started to drop after glucose was exhausted and until a certain low FBP level, PEP started to accumulate and remained at a high level during glucose starvation [159]. The authors proposed that the low FBP level reflecting low supply of glucose could serve as a way to preserve high PEP pool by inhibiting PYK which consumes PEP during sugar starvation for future rapid sugar uptake through PTS. Others, nonetheless, observed that such an activation relationship was also preserved in other organisms including those without PTS and remained conservative about the role of this FBP-PYK relation in glycolysis [164]. They suggested another possible role in which high FBP level could serve as a signal for PYK to remove the phosphoglycerate compounds in favour of a high flux through GAPDH which operated close to thermodynamic equilibrium and was thus sensitive to mass action.

Global cofactors: NADH/NAD^+ ratio

Another interesting example is the control of glycolytic flux by cofactors levels NADH/NAD^+ and ATP/ADP. NADH/NAD^+ ratio was first proposed by Garrigues *et al*. to be the controlling factor of the glycolytic flux (as well as the mixed-acid shift, which is reviewed in section 1.5.4) in a study on *L. lactis* NCDO2118 exponentially growing on three sugars, glucose, galactose and lactose, with decreasing glycolytic fluxes [198]. This was based on several observations: (i) *in vitro* activity of GAPDH almost completely inhibited by NADH/NAD^+ ratio higher than 0.05; (ii) NADH/NAD^+ ratio positively correlated with glycolytic flux and as high as 0.08 on glucose (severe inhibition of GAPDH expected); (iii) high pools of metabolites upstream of GAPDH including FBP, GAP and dihydroxyacetone phosphate (DHAP) (suggesting the insufficient GAPDH activity to metabolize GAP). A later study by the same group on MG1363 found the same correlation between NADH/NAD^+ ratio and glycolytic flux but the factors determining the ratio remained unknown [199].

Global cofactors: ATP/ADP ratio

Glycolytic kinetics in non-growing cells of *L. lactis* had then been studied using *in vivo* NMR by Neves *et al*. [158]. The kinetic model built in the study fitted with experimental data predicted that conversion of PEP into pyruvate by PYK is inhibited by high ATP surplus, i.e. high ATP/ADP ratio, which in turn inhibits NAD^+ regeneration by LDH and bounds the glycolytic flux. This somehow provided an explanation for the positive correlation between NADH/NAD^+ ratio and glycolytic flux

observed in other studies [198]. Later NMR study by the same group focusing on the role of NADH and NAD^+ found that GAPDH was able to sustain a flux as high as in the wild-type MG1363 in a LDH-knockout strain in which the NADH concentration was 1.5 mM while the inhibitory constant of NADH for GAPDH was found to be 0.4 mM [162]. The authors to a certain extent dismissed the control by GAPDH and NADH and proposed ATP, ADP and Pi as important regulatory metabolites in glycolysis. When interpreting these results, however, one should bear in mind that the cases that *in vivo* NMR studies were dealing with were non-growing *L. lactis* so it may not be directly applicable to the case where *L. lactis* is exponentially growing.

To test the *in vivo* role of ATP/ADP ratio in growing *L. lactis*, Koebmann *et al*. decreased the intracellular ATP/ADP ratio in MG1363 by expressing ATPase using a synthetic promoter library [79]. Surprisingly, for these strains growing exponentially on glucose, the glycolytic flux showed no significant change over a large range of ATP/ADP ratio from around 9 in the wild type to around 5 in the strain with the highest expression of ATPase. When these strains were in a non-growing state (achieved by resuspending cells in media without amino acids and vitamins), however, the glycolytic flux increased with ATPase activities until a level close to that in the growing wild type. These observations suggested the possibility that glycolysis was already at its maximal rate in the wild type. Another possible situation suggested by the authors was that although lowering the ATP/ADP ratio might stimulate glycolysis (e.g. by increasing the activities of kinases in the pay-off phase), it might eventually reduce the activity of PFK which becomes a bottleneck countering the effect, known as the risk of a 'turbo design' in which part of the desirable products are invested in the first place as input [200].

Other factors

Other sources of metabolic regulation thought to be important for regulating glycolytic flux include the inhibition of PYK by Pi [201], inhibition of PFK by PEP [202] and inhibition of GAPDH by NADH [198, 199]. Hoefnagel *et al*. integrated these three inhibitive relation and the activation of PYK by FBP in a single kinetic model with all rate equations and parameters adopted from literature without fitting [154]. The model succeeded in simulating the observed kinetic behaviour during glucose run-out experiments in other studies ([158]) including the rapid increase in PEP and Pi, decrease in ATP and slow depletion of FBP. The authors reasoned the following sequence of kinetic responses upon glucose depletion: (1) less Pi is retained in G6P, F6P and FBP; (2) Pi increases and inhibits PK; (3) PEP inceases due to inhibited PK and no glucose for PTS and thus less pyruvate available; (4) Less substrate for LDH and thus NADH accumulates; (5) GAPDH is inhibited by NADH.

1.5.3 Pyruvate metabolism

Since *L. lactis* does not have a complete and functional tricarboxylic acid (TCA) cycle and cannot perform oxidative phosphorylation due to the inability to synthesize heme [28, 182], glycolysis as the major energy generating pathway must operates at a high speed. Since only a small fraction of the sugar metabolized is required for biomass production (usually <10%, e.g. [203]), most of the pyruvate flux ends up as fermentation products through different pathways. *L. lactis* is usually a homolactic fermenting LAB. As described in section 1.3.2, there are two branches of pathways producing mixed acids and flavour compounds respectively from pyruvate other than homolactic fermentation in *L. lactis* (Figure 1.2A).

Homolactic fermentation

In the metabolism of *L. lactis*, at the pyruvate branch point, lactate is produced via a single reaction catalysed by lactate dehydrogenase (LDH). LDH converts pyruvate into lactate and generates NAD^+ from NADH at the same time. Several studies on the kinetics of LDH from *L. lactis* have been conducted [198, 199, 204]. From these studies, the K_m for pyruvate and NADH were found to be 1.5 – 3 mM and around 0.1 mM respectively. Also, FBP was found to be an activator of LDH with a micro-molar activation constant. Pi was considered to be an inhibition of LDH [204] but the inhibition was confirmed later to be negligible under physiological conditions [198, 199].

The expression of LDH is in general very robust as reflected by a fairly constant *in vitro* specific activity under different growth conditions, from strictly anaerobic, microaerobic to aerobic conditions [205, 206], or growth on different sugars [207]. LDH also appeared to be in huge excess compared to the *in vivo* flux it had in some studies (e.g. [207, 208]) and was shown to be able to sustain the same flux as in the wild type after about 40% reduction of its expression [191] (Table 1.1).

There are three genes in most genome-sequenced *L. lactis* strains, as observed from the UniProt database (http://www. uniprot.org), annotated as genes for LDH, named as *ldh*, *ldhB* and *ldhX* in both MG1363 and IL1403. *ldh* is the gene lying in the *las* operon following *pfk* and *pyk* and deemed to be the canonical gene for the LDH responsible for producing lactate in most cases [177]. The *las* operan has a *cre*-containing promoter and hence LDH, together with PFK and PYK, is transcriptionally activated by CcpA [188]. Whilst the role of *ldhX* remains unknown, *ldbB* has been found to be transcriptionally inactive when *ldh* was present and the transcription of *ldhB* was recovered with a significant capability of lactate production in an *ldh*-knockout strain after adaptive evolution [209]. The LDH synthesized from *ldhB* has later been characterized to have kinetic properties that depend heavily on the pH level and are quite different from the canonical LDH, e.g. activation by Pi at low pH [210].

Mixed-acid fermentation

Under anaerobic conditions, when the sugar uptake rate is constrained to be slow, for instance, by a low dilution rate in chemostat experiment (e.g. [40]), or by growth on slowly fermentable sugars such as maltose or galactose (e.g. [211, 212]), a significant fraction of pyruvate flux would be directed to the production of formate, acetate and ethanol, termed mixed-acid fermentation (Figure 1.6). The first step is the conversion of pyruvate into acetyl-coenzyme A (Ac-CoA) by either pyruvate formate lyase (PFL) or pyruvate dehydrogenase complex (PDHc). Ac-CoA can then be converted into acetyl-phosphate (Ac-P) by phosphotransacetylase (PTA) followed by acetate production by acetate kinase (ACK) which produces one ATP. Alternatively, Ac-CoA can be reduced into first acetaldehyde and then ethanol by a single enzyme alcohol dehydrogenase (ADH).

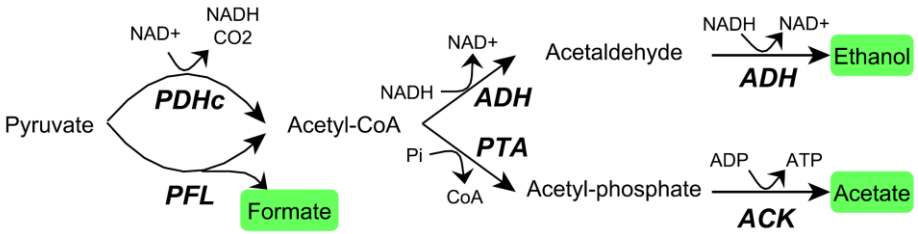

Figure 1.6. Mixed-acid fermentation pathway producing formate, acetate and ethanol.

Products excreted are shaded in green. Enzymes are in bold and italic style. Pi, inorganic phosphate; CoA, coenzymeA; PDHc, pyruvate dehydrogenase complex; PFL, pyruvate formate lyase; ADH, alcohol dehydrogenase; PTA, phosphotransacetylase; ACK, acetate kinase.

Of all these enzymes, two possible elementary routes are available for converting pyruvate into end products with proper redox balance. The generation of one pyruvate is accompanied by one NADH being reduced from NAD^+. Redox balance can therefore be kept by consuming one pyruvate with simultaneous oxidation of one NADH. The first route is one unit of pyruvate converted by PFL into Ac-CoA, followed by half of the Ac-CoA entering PTA-ACK pathway to produce acetate and the other half forming ethanol via ADH. The formate-acetate-ethanol ratio in this case is 2:1:1, which is the most common case observed in many studies under anaerobic conditions. This route generates 0.5 more ATP per pyruvate being catabolized. The second possible route is the production of one unit of CO2 and ethanol by PDHc and ADH but it has not been reported under anaerobic conditions due to low level and low activity of PDHc. On the contrary, under aerobic conditions, due to the expression of the NADH oxidase (NOX) and its activation by oxygen, PDHc activity coupled with acetate production with the aid of NOX for regeneration of NAD^+ has been observed in different studies [163, 205, 206].

Pyruvate formate-lyase

PFL in *L. lactis* has been manifested to be extremely vulnerable to exposure to oxygen as in *E. coli* [213]. It has been reported that the K_m for pyruvate of PFL in MG1363 was 0.4 mM, lower than that

of LDH and PFL was inhibited by triosephosphate pool with inhibitory constant equal to 0.7 mM and 1 mM for GAP and DHAP respectively [199]. The expression of PFL was usually found to be significantly induced for growth under anaerobic conditions at a low dilution rate in chemostat [206, 208] or on slowly fermentable sugars such as galactose [213].

The expression of *pfl* of MG1363, the gene encoding PFL, has been characterized [214]. A monocistronic mRNA for *pfl* was found. There are two sequences upstream of *pfl* with significant homology to the consensus of the global regulator FNR of *E. coli* which activates the transcription of *pfl* in *E. coli* anaerobically [215]. One of them even overlaps with the -35 promoter region. The genes of two proteins in *L. lactis* MG1363 homologous to FNR, FlpA and FlpB, were studied [216]. An *flpA* mutant was found to produce significantly more formate when growing on glucose or galactose but much less when growing on maltose compared to the wild type whereas no significant effect was observed for an *flpB* mutant and a double mutant. FlpA and FlpB have later been purified for studying their binding to DNA *in vitro* and FlpA was confirmed to recognize FNR site but appeared to work in the opposite direction to FNR because opposite to FNR, the binding was abolished by an iron-sulphur cluster and restored by exposure to air [217]. A later study on the expression of FlpA and FlpB indicated that transcription of *flpB* was much lower than *flpA* and was induced under anaerobic conditions while the transcription of *flpA* was not oxygen-responsive but required the presence of both FlpA and FlpB. Until now, there is no clear conclusion on the transcriptional regulation of *pfl* at the molecular level.

Pyruvate dehydrogenase complex

PDHc, another route for Ac-CoA formation from pyruvate, unlike PFL, produces one CO_2 and meanwhile generates one NADH from NAD^+. Kinetic studies on the kinetics of PDHc indicated that it was highly sensitive to high $NADH/NAD^+$ ratio [218, 219]. 50% and complete inhibition were observed at ratios of about 0.033 and 0.135 respectively in the studies, suggesting complete inhibition under strict anaerobiosis.

The expression of PDHc has usually been associated to growth under aerobic conditions [198, 199]. Under different growth conditions, however, conflicting results have been reported. PDH activity in MG1363 under anaerobic conditions has been found to be absent when growing on lactose [199]; or present at low but observable levels when growing either at 0.1 h^{-1} dilution rate or on glucose in batch (growth rate up to 0.9 h^{-1}) [205, 206]. It has also been found to increase >10-fold with aeration under microaerobic condition (air-to-nitrogen ratio from 0 to around 2) at a constant dilution rate of 0.1 h^{-1} [206] or without significant change in anaerobic, microaerobic or aerobic conditions for batch growth on glucose with high growth rates (>0.78 h^{-1} for all three cases) [205]. The well-known requirement of lipoate as a cofactor for PDHc is worthwhile to mention because *L. lactis* and some other LAB such

as *Enterococcus faecalis* lack the ability to synthesize lipoate and thus addition of lipoic acid into the growth media is necessary for PDHc activation [220].

Phosphotransacetylase, acetate kinase and alcohol dehydrogenase

For *L. lactis*'s PTA, ACK and ADH, little kinetic characterization has been performed except a recent study on PTA and ACK [221] and a very recent study on ACK isozymes [152]. PTA has been found to be inhibited by FBP and diacetyl [221]. In addition to these two compounds, ACK has also been found to be inhibited by GAP and PEP at concentrations within physiological ranges [152, 221]. The expression of these three enzymes was found to be in generally higher at lower growth rates in growth experiments on galactose, maltose or at low dilution rates in chemostat [179, 184, 207, 221].

Flavour compound production

Production of diacetyl, acetoin and 2,3-butanediol (2,3BTD) by *L. lactis*, all being C_4 flavour compounds, is very important in food industry. It has been associated with citrate fermentation [222, 223] as well as aerobic growth on sugars [224, 225]. In this pathway, first α-acetolactate synthase (ALS) catalyses the decarboxylation of two pyruvate to form one α-acetolactate, which upon further decarboxylation becomes one acetoin. 2,3BTD is produced from acetoin by 2,3BTD dehydrogenase (BTDDH). α-Acetolactate also reacts non-enzymatically with oxygen to form diacetyl which can be reduced to acetoin by acetoin dehydrogenase (ACETDH).

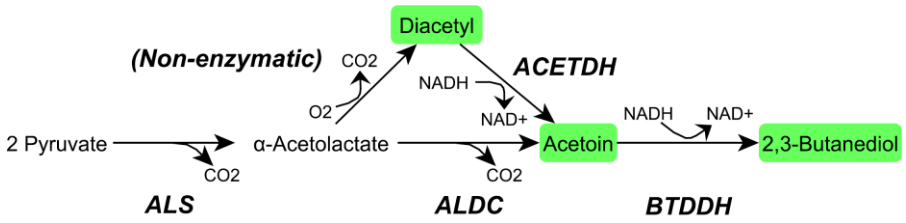

Figure 1.7. Flavour compound production from pyruvate.

Products excreted are shaded in green. Enzymes are in bold and italic style. The reaction producing diacetyl from α-acetolactate is non-enzymatic. ALS, α-acetolactate synthase; ALDC, α-acetolactate decarboxylase; ACETDH, acetoin dehydrogenase; BTDDH, 2,3-butanediol dehydrogenase.

The kinetics of ALS has been characterized for a *L. lactis* strain and showed strong positive cooperativity for pyruvate (Hill coefficient = 2.4) and a very high K_m for pyruvate equal to 50 mM [219]. Another study on another strain found a similar value of 30 mM [226]. In the study ALDC was also tested. Positive cooperativity was again observed with Hill coefficient equal to 1.89. The K_m for α-acetolactate estimated was 60 mM. For ACETDH and BTDDH, in a *L. lactis* strain, an enzyme capable of catalysing both reactions was isolated and K_m for acetoin and diacetyl were estimated to be 60 μM and 3.6 mM respectively [227].

Beside the precursor of several flavour compounds, α-acetolactate is also a metabolite connecting carbon and amino acid metabolism since it is a precursor of the branched-chain amino acids (BCAAs) leucine, isoleucine and valine (provided that a particular *L. lactis* strain is able to synthesize any of them). The expression of ALDC was found to be induced by the presence of leucine in media and inhibit growth of *L. lactis* NCDO2118 under valine starvation while disrupting the gene for ALDC succeeded in growth recovery under such a condition [228]. ALDC was attributed to the exhaustion of intracellular α-acetolactate so that valine could not be synthesized. The regulation of ALDC expression has later been investigated at transcriptional and translational levels [229].

In many studies, Fluxes through this flavour-producing pathway and acetate production increased concomitantly when *L. lactis* was granted extra ability to grow aerobically by either overexpressing NOX [56, 153, 163, 221] or supplementing heme or its precursor such as protoporphyrin IX for respiration [225, 230–232]. The reason for the redirection has not yet been fully elucidated. Comparison at the protein level between heme-dependent respiratiory and static conditions found that among glycolytic enzymes, the expression of phosphoglycerate mutase (PGM) and one isoform of GAPDH decreased markedly during respiration whereas the expression of PDHc and ALS was upregulated [233]. This may have some control on the distribution of pyruvate flux. For the case of NOX overexpression, the lower K_m for NADH of NOX compared to that of LDH and ADH has been ascribed to the phenomenon observed [163]. NOX outperforms LDH and ADH regarding NADH competition. This is compatible with the observation that other than the flavour-producing pathway, only acetate is produced via PDHc, PTA and ACK without formate and much ethanol production. PDHc may have high activity due to the expected low $NADH/NAD^+$ ratio. Meanwhile, PFL is inactivated under aerobic conditions [213].

1.5.4 Flux regulation of mixed-acid shift

The metabolic shift between homolactic fermentation and mixed-acid fermentation is intriguing in the sense that *L. lactis* prefers production of lactate with two ATP generated per glucose to production of mixed acids with three ATP generated per glucose. Such a shift from high-yield to low-yield metabolism, or equivalently use of energetically inefficient pathway, has been called overflow metabolism (usually for bacteria) [234, 235], or ‘crabtree effect’ for yeast and other organisms [236, 237], or ‘Warburg effect’ for tumor cells [238]. Unravelling the mechanism and the evolutionary advantage of this phenomenon is thus a very important biological question. In *L. lactis*, from the large amount of experimental evidence accumulated over the years, different factors and mechanisms have been proposed. They are divided into three aspects, protein level, metabolic level and environmental conditions. The possible evolutionary advantages are also discussed along the subsection.

Protein level

Elevated expression levels of enzymes in the mixed-acid branch have been reported when *L. lactis* grows at low dilution rates or on slowly fermentable sugars as described in the previous subsection. A study comparing the proteomes of *L. lactis* growing on glucose, growing on maltose and resting on maltose also revealed that expression of glycolytic enzymes was in general slightly down-regulated (<2-fold) for growth on maltose compared with growth on glucose while proteomes for *L. lactis* growing or resting on maltose were in general very similar [179].

Control analysis on different enzymes further emphasized the role of protein expression on the shift. PFL level in MG1363 has been modulated and strong control on formate flux was observed for growth on galactose (FCC > 1, estimated from the data in the article) but only weak control was found for growth on glucose (FCC ≈ 0.26) [239]. Modulation of LDH and PYK levels showed that there are a strong negative and positive control of formate flux and acetate flux by LDH and PYK respectively (FCCs close to -1 and 1) when growing on glucose [77, 191]. This means decreasing and increasing the expression of LDH and PYK respectively did increase the pyruvate flux distributed to mixed-acid fermentation. The same directions of control by LDH and PYK remained for growth on maltose, however, with much smaller FCCs (around -0.2 and 0.2) [240]. In another study, inhibition of the activity of GAPDH of *L. lactis* growing on lactose to different extents was achieved by adding increasing concentrations of iodoacetate [190]. A marked shift from mixed-acid to homolactic fermentation accompanied by decreasing growth rates was observed.

Beyond protein level

From the above experimental evidence, it is tempting to conclude that the mixed-acid shift is caused by the change in gene expression level but this was usually not the conclusion of most studies because there are other experimental results in which the shift could not be ascribed to change in gene expression level. For example, in the modulation of LDH and PYK levels [77, 191], the flux through the two reactions did not change apparently but they changed the formate flux, so it is reasonable to hypothesize that the change was caused by interactions between enzymes and metabolite, i.e. events at the metabolic level.

As aforementioned, proteomes for *L. lactis* growing or resting on maltose were in general very similar and no significant change was observed for glycolytic enzymes and enzymes in pyruvate metabolism [179]. However, while the growing cells produced mixed acids from maltose, the resting cells were found to produce lactate only. The glycolytic flux in resting cells was about 3-fold lower than that in growing cells, similar to the case of growth on glucose [79]. This study suggested that the flux distribution did not solely depend on the proteome. A similar conclusion has been drawn in the aforementioned study which calculated hierarchical and metabolic regulation coefficients by growing

MG1363 at different dilution rates [184]. Only the flux of ADH and possibly PFL appeared to be regulated by the protein expression level in conditions with different fermentation profiles.

A final example is a set of shift-up and shift-down experiments [208]. In the shift-up experiment, *L. lactis* MG1363 had been cultured to reach a steady state at a low dilution rate (0.1 h^{-1}) which produced mixed acid and the dilution rate was then instantaneously elevated to 0.5 h^{-1}. Switch to homolactic fermentation almost occurred at once, contrary to the hypothetical case of sole dependence on gene expression level in which a delayed switch should be observed due to the time required for regulation of expression. The shift-down experiment was conducted in a similar fashion but a reverse change of dilution rates. Unlike shifting up, in the shift-down experiment a profile of mixed-acid fermentation was gradually built up, suggesting the plausible dependence of the switch on gene expression. The results indicated the existence of a rapid regulatory mechanism for the switch from mixed-acid to homolactic fermentation, which is probably able to sense the glycolytic flux.

Metabolic level

LDH activation by FBP

In fact, allosteric regulation of the enzymes in pyruvate metabolism of *L. lactis* has long been proposed as a mechanism for the mixed-acid shift. Activation of LDH by FBP has first been proposed to regulate the shift since FBP is the only activator of LDH for growth on glucose and FBP level was found to be correlated with glycolytic flux [40]. The theory was however turned down convincingly by two later studies conducted by Garrigues *et al* on *L. lactis* NCDO2118 and MG1363 respectively [198, 199]. In these studies, full activation concentrations of LDH by FBP were measured to be 2 – 4 μM whereas the intracellular FBP concentration measured ranged from 0.3 mM to 118 mM, >50-fold higher than the activation concentration even for the case of the lowest FBP level.

NADH/NAD^+ ratio

Garrigues *et al*, in the same studies, instead proposed another mechanism for the switch which is caused by the change in NADH/NAD^+ ratio [198, 199]. Since GAPDH was found to be very sensitive to NADH/NAD^+ ratio, triose-phosphate (DHAP and GAP) accumulates when the ratio are high. Triose-phosphate then inhibits the activity of PFL and meanwhile LDH has a high activity because of high NADH/NAD^+ ratio, causing homolactic fermentation. When NADH/NAD^+ ratio is low, PFL is therefore not inhibited and the activity of LDH is lower. Combining with the higher affinity of PFL for pyruvate, mixed-acid fermentation is achieved. In the studies, positive correlation between NADH/NAD^+ ratio and glycolytic flux was observed. The model can therefore describe the homolactic and mixed-acid fermentation occurring at high and low glycolytic flux respectively. The inhibition of PFL by DHAP and GAP (first observed in *Streptococcus mutans* [241]) was confirmed *in vitro*. Their intracellular levels measured for exponentially growing cells in different conditions

also matched the hypothesis: being lower than the inhibitory constants in mixed-acid fermenting cells and being significantly higher than the constants in homolactic fermenting cells. This proposed mechanism is able to explain the rapid switch from mixed-acid to homolactic fermentation during the aforementioned shift-up experiment [208].

ATP/ADP surplus

The role of NADH/NAD^+ ratio was consistent with experimental evidences. How this ratio depends on substrate availability or glycolytic flux, however, was left unexplained. In fact, in the second of the two studies mentioned in the last paragraph, Garrigues *et al* proposed a more generalized theory stating that the switch depends on the balance of anabolic demand of ATP which is generated by catabolism [199]. It was based on the additional experiments in the study that compared the growth and fermentation pattern of *L. lactis* NCDO 2118 on galactose in media with different amino acid and vitamin contents. It was found that with fewer amino acid and vitamin contents, growth and glycolytic flux decreased as expected whereas fermentation switched from mixed-acid to homolactic unexpectedly. The authors thus proposed that under conditions of catabolic excess (growth on glucose) or anabolic limitation (growth in media with fewer amino acid and vitamin contents) in which ATP/ADP was predicted to be high, homolactic fermentation prevailed whereas under conditions of catabolic limitation and anabolic excess (growth on galactose in rich media), mixed-acid fermentation took place to maximize ATP. The concrete link between this theory and NADH/NAD^+ ratio was however not provided.

The proposed role of ATP/ADP surplus in the mixed-acid shift actually coincides with its role in glycolytic flux as discussed in section 1.5.2. The glycolytic flux in resting cells could be stimulated by lowering ATP/ADP ratio using ATPase, showing that high ATP/ADP level limited the flux [79]. A later study provided evidences supporting this assumed role of ATP/ADP [242]. For resting cells of *L. lactis* fermenting maltose which produced lactate only, reducing ATP/ADP ratio by adding monensin or valinomycin (ionophores known to induce ATPase activity) switched the fermentation pattern to mixed acids. Inhibition of ADH by the ATP and ADP pool was proposed as the caused since the measured level of ATP and ADP in resting cells brought 95% inhibition of ADH activity *in vitro*. Inhibition to a less extent by ATP and ADP was also observed for GAPDH and LDH.

The authors in the same study also compared growth on maltose with nitrogen limitation or growth arrested by chloramphenicol. In either case the decreasing growth rate was negatively correlated to increasing homolactic fermentation and the authors claimed that the change in fermentation pattern was due to change in growth rate instead of nitrogen content available. We think, however, this can be overly interpreted because chloramphenicol has long been known to inhibit bacterial growth by specifically inhibiting the assimilation of amino acids and therefore protein synthesis [243]. Thus

chloramphenicol addition and nitrogen limitation may actually have very similar effects on metabolism.

There is a final remark about the hypotheses of NADH/NAD^+ ratio and ATP/ADP surplus. The former has experimental support of the proposed mechanism but how it is related to the environment to which a cell is subject remains unclear. The latter, namely ATP/ADP surplus, provides a rationale of the switch and is also supported by some experimental evidence, but how it is related to the exact mechanism like the NADH/NAD^+ ratio remains unknown. Moreover, there have not yet been convincing experiments carried out as a proof of the proposed mechanism.

Environmental conditions

The most well-established environmental condition causing the occurrence of the mixed-acid shift is the catabolic limitation by either growth on slowly fermentable sugars or low availability of sugars in situation such as chemostat at low dilution rates. For growth under these conditions, when other anabolic limitations are active, such as less amino acid or vitamin availability as described previously, fermentation appears to shift back from mixed-acid to homolactic fermentation.

Environmental factors other than substrate availability including pH and temperature have also been found to influence the fermentation pattern. A study on *L. lactis* growing on maltose at different pH and temperatures revealed that *L. lactis* became more homolactic at lower pH compared to pH 6.5 and at higher temperature compared to 30 ˚C [244]. The authors suggested the inactivation of PFL at low pH found in *Streptococcus mutans* [241] and the increased ATP spent on maintenance at low pH or high temperatures as the reasons for the observed shift.

Evolutionary advantage

Despite the wealth of the knowledge regarding the metabolic shift (though an integrated consensus of the relative importance is still not available), the evolutionary advantage, as an ‘ultimate regulatory force’, of switching between a low-yield (homolactic fermentation) and high-yield (mixed-acid fermentation) metabolism remains far from clear. An advantage that has been sometimes cited in the literature is to inhibit the growth of other organisms by acidification of the environment due to fast lactate production but Teusink *et al*. argued that it may not be valid [164]. They reasoned that ‘cheater’ mutants that can grow faster by switching to high-yield metabolism and meanwhile survive the acidic environment should have evolved according to this hypothesis but it has never been observed for *L. lactis*.

Another hypothesis is the tradeoff between protein cost and ATP generation. On the one hand, mixed-acid fermentation generates one more ATP per hexose catabolized. On the other hand, mixed-acid fermentation requires three enzymes to be expressed while homolactic fermentation requires one only. Since protein expression also costs ATP and the rate of the cost should increase with growth rate due

to dilution by cell division, different strategies at different growth rates can be a result of growth rate optimization considering the ATP gain and protein cost of a pathway. This cannot be confirmed without a quantitative model. A very first model addressing this type of shift was the self-replicator model consisting of minimal elements for self-replication including one transport protein, ribosome, one anabolic pathway and two metabolic pathways, one with lower ATP yield but higher catalytic efficiency k_{cat} and one with higher ATP yield but lower k_{cat} [245]. The model did succeed in predicting a shift from high-yield metabolism to low-yield metabolism upon the increase of growth rate. A later attempt based on a similar rationale employed the genome-scale metabolic network of *L. lactis* IL1403 and applied flux balance analysis (FBA) with the constraints of molecular crowding to model the mixed-acid shift successfully [246]. Molecular crowding here refers to explicit consideration of the distribution of protein with the total amount being finite over all metabolic reactions. Each reaction has a maximum velocity equal to k_{cat} multiplied by the protein concentration assigned to that reaction.

This hypothesis, though logically sound, is yet to be verified experimentally. The very recent study mentioned several times previously conducted on MG1363 growing at different dilution rates with the aid of multi-omics techniques has been designed to test this hypothesis [184]. It was found that only the flux of ADH and possibly PFL was controlled at gene expression level and many other proteins appeared to be excessive than the necessary amounts to carry fluxes. This to a certain extent suggested that there was not a case in which tight control of gene expression was exerted to satisfy metabolic requirement minimally for protein-cost saving. One may however argue that while the excessive amount of most enzymes may bring other important evolutionary advantage, the gain from saving the cost of one or two enzymes, though little, can become significant in evolutionary sense. For one point that can be sure about, nonetheless, this hypothesis cannot explain the existence of a rapid shift mechanism because it is not related to the protein expression level.

Another evolutionary point of view that can be taken into consideration is the evolutionary game theory that has drawn increasing interest in the last decade [247–249]. It advocates defining objective function for optimization by considering the interactions between the organism, environment and other competing organisms (other players) as in game theory instead of simply maximizing growth rate. In this way of thinking, the objective function may no longer be the growth rate defined in genome-scale metabolic networks calculated by FBA which is basically an yield optimization but could be true rate optimization including the use of metabolically inefficient pathway. Or it is even possible to maximize the substrate depletion rate, regardless of the growth yield that such a strategy brings, to minimize the growth of other players.

A final remark about inferring the evolutionary advantage is that athough the same phenomenon of the shift of fermentation modes was observed at different condition, one should not simply draw the

same conclusion regarding the cause and effect. Under the conditions that *L. lactis* has long been adapted to, it is reasonable to think that the shift represents a way to optimize the growth rate or other fitness function. But under other conditions, the observed shift may be an effect of the evolved mechanism and advantage of the shift under those conditions may not be found. To properly study the evolutionary advantage of the shift, the evolutionary history, habitats and the ecological community of *L. lactis* should be put into considerations together.

1.6 Objectives and strategies

In sipte of the many efforts put on investigating the glycolysis and pyruvate metabolism of *L. lactis* in the past, especially about the mixed-acid shift, many elements in the proposed theory regarding the shift are required to be elucidated for a more comprehensive picture. Also, the widely studied laboratory strain *L. lactis* subsp. *lactis* IL1403 was found to remain homolactic even when growing on slowly fermentable sugars such as galactose [207]. By studying the fermentation behaviour of the strain and comparison with strains able to switch, further insights can be gained.

In this study, in response to the factors affecting the switching behaviour as reviewed in the previous section, namely gene expression level, metabolic level and environmental conditions, we aimed to study the mixed-acid fermentation of *L. lactis* subsp. *cremoris* MG1363 using the following strategies: (i) genetic perturbation, (ii) cofactor perturbation and (iii) growth at varying nutrient availability, in terms of amino acids. Growth behaviour on glucose and maltose of MG1363 respectively is usually compared and it is occasionally contrasted with IL1403. Maltose is chosen because it was observed to cause the most prominent mixed-acid shift in *L. lactis* MG1363.

1.6.1 Genetic perturbation

The roles of some mixed-acid-fermenting enzymes on mixed-acid fermentation remain to be elucidated, such as PFL, PTA, ACK and ADH, especially ACK which appears to be encoded by two different uncharacterized genes in many *L. lactis* strains.

1.7 reports the study of transcriptional activity of these enzymes and the modes of transcriptional regulation in the two widely studied laboratory strains, MG1363 and IL1403. The former exhibits mixed-acid shift to a large extent while the latter does not. Chapter 3 reports the results of modulation of PFL levels in MG1363 and IL1403 and the comparison. In Chapter 3, characterization of the two genes encoding ACK in *L. lactis* MG1363 is presented, including the transcription structure, enzyme kinetics and their physiological roles.

1.6.2 Cofactor perturbation

The role of NADH/NAD^+ in anaerobic growth of *L. lactis* was supported by comparing growth on different sugars or in different media [198, 199]. The question, however, that whether it truly controls

the pyruvate metabolism, remains unexamined to a large extent. Chapter 5 attempts to study the effect of perturbing NADH/NAD^+ under different conditions.

1.6.3 Nutrient availability

The effect of availability of nutrients other than sugars, especially amino acids, on the mixed-acid shift has only been studied roughly in [198, 199, 242]. Chapter 6 briefly summarizes some experimental findings in this respect from a bachelor project initiated by us and especially a general computational method developed and applied to look into the amino acid metabolism in the genome-scale metabolic network of *L. lactis* MG1363 [145] which has been pusblished and reprinted in Appendix A.

1.7 References

1. Khalid K (2011) An overview of lactic acid bacteria. *Int J Biosci* 1:1–13.
2. Stiles ME, Holzapfel WH (1997) Lactic acid bacteria of foods and their current taxonomy. *Int J Food Microbiol* 36:1–29. Available at: http://www.ncbi.nlm.nih.gov/pubmed/9168311.
3. Orla-Jensen S (1919) *Lactic Acid Bacteria* (Fred Host and Son, Copenhagen) Available at: http://books.google.dk/books?id=mxOnmgEACAAJ.
4. Makarova K et al. (2006) Comparative genomics of the lactic acid bacteria. *Proc Natl Acad Sci U S A* 103:15611–6. Available at: http://www.pubmedcentral.nih.gov/articlerender.fcgi?artid=2660350&tool=pmcentrez&rendertype=abstract.
5. Von Wright A, Axelsson L (2011) in *Lactic Acid Bacteria: Microbiological and Functional Aspects*, eds Lahtinen S, Ouwehand CA, Salminen S, von Wright A (CRC Press, London), pp 1–16.. 4th Ed.
6. Leroy F, De Vuyst L (2004) Lactic acid bacteria as functional starter cultures for the food fermentation industry. *Trends Food Sci Technol* 15:67–78. Available at: http://linkinghub.elsevier.com/retrieve/pii/S0924224403002085 [Accessed July 15, 2014].
7. Ljungh A, Wadstrom T (2006) Lactic acid bacteria as probiotics. *Curr Issues Intest Microbiol* 7:73–90.
8. Cunningham MW (2000) Pathogenesis of group A streptococcal infections. *Clin Microbiol Rev* 13:470–511.
9. Van Hylckama Vlieg JET et al. (2006) Natural diversity and adaptive responses of *Lactococcus lactis*. *Curr Opin Biotechnol* 17:183–90. Available at: http://www.ncbi.nlm.nih.gov/pubmed/16517150 [Accessed June 23, 2011].
10. Smit G, Smit B a, Engels WJM (2005) Flavour formation by lactic acid bacteria and biochemical flavour profiling of cheese products. *FEMS Microbiol Rev* 29:591–610. Available at: http://www.ncbi.nlm.nih.gov/pubmed/15935512 [Accessed September 3, 2014].
11. Urbach G (1995) Contribution of lactic acid bacteria to flavour compound formation in dairy products. *Int Dairy J* 5:877–903.
12. Zourari A, Accolas JP, Desmazeaud MJ (1992) Metabolism and biochemical characteristics of yogurt bacteria. A review. *Lait* 72:1–34.
13. Klaenhammer TR (1993) Genetics of bacteriocins produced by lactic acid bacteria. *FEMS Microbiol Rev* 12:39–85. Available at: http://doi.wiley.com/10.1111/j.1574-6976.1993.tb00012.x [Accessed September 15, 2014].
14. Nes IF et al. (1996) Biosynthesis of bacteriocins in lactic acid bacteria. *Antonie Van Leeuwenhoek* 70:113–28. Available at: http://www.ncbi.nlm.nih.gov/pubmed/8879403.
15. Stiles ME (1996) Biopreservation by lactic acid bacteria. *Antonie Van Leeuwenhoek* 70:331–345. Available at: http://www.ncbi.nlm.nih.gov/pubmed/8879414.
16. Guarner F, Schaafsma GJ (1998) Probiotics. *Int J Food Microbiol* 39:237–238.
17. Detmer A, Glenting J (2006) Live bacterial vaccines--a review and identification of potential hazards. *Microb Cell Fact* 5:23. Available at: http://www.pubmedcentral.nih.gov/articlerender.fcgi?artid=1538998&tool=pmcentrez&rendertype=abstract [Accessed September 10, 2014].
18. Robinson K, Chamberlain LM, Schofield KM, Wells JM, Le Page RW (1997) Oral vaccination of mice against tetanus with recombinant *Lactococcus lactis*. *Nat Biotechnol* 15:653–657.
19. De Vos WM, Hugenholtz J (2004) Engineering metabolic highways in Lactococci and other lactic acid bacteria. *Trends Biotechnol* 22:72–79. Available at: http://linkinghub.elsevier.com/retrieve/pii/S0167779903003354 [Accessed September 19, 2011].
20. Gaspar P, Carvalho AL, Vinga S, Santos H, Neves AR (2013) From physiology to systems metabolic engineering for the production of biochemicals by lactic acid bacteria. *Biotechnol Adv* 31:764–88. Available at: http://www.ncbi.nlm.nih.gov/pubmed/23567148 [Accessed July 14, 2014].
21. Hofvendahl K, Hahn-Hägerdal B (2000) Factors affecting the fermentative lactic acid production from renewable resources. *Enzyme Microb Technol* 26:87–107. Available at: http://www.ncbi.nlm.nih.gov/pubmed/10689064.

22. Mierau I, Kleerebezem M (2005) 10 years of the nisin-controlled gene expression system (NICE) in *Lactococcus lactis*. *Appl Microbiol Biotechnol* 68:705–17. Available at: http://www.ncbi.nlm.nih.gov/pubmed/16088349 [Accessed March 2, 2012].
23. Solem C, Dehli T, Jensen PR (2013) Rewiring *Lactococcus lactis* for ethanol production. *Appl Environ Microbiol* 79:2512–8. Available at: http://www.ncbi.nlm.nih.gov/pubmed/23377945 [Accessed August 11, 2013].
24. Berezina O V et al. (2010) Reconstructing the clostridial n-butanol metabolic pathway in Lactobacillus brevis. *Appl Microbiol Biotechnol* 87:635–46. Available at: http://www.ncbi.nlm.nih.gov/pubmed/20195860 [Accessed August 24, 2014].
25. Gaspar P, Neves AR, Gasson MJ, Shearman C a, Santos H (2011) High yields of 2,3-butanediol and mannitol in *Lactococcus lactis* through engineering of NAD^+ cofactor recycling. *Appl Environ Microbiol* 77:6826–35. Available at: http://www.pubmedcentral.nih.gov/articlerender.fcgi?artid=3187077&tool=pmcentrez&rendertype=abstract [Accessed September 2, 2014].
26. Hugenholtz J, Kleerebezem M (1999) Metabolic engineering of lactic acid bacteria: overview of the approaches and results of pathway rerouting involved in food fermentations. *Curr Opin Biotechnol* 10:492–497.
27. Pedersen MB, Iversen SL, Sørensen KI, Johansen E (2005) The long and winding road from the research laboratory to industrial applications of lactic acid bacteria. *FEMS Microbiol Rev* 29:611–24. Available at: http://www.ncbi.nlm.nih.gov/pubmed/15935510 [Accessed August 29, 2012].
28. Bolotin a et al. (2001) The complete genome sequence of the lactic acid bacterium *Lactococcus lactis* ssp. *lactis* IL1403. *Genome Res* 11:731–53. Available at: http://www.pubmedcentral.nih.gov/articlerender.fcgi?artid=311110&tool=pmcentrez&rendertype=abstract [Accessed July 13, 2011].
29. Schroeter J, Klaenhammer T (2009) Genomics of lactic acid bacteria. *FEMS Microbiol Lett* 292:1–6. Available at: http://www.ncbi.nlm.nih.gov/pubmed/19087207 [Accessed August 15, 2014].
30. Douillard FP, de Vos WM (2014) Functional genomics of lactic acid bacteria: from food to health. *Microb Cell Fact* 13:S8. Available at: http://www.microbialcellfactories.com/content/13/S1/S8 [Accessed September 2, 2014].
31. Makarova KS, Koonin E V (2007) Evolutionary genomics of lactic acid bacteria. *J Bacteriol* 189:1199–208. Available at: http://www.pubmedcentral.nih.gov/articlerender.fcgi?artid=1797341&tool=pmcentrez&rendertype=abstract [Accessed July 29, 2014].
32. Morelli L, Calleagri ML, Vogensen FK, von Wright A (2011) in *Lactic Acid Bacteria: Microbiological and Functional Aspects*, eds Salminen S, von Wright A, Lahtinen S, Ouwehand A (CRC Press, London), pp 17–37.. 4th Ed.
33. Bachmann H, Starrenburg MJC, Molenaar D, Kleerebezem M, van Hylckama Vlieg JET (2012) Microbial domestication signatures of *Lactococcus lactis* can be reproduced by experimental evolution. *Genome Res* 22:115–24. Available at: http://www.pubmedcentral.nih.gov/articlerender.fcgi?artid=3246198&tool=pmcentrez&rendertype=abstract [Accessed September 9, 2014].
34. Mendes-Soares H, Suzuki H, Hickey RJ, Forney LJ (2014) Comparative functional genomics of Lactobacillus spp. reveals possible mechanisms for specialization of vaginal lactobacilli to their environment. *J Bacteriol* 196:1458–1470.
35. De Vos WM (2011) Systems solutions by lactic acid bacteria: from paradigms to practice. *Microb Cell Fact* 10 Suppl 1:S2. Available at: http://www.pubmedcentral.nih.gov/articlerender.fcgi?artid=3231926&tool=pmcentrez&rendertype=abstract [Accessed August 12, 2014].
36. Claesson MJ et al. (2006) Multireplicon genome architecture of Lactobacillus salivarius. *Proc Natl Acad Sci U S A* 103:6718–23. Available at: http://www.pubmedcentral.nih.gov/articlerender.fcgi?artid=1436024&tool=pmcentrez&rendertype=abstract [Accessed September 11, 2014].
37. Siezen RJ et al. (2005) Complete sequences of four plasmids of *Lactococcus lactis* subsp. *cremoris* SK11 reveal extensive adaptation to the dairy environment. *Appl Environ Microbiol* 71:8371–8382.
38. Postma PW, Lengeler JW, Jacobson GR (1993) Phosphoenolpyruvate: carbohydrate phosphotransferase systems of bacteria. *Microbiol Rev* 57:543.
39. Carr FJ, Chill D, Maida N (2002) The lactic acid bacteria: a literature survey. *Crit Rev Microbiol* 28:281–370. Available at: http://www.ncbi.nlm.nih.gov/pubmed/12546196.
40. Thomas TD, Ellwood DC, Longyear VM (1979) Change from homo- to heterolactic fermentation by *Streptococcus lactis* resulting from glucose limitation in anaerobic chemostat cultures. *J Bacteriol* 138:109–17. Available at: http://www.pubmedcentral.nih.gov/articlerender.fcgi?artid=218245&tool=pmcentrez&rendertype=abstract.
41. Kandler O (1983) Carbohydrate metabolism in lactic acid bacteria. *Antonie Van Leeuwenhoek* 49:209–224.
42. Klein G, Pack a, Bonaparte C, Reuter G (1998) Taxonomy and physiology of probiotic lactic acid bacteria. *Int J Food Microbiol* 41:103–25. Available at: http://www.ncbi.nlm.nih.gov/pubmed/9704860.
43. Görke B, Stülke J (2008) Carbon catabolite repression in bacteria: many ways to make the most out of nutrients. *Nat Rev Microbiol* 6:613–24. Available at: http://www.ncbi.nlm.nih.gov/pubmed/18628769 [Accessed July 15, 2012].

44. Deutscher J, Francke C, Postma PW (2006) How phosphotransferase system-related protein phosphorylation regulates carbohydrate metabolism in bacteria. *Microbiol Mol Biol Rev* 70:939–1031. Available at: http://www.pubmedcentral.nih.gov/articlerender.fcgi?artid=1698508&tool=pmcentrez&rendertype=abstract [Accessed July 21, 2011].
45. Monod J (1942) Recherches sur la Croissance des Cultures Bactériennes. Dissertation (Hermann et Cie, Paris).
46. Titgemeyer F, Hillen W (2002) Global control of sugar metabolism: a Gram-positive solution. *Antonie Van Leeuwenhoek* 82:59–71. Available at: http://www.ncbi.nlm.nih.gov/pubmed/12369205.
47. Chopin A (1993) Organization and regulation of genes for amino acid biosynthesis in lactic acid bacteria. *FEMS Microbiol Rev* 12:21–37. Available at: http://www.ncbi.nlm.nih.gov/pubmed/8398216.
48. Kunji ERS, Mierau I, Hagting A, Poolman B, Konings WN (1996) The proteolytic systems of lactic acid bacteria. *Antonie Van Leeuwenhoek* 70:187–221. Available at: http://www.ncbi.nlm.nih.gov/pubmed/16628446.
49. Christensen JE, Dudley EG, Pederson J a, Steele JL (1999) Peptidases and amino acid catabolism in lactic acid bacteria. *Antonie Van Leeuwenhoek* 76:217–46. Available at: http://www.ncbi.nlm.nih.gov/pubmed/10532381.
50. Savijoki K, Ingmer H, Varmanen P (2006) Proteolytic systems of lactic acid bacteria. *Appl Microbiol Biotechnol* 71:394–406. Available at: http://www.ncbi.nlm.nih.gov/pubmed/16628446 [Accessed August 6, 2014].
51. Van de Guchte M et al. (2002) Stress responses in lactic acid bacteria. *Antonie Van Leeuwenhoek* 82:187–216. Available at: http://www.ncbi.nlm.nih.gov/pubmed/16961092.
52. Kuipers OP, Ruyter PGGA De, Kleerebezem M, Vos WM De (1998) Quorum sensing-controlled gene expression in lactic acid bacteria. *J Bacteriol* 64:15–21.
53. Kuipers OP, Beerthuyzen MM, de Ruyter PGG a., Luesink EJ, de Vos WM (1995) Autoregulation of Nisin Biosynthesis in *Lactococcus lactis* by Signal Transduction. *J Biol Chem* 270:27299–27304. Available at: http://www.jbc.org/cgi/doi/10.1074/jbc.270.45.27299 [Accessed September 7, 2014].
54. Kuipers OP, de Ruyter PG, Kleerebezem M, de Vos WM (1997) Controlled overproduction of proteins by lactic acid bacteria. *Trends Biotechnol* 15:135–40. Available at: http://www.ncbi.nlm.nih.gov/pubmed/9131833.
55. Ruyter PG De, Kuipers OP, de Vos WM (1996) Controlled gene expression systems for *Lactococcus lactis* with the food-grade inducer nisin. *Appl Environ Microbiol* 62:3662–3667.
56. Lopez de Felipe F, Kleerebezem M, de Vos WM, Hugenholtz J (1998) Cofactor engineering : a novel approach to metabolic engineering in *Lactococcus lactis* by controlled expression of NADH oxidase. *J Bacteriol* 180:3804–3808.
57. Hols P et al. (1999) Conversion of *Lactococcus lactis* from homolactic to homoalanine fermentation through metabolic engineering. *Nat Biotechnol* 17:588–92. Available at: http://www.ncbi.nlm.nih.gov/pubmed/10385325.
58. Hugenholtz J et al. (2000) *Lactococcus lactis* as a cell factory for high-level diacetyl production. *Appl Environ Microbiol* 66:4112–4114.
59. Sørvig E, Mathiesen G, Naterstad K, Eijsink VGH, Axelsson L (2005) High-level, inducible gene expression in Lactobacillus sakei and Lactobacillus plantarum using versatile expression vectors. *Microbiology* 151:2439–2449.
60. Mathiesen G, Sveen A, Piard J-C, Axelsson L, Eijsink VGH (2008) Heterologous protein secretion by Lactobacillus plantarum using homologous signal peptides. *J Appl Microbiol* 105:215–26. Available at: http://www.ncbi.nlm.nih.gov/pubmed/18298538 [Accessed September 17, 2014].
61. Nguyen T-T et al. (2011) A food-grade system for inducible gene expression in Lactobacillus plantarum using an alanine racemase-encoding selection marker. *J Agric Food Chem* 59:5617–24. Available at: http://www.ncbi.nlm.nih.gov/pubmed/21504147 [Accessed September 17, 2014].
62. Llull D, Poquet I (2004) New Expression System Tightly Controlled by Zinc Availability in *Lactococcus lactis* New Expression System Tightly Controlled by Zinc Availability in *Lactococcus lactis*. 70.
63. Diep DB, Mathiesen G, Eijsink VGH, Nes IF (2009) Use of lactobacilli and their pheromone-based regulatory mechanism in gene expression and drug delivery. *Curr Pharm Biotechnol* 10:62–73.
64. Peterbauer C, Maischberger T, Haltrich D (2011) Food-grade gene expression in lactic acid bacteria. *Biotechnol J* 6:1147–61. Available at: http://www.ncbi.nlm.nih.gov/pubmed/21858927 [Accessed August 27, 2014].
65. Hammer K, Mijakovic I, Jensen PR (2006) Synthetic promoter libraries--tuning of gene expression. *Trends Biotechnol* 24:53–5. Available at: http://www.ncbi.nlm.nih.gov/pubmed/16406119.
66. Dehli T, Solem C, Jensen PR (2012) Tunable promoters in synthetic and systems biology. *Subcell Biochem* 64:181–201. Available at: http://link.springer.com/10.1007/978-94-007-5055-5 [Accessed September 18, 2014].
67. Mijakovic I, Petranovic D, Jensen PR (2005) Tunable promoters in systems biology. *Curr Opin Biotechnol* 16:329–35. Available at: http://www.ncbi.nlm.nih.gov/pubmed/15961034 [Accessed September 18, 2014].
68. Jensen PR, Hammer K (1998) The Sequence of Spacers between the Consensus Sequences Modulates the Strength of Prokaryotic Promoters. *Microbiology* 64:82–87.
69. Jensen PR, Hammer K (1998) Artificial promoters for metabolic optimization. *Biotechnol Bioeng* 58:191–5. Available at: http://www.ncbi.nlm.nih.gov/pubmed/10191389.
70. Solem C, Jensen PR (2002) Modulation of Gene Expression Made Easy. *Appl Environ Microbiol* 68:2397–2403. Available at: http://aem.asm.org/cgi/doi/10.1128/AEM.68.5.2397-2403.2002 [Accessed January 24, 2012].
71. Koebmann B, Solem C, Jensen PR (2006) Control analysis of the importance of phosphoglycerate enolase for metabolic fluxes in *Lactococcus lactis* subsp. *lactis* IL1403. *IEE Proc - Syst Biol* 153:346–349. Available at: http://link.aip.org/link/IPSBDJ/v153/i5/p346/s1&Agg=doi [Accessed January 24, 2012].
72. Solem C, Koebmann B, Jensen PR (2008) Control analysis of the role of triosephosphate isomerase in glucose metabolism in *Lactococcus lactis*. *IET Syst Biol* 2:64–72. Available at: http://www.ncbi.nlm.nih.gov/pubmed/18397117 [Accessed January 24, 2012].

73. Solem C, Petranovic D, Koebmann B, Mijakovic I, Jensen PR (2010) Phosphoglycerate mutase is a highly efficient enzyme without flux control in *Lactococcus lactis*. *J Mol Microbiol Biotechnol* 18:174–80. Available at: http://www.ncbi.nlm.nih.gov/pubmed/20530968 [Accessed January 14, 2012].
74. Brøndsted L, Hammer K (1999) Use of the integration elements encoded by the temperate lactococcal bacteriophage TP901-1 to obtain chromosomal single-copy transcriptional fusions in *Lactococcus lactis*. *Appl Environ Microbiol* 65:752–758.
75. Christiansen B, Johnsen MG, Stenby E, Vogensen FK, Hammer K (1994) Characterization of the lactococcal temperate phage TP901-1 and its site-specific integration. *J Bacteriol* 176:1069–76. Available at: http://www.pubmedcentral.nih.gov/articlerender.fcgi?artid=205158&tool=pmcentrez&rendertype=abstract.
76. Breüner a, Brøndsted L, Hammer K (2001) Resolvase-like recombination performed by the TP901-1 integrase. *Microbiology* 147:2051–63. Available at: http://www.ncbi.nlm.nih.gov/pubmed/11495984.
77. Koebmann B, Solem C, Jensen PR (2005) Control analysis as a tool to understand the formation of the las operon in *Lactococcus lactis*. *FEBS J* 272:2292–303. Available at: http://www.ncbi.nlm.nih.gov/pubmed/15853813 [Accessed June 24, 2011].
78. Solem C, Koebmann BJ, Jensen PR (2003) Glyceraldehyde-3-phosphate dehydrogenase has no control over glycolytic flux in *Lactococcus lactis* MG1363. *J Bacteriol* 185:1564–1571. Available at: http://jb.asm.org/cgi/doi/10.1128/JB.185.5.1564-1571.2003 [Accessed September 27, 2014].
79. Koebmann BJ, Solem C, Pedersen MB, Nilsson D, Jensen PR (2002) Expression of Genes Encoding F1-ATPase Results in Uncoupling of Glycolysis from Biomass Production in *Lactococcus lactis*. *Appl Environ Microbiol* 68:4274–4282. Available at: http://aem.asm.org/cgi/doi/10.1128/AEM.68.9.4274-4282.2002 [Accessed January 24, 2012].
80. Koebmann BJ, Westerhoff H V, Snoep JL, Nilsson D, Jensen PR (2002) The Glycolytic Flux in *Escherichia coli* Is Controlled by the Demand for ATP. *J Bacteriol* 184:3909–3916. Available at: http://jb.asm.org/cgi/doi/10.1128/JB.184.14.3909-3916.2002 [Accessed January 24, 2012].
81. Koebmann B et al. (2002) The extent to which ATP demand controls the glycolytic flux depends strongly on the organism and conditions for growth. *Mol Biol* 29:41–5. Available at: http://www.springerlink.com/index/g1276wk2621hj62x.pdf [Accessed January 24, 2012].
82. Rud I, Jensen PR, Naterstad K, Axelsson L (2006) A synthetic promoter library for constitutive gene expression in Lactobacillus plantarum. *Microbiology* 152:1011–9. Available at: http://www.ncbi.nlm.nih.gov/pubmed/16549665 [Accessed September 18, 2014].
83. Otto R, de Vos WM, Gavrieli J (1982) Plasmid DNA in *Streptococcus cremoris* Wg2: influence of pH on selection in chemostats of a variant lacking a protease plasmid. *Appl Environ Mcrobiology* 43:1272–1277.
84. Leenhouts KJ, Kok JAN, Venema G (1991) Lactococcal plasmid pWVO1 as an integration vector for lactococci. *Appl Environ Microbiol* 57:2562–2567.
85. Maguin E, Duwat P, Hege T, Ehrlich D, Gruss A (1992) New thermosensitive plasmid for gram-positive bacteria. *J Bacteriol* 174:5633–8. Available at: http://www.pubmedcentral.nih.gov/articlerender.fcgi?artid=206509&tool=pmcentrez&rendertype=abstract.
86. Biswas I, Gruss A, Ehrlich SD, Maguin E (1993) High-efficiency gene inactivation and replacement system for gram-positive bacteria. *J Bacteriol* 175:3628–3635.
87. Leenhouts K, Venema G, Kok J (1998) A lactococcal pWV01-based integration toolbox for bacteria. 50:35–50.
88. Law J et al. (1995) A system to generate chromosomal mutations in *Lactococcus lactis* which allows fast analysis of targeted genes. *J Bacteriol* 177:7011–7018. Available at: http://www.pubmedcentral.nih.gov/articlerender.fcgi?artid=177576&tool=pmcentrez&rendertype=abstract [Accessed September 19, 2014].
89. Bourgeois P Le, Lautier M, Mata M, Ritzenthaler P, Le Bourgeois P (1992) New tools for the physical and genetic mapping of *Lactococcus* strains. *Gene* 111:109–14. Available at: http://www.ncbi.nlm.nih.gov/pubmed/1312498.
90. Solem C, Defoor E, Jensen PR, Martinussen J (2008) Plasmid pCS1966, a new selection/counterselection tool for lactic acid bacterium strain construction based on the oroP gene, encoding an orotate transporter from *Lactococcus lactis*. *Appl Environ Microbiol* 74:4772–5. Available at: http://www.pubmedcentral.nih.gov/articlerender.fcgi?artid=2519346&tool=pmcentrez&rendertype=abstract [Accessed September 6, 2011].
91. Pinto JPC et al. (2011) pSEUDO, a genetic integration standard for *Lactococcus lactis*. *Appl Environ Microbiol* 77:6687–90. Available at: http://www.pubmedcentral.nih.gov/articlerender.fcgi?artid=3187151&tool=pmcentrez&rendertype=abstract [Accessed September 18, 2012].
92. Goh YJ et al. (2009) Development and application of a upp-based counterselective gene replacement system for the study of the S-layer protein SlpX of Lactobacillus acidophilus NCFM. *Appl Environ Microbiol* 75:3093–105. Available at: http://www.pubmedcentral.nih.gov/articlerender.fcgi?artid=2681627&tool=pmcentrez&rendertype=abstract [Accessed September 11, 2014].
93. Douglas GL, Klaenhammer TR (2011) Directed chromosomal integration and expression of the reporter gene gusA3 in Lactobacillus acidophilus NCFM. *Appl Environ Microbiol* 77:7365–71. Available at: http://www.pubmedcentral.nih.gov/articlerender.fcgi?artid=3194874&tool=pmcentrez&rendertype=abstract [Accessed September 11, 2014].
94. Scott KP et al. (2000) Chromosomal integration of the green fluorescent protein gene in lactic acid bacteria and the survival of marked strains in human gut simulations. *FEMS Microbiol Lett* 182:23–27. Available at: http://doi.wiley.com/10.1111/j.1574-6968.2000.tb08867.x [Accessed September 19, 2014].

95. Low D et al. (1998) Role of *Streptococcus* thermophilus MR-1C capsular exopolysaccharide in cheese moisture retention? *Appl Environ Microbiol* 64:2147–2151.
96. Bhowmik T, Fernández L, Steele JL (1993) Gene replacement in Lactobacillus helveticus. *J Bacteriol* 175:6341–6344.
97. Frère J et al. (1998) A new theta-type thermosensitive replicon from Lactoccocus *lactis* as an integration vector for Enterococcus faecalis. *FEMS Microbiol Lett* 161:107–114.
98. Mills D a (2001) Mutagenesis in the post genomics era: tools for generating insertional mutations in the lactic acid bacteria. *Curr Opin Biotechnol* 12:503–9. Available at: http://www.ncbi.nlm.nih.gov/pubmed/11604329.
99. Lambert JM, Bongers RS, Kleerebezem M (2007) Cre-lox-based system for multiple gene deletions and selectable-marker removal in Lactobacillus plantarum. *Appl Environ Microbiol* 73:1126–35. Available at: http://www.pubmedcentral.nih.gov/articlerender.fcgi?artid=1828656&tool=pmcentrez&rendertype=abstract [Accessed September 22, 2014].
100. Petersen KV, Martinussen J, Jensen PR, Solem C (2013) Repetitive, marker-free, site-specific integration as a novel tool for multiple chromosomal integration of DNA. *Appl Environ Microbiol* 79:3563–9. Available at: http://www.pubmedcentral.nih.gov/articlerender.fcgi?artid=3675947&tool=pmcentrez&rendertype=abstract [Accessed September 11, 2014].
101. Alvarez MA, Herrero M, Suárez JE (1998) The site-specific recombination system of the Lactobacillus species bacteriophage A2 integrates in gram-positive and gram-negative bacteria. *Virology* 250:185–193.
102. Martin MC, Alonso JC, Suarez JE, Alvarez MA (2000) Generation of Food-Grade Recombinant Lactic Acid Bacterium Strains by Site-Specific Recombination. *Appl Environ Microbiol* 66:2599–2604. Available at: http://aem.asm.org/cgi/doi/10.1128/AEM.66.6.2599-2604.2000 [Accessed September 19, 2014].
103. Bruttin A, Foley S, Brüssow H (1997) The site-specific integration system of the temperate *Streptococcus* thermophilus bacteriophage phiSfi21. *Virology* 237:148–158.
104. Russell WM, Klaenhammer TR (2001) Efficient System for Directed Integration into the Lactobacillus acidophilus and Lactobacillus gasseri Chromosomes via Homologous Recombination. *Appl Environ Microbiol* 67:4361–4364. Available at: http://aem.asm.org/cgi/doi/10.1128/AEM.67.9.4361-4364.2001 [Accessed September 19, 2014].
105. Tsang P, Merritt J, Nguyen T, Shi W, Qi F (2005) Identification of genes associated with mutacin I production in *Streptococcus* mutans using random insertional mutagenesis. *Microbiology* 151:3947–55. Available at: http://www.ncbi.nlm.nih.gov/pubmed/16339939 [Accessed September 22, 2014].
106. Maguin E, Prévost H, Ehrlich SD, Gruss A (1996) Efficient insertional mutagenesis in lactococci and other Gram-positive bacteria. *J Bacteriol* 178:931–935.
107. Fernandez M, Kleerebezem M, Kuipers OP, Siezen RJ, van Kranenburg R (2002) Regulation of the metC-cysK Operon, Involved in Sulfur Metabolism in *Lactococcus lactis*. *J Bacteriol* 184:82–90. Available at: http://jb.asm.org/cgi/doi/10.1128/JB.184.1.82-90.2002 [Accessed September 6, 2013].
108. Nouaille S et al. (2004) Influence of lipoteichoic acid D-alanylation on protein secretion in *Lactococcus lactis* as revealed by random mutagenesis. *Appl Environ Microbiol* 70:1600–1607. Available at: http://aem.asm.org/cgi/doi/10.1128/AEM.70.3.1600-1607.2004 [Accessed September 22, 2014].
109. Licandro-Seraut H et al. (2012) Development of an efficient *In vivo* system (Pjunc-TpaseIS1223) for random transposon mutagenesis of Lactobacillus casei. *Appl Environ Microbiol* 78:5417–5423.
110. Perpetuini G et al. (2013) Identification of critical genes for growth in olive brine by transposon mutagenesis of Lactobacillus pentosus C11. *Appl Environ Microbiol* 79:4568–75. Available at: http://www.pubmedcentral.nih.gov/articlerender.fcgi?artid=3719503&tool=pmcentrez&rendertype=abstract [Accessed September 22, 2014].
111. Van Pijkeren J-P, Britton R a (2012) High efficiency recombineering in lactic acid bacteria. *Nucleic Acids Res* 40:e76. Available at: http://www.pubmedcentral.nih.gov/articlerender.fcgi?artid=3378904&tool=pmcentrez&rendertype=abstract [Accessed September 5, 2014].
112. Blais A, Dynlacht BD (2005) Constructing transcriptional regulatory networks. *Genes Dev* 19:1499–511. Available at: http://www.ncbi.nlm.nih.gov/pubmed/15998805 [Accessed June 17, 2011].
113. Zomer AL, Buist G, Larsen R, Kok J, Kuipers OP (2007) Time-resolved determination of the CcpA regulon of *Lactococcus lactis* subsp. *cremoris* MG1363. *J Bacteriol* 189:1366–81. Available at: http://www.pubmedcentral.nih.gov/articlerender.fcgi?artid=1797362&tool=pmcentrez&rendertype=abstract [Accessed November 10, 2011].
114. Zotta T et al. (2012) Inactivation of ccpA and aeration affect growth, metabolite production and stress tolerance in Lactobacillus plantarum WCFS1. *Int J Food Microbiol* 155:51–9. Available at: http://www.ncbi.nlm.nih.gov/pubmed/22326142 [Accessed September 22, 2014].
115. Guédon E, Sperandio B, Pons N, Ehrlich SD, Renault P (2005) Overall control of nitrogen metabolism in *Lactococcus lactis* by CodY, and possible models for CodY regulation in Firmicutes. *Microbiology* 151:3895–909. Available at: http://www.ncbi.nlm.nih.gov/pubmed/16339935 [Accessed November 9, 2011].
116. Den Hengst CD et al. (2005) Probing direct interactions between CodY and the oppD promoter of *Lactococcus lactis*. *J Bacteriol* 187:512–21. Available at: http://www.pubmedcentral.nih.gov/articlerender.fcgi?artid=543541&tool=pmcentrez&rendertype=abstract [Accessed January 24, 2012].
117. Petranovic D et al. (2004) Intracellular effectors regulating the activity of the *Lactococcus lactis* CodY pleiotropic transcription regulator. *Mol Microbiol* 53:613–21. Available at: http://www.ncbi.nlm.nih.gov/pubmed/15228538 [Accessed November 9, 2011].

118. Den Hengst CD et al. (2005) The *Lactococcus lactis* CodY regulon: identification of a conserved cis-regulatory element. *J Biol Chem* 280:34332–42. Available at: http://www.ncbi.nlm.nih.gov/pubmed/16040604 [Accessed September 23, 2014].
119. Magnani D, Barré O, Gerber SD, Solioz M (2008) Characterization of the CopR regulon of *Lactococcus lactis* IL1403. *J Bacteriol* 190:536–45. Available at: http://www.pubmedcentral.nih.gov/articlerender.fcgi?artid=2223693&tool=pmcentrez&rendertype=abstract [Accessed July 5, 2011].
120. Latorre M et al. (2014) Enterococcus faecalis reconfigures its transcriptional regulatory network activation at different copper levels. *Metallomics* 6:572–81. Available at: http://www.pubmedcentral.nih.gov/articlerender.fcgi?artid=4131723&tool=pmcentrez&rendertype=abstract [Accessed September 23, 2014].
121. Eckhardt TH, Skotnicka D, Kok J, Kuipers OP (2013) Transcriptional regulation of fatty acid biosynthesis in *Lactococcus lactis*. *J Bacteriol* 195:1081–9. Available at: http://www.pubmedcentral.nih.gov/articlerender.fcgi?artid=3571327&tool=pmcentrez&rendertype=abstract [Accessed September 6, 2013].
122. Larsen R, van Hijum S a FT, Martinussen J, Kuipers OP, Kok J (2008) Transcriptome analysis of the *Lactococcus lactis* ArgR and AhrC regulons. *Appl Environ Microbiol* 74:4768–71. Available at: http://www.pubmedcentral.nih.gov/articlerender.fcgi?artid=2519338&tool=pmcentrez&rendertype=abstract [Accessed September 23, 2014].
123. Riboulet-Bisson E et al. (2008) Characterization of the ers regulon of Enterococcus faecalis. *Infect Immun* 76:3064–3074.
124. Agustiandari H, Lubelski J, van den Berg van Saparoea HB, Kuipers OP, Driessen AJM (2008) LmrR is a transcriptional repressor of expression of the multidrug ABC transporter LmrCD in *Lactococcus lactis*. *J Bacteriol* 190:759–63. Available at: http://www.pubmedcentral.nih.gov/articlerender.fcgi?artid=2223683&tool=pmcentrez&rendertype=abstract [Accessed September 17, 2014].
125. Dressaire C et al. (2008) Growth rate regulated genes and their wide involvement in the *Lactococcus lactis* stress responses. *BMC Genomics* 9:343. Available at: http://www.pubmedcentral.nih.gov/articlerender.fcgi?artid=2526093&tool=pmcentrez&rendertype=abstract [Accessed September 23, 2013].
126. Lahtvee P-J et al. (2011) Multi-omics approach to study the growth efficiency and amino acid metabolism in *Lactococcus lactis* at various specific growth rates. *Microb Cell Fact* 10:12. Available at: http://www.pubmedcentral.nih.gov/articlerender.fcgi?artid=3049130&tool=pmcentrez&rendertype=abstract [Accessed March 2, 2012].
127. Li J, Bi Y, Dong C, Yang J, Liang W (2011) Transcriptome analysis of adaptive heat shock response of *Streptococcus* thermophilus. *PLoS One* 6:e25777. Available at: http://www.pubmedcentral.nih.gov/articlerender.fcgi?artid=3192767&tool=pmcentrez&rendertype=abstract [Accessed September 23, 2014].
128. Wels M, Overmars L, Francke C, Kleerebezem M, Siezen RJ (2011) Reconstruction of the regulatory network of Lactobacillus plantarum WCFS1 on basis of correlated gene expression and conserved regulatory motifs. *Microb Biotechnol* 4:333–44. Available at: http://www.pubmedcentral.nih.gov/articlerender.fcgi?artid=3818992&tool=pmcentrez&rendertype=abstract [Accessed September 23, 2014].
129. De Jong A, Hansen ME, Kuipers OP, Kilstrup M, Kok J (2013) The transcriptional and gene regulatory network of *Lactococcus lactis* MG1363 during growth in milk. *PLoS One* 8:e53085. Available at: http://www.pubmedcentral.nih.gov/articlerender.fcgi?artid=3547956&tool=pmcentrez&rendertype=abstract [Accessed September 11, 2014].
130. Rodionov DA (2007) Comparative genomic reconstruction of transcriptional regulatory networks in bacteria. *Chem Rev* 107:3467–97. Available at: http://www.pubmedcentral.nih.gov/articlerender.fcgi?artid=2643304&tool=pmcentrez&rendertype=abstract [Accessed September 8, 2014].
131. Ravcheev D a et al. (2013) Genomic reconstruction of transcriptional regulatory networks in lactic acid bacteria. *BMC Genomics* 14:94. Available at: http://www.pubmedcentral.nih.gov/articlerender.fcgi?artid=3616900&tool=pmcentrez&rendertype=abstract.
132. Novichkov PS et al. (2010) RegPrecise: a database of curated genomic inferences of transcriptional regulatory interactions in prokaryotes. *Nucleic Acids Res* 38:D111–8. Available at: http://www.pubmedcentral.nih.gov/articlerender.fcgi?artid=2808921&tool=pmcentrez&rendertype=abstract [Accessed August 7, 2012].
133. Thiele I, Palsson BØ (2010) A protocol for generating a high-quality genome-scale metabolic reconstruction. *Nat Protoc* 5:93–121. Available at: http://www.pubmedcentral.nih.gov/articlerender.fcgi?artid=3125167&tool=pmcentrez&rendertype=abstract [Accessed July 16, 2014].
134. Price ND, Reed JL, Palsson BØ (2004) Genome-scale models of microbial cells: evaluating the consequences of constraints. *Nat Rev Microbiol* 2:886–97. Available at: http://www.ncbi.nlm.nih.gov/pubmed/15494745 [Accessed July 11, 2014].
135. Lewis NE, Nagarajan H, Palsson BO (2012) Constraining the metabolic genotype–phenotype relationship using a phylogeny of in silico methods. *Nat Rev Micro* 10:291–305. Available at: http://dx.doi.org/10.1038/nrmicro2737.

136. Orth JD, Thiele I, Palsson BØ (2010) What is flux balance analysis? *Nat Biotechnol* 28:245–8. Available at: http://www.pubmedcentral.nih.gov/articlerender.fcgi?artid=3108565&tool=pmcentrez&rendertype=abstract [Accessed July 9, 2014].
137. Oberhardt MA, Palsson BØ, Papin JA (2009) Applications of genome-scale metabolic reconstructions. *Mol Syst Biol* 5:320. Available at: http://www.pubmedcentral.nih.gov/articlerender.fcgi?artid=2795471&tool=pmcentrez&rendertype=abstract [Accessed July 14, 2012].
138. Blazeck J, Alper H (2010) Systems metabolic engineering: genome-scale models and beyond. *Biotechnol J* 5:647–59. Available at: http://www.pubmedcentral.nih.gov/articlerender.fcgi?artid=2911524&tool=pmcentrez&rendertype=abstract [Accessed August 26, 2014].
139. Papp B, Notebaart R a, Pál C (2011) Systems-biology approaches for predicting genomic evolution. *Nat Rev Genet* 12:591–602. Available at: http://www.ncbi.nlm.nih.gov/pubmed/21808261 [Accessed July 11, 2014].
140. Oliveira AP, Nielsen J, Förster J (2005) Modeling *Lactococcus lactis* using a genome-scale flux model. *BMC Microbiol* 5:39. Available at: http://www.pubmedcentral.nih.gov/articlerender.fcgi?artid=1185544&tool=pmcentrez&rendertype=abstract [Accessed July 14, 2011].
141. Teusink B et al. (2006) Analysis of growth of Lactobacillus plantarum WCFS1 on a complex medium using a genome-scale metabolic model. *J Biol Chem* 281:40041–8. Available at: http://www.ncbi.nlm.nih.gov/pubmed/17062565 [Accessed September 4, 2011].
142. Pastink MI et al. (2009) Genome-scale model of *Streptococcus* thermophilus LMG18311 for metabolic comparison of lactic acid bacteria. *Appl Environ Microbiol* 75:3627–33. Available at: http://www.pubmedcentral.nih.gov/articlerender.fcgi?artid=2687286&tool=pmcentrez&rendertype=abstract [Accessed September 3, 2014].
143. Saulnier DM et al. (2011) Exploring metabolic pathway reconstruction and genome-wide expression profiling in Lactobacillus reuteri to define functional probiotic features. *PLoS One* 6:e18783. Available at: http://www.pubmedcentral.nih.gov/articlerender.fcgi?artid=3084715&tool=pmcentrez&rendertype=abstract [Accessed September 25, 2014].
144. Oddone GM, Mills D a, Block DE (2009) A dynamic, genome-scale flux model of *Lactococcus lactis* to increase specific recombinant protein expression. *Metab Eng* 11:367–81. Available at: http://www.ncbi.nlm.nih.gov/pubmed/19666133 [Accessed July 15, 2011].
145. Flahaut N a L et al. (2013) Genome-scale metabolic model for *Lactococcus lactis* MG1363 and its application to the analysis of flavour formation. *Appl Microbiol Biotechnol* 97:8729–39. Available at: http://www.ncbi.nlm.nih.gov/pubmed/23974365 [Accessed December 13, 2013].
146. Branco dos Santos F, de Vos WM, Teusink B, dos Santos FB (2013) Towards metagenome-scale models for industrial applications--the case of Lactic Acid Bacteria. *Curr Opin Biotechnol* 24:200–6. Available at: http://www.ncbi.nlm.nih.gov/pubmed/23200025 [Accessed August 9, 2014].
147. Smid EJ et al. (2005) Metabolic models for rational improvement of lactic acid bacteria as cell factories. *J Appl Microbiol* 98:1326–31. Available at: http://www.ncbi.nlm.nih.gov/pubmed/15916646 [Accessed January 14, 2012].
148. Van Niel EWJ, Palmfeldt J, Martin R, Paese M, Hahn-Hagerdal B (2004) Reappraisal of the regulation of Lactococcal L-lactate dehydrogenase. *Appl Environ Microbiol* 70:1843–1846. Available at: http://aem.asm.org/cgi/doi/10.1128/AEM.70.3.1843-1846.2004 [Accessed September 27, 2014].
149. Cao R, Zeidan A a, Rådström P, van Niel EWJ (2010) Inhibition kinetics of catabolic dehydrogenases by elevated moieties of ATP and ADP--implication for a new regulation mechanism in *Lactococcus lactis*. *FEBS J* 277:1843–52. Available at: http://www.ncbi.nlm.nih.gov/pubmed/20193044 [Accessed September 10, 2014].
150. Thomas TD (1976) Activator Specificity of pyruvate kinase from lactic Streptococci. *J Bacteriol* 125:1240–1242.
151. Veith N et al. (2013) Organism-adapted specificity of the allosteric regulation of pyruvate kinase in lactic acid bacteria. *PLoS Comput Biol* 9:e1003159. Available at: http://www.pubmedcentral.nih.gov/articlerender.fcgi?artid=3738050&tool=pmcentrez&rendertype=abstract [Accessed September 18, 2014].
152. Puri P, Goel A, Bochynska A, Poolman B (2014) Regulation of acetate kinase isozymes and its importance for mixed-acid fermentation in *Lactococcus lactis*. *J Bacteriol* 196:1386–93. Available at: http://www.ncbi.nlm.nih.gov/pubmed/24464460 [Accessed September 24, 2014].
153. Hoefnagel MHN et al. (2002) Metabolic engineering of lactic acid bacteria, the combined approach: kinetic modelling, metabolic control and experimental analysis. *Microbiology* 148:1003–13. Available at: http://www.ncbi.nlm.nih.gov/pubmed/11932446.
154. Hoefnagel MHN, van der Burgt A, Martens DE, Hugenholtz J, Snoep JL (2002) Time dependent response of glycolytic intermediates in a detailed glycolytic model of *Lactococcus lactis* during glucose run-out experiments. *Mol Biol Rep* 29:157–161.
155. Andersen AZ et al. (2009) The metabolic pH response in *Lactococcus lactis*: an integrative experimental and modelling approach. *Comput Biol Chem* 33:71–83. Available at: http://www.ncbi.nlm.nih.gov/pubmed/18829387 [Accessed August 16, 2011].
156. Levering J et al. (2012) Role of phosphate in the central metabolism of two lactic acid bacteria--a comparative systems biology approach. *FEBS J* 279:1274–90. Available at: http://www.ncbi.nlm.nih.gov/pubmed/22325620 [Accessed March 12, 2013].

157. Levering J, Kummer U, Becker K, Sahle S (2013) Glycolytic oscillations in a model of a lactic acid bacterium metabolism. *Biophys Chem* 172:53–60. Available at: http://www.ncbi.nlm.nih.gov/pubmed/23357412 [Accessed September 27, 2014].
158. Neves AR et al. (1999) *In vivo* nuclear magnetic resonance studies of glycolytic kinetics in *Lactococcus lactis*. *Biotechnol Bioeng* 64:200–12. Available at: http://www.ncbi.nlm.nih.gov/pubmed/10397856.
159. Voit E, Neves AR, Santos H (2006) The intricate side of systems biology. *Proc Natl Acad Sci U S A* 103:9452–7. Available at: http://www.pubmedcentral.nih.gov/articlerender.fcgi?artid=1480428&tool=pmcentrez&rendertype=abstract.
160. Voit EOO et al. (2006) Regulation of glycolysis in *Lactococcus lactis*: an unfinished systems biological case study. *IEE Proc - Syst Biol* 153:286. Available at: http://link.aip.org/link/IPSBDJ/v153/i4/p286/s1&Agg=doi [Accessed July 19, 2012].
161. Neves AR, Pool W a, Kok J, Kuipers OP, Santos H (2005) Overview on sugar metabolism and its control in *Lactococcus lactis* - the input from *in vivo* NMR. *FEMS Microbiol Rev* 29:531–54. Available at: http://www.ncbi.nlm.nih.gov/pubmed/15939503 [Accessed August 26, 2011].
162. Neves AR et al. (2002) Is the glycolytic flux in *Lactococcus lactis* primarily controlled by the redox charge? Kinetics of NAD(+) and NADH pools determined *in vivo* by 13C NMR. *J Biol Chem* 277:28088–98. Available at: http://www.ncbi.nlm.nih.gov/pubmed/12011086 [Accessed September 27, 2014].
163. Neves AR et al. (2002) Effect of Different NADH Oxidase Levels on Glucose Metabolism by *Lactococcus lactis*: Kinetics of Intracellular Metabolite Pools Determined by *In vivo* Nuclear Magnetic Resonance. *Appl Environ Microbiol* 68:6332–6342. Available at: http://aem.asm.org/cgi/doi/10.1128/AEM.68.12.6332-6342.2002 [Accessed July 12, 2012].
164. Teusink B, Bachmann H, Molenaar D (2011) Systems biology of lactic acid bacteria: a critical review. *Microb Cell Fact* 10:S11. Available at: http://www.microbialcellfactories.com/content/10/S1/S11 [Accessed September 22, 2011].
165. Hofmeyr JHS (2001) in *Proceedings of the 2nd International Conference on Systems Biology*, pp 291–300. Available at: http://www.siliconcell.net/sica/NWO-CLS/CellMath/OiOvoer/Hofmeyr_nutshell.pdf.
166. Cascante M et al. (2002) Metabolic control analysis in drug discovery and disease. *Nat Biotechnol* 20:243–249.
167. Fell DA (1998) Increasing the flux in metabolic pathways: A metabolic control analysis perspective. *Biotechnol Bioeng* 58:121–124. Available at: http://www.ncbi.nlm.nih.gov/pubmed/0010191380.
168. Rossell S, Solem C, Jensen PR, Heijnen JJ (2011) Towards a quantitative prediction of the fluxome from the proteome. *Metab Eng* 13:253–62. Available at: http://www.ncbi.nlm.nih.gov/pubmed/21296181 [Accessed September 26, 2014].
169. Rademaker JLW et al. (2007) Diversity analysis of dairy and nondairy *Lactococcus lactis* isolates, using a novel multilocus sequence analysis scheme and (GTG)5-PCR fingerprinting. *Appl Environ Microbiol* 73:7128–37. Available at: http://www.pubmedcentral.nih.gov/articlerender.fcgi?artid=2168189&tool=pmcentrez&rendertype=abstract [Accessed July 7, 2011].
170. Kelly WJ, Ward LJH, Leahy SC (2010) Chromosomal diversity in *Lactococcus lactis* and the origin of dairy starter cultures. *Genome Biol Evol* 2:729–44. Available at: http://www.pubmedcentral.nih.gov/articlerender.fcgi?artid=2962554&tool=pmcentrez&rendertype=abstract [Accessed August 23, 2011].
171. Chopin A, Chopin MC, Moillo-Batt A, Langella P (1984) Two plasmid-determined restriction and modification systems in *Streptococcus lactis*. *Plasmid* 11:260–263.
172. Tailliez P, Tremblay J, Ehrlich SD, Chopin A (1998) Molecular diversity and relationship within *Lactococcus lactis*, as revealed by randomly amplified polymorphic DNA (RAPD. *Systematic-and-Applied-Microbiology* 21:530–538. Available at: Tailliez, P: tailliez@diamant.jouy.inra.fr.
173. Gasson MJ (1983) Plasmid complements of *Streptococcus lactis* NCDO 712 and other lactic streptococci after protoplast-induced curing. *J Bacteriol* 154:1–9. Available at: http://www.pubmedcentral.nih.gov/articlerender.fcgi?artid=217423&tool=pmcentrez&rendertype=abstract.
174. Morello E et al. (2008) *Lactococcus lactis*, an efficient cell factory for recombinant protein production and secretion. *J Mol Microbiol Biotechnol* 14:48–58. Available at: http://www.ncbi.nlm.nih.gov/pubmed/17957110 [Accessed March 5, 2013].
175. Bahey-El-Din M, Gahan C, Griffin B (2010) *Lactococcus lactis* as a Cell Factory for Delivery of Therapeutic Proteins. *Curr Gene Ther* 10:34–45. Available at: http://www.eurekaselect.com/openurl/content.php?genre=article&issn=1566-5232&volume=10&issue=1&spage=34 [Accessed September 27, 2014].
176. Castro R et al. (2009) Characterization of the individual glucose uptake systems of *Lactococcus lactis*: mannose-PTS, cellobiose-PTS and the novel GlcU permease. *Mol Microbiol* 71:795–806. Available at: http://www.ncbi.nlm.nih.gov/pubmed/19054326 [Accessed January 14, 2012].
177. Cocaign-Bousquet M, Even S, Lindley ND, Loubière P (2002) Anaerobic sugar catabolism in *Lactococcus lactis*: genetic regulation and enzyme control over pathway flux. *Appl Microbiol Biotechnol* 60:24–32. Available at: http://www.ncbi.nlm.nih.gov/pubmed/12382039 [Accessed May 29, 2012].
178. Law J et al. (1995) A system to generate chromosomal mutations in *Lactococcus lactis* which allows fast analysis of targeted genes . A System To Generate Chromosomal Mutations in *Lactococcus lactis* Which Allows Fast Analysis of Targeted Genes. *Microbiology* 177:7011–18.

179. Palmfeldt J, Levander F, Hahn-Hägerdal B, James P (2004) Acidic proteome of growing and resting *Lactococcus lactis* metabolizing maltose. *Proteomics* 4:3881–98. Available at: http://www.ncbi.nlm.nih.gov/pubmed/15540167 [Accessed April 1, 2012].
180. Nilsson U, Radstrom P (2001) Genetic localization and regulation of the maltose phosphorylase gene, malP, in *Lactococcus lactis*. *Microbiology* 147:1565–1573.
181. Qian NY, Stanley GA, Hahn-Hagerdal B, Radstrom P (1994) Purification and characterization of two phosphoglucomutases from *Lactococcus lactis* subsp . *lactis* and their regulation in maltose- and glucose-utilizing cells. *J Bacteriol* 176:5304–5311.
182. Wegmann U et al. (2007) Complete genome sequence of the prototype lactic acid bacterium *Lactococcus lactis* subsp. *cremoris* MG1363. *J Bacteriol* 189:3256–70. Available at: http://www.pubmedcentral.nih.gov/articlerender.fcgi?artid=1855848&tool=pmcentrez&rendertype=abstract [Accessed June 14, 2011].
183. Linares DM, Kok J, Poolman B (2010) Genome sequences of *Lactococcus lactis* MG1363 (revised) and NZ9000 and comparative physiological studies. *J Bacteriol* 192:5806–12. Available at: http://www.pubmedcentral.nih.gov/articlerender.fcgi?artid=2953693&tool=pmcentrez&rendertype=abstract [Accessed July 10, 2011].
184. Puri P (2014) On the regulation of the metabolic shift and protein synthesis in *Lactococcus lactis*. Ph.D thesis, University of Groningen.
185. Jing Jing Ye, Reizer J, Cui X, Saier MH (1994) Inhibition of the phosphoenolpyruvate:lactose phosphotransferase system and activation of a cytoplasmic sugar-phosphate phosphatase in *Lactococcus lactis* by ATP-dependent metabolite-activated phosphorylation of serine 46 in the phosphocarrier protein HPr. *J Biol Chem* 269:11837–11844.
186. Guédon E, Jamet E, Renault P (2002) Gene regulation in *Lactococcus lactis*: the gap between predicted and characterized regulators. *Antonie Van Leeuwenhoek* 82:93–112. Available at: http://www.ncbi.nlm.nih.gov/pubmed/12369207.
187. Henkin TM (1996) The role of the CcpA transcriptional regulator in carbon metabolism in Bacillus subtilis. *FEMS Microbiol Lett* 135:9–15. Available at: http://dx.doi.org/10.1111/j.1574-6968.1996.tb07959.x.
188. Luesink EJ, van Herpen RE, Grossiord BP, Kuipers OP, de Vos WM (1998) Transcriptional activation of the glycolytic las operon and catabolite repression of the gal operon in *Lactococcus lactis* are mediated by the catabolite control protein CcpA. *Mol Microbiol* 30:789–98. Available at: http://www.ncbi.nlm.nih.gov/pubmed/10094627.
189. Poolman B, Bosman B, Kiers J, Konings WN (1987) Control of glycolysis by glyceraldehyde-3-phosphate dehydrogenase in *Streptococcus cremoris* and *Streptococcus lactis*. *J Bacteriol* 169:5887–5890.
190. Even S, Garrigues C, Loubiere P, Lindley ND, Cocaign-Bousquet M (1999) Pyruvate metabolism in *Lactococcus lactis* is dependent upon glyceraldehyde-3-phosphate dehydrogenase activity. *Metab Eng* 1:198–205. Available at: http://www.ncbi.nlm.nih.gov/pubmed/10937934.
191. Andersen HW, Pedersen MB, Hammer K, Jensen PR (2001) Lactate dehydrogenase has no control on lactate production but has a strong negative control on formate production in *Lactococcus lactis*. *Eur J Biochem* 268:6379–6389. Available at: http://www.ncbi.nlm.nih.gov/pubmed/11737192.
192. Andersen HW, Solem C, Hammer K, Jensen PR (2001) Twofold reduction of phosphofructokinase activity in *Lactococcus lactis* results in strong decreases in growth rate and in glycolytic flux. *J Bacteriol* 183:3458–67. Available at: http://www.pubmedcentral.nih.gov/articlerender.fcgi?artid=99644&tool=pmcentrez&rendertype=abstract [Accessed January 24, 2012].
193. Koebmann BJ, Andersen HW, Solem C, Jensen PR (2002) Experimental determination of control of glycolysis in *Lactococcus lactis*. 237–248.
194. Ter Kuile BH, Westerhoff H V (2001) Transcriptome meets metabolome: hierarchical and metabolic regulation of the glycolytic pathway. *FEBS Lett* 500:169–71. Available at: http://www.ncbi.nlm.nih.gov/pubmed/11445079.
195. Rossell S et al. (2006) Unraveling the complexity of flux regulation: a new method demonstrated for nutrient starvation in Saccharomyces cerevisiae. *Proc Natl Acad Sci U S A* 103:2166–71. Available at: http://www.pubmedcentral.nih.gov/articlerender.fcgi?artid=1413710&tool=pmcentrez&rendertype=abstract.
196. Even S, Lindley ND, Cocaign-Bousquet M (2003) Transcriptional, translational and metabolic regulation of glycolysis in *Lactococcus lactis* subsp. *cremoris* MG 1363 grown in continuous acidic cultures. *Microbiology* 149:1935–1944. Available at: http://mic.sgmjournals.org/cgi/doi/10.1099/mic.0.26146-0 [Accessed October 7, 2014].
197. Thompson J (1987) Regulation of sugar transport and metabolism in lactic acid bacteria. *FEMS Microbiol Lett* 46:221–231. Available at: http://www.sciencedirect.com/science/article/pii/0378109787901091.
198. Garrigues C, Loubiere P, Lindley ND, Cocaign-Bousquet M (1997) Control of the shift from homolactic acid to mixed-acid fermentation in *Lactococcus lactis*: predominant role of the NADH/NAD^+ ratio. *J Bacteriol* 179:5282–5287. Available at: http://www.pubmedcentral.nih.gov/articlerender.fcgi?artid=179393&tool=pmcentrez&rendertype=abstract.
199. Garrigues C, Mercade M, Cocaign-Bousquet M, Lindley ND, Loubiere P (2001) Regulation of pyruvate metabolism in *Lactococcus lactis* depends on the imbalance between catabolism and anabolism. *Biotechnol Bioeng* 74:108–15. Available at: http://www.ncbi.nlm.nih.gov/pubmed/11369999.
200. Teusink B, Walsh MC, van Dam K, Westerhoff H V (1998) The danger of metabolic pathways with turbo design. *Trends Biochem Sci* 23:162–169.
201. Collins LB, Terence D, Thomas TD (1974) Pyruvate kinase of *Streptococcus lactis*. *J Bacteriol* 120:52–8. Available at: http://www.pubmedcentral.nih.gov/articlerender.fcgi?artid=245729&tool=pmcentrez&rendertype=abstract.

202. Fordyce AM, Moore CH, Pritchard GG (1982) Phosphofructokinase from *Streptococcus lactis*. *Methods Enzymol* 90:77–82.
203. Cocaign-bousquet M, Garrigues C, Loubiere P, Lindley ND (1996) Physiology of pyruvate metabolism in *Lactococcus lactis*. *Antonie Van Leeuwenhoek* 70:253–267.
204. Crow VL, Pritchard GG (1977) Fructose 1,6-diphosphate-activated L-lactate dehydrogenase from *Streptococcus lactis*: kinetic properties and factors affecting activation. *J Bacteriol* 131:82–91. Available at: http://www.pubmedcentral.nih.gov/articlerender.fcgi?artid=235394&tool=pmcentrez&rendertype=abstract.
205. Nordkvist M, Jensen NBS, Villadsen J (2003) Glucose metabolism in *Lactococcus lactis* MG1363 under different aeration conditions: requirement of acetate to sustain growth under microaerobic conditions. *Appl Environ Microbiol* 69:3462–3468. Available at: http://aem.asm.org/cgi/doi/10.1128/AEM.69.6.3462-3468.2003 [Accessed August 13, 2014].
206. Jensen NB, Melchiorsen CR, Jokumsen KV, Villadsen J (2001) Metabolic behavior of *Lactococcus lactis* MG1363 in microaerobic continuous cultivation at a low dilution rate. *Appl Environ Microbiol* 67:2677–82. Available at: http://www.pubmedcentral.nih.gov/articlerender.fcgi?artid=92924&tool=pmcentrez&rendertype=abstract [Accessed January 24, 2012].
207. Even S, Lindley ND, Cocaign-Bousquet M (2001) Molecular physiology of sugar catabolism in *Lactococcus lactis* IL1403. *J Bacteriol* 183:3817–24. Available at: http://www.pubmedcentral.nih.gov/articlerender.fcgi?artid=95262&tool=pmcentrez&rendertype=abstract [Accessed January 24, 2012].
208. Melchiorsen CR, Jensen NBS, Christensen B, Jokumsen KV, Villadsen J (2001) Dynamics of pyruvate metabolism in *Lactococcus lactis*. *Biotechnol Bioeng* 74:271–279. Available at: http://www.ncbi.nlm.nih.gov/pubmed/11410851.
209. Bongers RS et al. (2003) IS981-mediated adaptive evolution recovers lactate production by *ldhb* transcription activation in a lactate dehydrogenase-deficient strain of *Lactococcus lactis*. *J Bacteriol* 185:4499–4507. Available at: http://jb.asm.org/cgi/doi/10.1128/JB.185.15.4499-4507.2003 [Accessed October 12, 2014].
210. Gaspar P et al. (2007) The lactate dehydrogenases encoded by the *ldh* and *ldhB* genes in *Lactococcus lactis* exhibit distinct regulation and catalytic properties - comparative modeling to probe the molecular basis. *FEBS J* 274:5924–36. Available at: http://www.ncbi.nlm.nih.gov/pubmed/17944947 [Accessed October 12, 2014].
211. Thomas TD, Turner KW, Crow VL (1980) Galactose fermentation by *Streptococcus lactis* and *Streptococcus cremoris*: pathways, products, and regulation. *J Bacteriol* 144:672–682.
212. Sjoberg A, Hahn-Hagerdal B (1989) β-Glucose-1-phosphate, a possible mediator for polysaccharide formation in maltose-assimilating *Lactococcus lactis*. *Appl Environ Microbiol* 55:1549–1554.
213. Melchiorsen CR et al. (2000) Synthesis and posttranslational regulation of pyruvate formate-lyase in *Lactococcus lactis*. *J Bacteriol* 182:4783–4788. Available at: http://jb.asm.org/cgi/doi/10.1128/JB.182.17.4783-4788.2000 [Accessed September 29, 2013].
214. Arnau J, Jørgensen F, Madsen SM, Vrang A, Hørsholm D- (1997) Cloning , Expression , and Characterization of the *Lactococcus lactis pfl* Gene, Encoding Pyruvate Formate-Lyase. *Microbiology* 179:5884–5891.
215. Sawers G (1993) Specific transcriptional requirements for positive regulation of the anaerobically inducible *pfl* operon by ArcA and FNR. *Mol Microbiol* 10:737–747.
216. Gostick DO et al. (1999) Two operons that encode FNR-like proteins in *Lactococcus lactis*. *Mol Microbiol* 31:1523–35. Available at: http://www.ncbi.nlm.nih.gov/pubmed/10200970.
217. Scott C, Guest JR, Green J (2000) Characterization of the *Lactococcus lactis* transcription factor FlpA and demonstration of an *in vitro* switch. *Mol Microbiol* 35:1383–93. Available at: http://www.ncbi.nlm.nih.gov/pubmed/10760139.
218. Snoep JL et al. (1993) Differences in sensitivity to NADH of purified pyruvate dehydrogenase complexes of Enterococcus faecalis , *Lactococcus lactis* , Azotobacter t ; inelandii and *Escherichia coli* : Implications for their activity *in vivo*. *FEMS Microbiol Lett* 114:279–284. Available at: http://www.ncbi.nlm.nih.gov/pubmed/8288104.
219. Snoep JL, Teixeira de Mattos MJ, Starrenburg MJ, Hugenholtz J (1992) Isolation, characterization, and physiological role of the pyruvate dehydrogenase complex and alpha-acetolactate synthase of *Lactococcus lactis* subsp. *lactis* bv. *diacetylactis*. *J Bacteriol* 174:4838–41. Available at: http://www.pubmedcentral.nih.gov/articlerender.fcgi?artid=206284&tool=pmcentrez&rendertype=abstract.
220. Snoep JL, van Bommel M, Lubbers F, de Mattos MJT, Neijssel OM (1993) The role of lipoic acid in product formation by Enterococcus faecalis NCTC 775 and reconstitution *in vivo* and *in vitro* of the pyruvate dehydrogenase complex. *J Gen Microbiol* 139:1325–1329.
221. Lopez de Felipe F, Gaudu P (2009) Multiple control of the acetate pathway in *Lactococcus lactis* under aeration by catabolite repression and metabolites. *Appl Microbiol Biotechnol* 82:1115–22. Available at: http://www.ncbi.nlm.nih.gov/pubmed/19214497 [Accessed September 29, 2013].
222. Hugenholtz J (1993) Citrate metabolism in lactic acid bacteria. *FEMS Microbiol Rev* 12:165–178. Available at: http://doi.wiley.com/10.1016/0168-6445(93)90062-E.
223. Pudlik AM, Lolkema JS (2011) Citrate uptake in exchange with intermediates in the citrate metabolic pathway in *Lactococcus lactis* IL1403. *J Bacteriol* 193:706–14. Available at: http://www.pubmedcentral.nih.gov/articlerender.fcgi?artid=3021216&tool=pmcentrez&rendertype=abstract [Accessed October 12, 2011].
224. Lopez de Felipe F, Starrenburg MJC, Hugenholtz J (1997) The role of NADH-oxidation in acetoin and diacetyl production from glucose in *Lactococcus lactis* subsp. *lactis* MG1363. *FEMS Microbiol Lett* 156:15–19.
225. Duwat P et al. (2001) Respiration capacity of the fermenting bacterium *Lactococcus lactis* and its positive effects on growth and survival. *J Bacteriol* 183:4509–4516.

226. Monnet C, Schmitt PP, Divies C (1994) Comparison of alpha-acetolactate synthase and alpha-acetolactate decarboxylase in *Lactococcus* spp. and Leuconostoc spp. *Biotechnol Lett* 16:257–262.
227. Gibson TD, Parker SM, Woodward JR (1991) Purification and characterization of diacetyl reductase from chicken liver and *Streptococcus lactis* and enzymic determination of diacetyl and diketones. *Enzyme Microb Technol* 13:171–178.
228. Goupil-Feuillerat N, Cocaign-Bousquet M, Godon J-J, Ehrlich SD, Renault P (1997) Dual role of alpha-acetolactate decarboxylase in *Lactococcus lactis* subsp . *lactis*. *J Bacteriol* 179:6285–6293.
229. Goupil-Feuillerat N, Corthier G, Godon J-J, Ehrlich SD, Renault P (2000) Transcriptional and translational regulation of α-acetolactate decarboxylase of *Lactococcus lactis* subsp . *lactis*. *J Bacteriol* 182:5399–5408.
230. Pedersen MB et al. (2008) Impact of aeration and heme-activated respiration on *Lactococcus lactis* gene expression: identification of a heme-responsive operon. *J Bacteriol* 190:4903–11. Available at: http://www.pubmedcentral.nih.gov/articlerender.fcgi?artid=2447008&tool=pmcentrez&rendertype=abstract [Accessed September 6, 2011].
231. Koebmann B et al. (2008) Increased biomass yield of *Lactococcus lactis* during energetically limited growth and respiratory conditions. *Biotechnol Appl Biochem* 50:25–33. Available at: http://www.ncbi.nlm.nih.gov/pubmed/17824842 [Accessed September 19, 2013].
232. Sijpesteijn AK (1970) Induction of cytochrome formation and stimulation of oxidative dissimilation by hemin in *Streptococcus lactis* and Leuconostoc mesenteroides. *Antonie Van Leeuwenhoek* 36:335–348.
233. Vido K et al. (2004) Proteome analyses of heme-dependent respiration in *Lactococcus lactis*: involvement of the proteolytic system. *J Bacteriol* 186:1648–1657. Available at: http://jb.asm.org/cgi/doi/10.1128/JB.186.6.1648-1657.2004 [Accessed October 12, 2014].
234. Vemuri GN, Altman E, Sangurdekar DP, Khodursky AB, Eiteman MA (2006) Overflow metabolism in *Escherichia coli* during steady-state growth: transcriptional regulation and effect of the redox ratio. *Appl Environ Microbiol* 72:3653–3661. Available at: http://www.pubmedcentral.nih.gov/articlerender.fcgi?artid=1472329&tool=pmcentrez&rendertype=abstract [Accessed November 28, 2013].
235. Russell JB (2007) The energy spilling reactions of bacteria and other organisms. *J Mol Microbiol Biotechnol* 13:1–11. Available at: http://www.ncbi.nlm.nih.gov/pubmed/17693707 [Accessed May 29, 2013].
236. De Deken RH (1966) The Crabtree effect: a regulatory system in yeast. *J Gen Microbiol* 44:149–156.
237. Van Dijken JP, Weusthuis RA, Pronk JT (1993) Kinetics of growth and sugar consumption in yeasts. *Antonie Van Leeuwenhoek* 63:343–352.
238. Vander Heiden MG, Cantley LC, Thompson CB (2009) Understanding the Warburg effect: the metabolic requirements of cell proliferation. *Science* 324:1029–1033.
239. Melchiorsen CR, Jokumsen KV, Villadsen J, Israelsen H, Arnau J (2002) The level of pyruvate-formate lyase controls the shift from homolactic to mixed-acid product formation in *Lactococcus lactis*. *Appl Microbiol Biotechnol* 58:338–44. Available at: http://www.ncbi.nlm.nih.gov/pubmed/11935185 [Accessed November 11, 2011].
240. Solem C, Koebmann B, Yang F, Jensen PR (2007) The las enzymes control pyruvate metabolism in *Lactococcus lactis* during growth on maltose. *J Bacteriol* 189:6727–30. Available at: http://www.pubmedcentral.nih.gov/articlerender.fcgi?artid=2045170&tool=pmcentrez&rendertype=abstract [Accessed September 6, 2011].
241. Takahashi S, Abbe K, Yamada T (1982) Purification of pyruvate formate-lyase from *Streptococcus* mutans and its regulatory properties. *J Bacteriol* 149:1034–1040. Available at: http://www.pubmedcentral.nih.gov/articlerender.fcgi?artid=216493&tool=pmcentrez&rendertype=abstract.
242. Palmfeldt J, Paese M, Hahn-Hägerdal B, Van Niel EWJ (2004) The pool of ADP and ATP regulates anaerobic product formation in resting cells of *Lactococcus lactis*. *Appl Environ Microbiol* 70:5477–84. Available at: http://www.pubmedcentral.nih.gov/articlerender.fcgi?artid=520924&tool=pmcentrez&rendertype=abstract [Accessed June 15, 2012].
243. Gale EF, Folkes JP (1953) The assimilation of amino-acids by bacteria. 15. Actions of antibiotics on nucleic acid and protein synthesis in Staphylococcus aureus. *Biochem J* 53:493.
244. Hofvendahl K, van Niel EWJ, Hahn-Hägerdal B (1999) Effect of temperature and pH on growth and product formation of *Lactococcus lactis* ssp . *lactis* ATCC 19435 growing on maltose. *Appl Environ Microbiol* 51:669–672.
245. Molenaar D, van Berlo R, de Ridder D, Teusink B (2009) Shifts in growth strategies reflect tradeoffs in cellular economics. *Mol Syst Biol* 5:323. Available at: http://www.pubmedcentral.nih.gov/articlerender.fcgi?artid=2795476&tool=pmcentrez&rendertype=abstract [Accessed July 18, 2012].
246. Van Hoek MJA, Merks RMH (2012) Redox balance is key to explaining full vs. partial switching to low-yield metabolism. *BMC Syst Biol* 6:22. Available at: http://www.pubmedcentral.nih.gov/articlerender.fcgi?artid=3384451&tool=pmcentrez&rendertype=abstract [Accessed March 7, 2013].
247. Pfeiffer T, Schuster S (2005) Game-theoretical approaches to studying the evolution of biochemical systems. *Trends Biochem Sci* 30:20–5. Available at: http://www.ncbi.nlm.nih.gov/pubmed/15653322 [Accessed April 28, 2014].
248. Schuster S, Pfeiffer T, Fell D a (2008) Is maximization of molar yield in metabolic networks favoured by evolution? *J Theor Biol* 252:497–504. Available at: http://www.ncbi.nlm.nih.gov/pubmed/18249414 [Accessed March 22, 2014].

249. Schuster S, de Figueiredo LF, Schroeter A, Kaleta C (2011) Combining Metabolic Pathway Analysis with Evolutionary Game Theory. Explaining the occurrence of low-yield pathways by an analytic optimization approach. *Biosystems* 105:147–153. Available at: http://www.sciencedirect.com/science/article/pii/S0303264711000876.
250. Castillo Martinez FA, Balciunas EM, Salgado JM, Domínguez González JM, Converti A, de Souza Oliveira RP. (2013) Lactic acid properties, applications and production: A review. *Trends Food Sci Technol* 30:70–83.

Chapter 2. Transcriptional activity of mixed-acid genes

2.1 Introduction

Many strains of *Lactococcus lactis* (*L. lactis*), including both subsp. *cremoris* and subsp. *lactis*, have been found to exhibit a metabolic shift from homolactic to mixed-acid fermentation when transiting from a fast fermentable sugar to one that is more slowly fermentable. In the former fermentation mode lactate is the main product whereas in the latter mode significant amounts of formate, acetate and ethanol are also produced. Table 2.1 summarizes the ability to exhibit a shift in fermentation mode for different strains that have been studied in the past. Most of the studied strains were found to exhibit the shift but two strains, *L. lactis* subsp. *lactis* ML8 and the widely studied laboratory strain *L. lactis* subsp. *lactis* IL1403, appeared to be unable to shift, though there has once been a study reporting the mixed-acid fermenting behavior of IL1403 when growing on maltose [1].

In this study, IL1403 and another extensively studied strain *L. lactis* subsp. *cremoris* MG1363, which exhibits the mixed-acid shift, were compared with respect to growth physiology, relative transcriptional activities of mixed-acid genes and elements of transcription regulation.

Table 2.1. Phenotype of *L. lactis* strains regarding shift in fermentation mode.

Subspecies	Strain	Shift to mixed-acid fermentation at low sugar uptake rates	Ref.
lactis	ML_3	Yes	[2, 3]
lactis	7962	Yes	[2]
lactis	ML_8	No	[2]
cremoris	E_8	Yes	[2]
cremoris	HP	Yes	[2]
lactis	65.1	Yes	[4, 5]
lactis	NCDO 2118	Yes	[6]
lactis	ATCC 19435	Yes	[7]
*cremoris**	MG1363	Yes	[8]
lactis	IL1403	No	[9]

*MG1363 is known to have *cremoris* genotype but *lactis* phenotype.

2.2 Materials and methods

2.2.1 Bacteria strains and plasmids

The two *L. lactis* strains, IL1403 and MG1363, were plasmid-free derivatives of *L. lactis* CNRZ157 (or IL594) [10] and *L. lactis* NCDO712 [11] respectively. Other *L. lactis* strains used were derived from the two strains. The plasmids pLB65 expressing the T901-1 integrase was used for mediating the site-specific integration into the chromosomal attachment site, *attB*, of pLB85, which contains a promoterless *gusA* reporter gene and a gene encoding erythromycin resistance [12]. *E. coli* ABLE-K (Stratagene) [13] was used for cloning purposes. Primers, plasmids and strains used or constructed in this study are listed in Table 2.2, Table 2.3 and Table 2.4 respectively.

Table 2.2. Primers used in the study.

Primer	RS	Amplified region	Sequence
3f	SpeI	upstream region of *pfl* in IL1403	atcgaactagtTGAGAGAAGATGATGAAGAC
3r	SalI		atcgagtcgacTTAATGTTCAAAGATATTTTCCGT
4f	XbaI	upstream region of *adhE* in IL1403	atcgatctagaTGGCTGGACAAATACTGA
4r	PstI		atcgactgcagTTAAGCGGCTTTTTTAGTTG
5f	XbaI	upstream region of *eutD* in IL1403	atcgatctagaTTGTTGATACAGATGACGA
5r	PstI		atcgactgcagTTACAGTGATTCAAAAAGTTCC
6f	XbaI	upstream region of *ackA1* in IL1403	atcgatctagaTTTTGCCATTTTCCTAGCTC
6r	PstI		atcgactgcagTTATGAACCAGCGTTAACTG
7f	XbaI	upstream region of *ackA2* in IL1403	atcgatctagaGAGATGTATGTTGACCGA
7r	PstI		atcgactgcagTTATTTTAATGACGAGGAGCC
8f	XbaI	upstream region of *pfl* in MG1363	atcgatctagaCCTCAGCAACATTTGTTC
8r	PstI		atcgactgcagTTATTTAAAACCATCCCAAGC
9f	SpeI	upstream region of *adhE* in MG1363	atcgaactagtGGTCATATTCCACGCGAT
9r	SalI		atcgagtcgacTTATGGAGCGGCTTTTTTAGTT
10f	SpeI	upstream region of *eutD* in MG1363	atcgaactagtAGATATTGAGGAAAGAGGAAG
10r	PstI		atcgactgcagTTACAGTGATTCAAAAAGTTCCA
11f	XbaI	upstream region of *ackA1* in MG1363	atcgatctagaGAGGATTTACTGACAAGTG
11r	PstI		atcgactgcagttaTGATGAACCAGCGTTTAC
12f	XbaI	upstream region of *ackA2* in MG1363	atcgatctagaTGAGATGTATGTTGACCG
12r	PstI		atcgactgcagttaTAATGATGAGGAGCCTG
CSO50	BamHI	verify chromosomal integration of pLB85	ggaaggatccCCCATAGTTCATCAGTTATC
CSO263	/		CGCGATCCAGACTGAATG

Each amplified region includes a short coding sequence (CDS) (20 – 50 bp) from the gene and a stop codon.

RS, restriction site.

Table 2.3. Plasmid used or constructed in the study.

Plasmid	Description	Antibiotic resistance
pLB65 [12]	Containing *orf1* expressing phage TP901-1 integrase	Cam
pLB85 [12]	Reporter vector containing a promoterless *gusA* gene and an *attP* site for integration into *attB* site on chromosomes in the presence of the TP901-1 integrase	Amp, Erm
pLB85-IL*pfl*	pLB85 containing *pfl* upstream region of IL1403 obtained with primer 3f, 3r	
pLB85-IL*adhE*	pLB85 containing *adhE* upstream region of IL1403 obtained with primer 4f, 4r	
pLB85-IL*eutD*	pLB85 containing *eutD* upstream region of IL1403 obtained with primer 5f, 5r	
pLB85-IL*ackA1*	pLB85 containing *ackA1* upstream region of IL1403 obtained with primer 6f, 6r	
pLB85-IL*ackA2*	pLB85 containing *ackA2* upstream region of IL1403 obtained with primer 7f, 7r	
pLB85-MG*pfl*	pLB85 containing *pfl* upstream region of MG1363 obtained with primer 8f, 8r	
pLB85-MG*adhE*	pLB85 containing *adhE* upstream region of MG1363 obtained with primer 9f, 9r	
pLB85-MG*eutD*	pLB85 containing *eutD* upstream region of MG1363 obtained with primer 10f, 10r	
pLB85-MG*ackA1*	pLB85 containing *ackA1* upstream region of MG1363 obtained with primer 11f, 11r	
pLB85-MG*ackA2*	pLB85 containing *ackA2* upstream region of MG1363 obtained with primer 12f, 12r	

Cam, chloramphenicol; Amp, ampicillin; Erm, erythromycin.

Table 2.4. Strains used or constructed in the study.

Strain	Description
IL1403 [10]	A plasmid-free strain derived from *L. lactis* subsp. *lactis* biovar *diacetylactis* CNRZ157
SC072	IL1403 containing pLB65
SC072/IL*pfl*	SCO72 with pLB85-IL*pfl* integrated
SC072/IL*eutD*	SCO72 with pLB85-IL*eutD* integrated
SC072/IL*ackA1*	SCO72 with pLB85-IL*ackA1* integrated
SC072/IL*ackA2*	SCO72 with pLB85-IL*ackA2* integrated
SC072/MG*pfl*	SCO72 with pLB85-MG*pfl* integrated
SC072/MG*eutD*	SCO72 with pLB85-MG*eutD* integrated
SC072/MG*ackA1*	SCO72 with pLB85-MG*ackA1* integrated
SC072/MG*ackA2*	SCO72 with pLB85-MG*ackA2* integrated
MG1363 [11]	A plasmid-free strain derived from *L. lactis* subsp. *cremoris* NCDO 712
LB436 [12]	MG1363 containing pLB65
LB436/IL*pfl*	SCO72 with pLB85-IL*pfl* integrated
LB436/IL*adhE*	SCO72 with pLB85-IL*adhE* integrated
LB436/IL*eutD*	SCO72 with pLB85-IL*eutD* integrated
LB436/IL*ackA1*	SCO72 with pLB85-IL*ackA1* integrated
LB436/IL*ackA2*	SCO72 with pLB85-IL*ackA2* integrated
LB436/MG*pfl*	SCO72 with pLB85-MG*pfl* integrated
LB436/MG*adhE*	SCO72 with pLB85-MG*adhE* integrated
LB436/MG*eutD*	SCO72 with pLB85-MG*eutD* integrated
LB436/MG*ackA1*	SCO72 with pLB85-MG*ackA1* integrated
LB436/MG*ackA2*	SCO72 with pLB85-MG*ackA2* integrated
ABLE-K [13]	An *E. coli* strain reducing the copy number of common cloning vectors

2.2.2 Antibiotics

When needed ampicillin, erythromycin or chloramphenicol were added at 100, 5 and 5 μg ml^{-1} for *L. lactis* respectively. Tetracycline and kanamycin were applied at 15 and 8 μg ml^{-1} for *E. coli* ABLE-K.

2.2.3 Culture media and conditions

E. coli strains were cultivated aerobically at 28 ˚C in lysogeny broth (LB) [14]. *L. lactis* was cultivated in M17 media or chemically defined SA media [15] at 30 ˚C without aeration, supplemented with 0.2% (w/v) glucose. For growth experiments, defined SA medium [15] devoid of sodium acetate and supplemented with nucleosides (adenosine, cytidine, guanosine, thymidine, uridine and inosine, 20 mg/L), α-lipoic acid (2 mg/L) and either glucose or maltose (0.2%) were used, abbreviated as GluSALN or MalSALN respectively. Growth experiments were conducted in flasks at 30 ˚C under static conditions with slow stirring. Optical density at 600 nm (OD_{600}) was regularly measured. To prepare a preculture, a single colony from an agar plate was inoculated into GluSALN or MalSALN media in dilution series. Growth experiments were started by inoculating an exponentially growing overnight culture selected from the dilution series into a flask containing the same medium, up to OD_{600} = 0.001 or 0.02 for growth on glucose or maltose respectively. Biological

triplicates for each experiment were performed. The previously found cell density equal to 0.36 g (dry weight) (gdw) per liter of SALN medium at OD_{600} = 1 was used for the calculation of specific rates [16].

2.2.4 Quantification of sugar and fermentation products

High-performance liquid chromatography (HPLC) was employed to measure the concentration of glucose, maltose, lactate, formate and acetate in the samples taken during the growth experiments as previously described [16]. The biomass yield on sugar $Y_{X/S}$ (gdw/C6-mol) was estimated by:

$$Y_{X/S} = \frac{1}{n_{C_6}}\frac{dX}{dS} = \frac{d(X/V)}{d(S/V)} = \frac{(\rho/OD_{600})}{n_{C_6}}\frac{d(OD_{600})}{dC} = \frac{0.36}{n_{C_6}}\frac{d(OD_{600})}{dC}$$

where S is the substrate (sugar), X is the biomass, V the culture volume, ρ the cell density and C the substrate concentration. $n_{C_6} = 1$ for glucose and 2 for maltose. It is therefore proportional to the slope of OD_{600} plotted against C6 concentration. Under the assumption of exponential growth ($dX/dt = \mu X$ where μ is the specific growth rate), the specific rate of consumption or production of substrate or product, respectively, or simply the substrate or product flux, were calculated as:

$$v = \frac{1}{X}\frac{dS}{dt} = \mu\frac{dS}{dX} = \frac{\mu}{0.36}\frac{dC}{d(OD_{600})}$$

2.2.5 DNA techniques

The method used to isolate the chromosomal DNA from *L. lactis* was modified from a previous method [17]. PCR amplification, restriction, ligation, transformation and plasmid purification from *E. coli* were performed following procedures described in Sambrook and Russell [18] and the description from the manufacturer of the enzymes used. Electrocompetent cells of *L. lactis* were grown in M17 broth supplemented with 10 g L^{-1} glucose and 10 g L^{-1} glycine and transformed by electroporation as described previously [19].

2.2.6 Construction of gusA reporter strains

The promoter containing region upstream a specific gene (≈500-bp) was PCR amplified and inserted into plasmid pLB85 and transformed into LB436 which expresses phage TP901-1 integrase as described previously [12] to construct strains reporting the promoter activity of mixed-acid genes. For SC072 which was derived from IL1403, since the *attB* site in IL1403 does not perfectly match the consensus for high-frequency integration, vectors derived from pLB85 were first transformed into and then purified from *E. coli*. It is noted that ampicillin instead of erythromycin was used as selection marker for *E. coli* transformation to avoid abnormal forms of plasmids observed (possibly multimer). *L. lactis* transformants were selected on GM17 with erythromycin and verified by sequencing using primers CSO50 and CSO263 (Table 2.2).

2.2.7 Measurement of β-glucuronidase activity

Exponentially growing culture at OD_{600}=0.6 was quenched on ice and harvested for *β*-glucuronidase assay. The procedure used for measuring *β*-glucuronidase activities was modified from Miller [20] and Israelsen et al. [21].

2.3 Results

2.3.1 Growth of MG1363 and IL1403

Before studying the difference between the two strains, the growth behavior and fermentation pattern of the strains should be confirmed. For this purpose, *L. lactis* MG1363 and IL1403 were cultivated on GluSALN or MalSALN media. Sugars were verified to be the limiting substrate for growth by the absence of sugar in cultures where growth had ceased. The growth rate and the fermentation pattern during exponential growth phase for each experiment were analyzed. Table 2.5 shows the specific growth rate and specific rates of consumption of sugars and production of lactate, formate, acetate and ethanol. The growth rate of both strains on glucose was indistinguishable from each other, around 1.15 h^{-1}, equivalent to a generation time of 36 minutes. Product formation as revealed by HPLC measurements was found to be homolactic, and only 5% (molar) of the pyruvate ended up as alternative products (Table 2.6).

Table 2.5. Specific rate of growth, sugar consumption and product formation.

	Growth rate (h^{-1})	Specific rate of consumption/production (mmol h^{-1} gdw^{-1})				
		Sugar	Lactate	Formate	Acetate	Ethanol
GluSALN						
MG1363	1.15 ± 0.04	25.9 ± 1.6	45.7 ± 1.2	1.8 ± 0.6	2.4 ± 0.2	0.3 ± 0.3
IL1403	1.15 ± 0.07	24.9 ± 1.6	42.2 ± 0.6	1.6 ± 0.2	1.8 ± 0.2	0.4 ± 0.4
MalSALN						
MG1363	0.61 ± 0.03	8 ± 0.4	12.6 ± 0.8	16.8 ± 1.5	9.6 ± 0.9	5.8 ± 0.8
IL1403	0.43 ± 0.01	9.8 ± 0.5	34.2 ± 2.4	3.8 ± 0.7	3.7 ± 0.8	0.2 ± 0.2

Table 2.6. Derived growth statistics.

	Carbon recovery	Formate %	Acetate + ethanol %	Biomass yield (gdw/ C_6-mol)
GluSALN				
MG1363	92% ± 3%	4% ± 1%	5% ± 1%	44.6 ± 4.2
IL1403	88% ± 5%	4% ± 1%	5% ± 1%	46.5 ± 5.5
MalSALN				
MG1363	92% ± 7%	57% ± 2%	55% ± 2%	38.3 ± 2.0
IL1403	97% ± 6%	10% ± 2%	10% ± 2%	22.1 ± 0.8

Carbon recovery was calculated as the sum of acetate, ethanol and lactate fluxes divided by the sugar uptake flux in C_3-mole. Formate percentage was the formate flux divided by the sum of formate and lactate fluxes. Acetate and ethanol percentage was the sum of acetate and ethanol fluxes divided by the sum of the two and lactate fluxes.

When growing on maltose, however, a notable higher growth rate of MG1363 (0.61 h^{-1}) than that of IL1403 (0.43 h^{-1}) was observed. Calculation of product fluxes indicated very different fermentation patterns between the two strains, prominently mixed-acid for MG1363 (≈55% mixed acids) and homolactic for IL1403 (10% mixed acids). Especially low in production was ethanol, basically close to zero production as in the case of growth on glucose. It is also worth noting that the maltose flux in IL1403 is slightly but systematically higher than that in MG1363 (8 replications throughout 1 year) (Table 2.5). Another observation is the significantly lower growth yield of IL1403 on maltose.

2.3.2 Strategy to identify *trans*- and *cis*-regulation of transcription

We aimed to study the regulation of the promoter activities of the mixed-acid genes in both MG1363 and IL1403. The genes include *pfl*, *eutD*, *ackA1*, *ackA2* and *adhE*, respectivey encoding for pyruvate formate-lyase (PFL), phosphotransacetylase (PTA), two acetate kinases (ACKs) and alcohol dehydrogenase (ADH). For the activity of promoter of gene G of strain A expressed in strain B, a single copy of a 500-bp upstream region of G from strain A followed by the gene *gusA*, encoding β-glucuronidase as a reporter, was created on the chromosome of strain B (see Figure 2.1 and 'construction of gusA reporter strains' in the method section for construction details).

For each gene, strains were constructed for measuring the promoter activity from MG1363 or IL1403 expressed in MG1363 or IL1403 respectively (Figure 2.2). The rationale behind this was to identify possible *trans*- and *cis*-regulatory elements. If the promoter activities of the two promoters are similar within a strain but the values differ between the two strains, *trans*-regulation specific to a strain is suggested. In contrast, if the activity of the promoter from a strain remains unchanged when expressed in both strains but is persistently different from that of the promoter from the other strain, *cis*-regulatory elements on either promoter region subject to regulation in both strains is suggested.

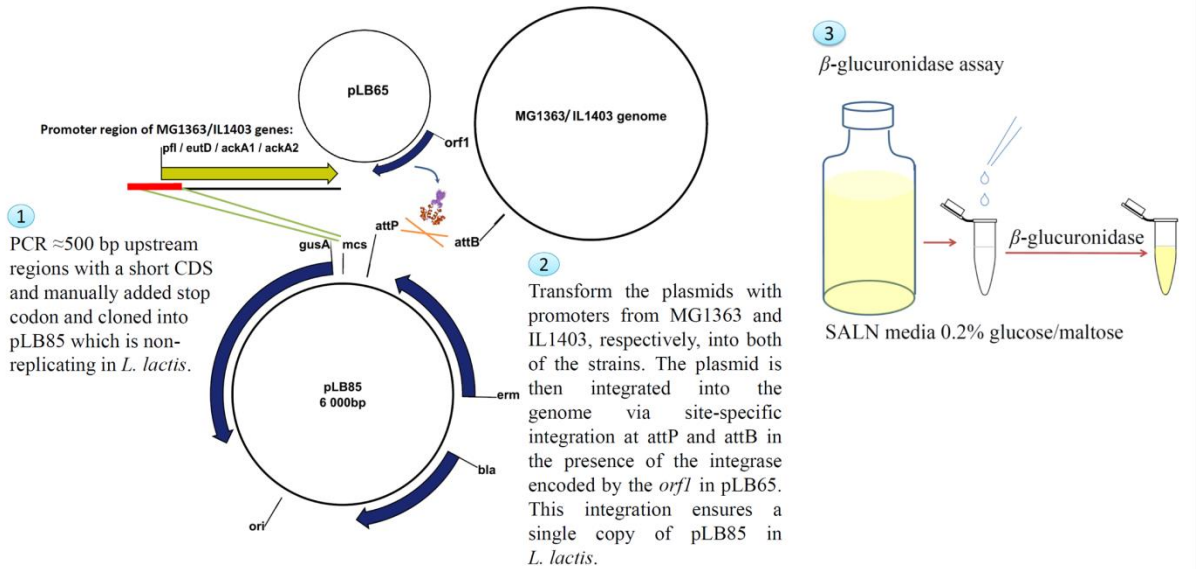

Figure 2.1. Construction for measuring promoter activities.

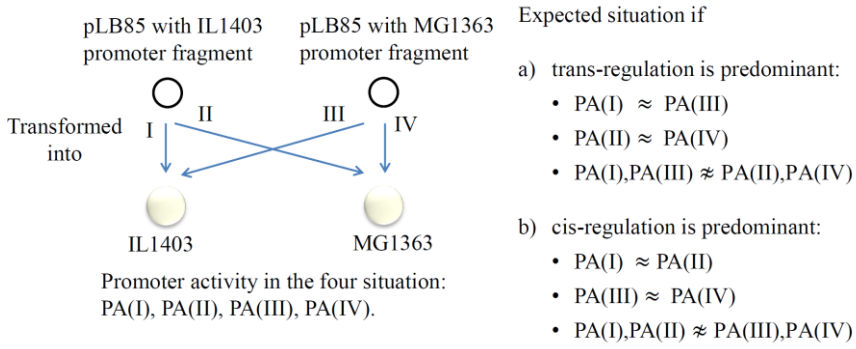

Figure 2.2. Identification of *trans*- and *cis*-regulation.

Compare activity of promoters from the two strains expressed in the two strains respectively.

PA, promoter activity.

pfl promoters

The activities of the *pfl* promoters of both strains were assayed (Figure 2.3). An obvious observation is the 10-fold induction of *pfl* promoters in all constructs for growth on maltose compared to growth on glucose. More interestingly, a surprisingly clear pattern resembling *trans*-regulation was seen. *pfl* promoters of both strains had very similar activities and they were 3-fold higher when expressed in MG1363 than in IL1403.

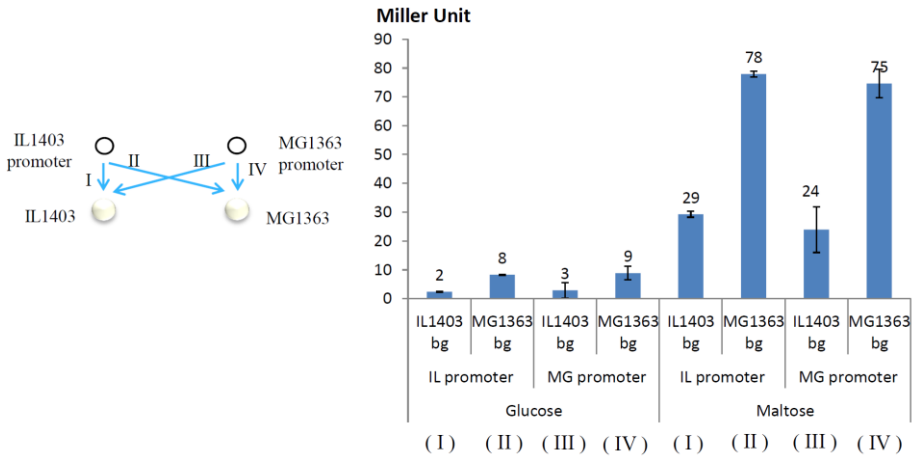

Figure 2.3. *pfl* promoter activities.

eutD promoters

For *eutD* promoters, similarly, induction for growth on maltose was observed (Figure 2.4). A sharp contrast to the case of *pfl* is a clear pattern resembling *cis*-regulation on *eutD* promoters. The *eutD* promoter of MG1363 always has an activity about 2 times higher than that of IL1403 and the levels are similar when expressed in both strains.

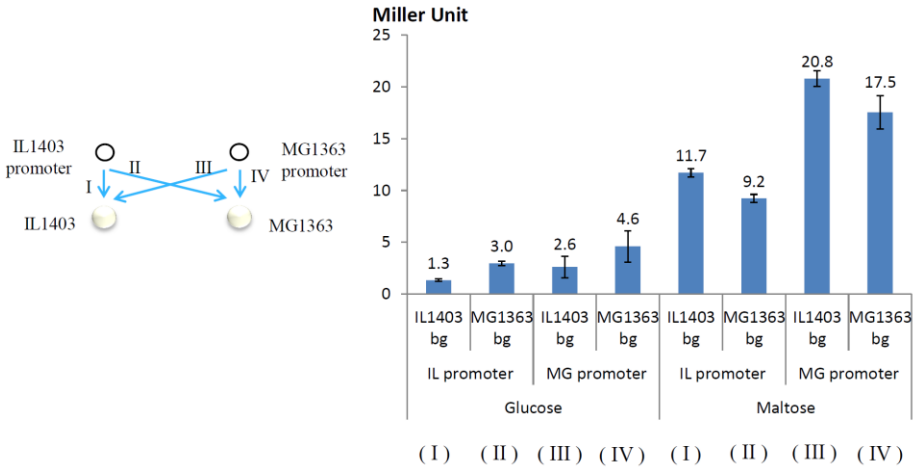

Figure 2.4. *eutD* promoter activities.

Promoter activities of ackA1 and ackA2

For the two *ackA* genes, no clear pattern could be observed . For *ackA1*, only a higher activity on maltose compared to glucose (≈2-fold) for all cases could be concluded. For *ackA2*, more significant induction on maltose was observed (≈10-fold). The promoter of IL1403 appeared to be more active than that of MG1363 and was particularly active in its original host IL1403.

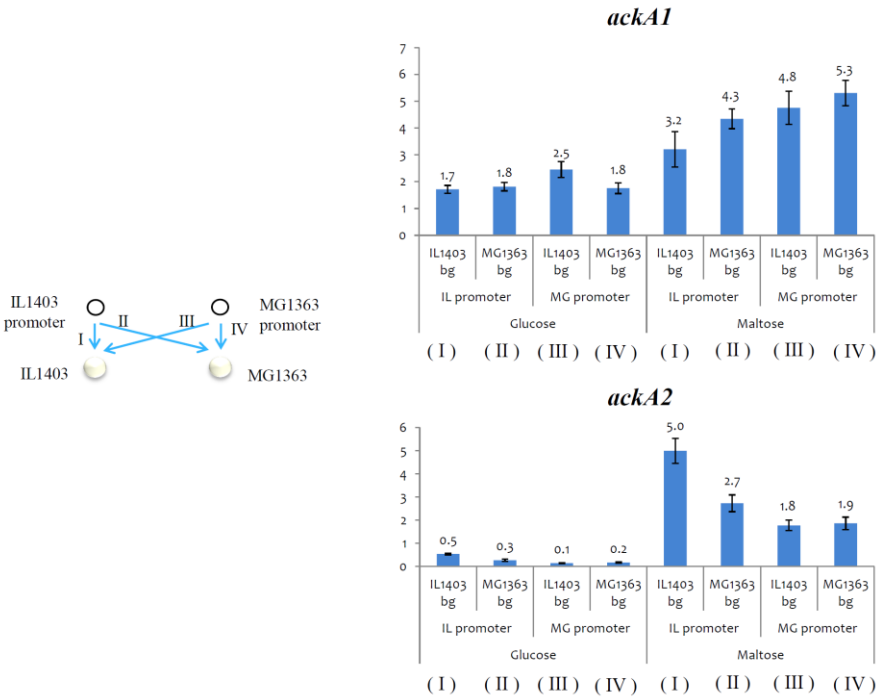

Figure 2.5. *ackA1, ackA2* promoter activities.

Promoter activities of adhE

For *adhE* promoter activity, only the promoter activities in MG1363 as the background were measured (Figure 2.6). The induction on maltose was very strong for MG1363's promoter (75-fold). The activity of IL1403's *adhE* promoter was two-fold to three-fold higher on maltose than that of MG1363's.

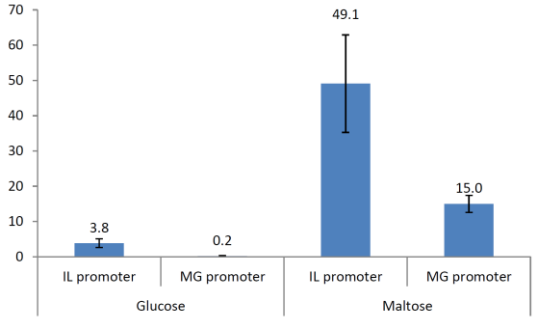

Figure 2.6. *adhE* promoter activities in MG1363.

2.4 Discussion

2.4.1 Homolactic fermentation in IL1403 confirmed

The growth experiments of IL1403 in MalSALN media supported two observations in Even et al. (2001) [9]. First, IL1403 largely remained homolactic even when growing on a slowly fermentable sugar (galactose in that study). Second, alcohol dehydrogenase (ADH) was probably not sufficiently functional as it was found in the previous study that ADH had an extremely low activity in IL1403 (10^2- to 10^3-fold lower than other fermentation enzymes) and in this study the ethanol production was very low, not comparable to the acetate production. In usual mixed-acid fermentation the production of the two products should be in the same order of magnitude.

The lower growth rate and biomass yield (as well as the final OD_{600}, data not shown) of IL1403 growing on maltose are probably results of decreased glycolytic flux limited by maltose uptake and the inability of IL1403 to switch into mixed-acid fermentation to get one more ATP per acetate produced. The effect of the lowered ATP production rate can be explained by the simplistic Pirt's equation:

$$v_{ATP} = \mu Y_{ATP/X} + v_{ATPm}$$

where v_{ATP} is the ATP production rate, μ the growth rate, $Y_{ATP/X}$ the ATP required for forming one unit of biomass, v_{ATPm} the rate of ATP needed for maintenance. Assume a constant maintenance and constant ATP requirement for biomass production, the growth rate decreases with the ATP production

rate. Then, during exponential growth, v_{ATP} is related to the ATP yield $Y_{ATP/S}$ and the biomass yield on substrate $Y_{X/S}$ as follows:

$$v_{ATP} = \frac{1}{X}\frac{d(ATP)}{dt} = \frac{Y_{ATP/S}}{X}\frac{dS}{dt} = Y_{ATP/S}(\mu\frac{dS}{dX}) = \mu\frac{Y_{ATP/S}}{Y_{X/S}}$$

Rearranging, we have:

$$Y_{X/S} = \frac{Y_{ATP/S}}{Y_{ATP/X}}\left(1 - \frac{v_{ATPm}}{v_{ATP}}\right)$$

Thus the biomass yield decreases with the ATP production rate and increases with the ATP yield on substrate.

Other factors could also contribute to the decreased ATP production in addition to the limited maltose uptake rate. (i) In the upstream maltose pathway, if more intracellular maltose is hydrolyzed by α-glucosidase than by maltose phosphorylase, the outcome is more glucose which needs ATP in order to be converted into G6P (Figure 1.4). The ATP yield is then lower than 2 moles per mole of C_6. But again the activity of α-glucosidase in *L. lactis* has not been determined. (ii) Compared to the PTS converting extracellular glucose to intracellular G6P in a single step, both ABC transporter transporting maltose and glucokinase produce extra protons while *L. lactis* maintains a high intracellular pH [22]. The extra protons produced may need to be pumped out of the cell by ATPase, using extra ATP. (iii) More ATP may be consumed in the whole cellular program for growth on maltose than on glucose, for instance, expression of additional enzymes for maltose assimilation.

2.4.2 Regulation of promoter activities

The activities of *pfl* promoters in different backgrounds suggested regulation by a *trans*-element in either strain. It could be a repressor in IL1403 or an activator in MG1363 not present in the other strain. A motif well matching the *cre* consensus at -114 (relative to the transcription start site) is present in both strains but it is not likely to be the reason since there have been *in vitro* and *in vivo* evidences showing the functionality of CcpA in IL1403 [23, 24]. Another candidate with higher possibility is FlpA in MG1363. It has been found to recognize the FNR consensus [25] which overlaps with the -35 promoter of *pfl* for both of the strains and once reported to affect the formate production in MG1363 [26]. No homolog of FlpA could be found in IL1403 but there is another FNR-like protein, RcfA, that however was unable to substitute FlpA in MG1363 [27].

For *eutD*, the regulation of promoter activity was more likely to be governed by *cis*-elements present in the promoter region. They could be sequence motifs matching the consensus of a certain activator targeting MG1363's promoter or a repressor targeting IL1403's promoter that exists in both strains. One possible candidate is a motif roughly matching the *cre* consensus present on MG1363

(TGGGGTCGATATTA), 257 bp upstream of the start codon and 165 bp upstream of a putative TGn -10 promoter (TGGTATACT). In IL1403, the corresponding sequence has lost the central CG element (TGGGGT**T**GATATTA) which is essential for CcpA recognition.

For the two *ackA* genes, the repression of *ackA2* on glucose is expected because it has been found to be subject to carbon catabolite repression and a *cre* consensus 22 bp upstream of the start codon is present just after a putative transcription start site [28]. Besides, the quite different activity profiles of the two promoters are interesting and worth further studying in the sense that the proteins encoded by the two genes (ACK) should be responsible for the same reaction. One hypothetical possible situation is that the ACK from *ackA1* produces acetate from acetyl-phosphate while that from *ackA2* is for the reverse direction. It was hypothesized because IL1403 does not exhibit significant mixed-acid fermentation, so acetyl-CoA is expected to be insufficient and acetate is one of the precursors. This coincides with the higher promoter activity of *ackA2* than *ackA1* for IL1403 growing on maltose.

Despite the insights provided by these results, a factor contributing to the expression level of a gene at the transcription level not taken into account using the present approach is the possibly varying gene dosage along the position of a gene in the genome. All transcriptional fusions were integrated into the same site on the chromosome, 18 kbp away from the origin of replication. *pfl*, for example, is located 618 and 657 kbp away from the origin in MG1363 and IL1403 respectively. The actual expression level may be different because the closer to the origin a gene is, the higher the expression level one can expect [29].

For the gene *adhE*, only the promoter activities in MG1363 were measured as the construction for IL1403 was not successful initially. Further attempts have not been made since later the focus had been shifted to PFL and ACKs, as reported in Chapter 3 and Chapter 1.

2.5 References

1. Palmfeldt J, Paese M, Hahn-Hägerdal B, Van Niel EWJ (2004) The pool of ADP and ATP regulates anaerobic product formation in resting cells of *Lactococcus lactis*. *Appl Environ Microbiol* 70:5477–84. Available at: http://www.pubmedcentral.nih.gov/articlerender.fcgi?artid=520924&tool=pmcentrez&rendertype=abstract [Accessed June 15, 2012].
2. Thomas TD, Turner KW, Crow VL (1980) Galactose fermentation by *Streptococcus lactis* and *Streptococcus cremoris*: pathways, products, and regulation. *J Bacteriol* 144:672–682.
3. Thomas TD, Ellwood DC, Longyear VM (1979) Change from homo- to heterolactic fermentation by *Streptococcus lactis* resulting from glucose limitation in anaerobic chemostat cultures. *J Bacteriol* 138:109–17. Available at: http://www.pubmedcentral.nih.gov/articlerender.fcgi?artid=218245&tool=pmcentrez&rendertype=abstract.
4. Sjoberg A, Hahn-Hagerdal B (1989) β-Glucose-1-phosphate, a possible mediator for polysaccharide formation in maltose-assimilating *Lactococcus lactis*. *Appl Environ Microbiol* 55:1549–1554.
5. Sjöberg A, Persson I, Quednau M, Hahn-Hägerdal B (1995) The influence of limiting and non-limiting growth conditions on glucose and maltose metabolism in *Lactococcus lactis* ssp. *lactis* strains. *Appl Microbiol Biotechnol* 42:931–938. Available at: http://www.springerlink.com/index/10.1007/BF00191193 [Accessed March 2, 2012].
6. Garrigues C, Loubiere P, Lindley ND, Cocaign-Bousquet M (1997) Control of the shift from homolactic acid to mixed-acid fermentation in *Lactococcus lactis*: predominant role of the NADH/NAD^+ ratio. *J Bacteriol* 179:5282–5287. Available at: http://www.pubmedcentral.nih.gov/articlerender.fcgi?artid=179393&tool=pmcentrez&rendertype=abstract.

7. Hofvendahl K, van Niel EWJ, Hahn-Hägerdal B (1999) Effect of temperature and pH on growth and product formation of *Lactococcus lactis* ssp . *lactis* ATCC 19435 growing on maltose. *Appl Environ Microbiol* 51:669–672.
8. Garrigues C, Mercade M, Cocaign-Bousquet M, Lindley ND, Loubiere P (2001) Regulation of pyruvate metabolism in *Lactococcus lactis* depends on the imbalance between catabolism and anabolism. *Biotechnol Bioeng* 74:108–15. Available at: http://www.ncbi.nlm.nih.gov/pubmed/11369999.
9. Even S, Lindley ND, Cocaign-Bousquet M (2001) Molecular physiology of sugar catabolism in *Lactococcus lactis* IL1403. *J Bacteriol* 183:3817–24. Available at: http://www.pubmedcentral.nih.gov/articlerender.fcgi?artid=95262&tool=pmcentrez&rendertype=abstract [Accessed January 24, 2012].
10. Chopin A, Chopin MC, Moillo-Batt A, Langella P (1984) Two plasmid-determined restriction and modification systems in *Streptococcus lactis*. *Plasmid* 11:260–263.
11. Gasson MJ (1983) Plasmid complements of *Streptococcus lactis* NCDO 712 and other lactic streptococci after protoplast-induced curing. *J Bacteriol* 154:1–9. Available at: http://www.pubmedcentral.nih.gov/articlerender.fcgi?artid=217423&tool=pmcentrez&rendertype=abstract.
12. Brøndsted L, Hammer K (1999) Use of the integration elements encoded by the temperate lactococcal bacteriophage TP901-1 to obtain chromosomal single-copy transcriptional fusions in *Lactococcus lactis*. *Appl Environ Microbiol* 65:752–758.
13. Greener A (1993) Expand your library by retrieving toxic clones with ABLE strains. *Strategies* 6:7–9.
14. Bertani G (2004) Lysogeny at mid-twentieth century: P1, P2, and other experimental systems. *J Bacteriol* 186:595–600.
15. Jensen PR, Hammer K (1993) Minimal requirements for exponential growth of *Lactococcus lactis*. *Appl Environ Microbiol* 59:4263–6.
16. Andersen HW, Solem C, Hammer K, Jensen PR (2001) Twofold reduction of phosphofructokinase activity in *Lactococcus lactis* results in strong decreases in growth rate and in glycolytic flux. *J Bacteriol* 183:3458–67. Available at: http://www.pubmedcentral.nih.gov/articlerender.fcgi?artid=99644&tool=pmcentrez&rendertype=abstract [Accessed January 24, 2012].
17. Johansen E, Kibenich A (1992) Characterization of *Leuconostoc* Isolates from Commercial Mixed Strain Mesophilic Starter Cultures. *J Dairy Sci* 75:1186–1191. Available at: http://linkinghub.elsevier.com/retrieve/pii/S0022030292778655 [Accessed August 12, 2013].
18. Sambrook J, Russell DW (1989) *Molecular cloning: a laboratory manual* (Cold Spring Harbor Laboratory Press Cold Spring Harbor New York). 2nd Ed.
19. Holo H, Nes IF (1989) High-frequency transformation, by electroporation, of *Lactococcus lactis* subsp. *cremoris* grown with glycine in osmotically stabilized media. *Appl Environ Microbiol* 55:3119–23. Available at: http://www.pubmedcentral.nih.gov/articlerender.fcgi?artid=203233&tool=pmcentrez&rendertype=abstract.
20. Miller JH (1972) *Experiments in molecular genetics* (Cold Spring Harbor Laboratory, New York (US)).
21. Israelsen H, Madsen SM, Vrang a, Hansen EB, Johansen E (1995) Cloning and partial characterization of regulated promoters from *Lactococcus lactis* Tn917-lacZ integrants with the new promoter probe vector, pAK80. *Appl Environ Microbiol* 61:2540–7. Available at: http://www.pubmedcentral.nih.gov/articlerender.fcgi?artid=167525&tool=pmcentrez&rendertype=abstract.
22. Van de Guchte M et al. (2002) Stress responses in lactic acid bacteria. *Antonie Van Leeuwenhoek* 82:187–216. Available at: http://www.ncbi.nlm.nih.gov/pubmed/16961092.
23. Aleksandrzak T, Kowalczyk M, Kok J, Bardowski J (2000) Regulation of carbon catabolism in *Lactococcus lactis*. *Prog Biotechnol* 17:61–66.
24. Kowalczyk M, Borcz B, Płochocka D, Bardowski J (2007) *In vitro* DNA binding of purified CcpA protein from *Lactococcus lactis* IL1403. *Acta Biochim Pol* 54:71–8. Available at: http://www.ncbi.nlm.nih.gov/pubmed/17356715.
25. Scott C, Guest JR, Green J (2000) Characterization of the *Lactococcus lactis* transcription factor FlpA and demonstration of an *in vitro* switch. *Mol Microbiol* 35:1383–93. Available at: http://www.ncbi.nlm.nih.gov/pubmed/10760139.
26. Gostick DO et al. (1999) Two operons that encode FNR-like proteins in *Lactococcus lactis*. *Mol Microbiol* 31:1523–35. Available at: http://www.ncbi.nlm.nih.gov/pubmed/10200970.
27. Akyol I, Shearman CA (2008) Regulation of *flpA*, *flpB* and *rcfA* promoters in *Lactococcus lactis*. *Curr Microbiol* 57:200–5. Available at: http://www.ncbi.nlm.nih.gov/pubmed/18600375 [Accessed August 29, 2012].
28. Zomer AL, Buist G, Larsen R, Kok J, Kuipers OP (2007) Time-resolved determination of the CcpA regulon of *Lactococcus lactis* subsp. *cremoris* MG1363. *J Bacteriol* 189:1366–81. Available at: http://www.pubmedcentral.nih.gov/articlerender.fcgi?artid=1797362&tool=pmcentrez&rendertype=abstract [Accessed November 10, 2011].
29. Cocaign-Bousquet M, Even S, Lindley ND, Loubière P (2002) Anaerobic sugar catabolism in *Lactococcus lactis*: genetic regulation and enzyme control over pathway flux. *Appl Microbiol Biotechnol* 60:24–32. Available at: http://www.ncbi.nlm.nih.gov/pubmed/12382039 [Accessed May 29, 2012].

Chapter 3. Mixed-acid fermentation controlled by pyruvate-formate lyase

3.1 Introduction

L. lactis subsp. *cremoris* MG1363 and subsp. *lactis* IL1403 have been confirmed to exhibit different extents of mixed-acid fermentation when growing on maltose in SALN media. In MG1363, 60% (in molar) of pyruvate ended up in mixed acids (formate, acetate and ethanol) whereas mixed acids accounted for only 10% of pyruvate distribution in IL1403 (1.7). Meanwhile, the transcriptional activity induced by *pfl* promoters was found to be 3-fold higher in MG1363 than in IL1403. *pfl* encodes for pyruvate formate-lyase (PFL), an oxygen sensitive enzyme producing formate and acetyl-CoA from pyruvate, and is the first enzyme of the mixed-acid pathway (see section 1.5.3). The lower transcription level of *pfl* could be a reason for the inability to shift from homolactic to mixed-acid fermentation in IL1403 as in the case of MG1363, for which PFL has been found to control the mixed-acid shift for growth on galactose [1].

In this study, to examine the role and functionality of PFL in IL1403, first PFL activities from IL1403 were introduced into a PFL-knockout strain derived from MG1363. Second, an attempt was made to modulate the level of PFL in IL1403.

3.2 Materials and methods

3.2.1 Bacteria strains and plasmids

All *L. lactis* strains were derived from MG1363 and IL1403. pCS1966 containing genes for erythromycin resistance and orotate transport was used for markerless *pfl* deletion in MG1363 [2]. pLB65 and pLB85-derived plasmids (described in section 2.2) were used for inserting a chromosomal copy of *pfl* preceded with a synthetic promoter library (SPL) in MG1363. The thermosensitive plasmid pGhost8 containing a gene encoding for tetracycline resistance was used for *gusA* insertion into IL1403's chromosome [3]. pRC1, non-replicating in *L. lactis*, was used for integrating synthetic promoters upstream of *pfl* in IL1403 by a single cross-over event [4]. *E. coli* MC1000 was used for cloning pCS1966- and pGhost8-derived plasmids [5]. *E. coli* ABLE-C (Stratagene) was used for cloning pRC1 [6]. Primers, plasmids and strains used or constructed in this study are listed in Table 3.1, Table 3.2 and Table 3.3 respectively.

Table 3.1. Primers used in the study.

Primer	RS	Amplified region / Description	Sequence (5' - 3')
CSO834	XbaI	*pfl* upstream	ctagtctagaCAAGTGATGTACCAAATGAC
CSO835	BamHI	in MG1363	cgcggatccTTTGAAATCTCCTTTGTTCT
CSO836	BamHI	*pfl* downstream	cgcggatccTTCTTAGTATTAAAAAATATAAAG
CSO837	XhoI	in MG1363	ggtactcgagTGTGATTCACCCCTATTTCT
CSO852	/	Verify *pfl* deletion	CTTGAATTCTGTTTGCTATTATC
CSO853	/		CTTTGTCAGCATCAATTACTTG
76f	XhoI	≈900 bp upstream region of *pfl* stop codon	actgactcgagGACTGATACTTATGTTGA
76r	HindIII	in IL1403	actgaaagcttTAAGAATTAGATGTTTGAAGTATGC
CSO380	HindIII	*E. coli* MG1655's *gusA*	gcatcaagcttaaggttGACCAGTATTATTATC
CSO381	PstI		tcggactgcagAGGAGAGTTGTTGATTCATTG
77f	PstI	≈900 bp downtream region of *pfl* stop	actgactgcagAAATTTAATGAATATTCGGTCTGTCAGT
77r	XbaI	codon in IL1403	actgatctagaATACAAGGGGAGAAAGGG
16f	XbaI	Synthetic promoter library for *pfl*, suitable for both MG1363 and IL1403	acgactagttctagaatnnnnnagtttattcttgacannnnnnnnnnnnnnntgrtataa tnnnnTTGTAATTTGAAACAGAAAGAAC
8f	XbaI	upstream region of *pfl* in MG1363	atcgatctagaCCTCAGCAACATTTGTTC
16r	SalI	Reverse primer for MG1363's *pfl*	actgagtcgacATTAGATATTTGAAGTGTGCATTACTTCTT CATC
54r	SalI	Reverse primer for IL1403's *pfl*	actgagtcgacAAGAATTAGATGTTTGAAGTATGC
78r	PstI	Reverse primer for truncated IL1403's *pfl*	actgactgcagttaGATATCAAGAACGATTGG

RS, restriction site.

Table 3.2. Plasmid used or constructed in the study.

Plasmid	Description	Resistance
pCS1966 [2]	A vector containing *oroP* for orotate transporter as a counterselection tool for deletion.	Erm
pCS1966-*pfl*	pCS1966 containing the upstream and downstream regions of *pfl* in MG1363 obtained with primers CSO834-837.	Erm
pGhost8 [3]	Thermosensitvie plasmid, non-replicating above 35 ˚C.	Tet
pGhost8-*gusA*	pGhost8 containing the upstream and downstream regions of *pfl* stop codon in IL1403, separated by *E. coli*'s gusA, PCR amplified with primers 76f, r, CSO380, 381 and 77f, r.	Tet
pLB65 [7]	Containing *orf1* expressing phage TP901-1 integrase	Cam
pLB85 [7]	Reporter vector containing a promoterless *gusA* gene and an *attP* site for integration into *attB* site on chromosomes in the presence of the TP901-1 integrase.	Amp, Erm
pLB85-SPL-MG*pfl*	pLB85 containing a synthetic promoter library preceding *pfl* of MG1363 PCR amplified with primer 16f, r.	Amp, Erm
pLB85-SPL-IL*pfl*	pLB85 containing a synthetic promoter library preceding *pfl* of IL1403 PCR amplified with primer 16f, 54r.	Amp, Erm
pLB85-WTP-MG*pfl*	pLB85 containing the wild-type promoter region and *pfl* of MG1363 PCR amplified with primers 8f, 16r	Amp, Erm
pRC1 [6]	A pBlue-script-derived vector, non-replicating in *L. lactis*.	Erm
pRC1-SPL-IL*pfl*	pRC1 containing a synthetic library preceding a truncated version of *pfl* of IL1403 (≈900 bp)	Erm

Erm, erythromycin; Tet, tetracycline; Cam, chloramphenicol; Amp, ampicillin.

Table 3.3. Strains used or constructed in the study.

Strain	Description
MG1363 [8]	A plasmid-free strain derived from *L. lactis* subsp. *cremoris* NCDO 712
IL1403 [9]	A plasmid-free strain derived from *L. lactis* subsp. *lactis* biovar *diacetylactis* CNRZ157
MG1363Δ*pfl*	*pfl*-knockout derived from MG1363 using pCS1966-*pfl*
SC100	MG1363Δ*pfl* containing pLB65
SC105 a – e	Strains with modulated expression of *pfl* from MG1363 by integration of pLB85-SPL-MG*pfl* into SC100
SC106 a – e	Strains with modulated expression of *pfl* from IL1403 by integration of pLB85-SPL-IL*pfl* into SC100
SC119	A strain with the wild-type promoter region and *pfl* of MG1363 by integration of pLB85-WTP-MG*pfl* into SC100
SC183	IL1403 with *gusA* inserted at *pfl* downstream, constructed using pGhost8-*gusA*
SC193 a – c	Strains with synthetic promoters preceding the native *pfl* in SC183 resulting from integrating pRC1-SPL-IL*pfl* into SC183's chromosome
MC1000 [5]	An *E. coli* strain used for cloning purposes
ABLE-K [6]	An *E. coli* strain reducing the copy number of common cloning vectors

3.2.2 Antibiotics

When needed, erythromycin, chloramphenicol, tetracycline were added at 5 μg ml^{-1} for *L. lactis* respectively. Erythromycin, tetracycline and kanamycin were applied at 150, 15 and 8 μg ml^{-1} for *E. coli*.

3.2.3 Gene deletion and insertion

pfl deletion was achieved by using the plasmid pCS1966 [2]. ≈900-bp regions upstream and downstream of the target to be deleted were PCR amplified (using primers CSO834 – 837) and inserted into pCS1966. The resulting plasmids were used as previously described [2]. For insertion of *gusA*, the sequence to be inserted was also PCR amplified (using primers CSO380, 381) and cloned in between the upstream and downstream regions (amplified using primers 76, 77) in pGhost8 [3].

3.2.4 Modulation of *pfl* expression in *L. lactis*

For modulating *pfl* expression in MG1363, first the native *pfl* was deleted followed by the transformation of pLB65 into the deletion strain, resulting in SC100. The vectors for strain construction were pLB85-SPL-MG*pfl* and pLB85-SPL-IL*pfl* containing a SPL preceding *pfl* of MG1363 and IL1403 amplified using primers 16f, 16r and 16f, 54r respectively. The vectors were directly transformed into SC100. The transformants became the SC105 and SC106 series of strains with modulated expression from MG1363 and IL1403 respectively via site-specific integration of the vectors at *attP*, *attB* sites in the presence of the integrase encoded from pLB65 [7]. For control, pLB85-WTP-MG*pfl* containing the wild-type promoter followed MG1363's *pfl* was also prepared. Transforming the vector yielded the strain

For modulation of *pfl* in IL1403, the *gusA* gene was inserted just downstream of *pfl* and the resultant strain was named SC183. For the integration vector, the fragment of a truncated version of *pfl* with a SPL was amplified using primers 16f and 78r. It was digested and inserted into pRC1 to become pRC1-SPL-IL*pfl*. It was then cloned through *E. coli* ABLE-C which reduced the copy number of plasmids to compensate the potential selective disadvantage of strong synthetic promoters. The transformants of the purified plasmids become the SC193 series of strains with different expression of *pfl*.

For the calculation of flux control coefficients (FCCs), a suitable curve $y = f(x)$ for flux as a function of *gusA* activity was fitted using Matlab® and the FCC was calculated as $xf'(x)/f(x)$.

3.2.5 Others

For culture media and conditions, quantification of sugars and fermentation products, other DNA techniques and measurement of β-glucuronidase activity, readers are referred to section 2.2.

3.3 Results

3.3.1 PFLs of MG1363 and IL1403 expressed in MG1363Δ*pfl*

The PFL of IL1403 (IL-PFL) and the PFL of MG1363 (MG-PFL) were expressed in MG1363Δ*pfl* to see if they behaved differently. This was done by integration of a copy of *pfl* either from MG1363 or IL1403 (MG-*pfl* or IL-*pfl*) following a SPL into the chromosome of MG1363 through the use of pLB85 (Figure 3.1). A control strain with the wild-type promoter region (WTP) followed by MG-*pfl* integrated in the same way was also constructed, called SC119. The library of clones with different expression of MG-*pfl* was called SC105 and the corresponding library of clones for IL-*pfl* was SC106.

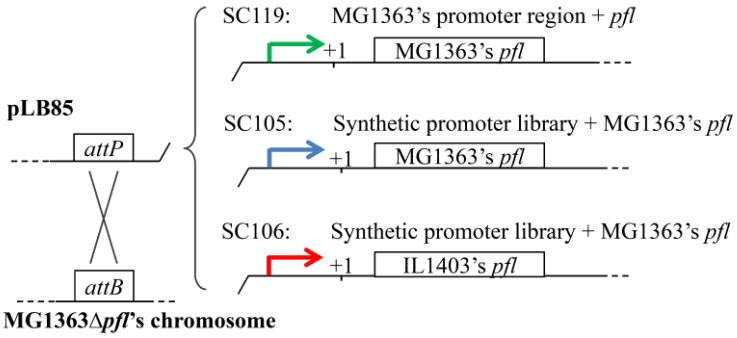

Figure 3.1. MG1363 derivatives with modulated PFL from MG1363 or IL1403.
'+1', transcription start site. The leader sequence is identical to that in MG1363's *pfl*.

The preliminary screening was done by quantifying the formate production in overnight culture of these strains (Figure 3.2). The preliminary screening showed that IL-PFL was indeed able to produce formate in significant amounts. The profile of formate production of the two libraries was very similar. Five strains from each library were selected for further characterization, named SC105a – e and

SC106a – e respectively. Growth experiments of these strains on glucose and maltose in SALN media were conducted respectively. Growth rate, production formation and *gusA* activity during exponential growth phase were measured (see Table 3.4 for all data).

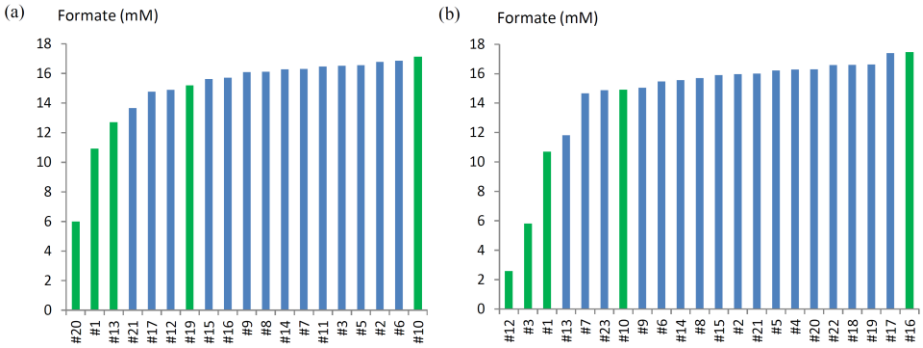

Figure 3.2. Screening of strains with modulated *pfl*.
Libraries of clones with modulated *pfl* from (a) MG1363 (library SC105) and (b) IL1403 (library SC106), respectively. Clones producing different amounts of formate in overnight cultures on maltose (in green bars) were selected for further characterization.

The *gusA* activity of the chosen strains ranged from 1 to 200 Miller units for growth on glucose and from around 10 to 400 Miller units for growth on maltose (Figure 3.3). The activity of all synthetic promoters appeared to have increased from 2- to 7-fold on maltose compared to glucose, with the fold change decreasing with the activity. The WTP in SC119 showed a 7-fold induction of activity on maltose compared to glucose, similar to the results in 1.7 (Figure 2.3). The fluxes of SC119 (Table 3.4) are also fairly comparable to the wild type MG1363 (Table 2.5).

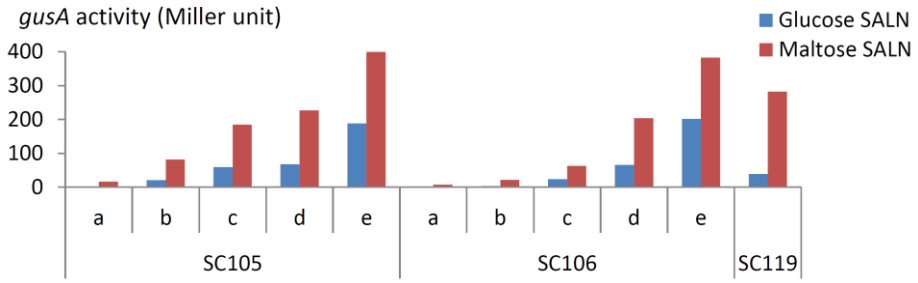

Figure 3.3. *gusA* activity of wild-type promoter and synthetic promoters.

Table 3.4. Growth data and gusA activities of SC105, SC106, SC100 and SC119.

	gusA activity (Miller unit)	Growth rate (h^{-1})	Specific rate of consumption/production (mmol h^{-1} gdw^{-1})				
			Sugar	Lactate	Formate	Acetate	Ethanol
Glucose SALN							
SC105a	2 ± 0.1	1.01 ± 0.01	23.3 ± 0.4	41 ± 0.6	-0.7 ± 0.3	1.8 ± 0.2	0.3 ± 0.1
SC105b	21 ± 0.3	1.01 ± 0.01	21.7 ± 0.6	41 ± 1.6	0.3 ± 0.1	2.4 ± 0.1	0.8 ± 0.5
SC105c	59 ± 1.1	0.98 ± 0.01	21.2 ± 1.1	40 ± 1.0	0.1 ± 0.3	3 ± 0.3	1.1 ± 0.5
SC105d	68 ± 1.2	0.98 ± 0.01	22.3 ± 0.5	38 ± 0.2	2.4 ± 0.4	2.7 ± 0.2	0.5 ± 0.05
SC105e	188 ± 3.5	0.94 ± 0.01	20.9 ± 0.5	38 ± 0.3	1.8 ± 0.5	2.9 ± 0.3	0.8 ± 0.1
SC106a	1 ± 0.1	1.01 ± 0.01	23.3 ± 0.2	41 ± 0.3	-0.7 ± 0.4	2.1 ± 0.4	0.3 ± 0.2
SC106b	3 ± 0.1	0.98 ± 0.01	23.6 ± 0.1	42 ± 0.2	-0.3 ± 0.4	1.6 ± 0	0.2 ± 0.1
SC106c	23 ± 0.4	1.00 ± 0.01	23.4 ± 0.5	41 ± 0.2	0.4 ± 0.2	2.4 ± 0.1	0.3 ± 0.1
SC106d	66 ± 2.0	0.99 ± 0.01	22.2 ± 0.7	39 ± 0.3	2.4 ± 0.5	2.8 ± 0.3	0.8 ± 0.6
SC106e	202 ± 3.7	0.91 ± 0.01	21.2 ± 0.5	38 ± 0.6	1.8 ± 0.6	2.8 ± 0.1	0.9 ± 0.2
SC100	N.D.	1.25 ± 0.03	25.0 ± 0.7	46 ± 1.3	-0.4 ± 0.1	1 ± 0.1	0.2 ± 0.1
SC119	39 ± 2.0	1.02 ± 0.02	23.2 ± 0.8	39 ± 1.1	1.8 ± 0.5	2.2 ± 0.2	N.D.
Maltose SALN							
SC105a	17 ± 0.4	0.43 ± 0.01	5.8 ± 0.8	20 ± 1.4	1.5 ± 0.2	2.2 ± 0.21	N.D.
SC105b	82 ± 2.8	0.50 ± 0.01	6.8 ± 0.6	18 ± 1.1	7.5 ± 0.4	5.1 ± 0.28	2.4 ± 0.4
SC105c	185 ± 1.5	0.54 ± 0.01	7.6 ± 0.5	16 ± 1.2	11 ± 0.7	7.1 ± 0.41	3.8 ± 0.6
SC105d	227 ± 2.8	0.56 ± 0.01	7.2 ± 0.6	13 ± 0.8	14 ± 0.9	8.8 ± 0.51	4.5 ± 0.7
SC105e	399 ± 15	0.59 ± 0.01	7.0 ± 0.6	10 ± 0.6	18 ± 1.1	11 ± 0.59	6.5 ± 0.8
SC106a	7 ± 0.2	0.39 ± 0.01	6.5 ± 0.6	19 ± 1.7	0.5 ± 0.1	1.3 ± 0.12	N.D.
SC106b	21 ± 1.6	0.41 ± 0.01	6.6 ± 0.5	20 ± 1.2	2.1 ± 0.3	2.2 ± 0.22	0.2 ± 0.5
SC106c	63 ± 1.9	0.49 ± 0.02	7.4 ± 0.9	20 ± 1.7	5.6 ± 0.5	4.9 ± 0.41	1.2 ± 0.8
SC106d	203 ± 8.9	0.56 ± 0.01	7.7 ± 0.6	14 ± 0.7	14 ± 0.8	8.6 ± 0.45	4.8 ± 1.3
SC106e	383 ± 17	0.59 ± 0.01	7.5 ± 0.1	11 ± 0.3	16 ± 0.4	10 ± 0.15	5.4 ± 0.2
SC100	N.D.	0.40 ± 0.02	7.5 ± 1.0	21 ± 2.3	-0.5 ± 0.1	0.5 ± 0.11	0.2 ± 0
SC119	282 ± 30	0.62 ± 0.01	8.0 ± 0.3	11 ± 1.0	17.3 ± 0.8	11 ± 1.02	5.9 ± 1.5

SC100, a *pfl*-deleted strain; SC105, strains SPL-MG-PFL; SC106, strains with SPL-IL-PFL; SC119, a strain with WTP-MG-PFL. N.D., not detectable.

3.3.2 Flux control by *pfl* expression level

Formate flux controlled by pfl expression

How the level of *pfl* expression controls the growth rate and different fluxes was investigated. An obvious question is the effect of *pfl* expression on formate production. For growth on glucose, the formate flux appeared to increase initially with *pfl* expression but decrease at high expression levels (SC105e and SC106e, see Figure 3.4a). The level of *pfl* expression level in the wild-type MG1363 and IL1403 might be estimated from the flux-response curve by comparing the formate fluxes in the wild types under the assumption that the formate flux responds to change in *pfl* expression similarly in IL1403. From the similar wild-type flux levels (from Table 2.5), similar *pfl* expression level was

suggested flux and control coefficients (FCCs) between 0.78 and 0.84 were estimated from curve fitting (Figure 3.4a(ii)).

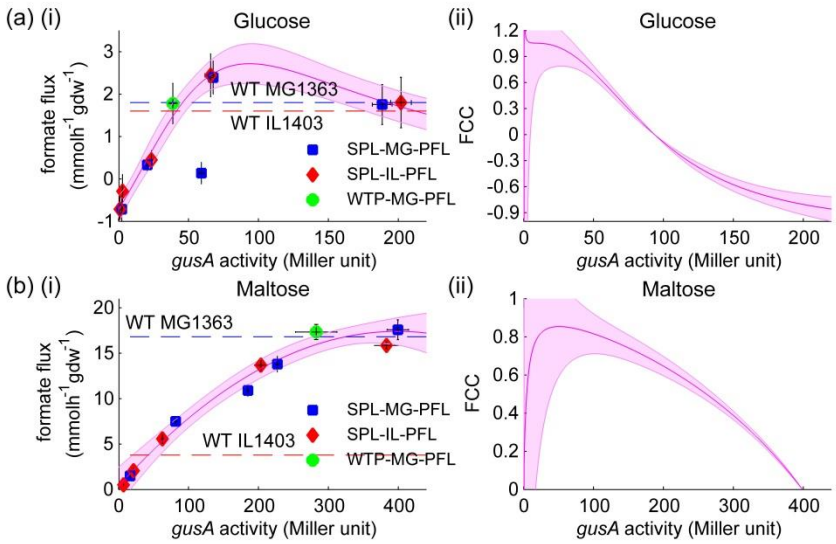

Figure 3.4. Dependence of formate flux on *pfl* expression.

SC105 (SPL-MG-PFL) (blue square), SC106 (SPL-IL-PFL) (red diamond), and SC119 (WTP-MG-PFL) (green circle) growing on (a) glucose or (b) maltose. (i) Formate flux and the derived (ii) flux control coefficient (FCC) plotted against *pfl* expression level. The fluxes in the wild-type IL1403 and MG1363 were provided for reference. SPL, synthetic promoter library; WTP, wild-type *pfl* promoter in MG1363.

For growth on maltose, a clear increasing trend of formate flux from 0 to ≈20 mmol $h^{-1}gdw^{-1}$ along with the increase of *pfl* expression level was observed (Figure 3.4b(i)). *pfl* expression in MG1363 and IL1403 estimated from the flux values and the flux-response curve was largely different from each other (≈340 and ≈40 Miller units respectively). The FCC decreases from 0.85 at the estimated wild-type IL1403's level to 0.31 at the estimated wild-type MG1363's level (Figure 3.4b(ii)).

Acetate fluxes controlled by PFL

Similar trends were observed for acetate production. Acetate flux increased initially but reached the apparent maximum level at ≈60 Miller units of *gusA* activity for growth on glucose while it kept increasing significantly for growth on maltose (Figure 3.5). The FCCs estimated for the glucose case are close to 0 and 0.19 for IL1403 and MG1363 respectively. The corresponding estimation for the maltose case is 0.52 and 0.33 respectively. It should be remarked, however, that the estimation is not consistent with the estimation from the formate flux data because different *pfl* expression levels reflected by *gusA* activity were estimated from data of different production fluxes. The issue will be discussed in later sections.

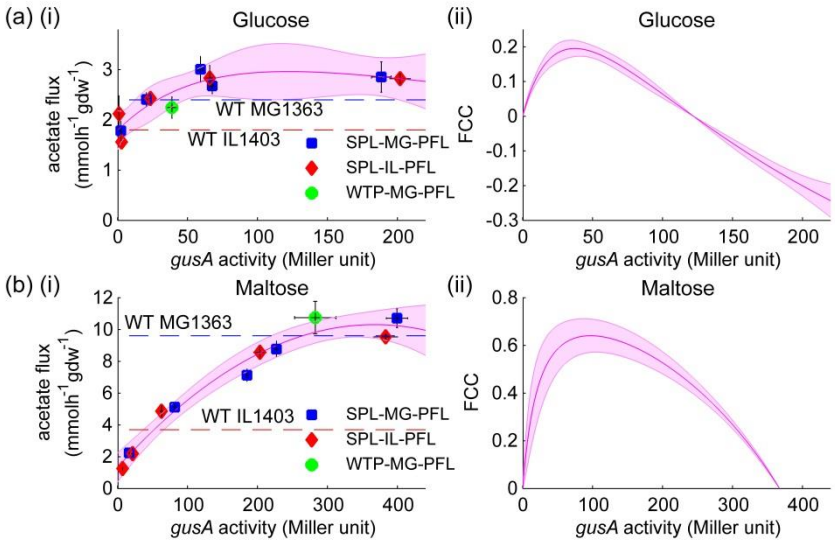

Figure 3.5. Dependence of acetate flux on *pfl* expression.

SC105 (SPL-MG-PFL), SC106 (SPL-IL-PFL), and SC119 (WTP-MG-PFL) growing on (a) glucose or (b) maltose. (i) Acetate flux and the derived (ii) FCC plotted against *pfl* expression level. The fluxes in the wild-type IL1403 and MG1363 were provided for reference. SPL, synthetic promoter library; WTP, wild-type *pfl* promoter in MG1363.

Ethanol fluxes controlled by PFL

Regarding ethanol production, for growth on glucose, no clear trend could be observed and the relative error of estimation of fluxes was large at such low values (Figure 3.6). For growth on maltose, an increasing pattern of ethanol flux along with the *pfl* expression level was observed. The estimated curve for FCC decreased from infinity initially because no ethanol production was observed at small positive *gusA* activities. The FCC tends to infinity when the value of the flux function approaches zero.

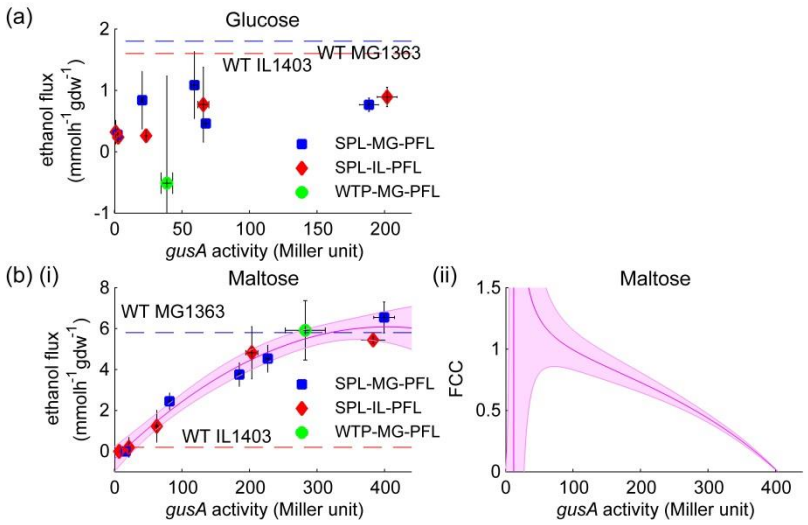

Figure 3.6. Dependence of ethanol flux on *pfl* expression.

SC105 (SPL-MG-PFL), SC106 (SPL-IL-PFL), and SC119 (WTP-MG-PFL) growing on (a) glucose or (b) maltose. (i) Ethanol flux and the derived (ii) FCC plotted against *pfl* expression level. The fluxes in the wild-type IL1403 and MG1363 were provided for reference. SPL, synthetic promoter library; WTP, wild-type *pfl* promoter in MG1363.

Negative control of lactate production by PFL

In contrast to the generally positive control of the mixed acids by PFL, lactate flux was found to be negatively controlled by *pfl* expression with a very small magnitude of negative FCC in the glucose case and a larger magnitude in the maltose case (Figure 3.7). Beside the flux control, it can also be seen that the wild-type lactate fluxes were out of the range of those of modulated strains in the glucose case. For growth on maltose, it is in particular interesting that the lactate flux of IL1403 (34 $mmolh^{-1}gdw^{-1}$) was almost 2-fold higher than all other strains, including strains with very low *gusA* activities (SC105a, SC106a, 20 $mmolh^{-1}gdw^{-1}$) and even the *pfl*-deletion strain (SC100, 21 $mmolh^{-1}gdw^{-1}$).

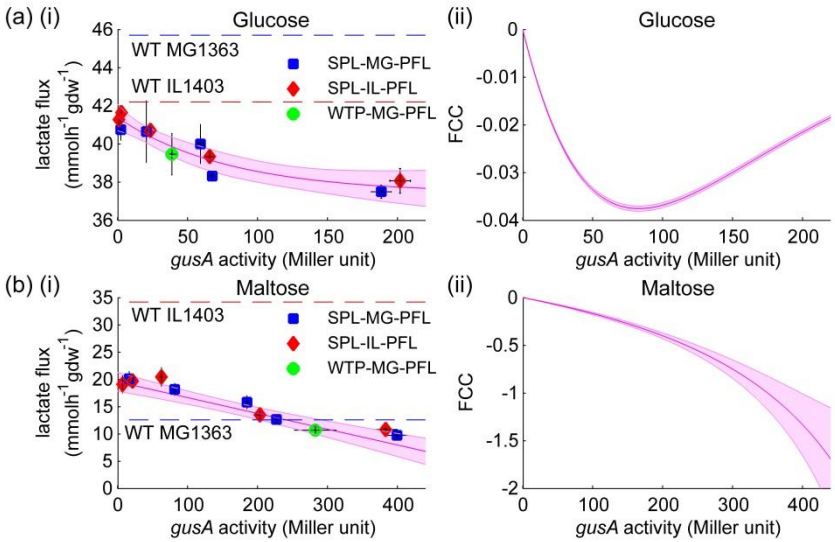

Figure 3.7. Dependence of lactate flux on *pfl* expression.

SC105 (SPL-MG-PFL), SC106 (SPL-IL-PFL), and SC119 (WTP-MG-PFL) growing on (a) glucose or (b) maltose. (i) Lactate flux and the derived (ii) FCC plotted against *pfl* expression level. The fluxes in the wild-type IL1403 and MG1363 were provided for reference. SPL, synthetic promoter library; WTP, wild-type *pfl* promoter in MG1363.

Control of glycolytic flux

The specific consumption rate of glucose roughly decreased with *pfl* expression with very low FCCs ranging from -0.04 to -0.01 (Figure 3.8). The corresponding values for IL1403 and MG1363 are apparently above those of modulated strains. For growth on maltose, the maximum glycolytic flux (with zero FCC) appeared to occur at an intermediate level of *pfl* expression, close to the level of SC119 which contained WTP-MG-PFL integrated in the attachment site *attB*. This maximum also almost coincides with the flux in MG1363. Consistent to the significantly higher lactate flux in the homolactic IL1403, the maltose flux was also substantially higher than all other strains.

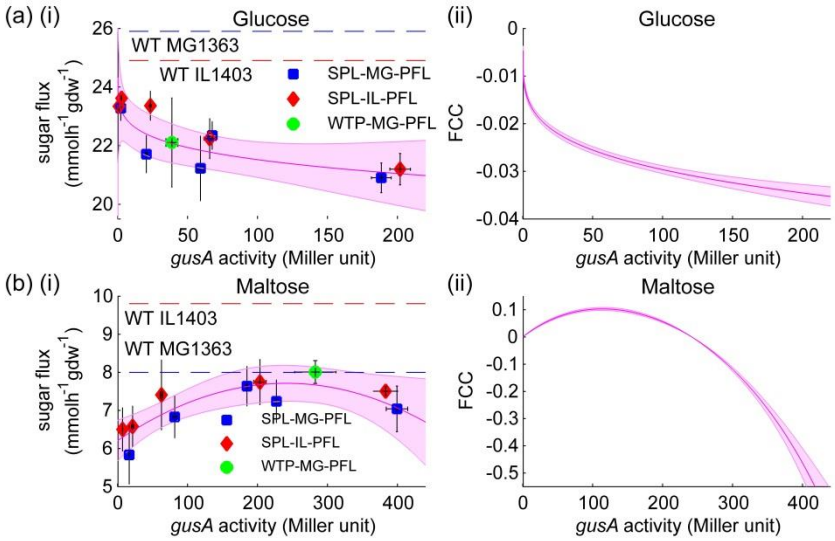

Figure 3.8. Dependence of glycolytic flux on *pfl* expression.

SC105 (SPL-MG-PFL), SC106 (SPL-IL-PFL), and SC119 (WTP-MG-PFL) growing on (a) glucose or (b) maltose. (i) Glycolytic flux and the derived (ii) FCC plotted against *pfl* expression level. The fluxes in the wild-type IL1403 and MG1363 were provided for reference. SPL, synthetic promoter library; WTP, wild-type *pfl* promoter in MG1363.

Maximum growth rate near the wild-type pfl level

For growth on glucose, the growth rate appeared to be quite constant at a level of ≈1 h^{-1} for *gusA* activity ≤ 70 Miller units and then started to drop, resulting in a curve of negative FCC (Figure 3.9). This includes the strain SC119 with WTP-MG-PFL. When the strains were grown on maltose, in contrast, a significant positive control of growth rate by *pfl* expression was observed initially and the maximum was then attained, also close to the level of SC119 which also had a growth rate very similar to the wild-type MG1363 (0.61 h^{-1}). The FCC therefore approached zero and became negative at higher *pfl* expression levels, corresponding to decreased growth rates in SC105e and SC106e. The growth rate of IL1403 is similar to that of strains with lowest *pfl* expression (SC105a, SC106a – b).

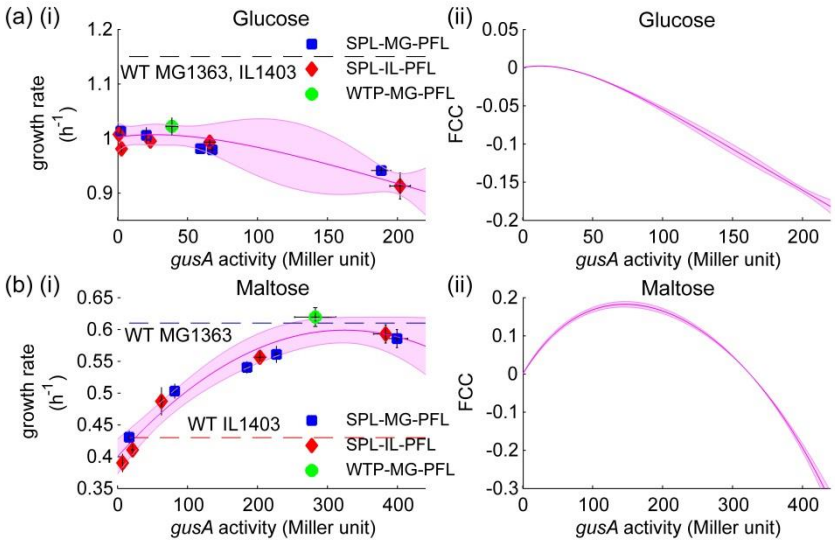

Figure 3.9. Dependence of growth rate on *pfl* expression.

SC105 (SPL-MG-PFL), SC106 (SPL-IL-PFL), and SC119 (WTP-MG-PFL) growing on (a) glucose or (b) maltose. (i) Growth rate and the derived (ii) FCC plotted against *pfl* expression level. The growth rates in the wild-type IL1403 and MG1363 were provided for reference. SPL, synthetic promoter library; WTP, wild-type *pfl* promoter in MG1363.

3.3.3 Yield on sugars

We also looked into the biomass and product yield on sugars (Figure 3.10). The patterns are in general very similar to the case of fluxes reported above. Here, however, several points not revealed by flux comparison are worth noting. First, for growth on glucose, the wild-type MG1363 and IL1403 showed higher growth rates, higher lactate fluxes than all other strains but their biomass and lactate yields on glucose indeed lied within the range of other strains (Figure 3.10a – b). Second, the biomass and lactate yield on glucose did not change significantly. Third, interestingly, SC119 containing WTP-MG-PFL did not have the highest biomass yield and the highest acetate yield which probably reflects the ATP yield although the strain had the apparently highest growth rate. MG1363 also had a slightly lower biomass and acetate yields than strains with highest *pfl* expression. The significance of this observation is discussed in the next section.

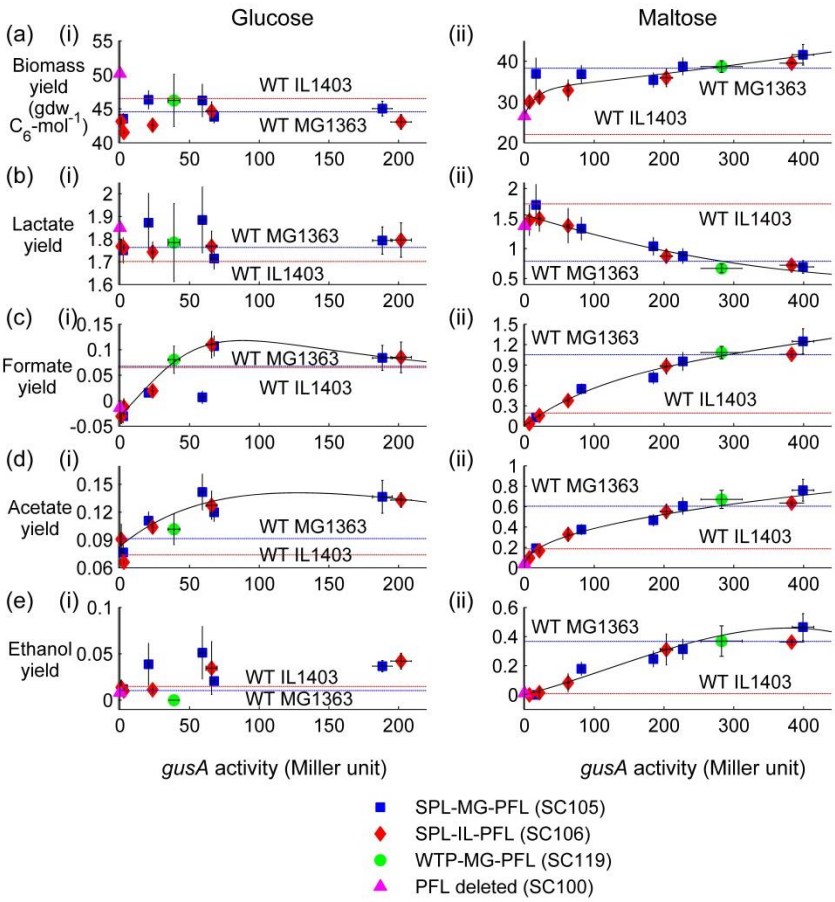

Figure 3.10. Biomass and product yield on sugars.

The (a) biomass, (b) lactate, (c) formate, (d) acetate and (e) ethanol yield on sugars for SC105 (SPL-MG-PFL) (blue square), SC106 (SPL-IL-PFL) (red diamond), SC119 (WTP-MG-PFL) (green circle) and SC100 (*pfl* deletion) (magenta triangle) growing on (i) glucose or (ii) maltose. Yields were calculated as growth rates or product fluxes divided by sugar fluxes in C_6 unit. The corresponding levels of MG1363 and IL1403 are marked by blue and red lines respectively.

SPL, synthetic promoter library; WTP, wild-type *pfl* promoter in MG1363.

3.3.4 Loss of formate-producing ability during the modulation of *pfl* in IL1403

To modulate *pfl* expression in IL1403, the reporter gene *gusA* following a proper leader sequence was inserted immediately after the native *pfl* in IL1403, resulting in the strain SC183 which produced blue spots on agar plates with X-gluc. The fragment from the *pfl* sequence to the region downstream of *pfl* used for the deletion by double crossover, including the inserted *gusA* in between, was confirmed to be correct by DNA sequencing. Then the plasmid pRC1-SPL-IL*pfl* was used to modulate *pfl* by integrating a SPL preceding *pfl* by a single-crossover event. A library of 9 strains, the SC193 series, was isolated. Preliminary tests on the formate-producing ability of SC183 and SC193 library, nonetheless, showed no formate production in all strains. The full copy of *pfl* in each strain and additionally the wild-type promoter region in SC183 were sequenced but no any mutation could be found (data not shown). The strains were therefore not further characterized. The possible reasons were discussed in the next section.

3.4 Discussion

3.4.1 Similar behaviour of MG-PFL and IL-PFL when expressed in MG1363

For testing the functionality of IL-PFL, both MG-PFL and IL-PFL were expressed in MG1363 where the native *pfl* had been deleted. The expression made used of the site-specific integration system at the attachment site using pLB85. The reporter gene *gusA* present on pLB85 could serve as an indicator of the expression level of *pfl* as an alternative to measure PFL activity directly which is not straightforward because of the extreme sensitivity of PFL toward oxygen [10]. Results of growth characterization indicated that the control of formate flux by both MG-PFL and IL-PFL was very similar. The change in growth rate and flux distribution in response to the change in MG-*pfl* and IL-*pfl* expression level were also very much alike. This suggested that IL-PFL should also be able to function properly in IL1403 provided that the PFL activating enzyme (PFL-AE) also expresses and functions properly in IL1403.

3.4.2 Flux control by PFL in MG1363

For growth on glucose, the growth rate, lactate flux and glycolytic flux were all negatively controlled by PFL, with very small negative FCCs (-0.04 ~ 0) at the estimated wild-type *pfl* levels for MG1363 and IL1403 respectively. Formate and acetate production fluxes meanwhile were positively controlled by PFL. The sum of FCCs for a flux by all enzymes is equal to 1 by the summation theorem of FCCs. Since previous studies found the FCC for formate flux by LDH and PYK is close to -1 and 1 respectively [11, 12]. The sum of FCCs of the rest of the reactions should be about 1, which is close to the value found for PFL. The sum of FCCs by enzymes other than LDH, PYK and PFL should thus be close to zero.

For growth on maltose, PFL appeared to have negative control on only lactate flux with FCC being close to zero (-0.06 ~ -0.04) and -0.6 ~ -0.7 at the estimated *pfl* levels for IL1403 and MG1363 respectively. Mixed-acid fluxes were positively controlled by PFL whereas the growth rate and glycolytic flux increased initially along *pfl* expression but decreased at larger levels after the maximum. The estimated FCCs were summarized in Table 3.5.

It should be noted again that the estimation of FCCs is dependent on the choice of fitted curves. In this study, general functions (exponential, power, rational, polynomial) were adopted and best fits in terms of lowest sum of squared residuals, highest coefficient of determination and fewer parameters were chosen. Some variations to the selected curves, however, can still be intuitively possible in some cases by looking at the plots. For example, for the formate and ethanol fluxes in the maltose case, good fits with more paramters registering maximum values at levels close to SC119 are also plausible. Similarly a curve fitting the lactate fluxes for growth on maltose with a minimum point attained at a level close to SC119 is another choice. This different selection of curves can lead to the conclusion of zero flux control by PFL on formate, ethanol and lactate flux at the wild-type level. More strains from

the libraries with *gusA* activity in the range of the estimated wild-type levels are required to be characterized for more accurate estimation.

Table 3.5. Estimated flux control coefficients (FCCs) at the wild-type *pfl* level.

		Glucose		Maltose	
		MG136	IL1403	MG1363	IL1403
Estimated relative *pfl* expression level in wild types (gusA activity in Miller unit)		30 ~ 40	30 ~ 40	270 ~ 290	30 ~ 40
FCC at the estimated wild-type level	Growth rate	-0.006 ~ -0.001		0.06 ~ 0.09	0.08 ~ 0.10
	Sugar	-0.02		-0.05 ~ -0.10	0.05 ~ 0.06
	Lactate	-0.03		-0.71 ~ -0.63	-0.06 ~ -0.04
	Formate	0.88 ~ 1.02		0.42 ~ 0.48	0.83 ~ 0.85
	Acetate	0.19		0.30 ~ 0.36	0.49 ~ 0.55
	Ethanol	/		0.47 ~ 0.53	1.38 ~ 1.63

3.4.3 Rate or yield optimization

An interesting observation from comparing flux and yield is that optimal growth rate in the wild-type MG1363 occurred at a sub-optimal growth yield and a sub-optimal ATP yield on maltose (positively correlated to acetate yield, assuming all sugar is converted into pyruvate in glycolysis). Homolactic fermentation has a lower ATP yield than mixed-acid fermentation and has been known to be out of the prediction by the well-known flux balance analysis (FBA) using genome-scale metabolic model if additional capacity constraints on flux were not added [13]. It is because FBA is in principle a method of yield optimization which, given the biomass reaction as the objective function, always selects a flux distribution with highest biomass yield and may not coincide with the flux distribution maximizing the true growth rate [14, 15]. The observation here apparently corresponds to this case, even happening in growth on maltose where ATP production rate should be the growth-limiting factor.

The data of the control strain SC119 with WTP-MG-PFL further supported this observation. SC119 was constructed in the same way as other strains with SPL-MG-PFL or SPL-IL-PFL. It behaved very similarly to the wild-type MG1363 for growth on maltose and had a *gusA* activity and biomass yield lower than SC105e and SC106e but still grew faster.

3.4.4 Comparison to previous results

Control of the shift from homolactic to mixed-acid fermentation in MG1363 has been demonstrated by Melchiorsen et al. (2002) [1]. In their study, similar pattern of flux control by PFL was observed. There are still several points of difference in our study. First, the functionality of IL-PFL was also tested and compared to MG-PFL. Second, the construction method was different from the previous study. In the previous study, two replicating plasmids expressing *pfl* with promoters of different strength were respectively transformed into MG1363 and a *pfl*-deleted strain. Multiple copies of *pfl*

were thus present in the constructed strains. In this study, all tested strains were constructed by site-specific chromosomal integration of *pfl* with synthetic promoters into SC100, ensuring a single copy on the chromosome. This precluded possible phenotypic differences brought by the existence of multiple copies of *pfl* and replicating plasmids. An obvious one is the more cellular resource spent on their replication. Third, we attempted to look into the control of different fluxes by estimating the flux control coefficients.

3.4.5 Unsuccessful modulation of *pfl* in IL1403

The absence of formate production in SC183 and the SC193 series suggested that PFL in these strains were not functional. The obvious possibility of mutation in the coding region and promoter region of *pfl* in SC183 was ruled out by sequencing. The lack of formate production might therefore be the result of mutation in PFL-activating enzyme (PFL-AE) which is required for PFL activity or other unknown reasons.

The results suggested that inserting *gusA* after *pfl* might be detrimental. Indeed, we also attempted to transform pLB85-SPL-IL*pfl* into IL1403 but no blue colonies on agar plates with X-gluc could be seen. A probable effect of inserting *gusA* into the transcription unit of *pfl* is increase in the transcription of *pfl* due to the increased mRNA stability of the longer transcript. This is supported by the ≈4-fold increase in *gusA* activity in strain SC119 compared to LB436/MG*pfl* (Table 2.4) when growing on either glucose or maltose (Figure 2.3 in Chapter 2 and Table 3.4). In both strains, the transcription of *gusA* is induced by the *pfl* promoter in MG1363. The difference lies in that in SC119 *gusA* is the second gene in an operon after *pfl* whereas the *gusA* in LB436/MG*pfl* directly follows the promoter.

If this is true, then this implied that significant overexpression of PFL in IL1403 might be lethal. The reason for IL1403 unfavorable of overexpressing PFL remains unknown. One possibility is the non-functionality of alcohol dehydrogenase downstream of PFL causing redox imbalance after PFL converts too much of the pyruvate into acetyl-CoA.

3.4.6 Possible reasons for the low formate production in IL1403

Different properties of IL-PFL and MG-PFL originating from the difference in the amino acid sequences is one of the possible causes for the lower formate production in IL1403. It has however been ruled out by the present study. Several other reasons for the low PFL activity in IL1403 are possible.

First, the PFL activating enzyme (PFL-AE) encoded by *pflA* might not be expressed sufficiently or not function properly in IL1403. It has long been known that PFL in *E. coli* requires activation by PFL-AE for catalytic activity [16] to protect PFL from irreversible oxygen cleavage [17]. Similar mechanisms activating PFL has been observed in *L. lactis* [10] and demonstrated *in vitro* using PFL

and PFL-AE from the closely related *Streptococcus mutans* [18, 19]. A study even showed that overexpressing PFL and PFL-AE simultaneously increased the formate-to-lactate ratio significantly in *Streptococcus bovis* [20].

Second, PFL might be expressed at a lower quantity in IL1403 as suggested by the study on promoter activity (Figure 2.3, Chapter 2) and the unsuccessful modulation of PFL in IL1403 suggested a high expression of IL1403 was probably unfavourable, unlike the case of MG1363.

Third, the flux might be controlled by other enzymes or regulated at the metabolic level. For example, the bi-functional alcohol dehydrogenase (ADH) in IL1403 might be defective or not expressed, as suggested in [21] (significant transcript abundance but low activity) and the close-to-zero ethanol production in our data (Table 2.5, Chapter 2). If this is the case, then the low PFL activity could be a result of metabolic regulation following the model proposed by Garrigues et al. [22]. Since one $NADH^+$ is not reduced for each pyruvate converted into acetate through PFL, phosphotransacetylase and acetate kinase in the absence of ADH activity, $NADH^+$ would accumulate and inhibit Glyceraldehyde 3-phosphate dehydrogenase (GAPDH). This would cause a large triose-phosphate pool which inhibits PFL. In this case, ADH or other NAD^+-producing enzymes are expected to have control on the formate flux. Interestingly, in this sense, the regulation of PFL by triose-phosphate can be a vital trait to prevent glycolysis from termination due to lack of NAD^+ regeneration during acetate production. This question can be answered by studying the evolutionary sequences of different fermentation enzymes and the regulatory mechanisms.

It should be noted that these possibilities are not mutually exclusive. Indeed, the first and second cases may be the evolutionary consequences of the third if the third is true.

3.5 Acknowledgement

We thank Jun Chen for help with constructing the strain MG1363Δ*pfl*.

3.6 References

1. Melchiorsen CR, Jokumsen KV, Villadsen J, Israelsen H, Arnau J (2002) The level of pyruvate-formate lyase controls the shift from homolactic to mixed-acid product formation in *Lactococcus lactis*. *Appl Microbiol Biotechnol* 58:338–44.
2. Solem C, Defoor E, Jensen PR, Martinussen J (2008) Plasmid pCS1966, a new selection/counterselection tool for lactic acid bacterium strain construction based on the oroP gene, encoding an orotate transporter from *Lactococcus lactis*. *Appl Environ Microbiol* 74:4772–5.
3. Maguin E, Duwat P, Hege T, Ehrlich D, Gruss A (1992) New thermosensitive plasmid for gram-positive bacteria. *J Bacteriol* 174:5633–8.
4. Bourgeois P Le, Lautier M, Mata M, Ritzenthaler P, Le Bourgeois P (1992) New tools for the physical and genetic mapping of *Lactococcus* strains. *Gene* 111:109–14.
5. Casadaban MJ, Cohen SN (1980) Analysis of gene control signals by DNA fusion and cloning in *Escherichia coli*. *J Mol Biol* 138:179–207.
6. Greener A (1993) Expand your library by retrieving toxic clones with ABLE strains. *Strategies* 6:7–9.
7. Brøndsted L, Hammer K (1999) Use of the integration elements encoded by the temperate lactococcal bacteriophage TP901-1 to obtain chromosomal single-copy transcriptional fusions in *Lactococcus lactis*. *Appl Environ Microbiol* 65:752–758.

8. Gasson MJ (1983) Plasmid complements of *Streptococcus lactis* NCDO 712 and other lactic streptococci after protoplast-induced curing. *J Bacteriol* 154:1–9.
9. Chopin A, Chopin MC, Moillo-Batt A, Langella P (1984) Two plasmid-determined restriction and modification systems in *Streptococcus lactis*. *Plasmid* 11:260–263.
10. Melchiorsen CR et al. (2000) Synthesis and posttranslational regulation of pyruvate formate-lyase in *Lactococcus lactis*. *J Bacteriol* 182:4783–4788.
11. Andersen HW, Pedersen MB, Hammer K, Jensen PR (2001) Lactate dehydrogenase has no control on lactate production but has a strong negative control on formate production in *Lactococcus lactis*. *Eur J Biochem* 268:6379–6389.
12. Koebmann B, Solem C, Jensen PR (2005) Control analysis as a tool to understand the formation of the las operon in *Lactococcus lactis*. *FEBS J* 272:2292–303.
13. Oliveira AP, Nielsen J, Förster J (2005) Modeling *Lactococcus lactis* using a genome-scale flux model. *BMC Microbiol* 5:39.
14. Schuster S, Pfeiffer T, Fell D a (2008) Is maximization of molar yield in metabolic networks favoured by evolution? *J Theor Biol* 252:497–504.
15. Teusink B et al. (2006) Analysis of growth of Lactobacillus plantarum WCFS1 on a complex medium using a genome-scale metabolic model. *J Biol Chem* 281:40041–8.
16. Knappe J et al. (1969) Pyruvate formate-lyase reaction in *Escherichia coli*: the enzymatic system converting an inactive form of the lyase into the catalytically active enzyme. *Eur J Biochem* 11:316–327.
17. Zhang W, Wong KK, Magliozzo RS, Kozarich JW (2001) Inactivation of pyruvate formate-lyase by dioxygen: defining the mechanistic interplay of glycine 734 and cysteine 419 by rapid freeze-quench EPR. *Biochemistry* 40:4123–30.
18. Yamamoto Y, Sato Y, Takahashi-Abbe S, Takahashi N, Kizaki H (2000) Characterization of the *Streptococcus* mutans pyruvate formate-lyase (PFL)-activating enzyme gene by complementary reconstitution of the *in vitro* PFL-reactivating system. *Infect Immun* 68:4773–4777.
19. Takahashi-Abbe S, Abe K, Takahashi N (2003) Biochemical and functional properties of a pyruvate formate-lyase (PFL)-activating system in *Streptococcus* mutans. *Oral Microbiol Immunol* 18:293–297.
20. Asanuma N, Hino T (2002) Molecular characterization and expression of pyruvate formate-lyase-activating enzyme in a ruminal bacterium, *Streptococcus* bovis. *Appl Environ Microbiol* 68:3352–3357.
21. Even S, Lindley ND, Cocaign-Bousquet M (2001) Molecular physiology of sugar catabolism in *Lactococcus lactis* IL1403. *J Bacteriol* 183:3817–24.
22. Garrigues C, Mercade M, Cocaign-Bousquet M, Lindley ND, Loubiere P (2001) Regulation of pyruvate metabolism in *Lactococcus lactis* depends on the imbalance between catabolism and anabolism. *Biotechnol Bioeng* 74:108–15.

Chapter 4. Acetate kinase isozymes confer robustness in acetate metabolism

Published in PLoS ONE (Public Library of Science), 9(3): e92256, doi:10.1371/journal.pone.0092256. Reprinted with permission.

Siu Hung Joshua Chan, Lasse Nørregaard, Christian Solem, Peter Ruhdal Jensen

4.1 Abstract

Acetate kinase (ACK) (EC no: 2.7.2.1) interconverts acetyl-phosphate and acetate to either catabolize or synthesize acetyl-CoA dependent on the metabolic requirement. Among all ACK entries available in UniProt, we found that around 45% are multiple ACKs in some organisms including more than 300 species but surprisingly, little work has been done to clarify whether this has any significance. In an attempt to gain further insight we have studied the two ACKs (AckA1, AckA2) encoded by two neighboring genes conserved in *Lactococcus lactis* (*L. lactis*) by analyzing protein sequences, characterizing transcription structure, determining enzyme characteristics and effect on growth physiology. The results show that the two ACKs are most likely individually transcribed. AckA1 has a much higher turnover number and AckA2 has a much higher affinity for acetate *in vitro*. Consistently, growth experiments of mutant strains reveal that AckA1 has a higher capacity for acetate production which allows faster growth in an environment with high acetate concentration. Meanwhile, AckA2 is important for fast acetate-dependent growth at low concentration of acetate. The results demonstrate that the two ACKs have complementary physiological roles in *L. lactis* to maintain a robust acetate metabolism for fast growth at different extracellular acetate concentrations. The existence of ACK isozymes may reflect a common evolutionary strategy in bacteria in an environment with varying concentrations of acetate.

4.2 Introduction

There are many examples where products of metabolism are excreted and later re-assimilated by organisms, e.g. acetate (OAc) in *E. coli* [1] and ethanol in yeast [2]. The ability to switch between dissimilation and assimilation of the same metabolite is an important trait for maximizing growth in a changing environment. The acetate switch is a prominent example of this type of behavior. Acetate is one of the main metabolic products, and re-assimilation happens in order to exploit an available carbon source for further biomass formation after the primary carbon source has been depleted. A general review of the switch in acetate metabolism can be found in Wolfe [3].

Lactococcus lactis (*L. lactis*) is an important Gram-positive model organism which belongs to the group of Lactic Acid Bacteria (LAB) and is widely used in cheese production. In *L. lactis*, acetate may also be excreted or assimilated, depending on the environmental conditions. Figure 4.1 summarizes the relevant metabolic reactions. Under anaerobic conditions *L. lactis* produces mainly lactate as well as formate, ethanol and acetate. The amounts of formate, ethanol and acetate become very significant when growth depends on slowly fermentable sugars like maltose and galactose [4]. Acetate can also be a precursor of Ac-CoA which is vital to *L. lactis* because Ac-CoA is a precursor in fatty acid biosynthesis [5], cysteine biosynthesis [6] and peptidoglycan biosynthesis [7], etc. Acetate is required for growth when other routes to Ac-CoA are blocked. In *L. lactis* there are three known pathways leading to Ac-CoA, including the pyruvate dehydrogenase complex (PDHc), pyruvate formate lyase (PFL) and phosphotransacetylase (PTA) in conjunction with acetate kinase (ACK) (Figure 4.1). PDHc is mainly active under aerobic conditions in the presence of the cofactor lipoic acid. Under strict anaerobiosis, PDHc was shown to have low activity [8] and growth depends on PFL in the absence of acetate [9], [10]. PFL is active only anaerobically due to inactivation by oxygen [11]. The PTA-ACK pathway, which converts acetate into Ac-CoA, can support growth when PDHc and PFL are both inactive provided that acetate is added to the media. If all the three known pathways leading to Ac-CoA are blocked, *L. lactis* is unable to grow [9]. A gene predicted to encode either the AMP-forming Ac-CoA synthetase (ACS) (which is important for Ac-CoA production from acetate in *E. coli* [3]) or acyl-CoA synthetase is also present in some *L. lactis* strains but no ACS activity has been reported. There are no other annotated genes in *L. lactis* encoding enzymes known to catalyze the conversion between Ac-CoA and acetate.

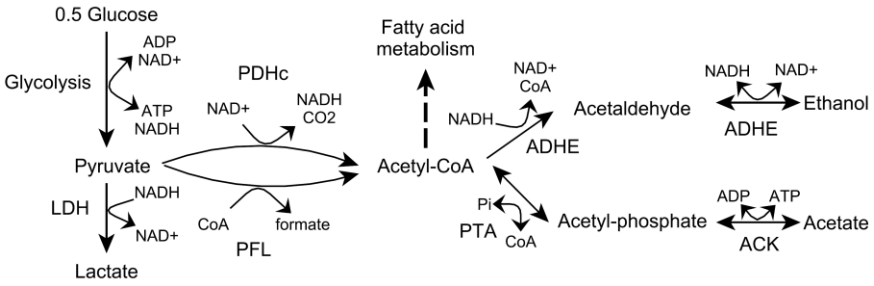

Figure 4.1. Pyruvate and Ac-CoA metabolism.

Pi: inorganic phosphate. CO_2: carbon dioxide. Enzyme names are in bold. LDH: lactate dehydrogenase. PFL: pyruvate formate lyase. PHDc: pyruvate dehydrogenase complex. PTA: phosphotransacetylase. ACK: acetate kinase. ADHE: bi-functional alcohol dehydrogenase. doi:10.1371/journal.pone.0092256.g001

Interestingly, in all available sequenced genomes of *L. lactis*, two well conserved neighboring homologous genes are predicted to encode ACK. A further search on all available ACK sequences shows that in fact >300 species have multiple ACKs, including some other LAB species. The

prevalence suggests a plausible advantage conferred by multiple ACK genes to *L. lactis* and other bacteria. In the literature, the kinetics and mechanism of ACK have long been a subject of study. The kinetics of ACK among different organisms has been characterized, e.g. [12]–[15]. Crystallographic studies, site-specific mutagenesis and sequence comparisons have revealed sites important for substrate binding and catalysis, e.g. [13], [16]–[19]. Several reaction mechanisms have also been proposed [20]–[22]. Despite the massive amount of literature on ACK, surprisingly, little work has been done on ACK isozymes which exist in many species, with the exception of one kinetic study in a spirochete [23].

In the hope of revealing the significance of ACK isozymes, in this study we investigated the two ACKs in *L. lactis* by sequence analysis, characterization of transcription structure, enzyme activity and effect on growth physiology.

4.3 Materials and methods

4.3.1 Bacterial strains and plasmids

All the *L. lactis* strains involved in this study were derived from the plasmid-free laboratory strain *L. lactis subsp. cremoris* MG1363 [24]. For overexpression of ACKs, *E. coli strain* M15 pREP4 groESL [25] was used. The plasmid pCS1966 containing genes encoding erythromycin resistance and an orotate transporter was used for markerless gene inactivation in *L. lactis* [26]. The plasmids pLB65, harboring a gene encoding a site-specific integrase, and pLB85, containing the *gusA* reporter gene and a gene encoding erythromycin resistance, were used for constructing strains needed for *in vivo* promoter strength assessment [27]. The primers, plasmids and strains used in the study are listed in Table B.1,Table B.2 and Table B.3 respectively.

4.3.2 Antibiotics

When needed erythromycin was added at 5 μg ml^{-1} for *L. lactis*. Ampicillin and kanamycin were applied at 100 μg ml^{-1} and 25 μg ml^{-1} respectively for *E. coli*.

4.3.3 Culture media and growth conditions

E. coli was grown aerobically at 37°C in Lysogeny Broth (LB). *L. lactis* strains were cultivated at 30°C without aeration in M17 broth supplemented with 2 g L^{-1} of glucose or in chemically defined SA medium [28] devoid of acetate and supplemented with 2 g L^{-1} of maltose (MSA). *L. lactis* growth experiments were carried out in flasks at 30°C under static conditions with slow stirring and optical density at 600 nm (OD_{600}) was measured regularly. As inoculum an over-night exponentially growing culture in the same medium was used and the start $OD_{600}\approx0.02$. The growth rate was calculated as the average of three replications. The cell density was correlated to the cell mass of *L. lactis* to be 0.36 g (dry weight) per liter of SA medium of $OD_{600} = 1$.

4.3.4 Quantification of maltose and fermentation products

HPLC was employed to measure the concentration of maltose, lactate, formate and acetate in the samples taken during the growth experiments as previously described [29].

4.3.5 DNA techniques

The method used to isolate the chromosomal DNA from *L. lactis* was modified from a previous method [30]. PCR amplification, restriction, ligation, transformation and plasmid purification from *E. coli* were performed following procedures described in Sambrook et al.[31] and the description from the manufacturer of the enzymes used. Electrocompetent cells of *L. lactis* were grown in M17 broth supplemented with 10 g L^{-1} glucose and 10 g L^{-1}glycine and transformed by electroporation as described previously [32].

4.3.6 Gene inactivation

Gene inactivation was achieved by deleting the whole gene or part of the gene containing the necessary active sites using the plasmid pCS1966 [26]. ≈800-bp regions upstream and downstream of the target to be deleted were PCR amplified and inserted into pCS1966. The resulting plasmids were used as previously described [26].

4.3.7 Construction of *gusA* reporter strains

The promoter containing region upstream a specific gene was PCR amplified and inserted into plasmid pLB85 and transformed into the desired *L. lactis* strain expressing phage TP901-1 integrase as described previously [27]. Transformants were selected on GM17 with erythromycin and verified by sequencing using primers CSO50 and CSO263 (Table B.1).

4.3.8 Rapid amplification of cDNA ends (RACE)

For RNA isolation, cells of MG1363 were harvested from an exponentially growing SA culture supplemented with 2 g L^{-1} glucose or maltose, with 2 μg ml^{-1} of lipoic acid and nucleosides. Cells were then resuspended in 200 μl Solution I (0.3 M sucrose and 0.01 M NaAc, pH 4.8) and 200 μl preheated Solution II (2% SDS and 0.01 M NaAc, pH 4.8). 400 μl phenol/acetate (phenol equilibrated with 100 mM NaAc, pH 4.8) was added and the mixture was disrupted by glass beads (106-μm diameter; Sigma, Prod. No. G4649) using a FastPrep (MP Biomedicals, Santa Ana, USA). The resulting lysate was centrifuged and the water phase was extracted by phenol/acetate two times and finally by phenol/acetate mixed with chloroform in a 1:1 ratio. RNA was precipitated by ethanol and dissolved in DEPC-treated water. RACE was performed using the SMARTer™ RACE cDNA Amplification Kit (Clontech) according to the instructions of the manufacturer.

4.3.9 Overproduction of *L. lactis* ACK in *E. coli*

The two ACK genes (*ackA1*, *ackA2*) from MG1363 were PCR amplified using primers 71f, 71r and 62f, 62r respectively. After digestion with BglII, SalI and BamHI, SalI respectively, the fragments were inserted into the vector pQE30 (Qiagen) digested with the same enzymes and subsequently introduced into the *E. coli* strain M15 pREP4*groESL* [25]. The strains were grown and His-tagged ACKs were produced via IPTG induction and purification on a Ni-NTA resin (Qiagen) according to the manufacturer's instruction. Purified protein was gel-filtrated on a PD-10 column (GE Healthcare) thereby transferring it to Solution A (50 mM Tris-HCl pH 7.5, 100 mM NaCl, 10% glycerol). Protein concentration was determined using Bradford Reagent (Sigma, Prod. No. B6916) and a protein standard (200 mg ml^{-1} BSA, Sigma, Prod. No. P5369), following the protocol provided by the manufacturer. The molecular weight of the protein was estimated by gel filtration using a HiPrep™ 16/60 Sephacryl™ S-300 High Resolution column (GE Healthcare) and a Gel Filtration Standard (BioRad, Cat. No. 151-1901). The mobile phase used was 0.05 M sodium phosphate, 0.15 M NaCl, pH 7.0 and the flow rate was 0.2 ml min^{-1}. Proteins were detected using the Ultimate 3000 Diode Array Detector (Dionex) at 280 nm.

4.3.10 Measurement of ACK activities

ACK activities were measured on either purified proteins or in cell extracts. Cell extracts were obtained by harvesting exponentially growing cells which were then resuspended in extract buffer [29] and disrupted by glass beads (106-µm diameter; Sigma, Prod. No. G4649) using a FastPrep (MP Biomedicals, Santa Ana, USA). The master buffer used for the assay was adapted from Goel et al. [33]: 100 mM HEPES, 50 mM NaCl, 400 mM potassium glutamate, 1 mM potassium phosphate and 10× diluted metal ions present in SA medium, adjusted to pH 7.5 with potassium hydroxide. For the production of acetate from Ac-P, the same assay mix was used as in Goel et al. [33]: master buffer, 5 mM $MgSO_4$, 2 mM D-glucose, 0.4 mM NAD^+, 8.5 U ml^{-1} hexokinase, 12.7 U ml^{-1} D-glucose 6-phosphate dehydrogenase, with varying amounts of ADP and Ac-P. For measurements of V_{max} in cell extracts, 3 mM ADP and 2 mM Ac-P were used. For the reverse direction, the assay mix was modified from a previous article [34]: master buffer, 4.2 mM $MgCl_2$, 1.7 mM phosphoenolpyruvate, 0.24 mM NADH, 9 U ml^{-1} pyruvate kinase, 12 U ml^{-1} lactate dehydrogenase, with varying amounts of ATP and potassium acetate. For measurement of V_{max} in cell extracts, 4 mM ATP and 200 mM acetate were used. The enzyme activities were determined by monitoring OD_{340} corresponding to the concentration of NADH using the Infinite® M1000 PRO microplate reader (TECAN) and the accompanying software Magellan. The 96-well microplates used were purchased from Greiner Bio-one (Cat. No. 655901).

4.3.11 Measurement of β-glucuronidase activity

The procedure used for measuring *β*-glucuronidase activities was modified from Miller [35]and Israelsen et al. [36].

4.3.12 Sequence analysis

Protein sequences were obtained from UniProt (http://www.uniprot.org/). Nucleotide sequences were downloaded from GenBank (http://www.ncbi.nlm.nih.gov/genbank/). Multiple alignments and phylogenetic construction were performed using MUSCLE [37] in CLC Main Workbench (http://www.clcbio.com/products/clc-main-workbench/). Phylogenies were visualized in FigTree (http://tree.bio.ed.ac.uk/software/figtree/). RNA secondary structure was predicted using Vienna RNA Web Services [38].

4.4 Results

4.4.1 Homologous sequences of AckA1 and AckA2 in *L. lactis* MG1363

Protein sequences of the two ACKs in MG1363, AckA1 and AckA2 encoded by *ackA1* and *ackA2* respectively, are homologous with an identity of 68%. Alignment to ACKs from *Salmonella typhimurium* and *Methanosarcina thermophila* (*M. thermophila*) whose structures are known [16], [17] (Figure B.1) showed conservation of active site, substrate, nucleotide triphosphate and metal binding sites except one residue in an ATP binding site (V331 of AckA1 and I331 of AckA2 respectively) which is also not conserved among other organisms. It is thus difficult to predict differences in enzymatic properties based on sequences alone.

4.4.2 Multiple ackA genes existing in *L. lactis* and many other species

To understand the evolutionary relationship between the ACKs from *Lactococcus* and other closely related LAB, a search for species with multiple acetate kinases was initiated. Under the genus *Lactococcus*, there are a total of 15 strains of three species, ten *L. lactis*, four *L. garvieae* and one *L. raffinolactis*. Interestingly, all *Lactococcus* strains except *L. raffinolactis* harbor two homologous ACK genes. For *Streptococcus* which is closest to *Lactococcus*, in contrast, among more than 500 strains with available ACK sequences, only 16 of them have two or more ACKs. It is however not a distinctive feature for *Lactococcus* but in fact a very general phenomenon in bacteria. Among the 11,100 entries predicted to encode ACKs in Uniprot, around 5,000 of them are not the unique gene for ACK in an organism. These multiple ACK genes exist in 2,242 strains from 320 species under 135 genera. Interested readers are referred to Appendix AB.2 for the complete list and the criteria for distinguishing multiple ACKs.

4.4.3 Two types of ACK conserved in *Lactococcus*

A multiple alignment including sequences from all *Lactococcus*, several *Streptococcus* and *Lactobacillus* representatives with the experimentally studied species as outgroup was performed to construct a phylogeny (Figure 4.2). From the phylogeny, it became clear that, except for *L. raffinolactis*, one ACK in each *Lactococcus* strain forms a monophyly and the other ACK in each strain forms another (filled triangles in Figure 4.2). A multiple alignment indicating the conserved differences of amino acid sequences between the two types of ACK in all *Lactococcus* strains is also shown in Fig. S2. For *Streptococcus* and *Lactobacillus*, similar but more complex relationships could be observed. For example, a *S. urinalis* strain has two ACKs more similar to ACKs in other species than to each other. One of the three ACKs of *Lb. sakei* also has a larger divergence with the other two ACKs than with the ACKs from bacteria in other phyla.

From the alignment of the two types of ACK in *L. lactis* with ACKs of known structure [16],[17], [39] (Figure B.2), it was observed that some important residues conserved within each type of ACK were different between the two types, e.g. position 331 (relative to MG1363's AckA1) in an ATP binding site and position 287–291 including a deletion on a helix containing an ATP binding site.

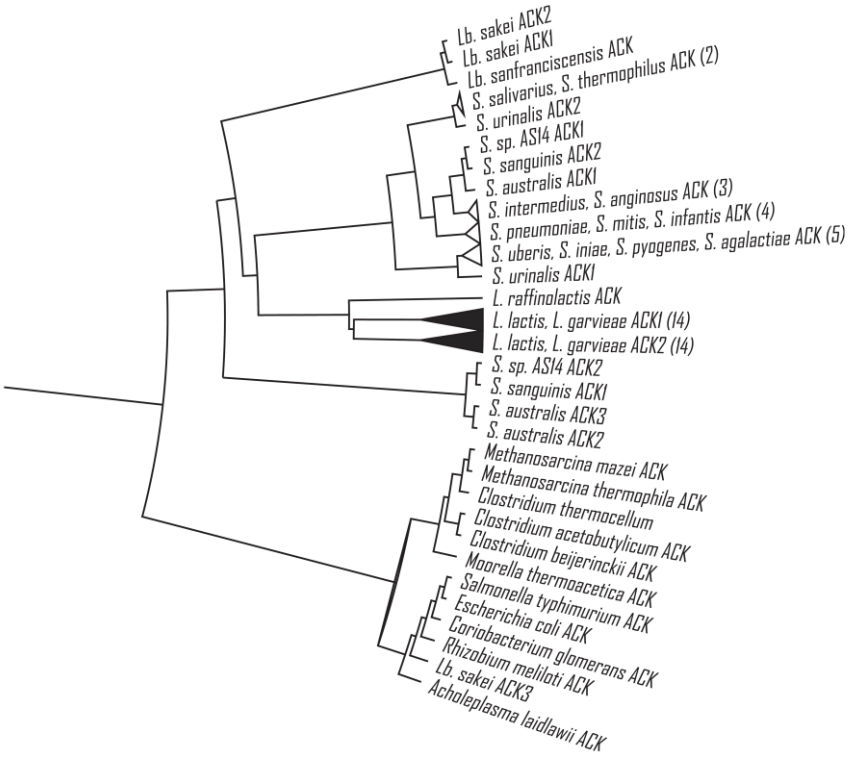

Figure 4.2. Phylogeny of acetate kinases from *Lactococcus*, *Streptococcus* and other species.

One ACK from each *L. lactis* and *L. garvieae* strain forms a monophyletic group and the other ACK forms another (filled triangles). A triangle represents a cluster of sequences lumped in one line and the number in the bracket is the size of the cluster. doi:10.1371/journal.pone.0092256.g002

4.4.4 Predicted transcription terminator between the two ACK genes in *L. lactis*

In all *L. lactis* strains, the genes for the two ACKs are neighbors of each other. In MG1363, the gene upstream was annotated as *ackA1* and the other as *ackA2*. To see if they form an operon, the intergenic RNA secondary structure was predicted using ViennaRNA Web Services [38]. A stem-loop structure followed by a poly-U sequence which is a potential transcription terminator located 8 bp downstream of the stop codon of *ackA1* was predicted (Figure 4.3). The prediction is conserved for all sequenced *L. lactis*.

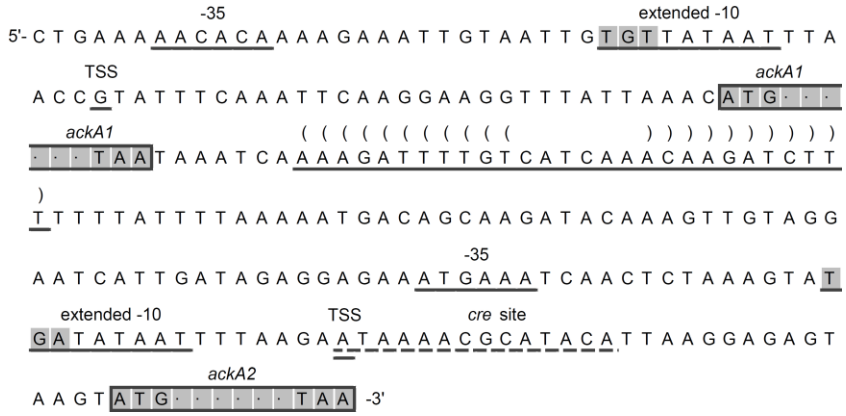

Figure 4.3. Nucleotide sequence upstream of *ackA1* and *ackA2*.

TSS: putative transcription start site. Putative −35 and extended −10 element are underlined. Shaded nucleotides in −10 element: TGn motif. *cre* site responsible for carbon catabolite repression is dotted underscored. Bracket pairs represent the base pairing in the predicted stem-loop structure which is conserved among all *L. lactis* strains. doi:10.1371/journal.pone.0092256.g003

4.4.5 Distinct transcription start sites for *ackA1* and *ackA2*

A 5′-end RACE was conducted on RNA samples from MG1363 growing on glucose and maltose respectively to locate the transcription start site (TSS) of the two *ackA* genes. For each gene, an individual TSS was identified and putative −35 element and extended −10 element containing a TGn motif [40] were proposed (Figure 4.3). We were unable to demonstrate the existence of an additional transcript containing both *ackA2* and *ackA1* although this should have been possible for the RACE approach used.

4.4.6 Distinct transcription units and activities

Reporter fusions were constructed as a quantitative approach to examine the transcription activity of *ackA1* and *ackA2*. Five resulting strains with fragments A–E (Figure 4.4a) respectively fused transcriptionally to *gusA* were grown on MSA medium and the *β*-glucuronidase activities were determined (Figure 4.4b).

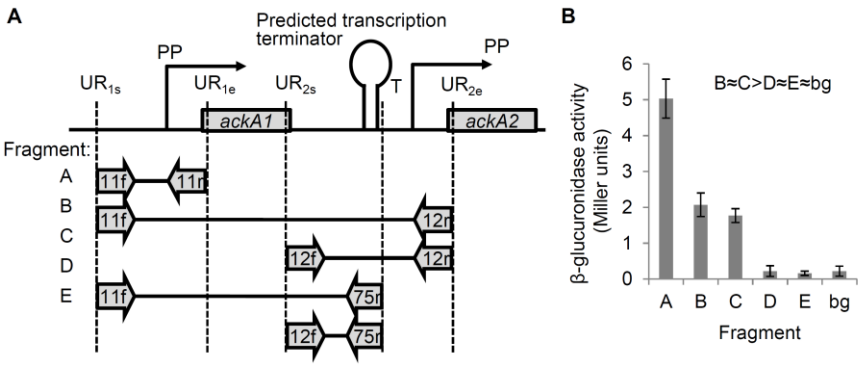

Figure 4.4. Transcription activities of *ackA* genes.

(A) Fragments used for transcriptional fusion. Numbers on arrows refer to primers in Table B.1. PP: putative promoter. UR_{1s}: ≈500 bp upstream of *ackA1*. UR_{1e}: ≈50 bp after the start codon of *ackA1*. UR_{2s}: ≈500 bp upstream of *ackA2*. UR_{2e}: ≈50 bp after the start codon of *ackA2*. T: position just after the predicted terminator. (B) The β-glucuronidase activities induced by the corresponding fragments. bg: background activity from the control strain without any promoter upstream of *gusA*. Error bars are equal to standard deviations of measurements on three replications. doi:10.1371/journal.pone.0092256.g004

Fragment A including the putative promoter (PP) of *ackA1* resulted in the highest activity of 5 Miller units. Fragment B includes both the PPs of *ackA1* and *ackA2* whereas fragment C includes only the PP of *ackA2*. They resulted in very similar activities (≈2 Miller units). This shows that the PP of *ackA1* had negligible effect on the transcription of *ackA2*. Fragment D and E, starting at the same 5′ end of fragment B and C respectively and both ending just after the predicted terminator but before the PP of *ackA2*, resulted in activities indistinguishable from the background activity ('bg' in Figure 4.4b). This demonstrates that the predicted terminator is effective and that the transcription of *ackA2* is governed by its own promoter.

4.4.7 Huge differences in k_{cat} and K_m for acetate

The molecular weights of the His-tagged ACKs were estimated to be 100 kDa for AckA1 and 84 kDa for AckA2 using gel filtration, close to a double of the monomer (43 kDa). Both proteins are concluded to be homodimeric. ACK activities of the enzymes were measured (Figure B.3). Both AckA1 and AckA2 were active in both directions. k_{cat} and K_m for all four substrates were estimated (Table 4.1). Two exceptional differences between AckA1 and AckA2 were first the much higher k_{cat} of AckA1 in both directions (8-fold higher for acetate production and 4-fold higher for the reverse) and second the much lower apparent K_m for acetate of AckA2 (1.87 mM) compared to that of AckA1 (22.07 mM).

Table 4.1. Estimated K_m and k_{cat} for AckA1 and AckA2.

		AckA1	AckA2
K_m (mM)	Ac-P	0.35 (0.02)	0.086 (0.02)
	ADP	0.94 (0.09)	1.15 (0.12)
	OAc	22.07 (1.05)	1.87 (0.29)
	ATP	0.086 (0.0078)	0.21 (0.12)
k_{cat} (s^{-1})	OAc →Ac-P	3234 (221)	394 (27)
	Ac-P→OAc	1033 (98)	282 (28)

Ac-P: acetyl-phosphate. OAc: acetate. Values in bracket represent the standard error of estimation from ≥20 data points. doi:10.1371/journal.pone.0092256.t001

4.4.8 Additive cell extract activities of mutant strains

To study the physiological roles of the two ACKs in *L. lactis*, three mutant strains, MG1363Δ*ackA1*, MG1363Δ*ackA2* and MG1363Δ*ackA1*Δ*ackA2*, were constructed by inactivating *ackA1*, *ackA2* and both respectively. V_{max} of ACK in MG1363 and the three mutant strains growing on MSA media were measured (Figure 4.5a). MG1363 showed the highest activity, followed by MG1363Δ*ackA2* and then MG1363Δ*ackA1*. MG1363Δ*ackA1*Δ*ackA2* had the lowest activity. An interesting observation was the additivity of the activities. When subtracting the activity in MG1363Δ*ackA1*Δ*ackA2* (which represents the background activity) from the activities in the other three strains, the sum of the activities in MG1363Δ*ackA1* and MG1363Δ*ackA2* was approximately equal to the activity in MG1363. The implication is discussed below.

To verify the much lower K_m for acetate of AckA2, V_{max} was also determined in the presence of 1 mM acetate (Figure 4.5b). MG1363Δ*ackA1* did show a higher activity than MG1363Δ*ackA2*. This is opposite to what was observed under normal assay conditions with 200 mM acetate and agrees with the differences in the K_m.

4.4.9 Slower acetate production by MG1363ΔackA1 at a high extracellular acetate concentration

To test whether the two ACKs performed differently *in vivo*, growth experiments of MG1363, MG1363Δ*ackA1*, MG1363Δ*ackA2* and MG1363Δ*ackA1*Δ*ackA2* were conducted on MSA media with or without 50 mM acetate. Figure 4.6 shows representative growth curves of the four strains and the average growth rates. In all experiments the wild type and single-deletion strains were able to grow up to an $OD_{600}\approx1$ where the HPLC analysis showed that the sugar had been consumed (data not shown). The double deletion strain MG1363Δ*ackA1*Δ*ackA2*stopped growing at a much lower cell density of $OD_{600}\approx0.1$. When acetate was absent, MG1363 and the two single deletion strains grew with similar growth rates about 0.45 h^{-1}. With 50 mM acetate present in the media, MG1363Δ*ackA1* had a significantly reduced growth rate of 0.38 h^{-1}, equal to a 20% reduction compared to MG1363 and MG1363Δ*ackA2* (0.49 h^{-1}).

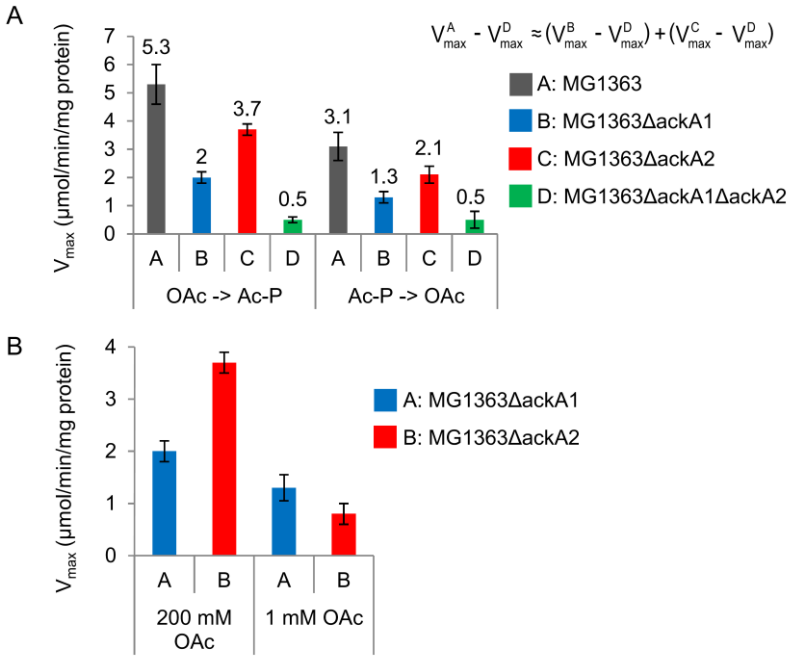

Figure 4.5. ACK activites in crude extracts of MG1363 and derived *ackA* deletion strains.

(A) Activities under normal assay conditions with 200 mM acetate. When subtracting the activity in MG1363Δ*ackA1*Δ*ackA2* (which represents background activity) from the activities in the other three strains, the sum of the activities in MG1363Δ*ackA1*and MG1363Δ*ackA2* was approximately equal to the activity in MG1363. (B) Activities of MG1363Δ*ackA1* and MG1363Δ*ackA2* in the presence of 1 mM or 200 mM of acetate (OAc). Error bars are equal to standard deviations of measurements on three replications. doi:10.1371/journal.pone.0092256.g005

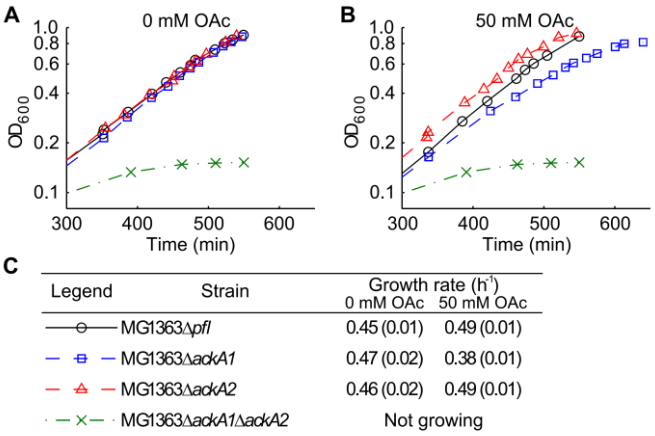

Figure 4.6. Representative growth curves and growth rates of MG1363 and derived *ackA* deletion strains.

Growth with (A) 0 mM and (B) 50 mM acetate. Only data obtained 5 hours after the start of the experiments are plotted for better visualization. (C) Table showing the legend and average growth rates. Values in brackets represent standard deviations of three replications. doi:10.1371/journal.pone.0092256.g006

The product formation from the three growing strains was also measured (Table 4.2). In the absence of acetate, the distribution of fermentation products was very similar for all three strains. Since MG1363Δ*ackA1*Δ*ackA2* was unable to grow and produce acetate after OD_{600}≈0.1, the acetate

production in MG1363Δ*ackA1* and MG1363Δ*ackA2* can be attributed to AckA2 and AckA1 respectively. This implies that both individual ACKs were able to sustain a flux equal to that in the wild type where both ACKs were present. In the presence of 50 mM acetate, however, the reduced acetate production rate concomitant with the reduced growth rate (Figure 4.6c), formate production rate and maltose uptake rate in MG1363Δ*ackA1* reveals that the flux entering the mixed acid branch decreased while the lactate flux remained unchanged (Table 4.2). This indicates that AckA2 alone in MG1363Δ*ackA1* was unable to maintain the same flux as in MG1363 and MG1363Δ*ackA2*where AckA1 was present. It can thus be concluded that AckA1 performed better than AckA2 in acetate production in the presence of a high concentration of acetate (50 mM) in the media.

Table 4.2. Average specific rates of consumption of maltose, production of lactate, formate and acetate of MG1363, MG1363Δ*ackA1* and MG1363Δ*ackA2* at 0 or 50 mM of extracellular acetate.

	Specific rate of consumption/production (mmol h^{-1} gdw^{-1})							
	MSA, 0 mM OAc				MSA, 50 mM OAc			
	maltose	lactate	formate	acetate	maltose	lactate	formate	acetate
MG1363	7.9 (0.5)	20.6 (1.5)	12.5 (0.9)	7.5 (0.8)	8.3 (0.6)	20.1 (1.6)	14.0 (1.4)	7.9 (0.9)
MG1363Δ*ackA1*	8.0 (0.5)	19.9 (1.4)	12.7 (1.0)	8.0 (0.4)	7.2 (0.5)	19.0 (1.8)	8.9 (1.0)	5.1 (1.0)
MG1363Δ*ackA2*	7.3 (0.6)	18.8 (1.1)	12.5 (1.2)	7.4 (0.4)	8.0 (0.6)	18.0 (1.1)	14.3 (1.2)	7.7 (0.7)

OAc: acetate. Values in brackets represent standard deviations of three replications. doi:10.1371/journal.pone.0092256.t002

4.4.10 Slower acetate uptake by MG1363ΔackA2Δ*pfl* at low acetate concentrations

An acetate-assimilating growth condition was created by excluding lipoic acid from the medium and knocking out PFL in the *ackA* deletion strains. The PFL-deleted strains, MG1363Δ*pfl*, MG1363Δ*ackA1*Δ*pfl*, MG1363Δ*ackA2*Δ*pfl* and MG1363Δ*ackA1*Δ*ackA2*Δ*pfl*, were grown in MSA media supplemented with acetate. Figure 4.7 shows the growth in media supplemented with no acetate, 8 mM, 12 mM and 50 mM acetate respectively. When acetate was absent, all four strains stopped growing at OD_{600}≈0.1 (Figure 4.7a), showing that the cells depended on acetate for growth beyond this point. When acetate was added to the media, further growth could be seen for all strains except MG1363Δ*ackA1*Δ*ackA2*Δ*pfl*. A clear transition occurred between OD_{600} = 0.2 and 0.3, after which growth depends on acetate. The final OD_{600} was around 0.6 where HPLC analysis indicated that all maltose had been consumed.

Very slow acetate-dependent growth was observed for MG1363Δ*ackA2*Δ*pfl* at 8 or 12 mM of extracellular acetate, >10-fold slower than MG1363Δ*ackA1*-Δ*pfl* and MG1363Δ*pfl* (Figure 4.7b, c). MG1363Δ*ackA1*Δ*pfl* also grew even faster than MG1363Δ*pfl* at these acetate concentrations. When the acetate concentration increased to 50 mM, however, the growth rates were similar for all three strains (0.22–0.23 h^{-1}, Figure 4.7d).

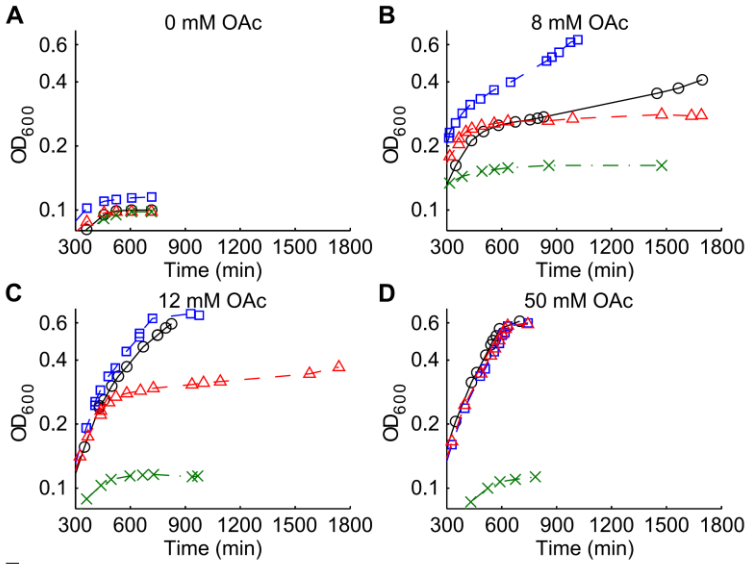

E

Legend	Strain	Growth rate (h^{-1}) 8 mM OAc	12 mM OAc	50 mM OAc
—○—	MG1363Δ*pfl*	0.036 (0.002)	0.09 (0.01)	0.23 (0.003)
— □ —	MG1363Δ*ackA1*Δ*pfl*	0.066 (0.006)	0.16 (0.01)	0.22 (0.004)
— △ —	MG1363Δ*ackA2*Δ*pfl*	0.005 (0.001)	0.01 (0.002)	0.22 (0.001)
·—×—·	MG1363Δ*ackA1*Δ*ackA2*Δ*pfl*	Not growing		

Figure 4.7. Representative growth curves of MG1363Δ*pfl* and derived *ackA-pfl* deletion strains.
Growth with (A) 0 mM, (B) 8 mM, (C) 12 mM and (D) 50 mM acetate. Only data obtained 5 hours after the start of the experiments are plotted for better visualization. (E) Table showing the legend and average growth rates. Values in brackets represent standard deviations of three replications. doi:10.1371/journal.pone.0092256.g007

The consumption of acetate was also quantified (Table 4.3). The acetate uptake rate of MG1363Δ*ackA1*Δ*pfl* was significantly higher than that of MG1363Δ*pfl* (2–3 fold) and MG1363Δ*ackA2*Δ*pfl* (>6 fold) at 8 or 12 mM extracellular acetate. They were nonetheless indistinguishable at 50 mM extracellular acetate. Since MG1363Δ*ackA1*Δ*ackA2*Δ*pfl* did not show acetate-dependent growth, the acetate uptake in MG1363Δ*ackA1*Δ*pfl* and MG1363Δ*ackA2*Δ*pfl* could be attributed to the presence of AckA2 and AckA1 respectively. It can thus be concluded that at a high acetate concentration (50 mM), both individual ACKs were able to take up acetate as fast as in MG1363Δ*pfl* whereas at low acetate concentrations (≤12 mM), AckA2 has a significant higher capability for acetate uptake than AckA1.

Table 4.3. Average specific rates of consumption of maltose, acetate and production of lactate of MG1363Δ*pfl*, MG1363Δ*ackA1*Δ*pfl* and MG1363Δ*ackA2*Δ*pfl*.

	Specific consumption/production rate (mmol h^{-1} gdw^{-1})								
	8 mM OAc			12 mM OAc			50 mM OAc		
	maltose	lactate	acetate	maltose	lactate	acetate	maltose	lactate	acetate
MG1363Δ*pfl*	1.3 (0.1)	2.8 (0.2)	0.02 (0.003)	2.7 (0.3)	8.1 (1.0)	0.16 (0.02)	7.1 (0.4)	28 (1)	2.5 (0.5)
MG1363Δ*ackA1*Δ*pfl*	2.1 (0.2)	5.5 (0.7)	0.06 (0.02)	3.7 (0.3)	12.1 (1.0)	0.27 (0.02)	6.8 (0.2)	27 (1)	2.6 (0.4)
MG1363Δ*ackA2*Δ*pfl*	0.2 (0.03)	0.54 (0.09)	N.D.	0.3 (0.05)	0.8 (0.4)	0.04 (0.01)	6.7 (0.3)	27 (1)	2.6 (0.5)

Formate production was not detectable in all cases. Values in brackets represent standard deviations of three replications. N.D.: not detectable. doi:10.1371/journal.pone.0092256.t003

4.5 Discussion

4.5.1 Prevalence of multiple ACKs in bacteria

ACK sequence data from Uniprot revealed that the existence of multiple ACKs is a very common phenomenon in bacteria which is interesting and emphasizes its possible importance. Unfortunately, there are few studies on ACK isozymes in the literature except for a spirochete [23]. We believed that the importance of ACK isozymes on acetate metabolism is being neglected while the acetate metabolism in bacteria is still a subject under active research, for instances, current generation of *Geobacter sulfurreducens*'s growth on acetate [41] and acetate dependency of the probiotic *Lactobacillus johnsonii* [42]. Interestingly, the strains used in the two studies also have multiple ACKs. Knowledge on ACK isozymes in these organisms may provide insights into these studies and their applications. The current study attempts to fill the gap by studying the two ACKs in *L. lactis* at different levels.

4.5.2 *ackA1* and *ackA2* in *L. lactis* probably resulted from gene duplication

Protein sequence analysis revealed the conserved differences between the two ACKs found in *Lactococcus*. This brought an insight into the potential evolutionary advantage of having ACK isozymes. From the simple phylogenetic analysis, the two *ackA* genes may have resulted from a duplication event in a common ancestor of *Lactococcus* which had already been differentiated from *Streptococcus*. To prove this point, however, a more formal phylogenetic analysis is required.

4.5.3 AckA1 and AckA2 in MG1363 being isozymes rather than subunits

With respect to the expression of *ackA1* and *ackA2*, our results suggest that the two genes are transcribed individually rather than in an operon. This is actually consistent with the Northern Blot results in Lopez de Felipe and Gaudu (2009) [43] where a transcript of around 1 kb was found for *ackA1*. Interestingly, in their study, *ackA1* was assumed to encode one subunit of ACK in *L. lactis*. This question may be worth asking because the two ACKs are in fact homologous to each other.

In the current study, nevertheless, the state of being isozymes rather than subunits of one ACK for the two *ackA* gene products was assumed for several reasons. First, we found that the individual His-tagged enzymes could catalyze the reaction in both directions. Second, the *ackA* mutant strains could produce as well as utilize acetate. Third, the crude extracts from *ackA* mutant strains showed additive activities ($V_{\max}^{MG1363} = V_{\max}^{MG1363\Delta ackA1} + V_{\max}^{MG1363\Delta ackA2} - V_{\max}^{MG1363\Delta ackA1\Delta ackA2}$). If a hetero-oligomeric form of ACK with different kinetic properties exists, the additivity is less likely to hold. Fourth, most of the ACKs reported in the literature appear to be homodimeric [16], [17],[22], [44]–[47]. Finally, we have data analogous to those in Fig. 4b showing that when growing on glucose, the promoter activity of *ackA2* was 10-fold lower than that of *ackA1* and was close to the value of background activity (unpublished results). This is consistent with the *cre* site identified 6 bp downstream of the *ackA2*'s TSS (Fig. 3) which is subject to carbon catabolite repression [48]. In light of this huge difference

between the transcriptional activities, it is unlikely that the two gene products from *ackA1* and *ackA2* form one protein complex. However, the possibility that hetero-oligomeric ACK exists cannot be entirely ruled out.

4.5.4 Possible different roles suggested by enzyme kinetics

From the His-tagged purified enzymes, AckA1 was shown to have much higher turnover number k_{cat} than AckA2 whereas AckA2 has a higher affinity towards acetate. The apparent K_m is the lowest of all the reported ACKs where K_m for acetate usually is notoriously high (the highest being 300 mM in *E. coli* [13]). The kinetic properties of the two ACKs thus suggest a possible complementary role in metabolism. For the effect of His-tagging on enzymes, we have looked into the 3D structure of the ACK from *M. thermophile* (PDB ID: 1TUY) [22] which is homologus to AckA1 and AckA2 in *L. lactis*. The first few residues from the N-terminus are outside the catalytic core. Together with the consistency between the assays on purified enzymes and crude extracts, we believed that the His-tag is unlikely to interfere with the reaction.

4.5.5 Physiological roles of ACK reported in literature

Among the ACKs reported previously, some were found to have ATP production as their primary physiological role while some are more likely to be responsible for acetate activation. For instance, the ACK in *Lactobacillus sanfranciscensis* was suggested to take the role of ATP formation [13]. The ACKs in *Bacillus subtilis* were shown to be non-essential for growth on acetate and meanwhile important for excretion of excess carbohydrate by producing acetate [49].

With respect to examples of acetate activation, in *Corynebacterium glutamicum*, ACK activities were proven to be necessary for growth on acetate [50]. Another interesting case is *M. thermophile* which is acetotrophic. The K_m for acetate of the ACK from *M. thermophile*was found to be 22 mM [18]. Site-directed mutagenesis in the same study revealed that only a single-residue mutation could cause a 10-fold lower K_m for acetate concomitant with a 6-fold reduction in k_{cat}. This striking similarity between the pair of ACKs in *M. thermophile* (wild-type and mutated) and the pair of ACKs in *L. lactis* (AckA1 and AckA2) leaves a possible hint for how AckA1 and AckA2 differentiated and specialized. The author suggested that the sacrifice of a low K_m in return for a high k_{cat} conferred the advantage of more rapid acetate uptake to *Methanosarcina* species in an environment with a high acetate concentration [18].

These are only a few examples among many different studies. It must be noted that despite the particular functions of ACK demonstrated in the mentioned studies, one should not exclude other possibilities. The physiological role might be dependent on the nutrients available and complementary to other enzymes like the AMP-forming ACS in bacteria. For example, in *E. coli*, a number of studies on ACK-deficient mutants showed that PTA-ACK is the primary pathway for acetate production, e.g. [51], [52]. Other studies found that it is important for growth on high acetate concentration (≥25

mM) whereas growth on low acetate concentration (≤2.5 mM) depends on ACS [1], [53] (reviewed in [3]). This example of PTA-ACK complementary to ACS in *E. coli* also resembles AckA1 and AckA2 in the sense that ACS has a much lower K_m for acetate (0.2 mM) and lower V_{max} [53]. The difference lies in the irreversibility of ACS in *E. coli* and the dependence of AckA2 on PTA to produce Ac-CoA in *L. lactis*. A final example is a spirochete with two ACKs [23]. They had a lower K_m for Ac-P and acetate respectively. The authors mentioned the possibility of the two ACKs being specialized in different directions respectively.

4.5.6 Growth on maltose as a test of the physiological roles in *L. lactis*

To find out whether the two ACKs have different physiological roles, mutant strains were constructed and their response to acetate during growth was examined. In our growth experiments, maltose was chosen as the carbon source because for MG1363 growing on maltose, a more significant amount of formate, acetate and ethanol is produced than on glucose [54]. Via growth on maltose the capacity of the two ACKs to bear a high flux from glycolysis can be tested. Another reason is the much lower ATP/ADP ratio in *L. lactis* when growing on maltose than on glucose. The ATP/ADP ratio in MG1363 was around 9 when growing on glucose [55] and was around 4 when growing on maltose [56]. The lower ATP/ADP ratio provided a more stringent condition for acetate uptake in the mutant strains.

4.5.7 Complementary roles in acetate metabolism

Our results show that under favorable conditions either one of the ACKs is sufficient for the dual function of acetate production and uptake. In an environment where the concentrations of acetate, lipoic acid (activating PDHc) and oxygen (inactivating PFL) are varying, nonetheless, AckA1 and AckA2 have their own advantages and complement each other to allow fast growth at different extracellular acetate concentrations. In an environment with high acetate concentration (50 mM), AckA1 showed its superior capability of acetate production. This is consistent with the kinetic properties *in vitro*. The much higher affinity for acetate of AckA2 probably led to a larger effect of product inhibition by extracellular acetate diffused into the cells. In contrast, in a dynamic environment where PFL and PDHc are inactive, e.g. containing oxygen and without lipoic acid, our results from the growth experiments of PFL and ACK defective strains show that AckA2 is important for acetate uptake when the acetate source is scarce (≤12 mM). The lower growth yield compared to PFL-effective strains (OD_{600} = 0.6 vs 1) was probably a result of loss of the ATP generated from acetate production combined with additional ATP consumed for acetate uptake.

Another possible function of the two ACKs that should not be overlooked is the emergent properties of combining the isozymes. A possibility is thus a switch to fine-tune the direction and rate of the reaction in response to the cellular requirement by altering the expression of the two *ackA* genes. It would be interesting to look into the regulation of the expression of*ackA1* and *ackA2* to examine this hypothesis.

4.5.8 PTA-ACK as the only pathway interconverting Ac-CoA and acetate in *L. lactis*

The inability of MG1363Δ*ackA1*Δ*ackA2* and MG1363Δ*ackA1*Δ*ackA2*Δ*pfl* to grow on MSA media suggests the absence of other pathways involved in the interconversion between Ac-CoA and acetate. For MG1363Δ*ackA1*Δ*ackA2*, the only known pathway left for catabolizing Ac-CoA is the NAD^+-generating bi-functional alcohol dehydrogenase (ADHE) because of the lack of ACKs. The redox imbalance could lead to the accumulation of toxic intermediate metabolites such as acetaldehyde which prevents growth. For MG1363Δ*ackA1*Δ*ackA2*Δ*pfl*, no acetate was assimilated to form Ac-CoA to satisfy anabolic requirements. If other pathways for either direction exist, one of the strains should be able to grow. Thus, these results further emphasize the importance of AckA1 and AckA2 in the acetate metabolism of *L. lactis*. For the initial growth up to OD_{600}≈0.1 of the two strains, it was found to be caused by the small amounts of lipoic acid present as impurity in the amino acids composing the media which could activate PDHc. Adding lipoic acid to these cultures indeed allowed growth beyond OD_{600} = 0.1 and growth experiments in media with reduced amounts of amino acids showed that these strains stopped growing at a lower OD_{600} whereas the wild-type MG1363 was unaffected (data not shown). This indicated the presence of small amounts of lipoic acid in the amino acid stock which caused the initial growth of MG1363Δ*ackA1*Δ*ackA2* and MG1363Δ*ackA1*Δ*ackA2*Δ*pfl*.

4.6 Conclusions

In conclusion, the present study demonstrated the different and yet complementary roles of the two acetate kinases in *L. lactis* MG1363 with one being specialized in acetate production and the other in acetate uptake. It was observed from the sequence and phylogenetic analysis, supported with transcriptional analysis and the enzyme kinetics, and finally confirmed by the different growth behavior of mutant strains harboring only *ackA1* and *ackA2* respectively. The findings can be of great significance in bacterial metabolism in light of the fact that more than 300 species of organisms actually have multiple ACKs. Evolution to multiple ACKs specialized in complementary functions may be a common strategy in bacteria in response to the dual nature of acetate which can be an essential substrate but also an inhibitor for growth depending on environmental conditions.

4.7 Acknowledgments

We thank Jun Chen for help with constructing the strain MG1363Δ*pfl*. We also thank the transnational SysMOLAB2 consortium for a fruitful discussion.

4.8 Author contributions

Conceived and designed the experiments: SHJC CS PRJ. Performed the experiments: SHJC LN. Analyzed the data: SHJC LN. Contributed reagents/materials/analysis tools: SHJC LN CS RPJ. Wrote the paper: SHJC LN CS PRJ.

4.9 References

1. Brown TDK, Jones-Mortimer MC, Kornberg HL (1977) The enzymic interconversion of acetate and acetyl-coenzyme A in *Escherichia coli*. *J Gen Microbiol* 102: 327–336.
2. Skoog K, Hahn-Hägerdal B, Degn H, Jacobsen JP, Jacobsen HS (1992) Ethanol reassimilation and ethanol tolerance in *Pichia stipitis* CBS 6054 as studied by 13C nuclear magnetic resonance spectroscopy. *Appl Environ Microbiol* 58: 2552–2558.
3. Wolfe AJ (2005) The acetate switch. *Microbiol Mol Biol Rev* 69: 12–50. doi:10.1128/MMBR.69.1.12-50.2005.
4. Thomas TD, Ellwood DC, Longyear VM (1979) Change from homo- to heterolactic fermentation by *Streptococcus lactis* resulting from glucose limitation in anaerobic chemostat cultures. *J Bacteriol* 138: 109–117.
5. Eckhardt TH, Skotnicka D, Kok J, Kuipers OP (2013) Transcriptional regulation of fatty acid biosynthesis in *Lactococcus lactis*. *J Bacteriol* 195: 1081–1089. doi:10.1128/JB.02043-12.
6. Fernandez M, Kleerebezem M, Kuipers OP, Siezen RJ, van Kranenburg R (2002) Regulation of the metC-cysK Operon, Involved in Sulfur Metabolism in *Lactococcus lactis*. *J Bacteriol* 184: 82–90. doi:10.1128/JB.184.1.82-90.2002.
7. Delcour J, Ferain T, Deghorain M, Palumbo E, Hols P (1999) The biosynthesis and functionality of the cell-wall of lactic acid bacteria. *Antonie Van Leeuwenhoek* 76: 159–184.
8. Snoep JL, de Graef MR, Westphal AH, de Kok A, Teixeira de Mattos MJ, et al. (1993) Differences in sensitivity to NADH of purified pyruvate dehydrogenase complexes of *Enterococcus faecalis*, *Lactococcus lactis*, *Azotobacter vinelandii* and *Escherichia coli*: Implications for their activity *in vivo*. *FEMS Microbiol Lett* 114: 279–284.
9. Henriksen CM, Nilsson D (2001) Redirection of pyruvate catabolism in *Lactococcus lactis* by selection of mutants with additional growth requirements. *Appl Microbiol Biotechnol* 56: 767–775. doi:10.1007/s002530100694.
10. Melchiorsen CR, Jokumsen KV, Villadsen J, Israelsen H, Arnau J (2002) The level of pyruvate-formate lyase controls the shift from homolactic to mixed-acid product formation in *Lactococcus lactis*. *Appl Microbiol Biotechnol* 58: 338–344. doi:10.1007/s00253-001-0892-5.
11. Melchiorsen CR, Jokumsen KV, Villadsen J, Johnsen MG, Israelsen H, et al. (2000) Synthesis and Posttranslational Regulation of Pyruvate Formate-Lyase in *Lactococcus lactis*. *J Bacteriol* 182: 4783–4788. doi:10.1128/JB.182.17.4783-4788.2000.
12. Nakajima H, Suzuki K, Imahori K (1978) Purification and properties of acetate kinase from *Bacillus stearothermophilus*. *J Biochem* 84: 193–203.
13. Knorr R, Ehrmann M a, Vogel RF (2001) Cloning, expression, and characterization of acetate kinase from *Lactobacillus sanfranciscensis*. *Microbiol Res* 156: 267–277. doi:10.1078/0944-5013-00114.
14. Aceti DJ, Ferry JG (1988) Purification and Characterization of Acetate Kinase from Acetate- grown *Methanosarcina thermophila*. *J Biol Chem* 263: 15444–15448.
15. Miles RD, Gorrell A, Ferry JG (2002) Evidence for a transition state analog, MgADP-aluminum fluoride-acetate, in acetate kinase from *Methanosarcina thermophila*. *J Biol Chem* 277: 22547–22552. doi:10.1074/jbc.M105921200.
16. Buss KA, Ingram-Smith C, Ferry JG, Sanders D a, Hasson MS (1997) Crystallization of acetate kinase from *Methanosarcina thermophila* and prediction of its fold. *Protein Sci* 6: 2659–2662. doi:10.1002/pro.5560061222.
17. Chittori S, Savithri HS, Murthy MRN (2012) Structural and mechanistic investigations on *Salmonella typhimurium* acetate kinase (AckA): identification of a putative ligand binding pocket at the dimeric interface. *BMC Struct Biol* 12: 24. doi:10.1186/1472-6807-12-24.
18. Singh-Wissmann K, Ingram-Smith C, Miles RD, Ferry JG (1998) Identification of Essential Glutamates in the Acetate Kinase from *Methanosarcina thermophila*. *J Bacteriol* 180: 1129–1134.
19. Miles RD, Iyer PP, Ferry JG (2001) Site-directed mutational analysis of active site residues in the acetate kinase from *Methanosarcina thermophila*. *J Biol Chem* 276: 45059–45064. doi:10.1074/jbc.M108355200.
20. Ishikawa H, Shiroshima M, Widjaja A (1995) Kinetics and mechanism of acetate kinase from *Bacillus stearothermophilus*. *J Chem Eng Japan* 28: 517–524.
21. Spector LB (1980) Acetate kinase : A triple-displacement enzyme. *Proc Natl Acad Sci U S A* 77: 2626–2630.
22. Gorrell A, Lawrence SH, Ferry JG (2005) Structural and kinetic analyses of arginine residues in the active site of the acetate kinase from *Methanosarcina thermophila*. *J Biol Chem* 280: 10731–10742. doi:10.1074/jbc.M412118200.
23. Harwood CS, Canale-Parola E (1982) Properties of acetate kinase isozymes and a branched-chain fatty acid kinase from a spirochete. *J Bacteriol* 152: 246–254.
24. Gasson MJ (1983) Plasmid complements of *Streptococcus lactis* NCDO 712 and other lactic streptococci after protoplast-induced curing. *J Bacteriol* 154: 1–9.
25. Amrein KE, Takacs B, Stieger M, Molnos J, Flint NA, et al. (1995) Purification and characterization of recombinant human p50csk protein-tyrosine kinase from an *Escherichia coli* expression system overproducing the bacterial chaperones GroES and GroEL. *Proc Natl Acad Sci U S A* 92: 1048–1052.
26. Solem C, Defoor E, Jensen PR, Martinussen J (2008) Plasmid pCS1966, a new selection/counterselection tool for lactic acid bacterium strain construction based on the oroP gene, encoding an orotate transporter from *Lactococcus lactis*. *Appl Environ Microbiol* 74: 4772–4775. doi:10.1128/AEM.00134-08.
27. Brøndsted L, Hammer K (1999) Use of the integration elements encoded by the temperate lactococcal bacteriophage TP901-1 to obtain chromosomal single-copy transcriptional fusions in *Lactococcus lactis*. *Appl Environ Microbiol* 65: 752–758.
28. Jensen PR, Hammer K (1993) Minimal Requirements for Exponential Growth of *Lactococcus lactis*. *Appl Environ Microbiol* 59: 4263–4266.
29. Andersen HW, Solem C, Hammer K, Jensen PR (2001) Twofold reduction of phosphofructokinase activity in *Lactococcus lactis* results in strong decreases in growth rate and in glycolytic flux. *J Bacteriol* 183: 3458–3467. doi:10.1128/JB.183.11.3458-3467.2001.

30. Johansen E, Kibenich A (1992) Characterization of *Leuconostoc* Isolates from Commercial Mixed Strain Mesophilic Starter Cultures. *J Dairy Sci* 75: 1186–1191. doi:10.3168/jds.S0022-0302(92)77865-5.
31. Sambrook J, Russell DW (1989) Molecular cloning: a laboratory manual. 2nd ed. Cold Spring Harbor Laboratory Press Cold Spring Harbor New York.
32. Holo H, Nes IF (1989) High-Frequency Transformation, by Electroporation, of *Lactococcus lactis* subsp. *cremoris* Grown with Glycine in Osmotically Stabilized Media. *Appl Environ Microbiol* 55: 3119–3123.
33. Goel A, Santos F, Vos WM De, Teusink B, Molenaar D (2012) Standardized assay medium to measure *Lactococcus lactis* enzyme activities while mimicking intracellular conditions. *Appl Environ Microbiol* 78: 134–143. doi:10.1128/AEM.05276-11.
34. Andersch W, Bahl H, Gottschalk G (1983) Level of Enzymes Involved in Acetate , Butyrate , Acetone and Butanol Formation by *Clostridium acetobutylicum*. *Appl Microbiol Biotechnol* 18: 327–332.
35. Miller JH (1972) Experiments in molecular genetics. New York (US): Cold Spring Harbor Laboratory.
36. Israelsen H, Madsen SM, Vrang a, Hansen EB, Johansen E (1995) Cloning and partial characterization of regulated promoters from *Lactococcus lactis* Tn917-lacZ integrants with the new promoter probe vector, pAK80. *Appl Environ Microbiol* 61: 2540–2547.
37. Edgar RC (2004) MUSCLE: multiple sequence alignment with high accuracy and high throughput. *Nucleic Acids Res* 32: 1792–1797. doi:10.1093/nar/gkh340.
38. Gruber AR, Lorenz R, Bernhart SH, Neuböck R, Hofacker IL (2008) The Vienna RNA websuite. *Nucleic Acids Res* 36: W70–4. doi:10.1093/nar/gkn188.
39. Buss KA, Cooper DR, Ingram-Smith C, Ferry JG, Sanders DA, et al. (2001) Urkinase: structure of acetate kinase, a member of the ASKHA superfamily of phosphotransferases. *J Bacteriol* 183: 680–686. doi:10.1128/JB.183.2.680-686.2001.
40. Browning DF, Busby SJ (2004) The regulation of bacterial transcription initiation. *Nat Rev Microbiol* 2: 57–65. doi:10.1038/nrmicro787.
41. Meng J, Xu Z, Guo J, Yue Y, Sun X (2013) Analysis of enhanced current-generating mechanism of *Geobacter sulfurreducens* strain via model-driven metabolism simulation. *PLoS One* 8: e73907. doi:10.1371/journal.pone.0073907.
42. Hertzberger RY, Pridmore RD, Gysler C, Kleerebezem M, Teixeira de Mattos MJ (2013) Oxygen relieves the CO2 and acetate dependency of *Lactobacillus johnsonii* NCC 533. *PLoS One* 8: e57235. doi:10.1371/journal.pone.0057235.
43. Lopez de Felipe F, Gaudu P (2009) Multiple control of the acetate pathway in *Lactococcus lactis* under aeration by catabolite repression and metabolites. *Appl Microbiol Biotechnol* 82: 1115–1122. doi:10.1007/s00253-009-1897-8.
44. Kahane I, Muhlrad A (1979) Purification and Properties of Acetate Kinase from *Acholeplasma laidlawii*. *J Bacteriol* 137: 764–772.
45. Fox DK, Roseman S (1986) Isolation and characterization of homogeneous acetate kinase from *Salmonella typhimurium* and *Escherichia coli*. *J Biol Chem* 261: 13487–13497.
46. Lin WR, Peng Y, Lew S, Lee CC, Hsu JJ, et al. (1998) Purification and Characterization of Acetate Kinase from *Clostridium thermoaceticum*. *Tetrahedro*n 54: 15915–15925.
47. Bowman CM, Valdez RO, Nishimura JS (1976) Acetate Kinase from *Veillonella alcalescens*. *J Biol Chem* 251: 3117–3121.
48. Zomer AL, Buist G, Larsen R, Kok J, Kuipers OP (2007) Time-resolved determination of the CcpA regulon of *Lactococcus lactis* subsp. *cremoris* MG1363. *J Bacteriol* 189: 1366–1381. doi:10.1128/JB.01013-06.
49. Grundy FJ, Waters D a, Allen SH, Henkin TM (1993) Regulation of the *Bacillus subtilis* acetate kinase gene by CcpA. *J Bacteriol* 175: 7348–7355.
50. Gerstmeir R, Wendisch VF, Schnicke S, Ruan H, Farwick M, et al. (2003) Acetate metabolism and its regulation in *Corynebacterium glutamicum*. *J Biotechnol* 104: 99–122. doi:10.1016/S0168-1656(03)00167-6.
51. Kakuda H, Shiroishi K, Hosono K, Ichihara S (1994) Construction of Pta-Ack pathway deletion mutants of *Escherichia coli* and characteristic growth profiles of the mutants in a rich medium. *Biosci Biotechnol Biochem* 58: 2232–2235.
52. Contiero J, Beatty C, Kumari S, DeSanti CL, Strohl WR, et al. (2000) Effects of mutations in acetate metabolism on high-cell-density growth of *Escherichia coli*. *J Ind Microbiol Biotechnol* 24: 421–430. doi:10.1038/sj.jim.7000014.
53. Kumari S, Tishel R, Eisenbach M, Wolfe AJ (1995) Cloning, characterization, and functional expression of *acs*, the gene which encodes acetyl coenzyme A synthetase in *Escherichia coli*. *J Bacteriol* 177: 2878–2886.
54. Solem C, Koebmann B, Yang F, Jensen PR (2007) The las enzymes control pyruvate metabolism in *Lactococcus lactis* during growth on maltose. *J Bacteriol* 189: 6727–6730. doi:10.1128/JB.00902-07.
55. Koebmann BJ, Solem C, Pedersen MB, Nilsson D, Jensen PR (2002) Expression of Genes Encoding F1-ATPase Results in Uncoupling of Glycolysis from Biomass Production in *Lactococcus lactis*. *Appl Environ Microbiol* 68: 4274–4282. doi:10.1128/AEM.68.9.4274-4282.2002.
56. Koebmann B, Blank LM, Solem C, Petranovic D, Nielsen LK, et al. (2008) Increased biomass yield of *Lactococcus lactis* during energetically limited growth and respiratory conditions. *Biotechnol Appl Biochem* 50: 25–33. doi:10.1042/BA20070132.

Chapter 5. Influence of NADH/NAD$^+$ on mixed-acid fermentation

5.1 Introduction

The cofactor ratio NADH/NAD$^+$ has been proposed as a key determinant of the switch between homolactic fermentation and mixed-acid fermentation in *L. lactis* [1, 2]. In these two early studies, a higher NADH/NAD$^+$ ratio and higher triosephosphate pool, especially glyceraldehyde 3-phosphate (GAP), were observed at higher glycolytic fluxes. Together with the findings by *in vitro* enzyme assay that pyruvate formate-lyase (PFL) was inhibited by GAP and that glyceraldehyde 3-phosphate dehydrogenase (GAPDH) was very sensitive to high NADH/NAD$^+$ ratio, the authors of the two studies established the model in which a high NADH/NAD$^+$ ratio accompanying a high glycolytic flux activates lactate dehydrogenase (LDH), inhibits GAPDH and thus cause a high GAP pool which in turn inhibits PFL, resulting in homolactic fermentation. Mixed-acid fermentation was proposed to take place conversely when the glycolytic flux is low.

This mechanism, however, was only concluded from the difference in measured metabolite concentrations and enzyme activities. The question of whether change in the NADH/NAD$^+$ ratio would in fact cause any change in the fermentation mode of *L. lactis* remains to be tested *in vivo*. There have been attempts to perturb the redox state by introducing NADH oxidase (NOX) activities [3–6]. Growth in these cases, nonetheless, had to be aerobic for NOX to be active while the pyruvate metabolism of *L. lactis* changes significantly under aerobic conditions compared with anaerobic conditions, e.g. no formate production due to PFL inactivated by oxygen [7], flavour compound production [8, 9].

In this study, we tested the proposed roles of NADH/NAD$^+$ on the shift of fermentation modes in *L. lactis* growing on maltose by introducing enzyme activities to perturb the ratio anaerobically. Formate dehydrogenase (FDH) which produces CO_2 and NADH from formate and NAD$^+$ has recently been introduced into *L. lactis* MG1363 [10]. It was found that flux towards mixed-acid fermentation decreased and the ethanol-to-acetate ratio increased. Here the enzyme, 2,3-butanediol dehydrogenase (23BDH), was introduced for NAD$^+$ regeneration by converting acetoin supplemented in the media into 2,3-butanediol (23BD) (Figure 5.1).

In the ideal case, a system for studying the effect of cofactors perturbation should be isolated from the rest of the metabolism except the exchange of cofactors. Here, under anaerobic conditions, overexpressing 23BDH can be a good approximation of an ideal system based on the following observations: (i) the flavour compounds diacetyl, acetoin and 23BD are generally not produced or produced at very low amounts under anaerobic or microaerobic conditions [8, 9, 11]; (ii) acetolactate synthase (ALS) has very low activity in non-aerated conditions [8, 11]; acetolactate decarboxylase (ALDC) favors the acetoin-forming direction ($\Delta_r G^\circ$ estimated to be -1.7 or -1 kcal/mol in MetaCyc [12]) and requires the fixation of CO_2 for the acetoin-consuming direction; (iii) diacetyl formation

from α-acetolactate requires oxygen; and (iv) diacetyl reductase (DAR) is irreversible. Under anaerobic conditions, therefore, since the flux going into the flavour-forming pathway is absent or negligible and meanwhile acetoin from the medium is unlikely to induce fluxes in reverse directions affecting the upstream metabolism, the overexpression of 23BDH with provided extracellular acetoin can be considered to reasonably approximate an ideal system to perturb NADH/NAD^+ under anaerobic conditions.

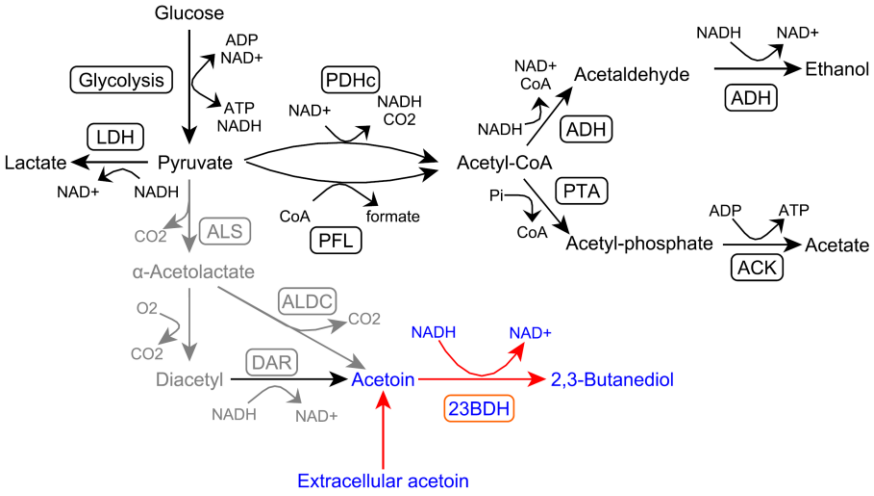

Figure 5.1. Introducing NAD^+-regenerating enzyme activities.

Reactions in color refer to introduced activities to regenerate NAD^+. Reactions in grey are thought to have low or no activity under anaerobic conditions. Enzyme or pathway names are in round rectangles. The stoichiometry from glucose to pyruvate, and from pyruvate to α-acetolactate is 1 to 2 and 2 to 1 respectively, with all other reactions being 1 to 1. LDH, lactate dehydrogenase; PDHc, pyruvate dehydrogenase complex; PFL, pyruvate formate-lyase; ADH, bi-functional alcohol dehydrogenase; PTA, phosphotransacetylase; ACK, acetate kinase; ALS, acetolactate synthase; ALDC, acetolactate decarboxylase; DAR, diacetyl reductase; 23BDH, 2,3-butanediol dehydrogenase. The reaction producing diacetyl from α-acetolactate is non-enzymatic.

5.2 Materials and methods

5.2.1 Bacteria strains and plasmids

All *L. lactis* strains were derived from MG1363 and IL1403. For introducing 23BDH activities, pCS4701 and pCS4639, each containing a synthetic codon-optimized operon consisting of *budC/dar* (encoding diacetyl/acetoin reductase, accession no. AF098800) from *Klebsiella pneumonia* and *budC/bdh* (encoding L-23BDH, accession no. AB009078) from *Brevibacterium saccharolyticum* ordered from GenScript following a synthetic promoter (kindly provided by Christian Solem), were used. Plasmids and strains used or constructed in this study are listed in Table 5.1 and Table 5.2 respectively.

Table 5.1. Plasmid used in the study.

Plasmid	Description
pCI372 [13]	Shuttle vector between *E. coli* and *L. lactis*; chloramphenicol resistence
pCS4639	pCI372 derivatives, each carrying a synthetic promoter followed by a synthetic codon-optimized operon consisting of *budC/dar* (encoding diacetyl/acetoin reductase, accession no. AF098800) from
pCS4701	*Klebsiella pneumonia* and *budC/bdh* (encoding L-23BDH, accession no. AB009078) from *Brevibacterium saccharolyticum* ordered from GenScript; chloramphenicol resistence

Table 5.2. Strains used or constructed in the study.

Strain	Description
Parent strain	
MG1363 [14]	A plasmid-free strain derived from *L. lactis* subsp. *cremoris* NCDO 712
IL1403 [15]	A plasmid-free strain derived from *L. lactis* subsp. *lactis* biovar *diacetylactis* CNRZ157
MG/SP1-*bdh*	MG1363 transformed with pCS4701; Cam^r
MG/SP2--*bdh*	MG1363 transformed with pCS4639; Cam^r
IL/SP1-*bdh*	IL1403 transformed with pCS4701; Cam^r

Cam^r, chloramphenicol resistence

5.2.2 Culture media and conditions

L. lactis was cultivated in M17 media or chemically defined SA media [16] at 30 ˚C without aeration, supplemented with 0.2% (w/v) glucose (GM17). When needed chloramphenicol were added at 5 μg ml^{-1} for *L. lactis* respectively. For growth experiments, defined SA media devoid of sodium acetate and supplemented with nucleosides (adenosine, cytidine, guanosine, thymidine, uridine and inosine, 20 mg/L), α-lipoic acid (2 mg/L) and either glucose or maltose (0.2%) were used, abbreviated as GluSALN or MalSALN respectively. To enable the detection of acetoin consumption and 23BD production by HPLC, in some cases, the buffer MOPS used in normal SALN media was replaced by 1.9% β-glycerophosphate (BPG), which is applied in the M17 media. The resultant medium is denoted by SALN(BPG) medium. Growth experiments were conducted in flasks at 30 ˚C under static conditions with slow stirring. Optical density at 600 nm (OD_{600}) was regularly measured. To prepare a preculture, a single colony from an agar plate was inoculated into GluSALN or MalSALN media in dilution series. Growth experiments were started by inoculating an exponentially growing overnight culture selected from the dilution series into a flask containing the same medium, up to OD_{600} = 0.001 or 0.02 for growth on glucose or maltose respectively. Biological triplicates for each experiment were performed. The cell density equal to 0.36 g (dry weight) (gdw) per liter of SALN medium at OD_{600} = 1 was used for the calculation of specific rates.

5.2.3 Quantification of sugar and fermentation products

High-performance liquid chromatography (HPLC) was employed to measure the concentration of glucose, maltose, lactate, formate, acetate, ethanol, acetoin and 23BD in the samples taken during the

growth experiments as previously described [17]. Specific rates of consumption/production for mid-exponential growth phase ($OD_{600} \approx 0.4 – 0.6$) were calculated Carbon recovery was calculated as the sum of acetate, ethanol and lactate fluxes divided by sugar uptake flux in C_3-mole.

5.2.4 Extraction and quantification of NADH and NAD^+

Growing culture of *L. lactis* in the mid-exponential phase (OD_{600}=0.4) was quenched by liquid nitrogen and stored at -20 ˚C. Extraction and quantification of nicotinamide adenine dinucleotides were performed using the kit NAD/NADH-Glo™ Assay (Promega) following the instruction of the provided manual. NAD^+ and NADH were extracted by heating in acidic and basic solutions respectively. They were then individually quantified by a luciferase assay perform on 96-well white microplates (Greiner Bio-one, cat. no. 655904) using the Infinite® M1000 PRO microplate reader (TECAN). Intracellular concentrations were estimated by assuming that 1 g (dry weight) of cells corresponded to 1.67 ml of intracellular volume [18].

5.2.5 DNA techniques

Electrocompetent cells of *L. lactis* were grown in M17 broth supplemented with 10 g L^{-1} glucose and 10 g L^{-1} glycine and transformed by electroporation as described previously [19].

5.2.6 Measurement of 2,3-butanediol dehydrogenase activity

Exponentially growing culture at OD_{600}=0.6 was quenched on ice and harvested, then resuspended in extract buffer [17] and disrupted by glass beads (106-μm diameter; Sigma, Prod. No. G4649) using a FastPrep (MP Biomedicals, Santa Ana, USA). The master buffer used for the assay was adapted from Goel et al. [20]: 100 mM HEPES, 50 mM NaCl, 400 mM potassium glutamate, 1 mM potassium phosphate and 10× diluted metal ions present in SA medium, adjusted to pH 7.5 with potassium hydroxide. The reaction mix included the master buffer, 5 mM acetoin and 0.25 mM NADH. The enzyme activities were determined by monitoring OD_{340} corresponding to the concentration of NADH using the Infinite® M1000 PRO microplate reader (TECAN) and the accompanying software Magellan. The 96-well microplates used were purchased from Greiner Bio-one (Cat. No. 655901). Protein concentration was determined using Bradford Reagent (Sigma, Prod. No. B6916) and a protein standard (200 mg ml^{-1} BSA, Sigma, Prod. No. P5369), following the protocol provided by the manufacturer.

5.3 Results

5.3.1 Introduction of 2,3-butanediol dehydrogenase activity

To introduce 23BDH activity, the vector pCS4701 containing a gene encoding 23BDH following a synthetic promoter was transformed into MG1363 and IL1403 respectively. The resultant strains derived from MG1363 and IL1403 were called MG/SP1-*bdh* and IL/SP1-*bdh* respectively.

As a preliminary test, the fermentation products of MG1363, MG/SP1-*bdh*, IL1403 and IL/SP1-*bdh* in overnight cultures in MalSALN media were quantified (Figure 5.2). For MG/SP1-*bdh*, the fermentation pattern was very similar to that of the wild-type MG1363. When the substrate of 23BDH, acetoin, was added into the medium, however, substantial increase in acetate (from 5.3 to 8.3 mM) and decrease in ethanol (from 4.6 to 1.9 mM) were observed. The formate produced was also reduced (from 11.5 to 10 mM). For IL/SP1-*bdh*, while in the absence of acetoin, it behaved similarly, interestingly, the formate production increased substantially (from 1.4 to 3.8 mM) and the effect for acetate was even more pronounced (from 0.8 to 4 mM).

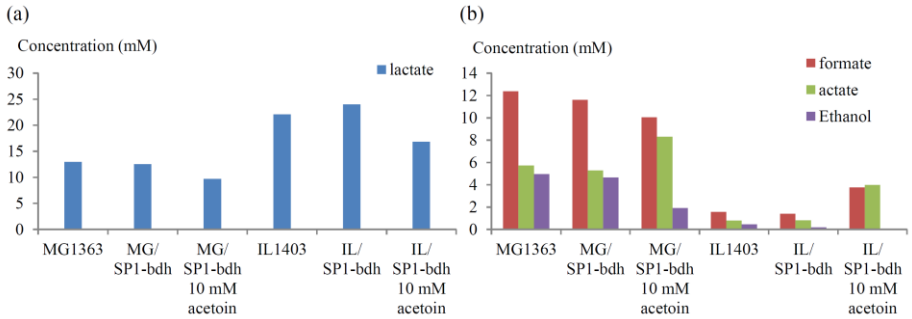

Figure 5.2. Products in overnight cultures in MalSALN media with/without acetoin.
(a) Lactate concentrations and (b) formate, acetate and ethanol concentrations.

5.3.2 Faster growth of MG/SP1-*bdh* in the presence of acetoin in the media

To further investigate the effect of 23BDH activity and the presence of acetoin in media on the fermentation pattern, growth experiments of MG1363 and MG/SP1-*bdh* were conducted in MalSALN media with 0, 5 mM (MG/SP1-*bdh* only) or 20 mM acetoin. Interestingly, the growth rate of MG/SP1-*bdh* increased from 0.61 h^{-1}, a value close to the wild-type MG1363, to 0.67 h^{-1} and 0.72 h^{-1} as extracellular acetoin increased from 0 to 5 mM and 20 mM respectively (Figure 5.3a). Meanwhile, 20 mM acetoin present in the medium appeared to inhibit the growth of MG1363 slightly.

The specific maltose consumption rates of MG/SP1-*bdh* were in all cases lower than MG1363 growing in the medium with no acetoin (Figure 5.3b). Since the growth rates of MG/SP1-*bdh* are higher, the biomass yields (= growth rate / maltose flux) on maltose of MG/SP1-*bdh* were higher than those of MG1363.

5.3.3 Flux directed towards acetate production

When growing on media with acetoin, MG/SP1-*bdh* exhibited significant redirection of pyruvate flux compared to MG1363. For MG1363, the fermentation shifted to a more homolactic one in the presence of 20 mM action. For MG/SP1-*bdh*, no substantial change in lactate and formate production was observed for growth with zero or 5 mM acetoin (Figure 5.3c, d). At 20 mM acetoin, while the formate flux dropped similarly, the lactate production in MG/SP1-*bdh* also decreased in contrast to

the increase in MG1363. The most pronounced effect was observed in acetate production, which significantly increased with acetoin concentration in MG/SP1-*bdh* (Figure 5.3e). The case of 20 mM is in particular interesting because the acetate flux (15 mmolh^{-1}gdw^{-1}) was much larger than the formate flux (6 mmolh^{-1}gdw^{-1}). This situation seldom happened in anaerobic conditions. Meanwhile, ethanol production was reduced significantly to virtually zero production at 20 mM acetoin (Figure 5.3f). The complete data are shown in Table C.1 and Table C.2 in Appendix C.

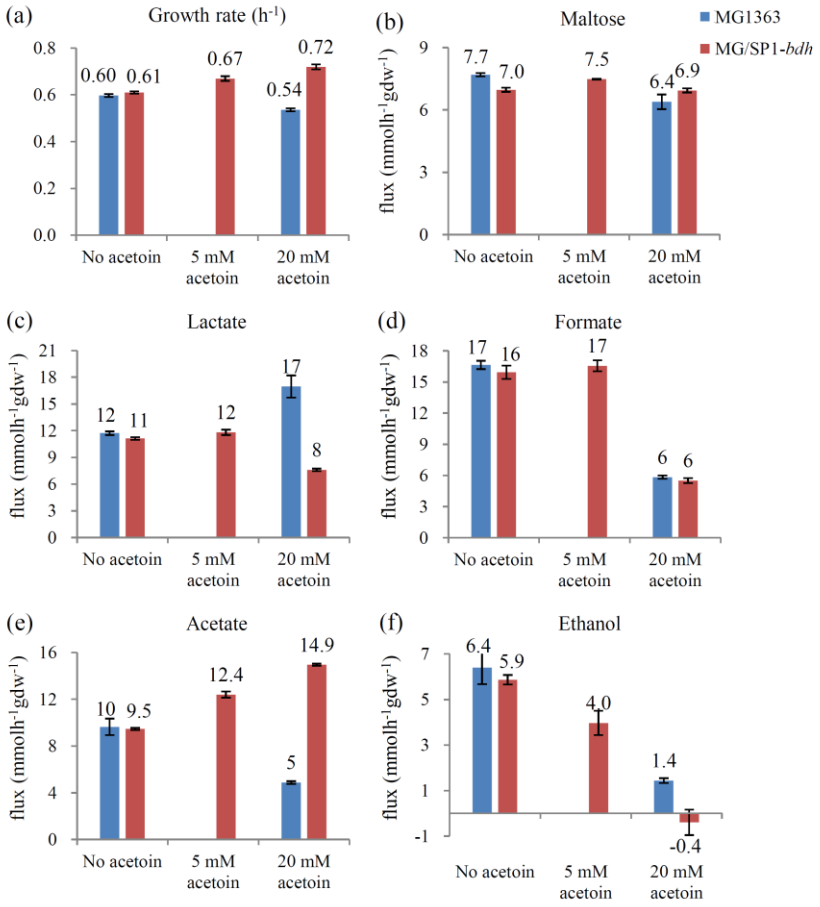

Figure 5.3. Growth rates, fluxes of MG1363 and MG/SP1-*bdh* growing in MalSALN.

(a) Growth rates, specific rates of (b) maltose consumption, (c) lactate, (d) formate, (e) acetate and (f) ethanol production of MG1363 and MG/SP1-*bdh* growing in MalSALN with no acetoin, 5 mM (MG/SP1-*bdh*) or 20 mM acetoin were shown.

5.3.4 No change in growth rate in media devoid of lipoic acid

MG1363 and MG/SP1-*bdh* were also cultivated in MalSAN media which was devoid of lipoic acid, the essential cofactor of pyruvate dehydrogenase complex (PDHc) at acetoin concentrations of 0, 10 and 20 mM (Table 5.3). Interestingly, the growth rate of MG/SP1-*bdh* was constantly about 0.6 h^{-1} along the increase of acetoin concentrations. While the change in fermentation pattern in the presence of acetoin was in general similar to the growth in MalSALN, the decreases in formate production (from 16 to 11 or 12 mmolh^{-1}gdw^{-1}) and increases in acetate production (from 9 to 10 or 11 mmolh^{-1}gdw^{-1}) at higher acetoin concentrations were less pronounced. An obvious difference is the acetate

flux being lower than the formate flux in all cases contrary to the case of MG/SP1-*bdh* growing in MalSALN with 20 mM acetoin.

Table 5.3. MG1363 and MG/SP1-*bdh* growing in MalSAN with or without acetoin.

Strain	Acetoin added	Growth rate (h^{-1})	Specific rate of sugar consumption and product formation ($mmolh^{-1}gdw^{-1}$)				
			Maltose	Lactate	Formate	Acetate	Ethanol
MG1363	0	0.60	8.2	13	19	10	10.5
	20 mM	0.47	7.0	17	6	4	1.9
MG/SP1-*bdh*	0	0.58	8.0	14	16	9	8.1
	10 mM	0.56 ± 0.01	7.2 ± 0.4	10 ± 0.4	11 ± 0.3	10 ± 0.1	0.3 ± 0.1
	20 mM	0.59 ± 0.01	7.4 ± 0.1	10 ± 0.4	12 ± 0.3	11 ± 0.1	0.2 ± 0.2

5.3.5 Unexpected lower carbon recovery in MG/SP1-*bdh* at ≥ 10mM acetoin

When checking the carbon balance in the growth experiments, it was found that only 80% of carbon was recovered from the product for MG/SP1-*bdh* growing on MalSALN with 20 mM acetoin. For growth on MalSAN with 10 or 20 mM acetoin, the recovery even reduced to 70%. The recovery was significantly lower than that of other conditions (≥ 90%), which was generally observed in previous experiments.

5.3.6 Growth of MG1363, MG/SP2-*bdh* and MG/SP1-*bdh* in MalSALN(BGP)

In light of the uncharacterized effect of ≥ 10mM acetoin which deviated the carbon balance very significantly, in the subsequent experiments, only 5 mM acetoin was applied to the media in which the carbon recovery remained at a high level (Table C.2). To more clearly quantify the effect of the NAD^+-regenerating activity brought by 23BDH, the strain MG/SP2--*bdh*, which is MG1363 transformed with pCS4639 containing a weaker promoter than that in pCS4701, was also characterized. Finally, to allow the quantification of acetoin and 2,3-butanediol by HPLC, the buffer MOPS used in normal SALN media was replaced by 1.9% β-glycerophosphate which acts as buffer in the M17 medium.

The results of growth in MalSALN(BPG) were in general similar to those in MalSALN except the overall lower growth rates (Figure 5.4). MG/SP2--*bdh* and MG/SP1-*bdh*, when supplemented with 5 mM acetoin, grew slightly faster than the wild-type MG1363 albeit they had lower maltose uptake fluxes (Table 5.4).

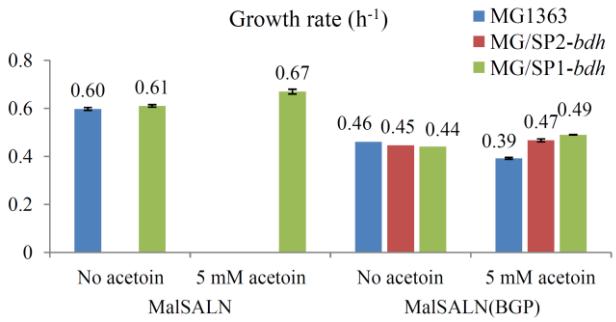

Figure 5.4. Growth rates in MalSALN or MalSALN(BGP) media.
Growth of MG/SP1-*bdh* was not tested in MalSALN

Table 5.4. Specific rates of MG1363, MG/SP2--*bdh* and MG/SP1-*bdh* growing in MalSALN(BGP).

Acetoin added	Strain	Growth rate (h^{-1})	Specific rate of sugar consumption/product formation ($mmolh^{-1}gdw^{-1}$)				
			Maltose	Lactate	Formate	Acetate	Ethanol
0	MG1363	0.46	7.3	10	17.5	9.6	6.6
	MG/SP2--*bdh*	0.45	7.1	11	16.3	9.1	6.4
	MG/SP1-*bdh*	0.44	7.0	12	16.2	9.2	5.5
5 mM	MG1363	0.39 ± 0.004	7.8 ± 0.3	17 ± 0.4	9.2 ± 0.3	6.6 ± 0.1	2.3 ± 0.2
	MG/SP2--*bdh*	0.47 ± 0.006	6.8 ± 0.1	13 ± 0.3	14.7 ± 0.9	10.0 ± 0.1	4.3 ± 0.1
	MG/SP1-*bdh*	0.49 ± 0.002	7.0 ± 0.1	10 ± 0.2	16.4 ± 0.7	11.7 ± 0.2	3.6 ± 0.2

Acetate and ethanol production significantly increased and decreased respectively while the formate flux was reduced slightly and no significant change in lactate flux was observed when comparing MG/SP2--*bdh* and MG/SP1-*bdh* growing at 5 mM acetoin to MG1363 growing without acetoin (Table 5.4). The changes in growth rate, acetate and ethanol production were found to be correlated with the *in vitro* activity of 23BDH in the strains and so were the increases in acetoin consumption and 23BD production (Figure 5.5). No production of diacetyl was observed.

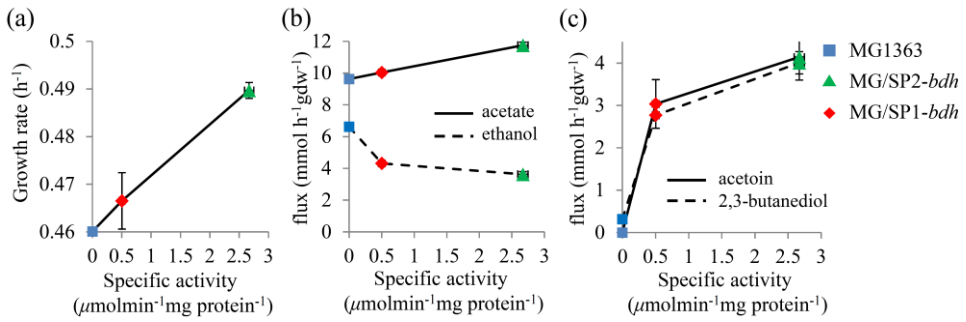

Figure 5.5. Fluxes of MG1361, MG/SP2--*bdh* and MG/SP1-*bdh* plotted against 23BDH activity.
(a) Growth rate, (b) acetate, ethanol, (c) acetoin (uptake) and 2,3-butanediol (23BD) fluxes plotted against the specific activity of 23BDH measured in MG/SP2--*bdh* and MG/SP1-*bdh*. MG1363 growing without acetoin was assumed to have zero activity.

Here we compared to MG1363 growing without acetoin and assigned a zero specific 23BDH activity to this case because no acetoin was added to the medium and no acetoin was detectable while 23BD was produced at a very low rate of 0.3 $mmolh^{-1}gdw^{-1}$, compared to the pyruvate flux of 29 $mmolh^{-1}gdw^{-1}$. It is also because in the ideal case, 23BDH acts as an isolated system exchanging only NADH and NAD^+ with the rest of the metabolism in the presence of acetoin or 23BD, so there would be no activity in the absence of any substrates. Furthermore, although for MG1363 growing at 5 mM acetoin, a very low 23BDH activity concomitant with acetoin consumption and 23BD production at rates lower than MG/SP2--*bdh* and MG/SP1-*bdh* were measured (see Table C.5 in Appendix C for the data), the case appeared to be not a good reference that was comparable with others because it grew substantially slower and deviated to a more homolactic mode of fermentation in the presence of 5 mM extracellular acetoin. More discussion can be found below in 'Unexpected effect of extracellular acetoin'.

5.3.7 Slower growth of MG/SP2-*bdh* and MG/SP1-*bdh* on glucose

The three strains were also cultivated on glucose under the same conditions. Similar to the case of maltose, when supplied with 5 mM acetoin, MG/SP2--*bdh* and MG/SP1-*bdh* had slightly lower glycolytic fluxes and significantly more acetate production compared to MG1363 which similarly appeared to be more homolactic in the presence of 5 mM acetoin (Table 5.5). Moreover, MG/SP1-*bdh* consumed acetoin and produced 23BD at highest rates to which MG/SP2--*bdh* was second (Table C.5 in Appendix C).

Table 5.5. Specific rates of MG1363, MG/SP2--*bdh* and MG/SP1-*bdh* growing in GluSALN(BGP).

Acetoin added	Strain	Growth rate (h^{-1})	Specific rate of sugar consumption/product formation ($mmolh^{-1}gdw^{-1}$)				
			Glucose	Lactate	Formate	Acetate	Ethanol
0	MG1363	0.99	24.8	45.0	2.1	1.7	-0.22
	MG/SP2--*bdh*	0.98	24.0	47.2	2.3	2.0	0.83
	MG/SP1-*bdh*	0.97	25.4	45.6	2.1	1.9	-0.33
5 mM	MG1363	0.98 ± 0.01	24.5 ± 0.6	46.3 ± 1.1	1.1 ± 0.1	1.0 ± 0.2	0.5 ± 0.6
	MG/SP2--*bdh*	0.95 ± 0.00	23.5 ± 0.5	39.7 ± 0.8	0.6 ± 0.1	3.1 ± 0.1	-0.3 ± 0.5
	MG/SP1-*bdh*	0.95 ± 0.00	23.3 ± 0.3	37.3 ± 0.9	0.4 ± 0.2	5.1 ± 0.2	0.1 ± 0.2

Despit the resemblance, several distinctive features of interest could also been observed. First, MG/SP2--*bdh* and MG/SP1-*bdh* grew slower than MG1363 when extracellular acetoin was present (Table 5.5). Second, lactate flux decreased whereas ethanol production remained indefinite. For each replicate of the same experimental conditions, either production or consumption of ethanol at a very low rate might be measured. This indeed appeared to be a feature commonly observed for growth on glucose in our experimental setup (e.g. Table 2.5 in Chapter 2). Third, the production of formate by MG/SP2--*bdh* and MG/SP1-*bdh* was lower than that of MG1363 growing at 5 mM acetoin. More interestingly, it was much less than the production of acetate.

5.3.8 Increased NADH/NAD$^+$ ratio

Concentrations of NADH and NAD$^+$ of cultures in MalSALN(BGP) and GluSALN(BGP) were quantified. The NADH/NAD$^+$ ratio measured in MG1363 growing on glucose or maltose was comparable to previous studies (e.g. [2]) and was higher on glucose than on maltose (Table 5.6). For MG/SP2--*bdh* and MG/SP1-*bdh*, surprisingly, their measured NADH/NAD$^+$ ratios were higher than that of MG1363. The increase was most significant for growth on maltose, from 0.06 in MG1363 to 0.26 in MG/SP2--*bdh* and 0.37 in MG/SP1-*bdh*, whereas the increase in the ratio of MG/SP2--*bdh* and MG/SP1-*bdh* compared to MG1363 growing on maltose without acetoin was much smaller. For growth on maltose, the concentrations of both NADH and NAD$^+$ increased in MG/SP1-*bdh* and MG/SP2-*bdh* whereas for growth on glucose, NAD$^+$ concentration showed no significiant change.

5.4 Discussion

5.4.1 Strategy to perturb NADH/NAD$^+$

In this study, 23BDH together with acetoin added to media was proposed as an approximation for an ideal system which perturbs the NADH/NAD$^+$ ratio by converting NADH into NAD$^+$ and is isolated from the rest of the metabolism. While under aerobic conditions NOX is a good choice, under anaerobic conditions the construction of such a system is not straightforward because of the complexity of the metabolic network. The design of the present system was based on the knowledge on *L. lactis* to try to find a reaction with low activity whose substrate and product can both be easily transported into and out of the cells.

Table 5.6. Measurements of NADH/NAD$^+$ ratio and their intracellular concentrations.

	0 mM acetoin			5 mM acetoin		
	MG1363	MG/SP2--bdh	MG/SP1-bdh	MG1363	MG/SP2--bdh	MG/SP1-bdh
MalSALN (BGP)						
NADH (mM)	0.08	0.09	0.13	0.02 ± 0.01	0.13 ± 0.03	0.20 ± 0.04
NAD$^+$ (mM)	1.01	0.88	0.92	0.33 ± 0.06	0.51 ± 0.07	0.55 ± 0.03
NAD(H) pool (mM)	1.09	0.96	1.04	0.35 ± 0.07	0.64 ± 0.10	0.76 ± 0.07
NADH/NAD$^+$	0.08	0.10	0.14	0.06 ± 0.02	0.26 ± 0.05	0.37 ± 0.06
GluSALN (BGP)						
NADH (mM)				0.19 ± 0.03	0.19 ± 0.01	0.28 ± 0.05
NAD$^+$ (mM)		Not determined		0.91 ± 0.07	0.80 ± 0.03	0.88 ± 0.09
NAD(H) pool (mM)				1.11 ± 0.10	0.99 ± 0.03	1.16 ± 0.14
NADH/NAD$^+$				0.21 ± 0.02	0.24 ± 0.01	0.31 ± 0.03

NAD(H) pool is the sum of the concentrations of NADH and NAD$^+$.

Characterization of growth and fermentation pattern and quantification of NADH/NAD$^+$ ratio showed that the growth of MG/SP2--*bdh* and MG/SP1-*bdh* which contain plasmids expressing 23BDH was

similar to MG1363 in the absence of acetoin but significantly different in the presence of acetoin. This indicated that the difference originated from the conversion of acetoin into 23BD by the 23BDH activity expressed in MG/SP2--*bdh* and MG/SP1-*bdh*. This is strongly supported by the similar measured rates of acetoin consumption and 23BD production. In this sense, the introduced system can answer the question of the effect of NADH/NAD^+ ratio on fermentation modes to a certain extent except a disadvantage described below.

5.4.2 Unexpected effect of extracellular acetoin on MG1363

From experimental data regarding MG1363, the presence of acetoin in media appeared to turn the fermentation mode into more homolactic and even with carbon lost probably to other pathways at a higher acetoin concentration of 20 mM. This to a certain extent confused the interpretation of the results. A hypothesis that can explain the phenomenon and fit the data is that acetoin inhibits the activity of PFL. The formate production of MG1363 in either MalSALN(BGP) or GluSALN(BGP) was 2-fold lower in the presence of 5 mM acetoin present. In fact, we observed that for MG/SP2--*bdh* and MG/SP1-*bdh* growing in MalSALN(BGP) with 5 mM acetoin, the formate production rate increased in the early exponential phase (OD_{600} = 0.15 – 0.3) and became fairly constant in the reported mid-exponential phase (OD_{600} = 0.35 – 0.6) along with the decrease of acetoin concentration in the media (data not shown). Meanwhile, the consumption rate of sugar, production rate of lactate and acetate remained constant over the entire range.

This hypothesis can explain the slower growth of MG1363 in the presence of acetoin because the acetate production and thus ATP production rate were limited by the supply of acetyl-CoA by PFL. The exact effect of acetoin requires further investigation. For the system to work in a more elegent way, for example, acetoin can be added at a lower amount (say 1 mM) and growth is characterized at a lower cell density or weaker synthetic promoters can be used so that acetoin is consumed slow but steadily. Chemostat can also be used in which the acetoin concentration can be finetuned to a low level enough for full activity.

5.4.3 PDHc activity in anaerobic conditions

Another side observation of the study is the suspected activity of pyruvate dehydrogenase complex (PDHc) which oxidases pyruvate into acetyl-CoA. In the literature, PDHc was proposed to be inactive anaerobically due to the high NADH/NAD^+ ratio [21] and was found to have low or no expression anaerobically [2, 8, 11]. In our results, PDHc activity was suggested by the larger acetate flux than formate flux when MG/SP1-*bdh* grew in MalSALN with 20 mM acetoin and GluSALN(BPG) with 5 mM acetoin. In contrast, the acetate flux was lower and very close to the formate flux for the slower growth of MG/SP1-*bdh* in MalSAN without α-lipoic acid, an essential cofactor for PDHc activity that *L. lactis* is auxotrophic for. This further supported that PDHc was indeed active under such conditions. These cases with acetate production probably supported by PDHc activity can be interpreted as an

altermative acetate-producing capacity brought by PDHc when PFL was not available, very much alike the case of aerobic growth where PFL was inactivated by oxygen, PDHc was found to be active and acetate was produced [11]. The magnitude of the PDHc activity observed in this study has rarely been reported in the literature.

5.4.4 Shift towards acetate production in MG1363 and additionally formate production in IL1403

From different sets of experiments, it is clear that in MG1363, additional NAD^+-regenerating activities brought by 23BDH had a positive control on acetate production flux. For growth on maltose, the flux was redirected from ethanol production and allowed faster growth. This corresponds well to the recent results which found an increased ethanol-to-acetate ratio and meanwhile a slower growth rate when introducing FDH activity into MG1363 to produce NADH from NAD^+ by oxidizing formate into CO_2 [10]. The effect on formate production, however, could not be concluded because it coincided with the apparent inhibitory effect of acetoin on formate production.

For growth on glucose, the increase in acetate production was redirected from lactate production. The decrement in formate flux in MG/SP2--*bdh* and MG/SP1-*bdh* can be savely considered as an effect of the additional NAD^+-regenerating activity because the formate flux of MG1363 growing with 5 mM acetoin which did not consume acetoin was even higher than that of MG/SP2--*bdh* and MG/SP1-*bdh* which consumed acetoin down to 4 mM and 3 mM respectively (data not shown). Consequently, the inhibitory effect of acetoin on formate production had to be less significant in MG/SP2--*bdh* and MG/SP1-*bdh* than MG1363. The effect should thus originate from the additional NAD^+-regenerating activity.

The mechanism of the redirection of flux from ethanol production in the maltose case or from lactate in the glucose case is not clear. It might be simply the competition of NADH between lactate dehydrogenase (LDH), alcohol dehydrogenase (ADH) and 23BDH. For the inhibition of formate production on glucose, one possible explanation is the higher $NADH/NAD^+$ ratio. By the model proposed in [1, 2], this would inhibit GAPDH and cause a higher GAP pool, which inhibits PFL, to accumulate for maintaining a high glycolytic flux.

From the test of IL1403 and IL/SP1-*bdh* in overnight culture, however, a more than two-fold increase of both formate and acetate were observed in the presence of extracellular acetoin. This suggested that acetoin may not be inhibitory to the mixed-acid fermentation pathway in IL1403 as in MG1363. Moreover, the more mixed-acid fermentation pattern in IL1403 caused by the additional NAD^+-regenerating activity to a certain extent confirm one of the conjecture made in Chapter 3 of why IL1403 remains homolactic even at low glycolytic flux. However, more efforts are required to characterize IL1403 and IL/SP1-*bdh* for more concrete conclusions.

5.4.5 Counterintuitive NADH/NAD^+ ratio

Among all the results, the most confusing one is the higher NADH/NAD^+ ratio measured. Intuitively, introducing a reaction that acts in the direction of NAD^+ production should lower the NADH/NAD^+ ratio. From the flux data, it seems that the reason is the additional NAD^+-producing flux by 23BDH could not compensate the decrease in the other NAD^+-producing flux (summarized in Table 5.7). This might involve some very interesting kinetic behavior which can be studied through kinetic modeling, for example, oscillation of the system. This might also help to explain why PDHc appeared to be active under a high NADH/NAD^+ ratio. The worst possibility is that the quantification procedure was problematic and thus caused large systematic errors in all experiments.

Table 5.7. Estimated net production of NADH from glycolysis and fermentation.

Strain	Flux through pathway/enzyme ($mmolh^{-1}gdw^{-1}$)					Net NADH production* ($mmolh^{-1}gdw^{-1}$)
	Glycolysis (C_6-mol)	LDH	PDHc	ADH	23BDH	
GluSALN(BGP)						
MG1363	24.8	45.0	0	-0.22	0	5.0
MG/SP1-*bdh*	23.3	37.3	4.7	0.1	6.7	7.1
MalSALN(BGP)						
MG1363	14.6	10	0	6.6	0.3	5.7
MG/SP1-*bdh*	14.0	10	0	3.6	4.0	6.8

* Production = 2 × glycolysis + PDHc; consumption = LDH + 2 × ADH + 23BDH. 23BDH, 2,3-butanediol dehydrogenase; ADH, alcohol dehydrogenase; PDHc, pyruvate dehydrogenase complex.

5.5 References

1. Garrigues C, Loubiere P, Lindley ND, Cocaign-Bousquet M (1997) Control of the shift from homolactic acid to mixed-acid fermentation in *Lactococcus lactis*: predominant role of the NADH/NAD^+ ratio. *J Bacteriol* 179:5282–5287. Available at: http://www.pubmedcentral.nih.gov/articlerender.fcgi?artid=179393&tool=pmcentrez&rendertype=abstract.
2. Garrigues C, Mercade M, Cocaign-Bousquet M, Lindley ND, Loubiere P (2001) Regulation of pyruvate metabolism in *Lactococcus lactis* depends on the imbalance between catabolism and anabolism. *Biotechnol Bioeng* 74:108–15. Available at: http://www.ncbi.nlm.nih.gov/pubmed/11369999.
3. Lopez de Felipe F, Kleerebezem M, de Vos WM, Hugenholtz J (1998) Cofactor engineering : a novel approach to metabolic engineering in *Lactococcus lactis* by controlled expression of NADH oxidase. *J Bacteriol* 180:3804–3808.
4. Neves AR et al. (2002) Effect of different nadh oxidase levels on glucose metabolism by *Lactococcus lactis*: kinetics of intracellular metabolite pools determined by *in vivo* nuclear magnetic resonance. *Appl Environ Microbiol* 68:6332–6342. Available at: http://aem.asm.org/cgi/doi/10.1128/AEM.68.12.6332-6342.2002 [Accessed July 12, 2012].
5. Hoefnagel MHN et al. (2002) Metabolic engineering of lactic acid bacteria, the combined approach: kinetic modelling, metabolic control and experimental analysis. *Microbiology* 148:1003–13. Available at: http://www.ncbi.nlm.nih.gov/pubmed/11932446.
6. Lopez de Felipe F, Gaudu P (2009) Multiple control of the acetate pathway in *Lactococcus lactis* under aeration by catabolite repression and metabolites. *Appl Microbiol Biotechnol* 82:1115–22. Available at: http://www.ncbi.nlm.nih.gov/pubmed/19214497 [Accessed September 29, 2013].
7. Melchiorsen CR et al. (2000) Synthesis and posttranslational regulation of pyruvate formate-lyase in *Lactococcus lactis*. *J Bacteriol* 182:4783–4788. Available at: http://jb.asm.org/cgi/doi/10.1128/JB.182.17.4783-4788.2000 [Accessed September 29, 2013].

8. Nordkvist M, Jensen NBS, Villadsen J (2003) Glucose metabolism in *Lactococcus lactis* MG1363 under different aeration conditions: requirement of acetate to sustain growth under microaerobic conditions. *Appl Environ Microbiol* 69:3462–3468. Available at: http://aem.asm.org/cgi/doi/10.1128/AEM.69.6.3462-3468.2003 [Accessed August 13, 2014].
9. Duwat P et al. (2001) Respiration capacity of the fermenting bacterium *Lactococcus lactis* and its positive effects on growth and survival. *J Bacteriol* 183:4509–4516.
10. Dehli TI (2013) Engineering *Lactococcus lactis* towards butanol production and increased butanol tolerance. Dissertation (Technical University of Denmark).
11. Jensen NB, Melchiorsen CR, Jokumsen KV, Villadsen J (2001) Metabolic behavior of *Lactococcus lactis* MG1363 in microaerobic continuous cultivation at a low dilution rate. *Appl Environ Microbiol* 67:2677–82. Available at: http://www.pubmedcentral.nih.gov/articlerender.fcgi?artid=92924&tool=pmcentrez&rendertype=abstract [Accessed January 24, 2012].
12. Caspi R et al. (2014) The MetaCyc database of metabolic pathways and enzymes and the BioCyc collection of Pathway/Genome Databases. *Nucleic Acids Res* 42.
13. Hayes F, Daly C, Fitzgerald GF (1990) Identification of the minimal replicon of *Lactococcus lactis* subsp. *lactis* UC317 plasmid pCI305. *Appl Environ Microbiol* 56:202–9. Available at: http://www.pubmedcentral.nih.gov/articlerender.fcgi?artid=183273&tool=pmcentrez&rendertype=abstract.
14. Gasson MJ (1983) Plasmid complements of *Streptococcus lactis* NCDO 712 and other lactic streptococci after protoplast-induced curing. *J Bacteriol* 154:1–9. Available at: http://www.pubmedcentral.nih.gov/articlerender.fcgi?artid=217423&tool=pmcentrez&rendertype=abstract.
15. Chopin A, Chopin MC, Moillo-Batt A, Langella P (1984) Two plasmid-determined restriction and modification systems in *Streptococcus lactis*. Plasmid 11:260–263.
16. Jensen PR, Hammer K (1993) Minimal requirements for exponential growth of *Lactococcus lactis*. *Appl Environ Microbiol* 59:4263–6.
17. Andersen HW, Solem C, Hammer K, Jensen PR (2001) Twofold reduction of phosphofructokinase activity in *Lactococcus lactis* results in strong decreases in growth rate and in glycolytic flux. *J Bacteriol* 183:3458–67. Available at: http://www.pubmedcentral.nih.gov/articlerender.fcgi?artid=99644&tool=pmcentrez&rendertype=abstract [Accessed January 24, 2012].
18. Koebmann BJ, Solem C, Pedersen MB, Nilsson D, Jensen PR (2002) Expression of genes encoding F1-ATPase results in uncoupling of glycolysis from biomass production in *Lactococcus lactis*. *Appl Environ Microbiol* 68:4274–4282. Available at: http://aem.asm.org/cgi/doi/10.1128/AEM.68.9.4274-4282.2002 [Accessed January 24, 2012].
19. Holo H, Nes IF (1989) High-frequency transformation, by electroporation, of *Lactococcus lactis* subsp. *cremoris* grown with glycine in osmotically stabilized media. *Appl Environ Microbiol* 55:3119–23. Available at: http://www.pubmedcentral.nih.gov/articlerender.fcgi?artid=203233&tool=pmcentrez&rendertype=abstract.
20. Goel A, Santos F, Vos WM De, Teusink B, Molenaar D (2012) Standardized assay medium to measure *Lactococcus lactis* enzyme activities while mimicking intracellular conditions. *Appl Environ Microbiol* 78:134–43. Available at: http://www.pubmedcentral.nih.gov/articlerender.fcgi?artid=3255609&tool=pmcentrez&rendertype=abstract [Accessed March 12, 2013].
21. Snoep JL et al. (1993) Differences in sensitivity to NADH of purified pyruvate dehydrogenase complexes of Enterococcus faecalis , *Lactococcus lactis* , Azotobacter t ; inelandii and *Escherichia coli* : Implications for their activity *in vivo*. *FEMS Microbiol Lett* 114:279–284. Available at: http://www.ncbi.nlm.nih.gov/pubmed/8288104.

Chapter 6. Amino acid metabolism and fermentation modes

6.1 Introduction

In addition to the gene expression level and cofactor level, the nutrient availability has once been shown to be one of the factors influencing the fermentation modes. Garrigues et al. observed that for *L. lactis* growing on the same carbon source galactose, the richer the medium was, the faster the growth rate was and unexpectedly the more mixed-acid the fermentation became [1]. This disproved the hypothesis that the extent of mixed-acid fermentation is simply negatively correlated to the growth rate. Moreover from these experimental results, the authos proposed the theory that the mixed-acid switch depends on the balance between catabolism and anabolism. When the catabolic flux is the growth-limiting factor for reasons such as growth on slowly fermentable sugars like galactose, mixed acids are produced for ATP maximization by acetate production whereas when other anabolic requirements such as amino acid (AA) biosynthesis are limiting for growth, homolactic fermentation prevails.

In our previous study, the same pattern was observed for *L. lactis* MG1363 growing on maltose in the define SA medium omitting certain AAs [2]. Some of the results are summerized in

Table 6.1. Different AAs could have very different effects on both growth rate and mixed-acid fermentation.

In this study, we attempted to explore this aspect from the computational perspective by using the recently published genome-scale metabolic network for MG1363 and a set of experimental data from that publication [3]. Elementry flux modes (EFMs) were chosen as the tool for metabolic pathway analysis [4] because they represent all the minimal functional units in a metabolic network which may reveal unexpected connections between different metabolic activities.

Table 6.1. Selected results about the impact of amino acid availability on mixed-acid fermentation[1].

Medium [2]	Growth rate (h^{-1})	Formate % [3]
SALN	0.65	56%
SALN ÷ cysteine	0.64	45%
SALN ÷ phenylalanine	0.59	36%
SALN ÷ alanine	0.58	52%
SALN ÷ lysine	0.55	45%
SALN ÷ threonine	0.43	30%

[1] Adapted from [2].

[2] 0.2% maltose, SA medium supplemented with α-lipoic acid and nucleosides (SALN).

[3] Formate percentage was calculated as: $flux_{formate} / (flux_{formate} + flux_{lactate})$

6.2 Results and discussion

6.2.1 Computational method developed

A decomposition method termed 'minimal branching decomposition' (MBD) was developed to interpret a flux distribution in terms of a set of EFMs with an overall minimum number of branching pathways with respect to a given set of metabolites. By choosing amino acids as the set of metabolites with minimum branching pathways involving them, the computational method was applied to a flux distribution estimated from the experimental data of MG1363 exhibiting significant mixed-acid fermentation [3]. This may reveal the distribution of the amino acid fluxes into different metabolic activities including catabolism as well as biomass formation.

The computational method, as a method of representing flux distributions by EFMs that is applicable to general metabolic networks, has been published. Please see Appendix A for the full paper which includes the derivation, validation and application of the method to the amino acid metabolism of *L. lactis* MG1363 and other metabolic models.

6.2.2 Amino acid utilization and mixed-acid fermentation

Here more discussion is presented regarding the relationship between amino acid metabolism and mixed-acid fermentation in addition to the results presented in the article in Appendix A. Table 6.2 shows the rates of production of fermentation products and consumption of glucose and amino acids of the estimated flux distribution and the EFMs decomposing it. The redox balance and ATP production from the module of glycolysis and fermentation pathways were also calculated.

Lactate production was only involved in two of the EFMs which were redox-balanced in the module of glycolysis and fermentation pathways. In all other modes acetate and formate were produced. An interesting observation is that the module of glycolysis and fermentation in the overall flux distribution was indeed redox-unbalanced with net production in NADH. Flahaut et al. has ascribed this to the production of flavour compounds from amino acids which oxidized NADH and shared the role of alcohol dehydrogenase to allow more acetate production [3].

In our resolution of the flux distribution by EFMs, the same could be observed. EFM 5, 6 and 13 in Table 6.2 together accounted for 80% of the net NADH produced in glycolysis. In these modes, 50% or less carbon from glucose uptake ended up in acetate production. All or most of the rest of carbon entered into the amino acid metabolism and participated in flavour compound production together with the amino acids assimilated in these EFMs, glycine, threonine and methionine. The flavour compounds produced in these three modes accounted for 60% of all flavour compound production. These NAD^+-regenerating pathways in additional to fermentation contributed to around 10% of the ATP and acetate production. In the sugar-uptake-limited case being analysed (chemostat at dilution rate of $0.05h^{-1}$), this 10% contribution is expected to be quite important for growth. This finding also

supports the finding in Chapter 5 which suggested additional NAD^+-regenerating activities switched the metabolism towards acetate production.

Another interesting observation is that even though the overall carbon recovery was lower than 100% indicating some glucose ended up in products or biomass other than lactate, formate, acetate and ethanol, EFMs with recovery higher than 100% might actually be active. In EFM 7 and 14, though at small fluxes, formate and acetate were directly produced from cysteine and serine.

The above analysis provided hints for the possible connection of amino acid metabolism and the mixed-acid fermentation, in particular acetate production. The flux distribution being analyzed, however, is only one of the infinitely many possible solutions of the flux space constrained by exchange fluxes. A more comprehensive framework considering the whole feasible flux space and EFMs simultaneously should allow more systematic assessment of the significance of the decomposition by EFMs.

6.3 References

1. Garrigues C, Mercade M, Cocaign-Bousquet M, Lindley ND, Loubiere P (2001) Regulation of pyruvate metabolism in *Lactococcus lactis* depends on the imbalance between catabolism and anabolism. *Biotechnol Bioeng* 74:108–15. Available at: http://www.ncbi.nlm.nih.gov/pubmed/11369999.
2. Aminzadeh A. (2014) The effect of amino acids and specific enzyme activities on mixed-acid production in *L. lactis.* Bachelor thesis, Technical University of Denmark.
3. Flahaut NAL, Wiersma A, van de Bunt B, Martens DE, Schaap PJ, Sijtsma L, dos Santos VAM, de Vos WM. (2013) Genome-scale metabolic model for *Lactococcus lactis* MG1363 and its application to the analysis of flavour formation. *Appl Microbiol Biotechnol* 97:8729–39. Available at: http://www.ncbi.nlm.nih.gov/pubmed/23974365 [Accessed December 13, 2013].
4. Schuster S, Hilgetag C (1994) On elementary flux modes in biochemical reaction systems at steady state. *J Biol Syst* 2:165–182.

Substrate/ Product		Flux (mmolh^{-1}gdw^{-1})															
		Flux distrib.	EFM[a]														
			1	2	3	4	5	6	7	8	9	10	11	12	13	14	15
Production	Lactate	0.606									0.365		0.2				
	Formate	2.305	0.235	0.0065	0.863	0.8817	0.04	0.07	0.01	0.0068	0.042	0.0014		0.005	0.106	0.01	0.035
	Acetate	1.213	0.120	0.0043	0.449	0.4439	0.04	0.03	0.01	0.0046	0.037	0.0011		0.002	0.046	0.01	0.016
	Ethanol	0.994	0.115	0.0022	0.414	0.4370				0.0014		0.0003		0.002	0.009		0.014
Uptake	Glucose	1.523	0.135	0.0029	0.445	0.4591	0.04	0.05		0.0024	0.192	0.0008	0.1	0.002	0.054		0.021
	Ala	0.039	0.006	0.0002	0.012					0.0015	0.010	0.0002					0.008
	Arg	0.009	0.003	0.0001	0.006												
	Asp	0.008		0.0002	0.008												
	Cys	0.031	0.004	0.0001	0.007											0.01	0.010
	Glu	0.046	0.013	0.0005	0.026	0.0004				0.0004	0.003	0.00004					0.002
	Gly	0.046	0.004	0.0002	0.008			0.03									
	His	0.004	0.001	0.0000	0.002												
	Ile	0.018	0.006	0.0002	0.012												
	Leu	0.049	0.018	0.0004	0.028	0.0016											
	Lys	0.018	0.004	0.0001	0.008	0.0004				0.0004	0.003	0.00004					0.002
	Met	0.005	0.001	0.0001	0.003										0.001		
	Phe	0.008	0.003	0.0001	0.005												
	Ser	0.085	0.010	0.0022	0.019				0.01	0.0044	0.043	0.0006					
	Thr	0.062	0.005	0.0002	0.009	0.0098	0.04										
	Val	0.016	0.005	0.0002	0.010												
Glycolysis + fermentation pathways:																	
NADH production[b]		2.9	0.2	0.0047	0.87	0.89	0.08	0.10	0	0.003	0.37	0.0009	0.2	0.005	0.11	0	0.03
NADH consumption[c]		2.6	0.2	0.0045	0.83	0.87		0.03	0	0.003	0.37	0.0005	0.2	0.005	0.02	0	0.03
NADH net production		0.3	0	0.0002	0.04	0.02	0.08	0.07	0	0.000	0.00	0.0004	0	0	0.09	0	0.00
ATP production[d]		4.1	0.3	0.0082	1.29	1.32	0.12	0.13	0.01	0.006	0.39	0.0015	0.2	0.007	0.15	0.01	0.03
ATP production %		100%	8%	0%	32%	33%	3%	3%	0%	0%	10%	0%	6%	0%	4%	0%	1%
Carbon recovery[e]		92%	87%	113%	97%	96%	50%	33%	∞[f]	124%	104%	78%	100%	100%	51%	∞[f]	74%

Table 6.2. Production and uptake fluxes of the estimated flux distribution and its decomposition by EFMs.

[a] Four EFMs with ≤ 0.1% of the sum of fluxes of the flux distribution were not shown.

[b] NADH production from glycolysis was equal to the flux of GAPDH.

[c] NADH consumption by fermentation modes was calculated as the sum of flux through LDH and 2 × flux through ADH.

[d] ATP production was calculated as the sum of fluxes through PGK, PYK and ACK subtracted by the flux through PFK.

[e] Carbon recovery was calculated as the sum of production of lactate, acetate and ethanol divided by the consumption of glucose.

[f] Carbon recovery equal to inifinity implies fermentation products produced from carbon sources other than glucose.

Chapter 7. Conclusion and future directions

7.1 Conclusion

In the present study, efforts have been made to investigate the switch between homolactic fermentation and mixed-acid fermentation influenced by three aspects of metabolism, namely the level of gene expression in the pathway for mixed-acid fermentation, the level of the cofactor NADH/NAD^+ and the availability of amino acids as nutrients.

7.1.1 Different promoter activities of mixed-acid genes

At the level of gene expression, the promoter activities of the genes in the pathway branch that produces formate, acetate and ethanol were compared between the two important laboratory strains MG1363 and IL1403 which differ from each other with respect to the mixed-acid switch. The results suggested that different types of regulatory elements governed the transcriptional regulation of different genes in the two strains, including the obvious indication of *trans*-regulation on pyruvate formate-lyase (PFL) and *cis*-regulation on phosphotransacetylase (PTA), as well as the more unobvious regulation pattern for the two genes encoding for acetate kinase (ACK).

7.1.2 Contrl on mixed-acid fermentation by pyruvate formate-lyase

The difference observed in the promoter activity of PFL between the two strains led to the attempt to modulating the expression of PFL in both MG1363 and IL1403. For MG1363, consistent with results from the literature, PFL was found to have control on the mixed-acid switch. In particular, complementary to the previous control analysis which implied the existence of one or more reactions positively controlling the formate flux in the wild-type MG1363 growing on glucose, we estimated a control coefficient close to one by PFL on the formate flux at the wild-type PFL level for growth on glucose. For IL1403, however, the modulation was not successful and this suggested that a high expression of PFL might be lethal. Overexpressing PFL is thus probably not the first step to take to restore a mixed-acid-fermenting phenotype of IL1403.

7.1.3 Complementary roles of acetate kinase isozymes

Meanwhile, the interesting observation that one of the genes for ACK was the only gene having a higher promoter activity in IL1403 than in MG1363 gave rise to the conjecture that the two genes for ACK might play different roles in acetate metabolism. We then characterized the two genes in MG1363. We found different kinetic properties of the two ACKs encoded by the two genes and their complementary roles for acetate production and uptake under different conditions. It was also observed that the existence of acetate kinase isozymes was very common among bacteria.

7.1.4 Acetate production induced by additional NAD^+-regenerating activities

At the level of metabolic regulation, we tested the proposed roles of the cofactors NADH and NAD^+ on the mixed-acid switch by introducing an enzyme activity to approximate an ideal isolated system that only oxidized NADH from the metabolism to NAD^+ anaerobically. The construction partially restored the mixed-acid fermenting ability in IL1403 as reflected by a substantial increase in formate and acetate production. For MG1363, no any positive effect on formate production was observed but significant increase in acetate and decrease in ethanol were observed. An interesting observation was the apparent high flux through pyruvate dehydrogenase complex which has not been reported in the literature.

7.1.5 Connection between amino acid metabolism and fermentation modes

The extent of the mixed-acid fermentation of MG1363 was found to depend on amino acid availability and individual amino acids could have largly different impact. Meanwhile, a computational method for combining metabolic flux analysis and elementary mode analysis was developed and applied to a flux distribution estimated from experimental data. Elementary modes connecting amino acid metabolism and fermentation modes were observed.

7.2 Future directions

Based on the results from the current studies, many interesting questions are worth futher research. They are described below.

7.2.1 Identify transcriptional regulators and *cis*-regulatory elements

In Chapter 2, *trans*-regulatory elements for the transcriptional regulation of *pfl*, probably activators for growth on maltose or repressors for growth on glucose were suggested to exist. The exact genetic element responsible for this observation can be identified through random mutagenesis using existing tools such as insertional sequence ISS1 for *L. lactis* and subsequent screening for the loss of reporter activity on maltose or gain on glucose.

Moreover, *cis*-regulatory elements regulating the transcription of *eutD*, the gene for phosphotransacetylase, were also expected to exist and the mutated *cre* site upstream of *eutD* in IL1403 was proposed as a candidate. It can be tested by restoring the *cre* site in IL1403.

7.2.2 Restore the phenotype of mixed-acid fermentation for IL1403

In Chapter 3, the modulation of PFL in IL1403 turned out to be unsuccessful while in Chapter 5 the formate- and acetate- producing ability of IL1403 was increased. Further efforts can be made to restore the mixed-acid-fermenting phenotype of IL1403.

7.2.3 Characterize acetate-dependent growth of IL1403

In Chapter 4 only the ACK isozymes of MG1363 were studied though the study was originally motivated by a stronger induction of the promoter of one of the ACKs in IL1403 whose ortholog in MG1363 was later found to be specialized in acetate uptake. It would be interesting to compare the acetate-dependent growth of IL1403 to that of MG1363 and see whether the effect in IL1403 is even more pronounced.

7.2.4 Model the perturbation of NADH/NAD^+ ratio

In Chapter 5, introducing an NADH-consuming enzyme unexpectedly resulted in increase in the measured NADH/NAD^+ ratio. If the trend of the measurement is correct, very interesting kinetic behaviour may be involved in this situation. Kinetic modeling would be a powerful tool to make sense of the observation.

7.2.5 Study the effect of another important cofactors, ATP/ADP ratio

Beside NADH/NAD^+, in the literature, the ATP/ADP ratio has also been proposed to be an important factor of the mixed-acid switch. It would be interesting to perturb the ATP/ADP ratio by introducing ATPase activities as in previous studies.

7.2.6 Comprehensive computational analysis on the connection between amino acid metabolism and fermentation modes

For a more in-depth understanding of the relationship between amino acid metabolism and fermentation modes, a more comprehensive computational analysis using genome-scale models and elementary modes can be performed. The experimental data of growth in media with different amino acid compositions, together with other availabile –omics data such as gene-expression data can be integrated for identifying active subnetworks. Such analysis is expected to shed light on some unobvious pathways or hidden regulation between the two subsystems.

Appendix A Estimating biological elementary flux modes that decompose a flux distribution by the minimal branching property

Published in Bioinformatics (Oxford University Press), 30 (22):3232-3239, doi:10.1093/bioinformatics/btu529. Reprinted with permission.

Siu Hung Joshua Chan1[1], Christian Solem[1], Peter Ruhdal Jensen[1] and Ping Ji[2]

[1]Systems Biotechnology and Biorefining, National Food Institute, Technical University of Denmark

[2]Department of Industrial and Systems Engineering, The Hong Kong Polytechnic University

A.1 Abstract

Motivation: Elementary flux mode (EFM) is a useful tool in constraint-based modeling of metabolic networks. The property that every flux distribution can be decomposed as a weighted sum of EFMs allows certain applications of EFMs to studying flux distributions. The existence of biologically infeasible EFMs and the non-uniqueness of the decomposition, however, undermine the applicability of such methods. Efforts have been made to find biologically feasible EFMs by incorporating information from transcriptional regulation and thermodynamics. Yet, no attempt has been made to distinguish biologically feasible EFMs by considering their graphical properties. A previous study on the transcriptional regulation of metabolic genes found that distinct branches at a branch point metabolite usually belong to distinct metabolic pathways. This suggests an intuitive property of biologically feasible EFMs, i.e. minimal branching.

Results: We developed the concept of minimal branching EFM and derived the minimal branching decomposition (MBD) to decompose flux distributions. Testing in the core *Escherichia coli* metabolic network indicated that MBD can distinguish branches at branch points and greatly reduced the solution space in which the decomposition is often unique. An experimental flux distribution from a previous study on mouse cardiomyocyte was decomposed using MBD. Comparison with decomposition by a minimum number of EFMs showed that MBD found EFMs more consistent with established biological knowledge, which facilitates interpretation. Comparison of the methods applied to a complex flux distribution in *Lactococcus lactis* similarly showed the advantages of MBD. The minimal branching EFM concept underlying MBD should be useful in other applications.

A.2 Introduction

Metabolic networks consisting of biochemical reactions and compounds in a cell have proven to be an extremely useful in silico tool to study cellular metabolism (Edwards and Palsson, 1999; Oberhardt et al., 2009; Price et al., 2004). The structure of a metabolic network is reflected in the stoichiometric matrix S, and the state of the network is embodied in the flux distribution (FD) **v**, which is a vector

containing all reaction rates in the network. Based on the well-established quasi-steady-state assumption, $\mathbf{v}$ can be constrained in a polyhedral cone ($\mathbf{Sv}=\mathbf{0}$, $\mathbf{v}_{ub} \geq \mathbf{v} \geq \mathbf{v}_{lb}$) and studied using a series of so-called constraint-based reconstruction and analysis (COBRA) methods (Lewis et al., 2012).

One of the approaches of theoretical importance and application value is the elementary flux mode (EFM) analysis (Schuster and Hilgetag, 1994). An EFM is a FD with a minimal number of active reactions that together satisfy the steady-state condition. It is thus a minimal metabolic pathway in a metabolic network. EFMs have been successfully applied to examine network structures, explore newmetabolic pathways, suggest rational strain design, etc. (reviewed in Trinh et al., 2009; Zanghellini et al., 2013).

Another property of EFMs useful for studying FDs is that every FD $\mathbf{v}$ is a non-negative sum of EFMs:

$$\mathbf{v} = \sum_{k=1}^{K} \alpha_k \mathbf{e}_k \tag{1}$$

where $\mathbf{e}_1 \cdots \mathbf{e}_K$ are all EFMs of the network, and α_k is the corresponding weight coefficient. This decomposition of FDs from EFMs or extreme pathways (another type of pathways with a similar definition) has been investigated and applied to certain biological studies by choosing particular decompositions [reviewed in Chan and Ji (2011)]. The usefulness of these methods, however, is limited for two main reasons. First, the practical computation of the decomposition requires the set of all EFMs *a priori*, which is usually not available in large-scale networks owing to combinatorial explosion. This computational issue can be overcome in two ways, either by sampling EFMs (Machado et al., 2012; Tabe-Bordbar and Marashi, 2013) or by finding EFMs with particular properties to solve for the decomposition without requiring the entire set of EFMs (Chan and Ji, 2011; de Figueiredo et al., 2009; Ip et al., 2011; Pey and Planes, 2014; Rezola et al., 2011). The second limitation is the non-uniqueness of decomposition and its dependence on the choice of algorithms or optimization objective (Zanghellini et al., 2013). The ambiguity severely weakens the biological significance of decomposition. Poolman et al. (2004) has proposed a method to obtain unique decompositions by combining EFMs with variable weights into compound modes with unique weights. Another method for unique decompositions is the minimization of the sum of squares of weights (Schwartz and Kanehisa, 2005, 2006), but the resulting decomposition can be dependent on how EFMs are scaled.

The usefulness of EFMs can be enhanced by finding biologically feasible EFMs. Attempts have been made to incorporate transcriptional regulatory information to enumerate biologically feasible EFMs (Jungreuthmayer et al., 2013) and to rule out thermodynamically infeasible EFMs (Jol et al., 2012).

These approaches integrating information other than stoichiometry did give promising results. The information, for instance, metabolomics data and transcriptomics data, however, is not always available. Surprisingly, all the proposedmethods to find EFMs or to choose decomposition have notmade full use of their graphical properties, which should be intuitively important for interpreting EFMs. An earlier study on the co-regulation of metabolic pathways found that transcriptional regulation tends to favor linear metabolic flow by co-expressing only distinct branches at metabolic branch points (Ihmels et al., 2004). This means, in Figure A.1 where '*A*' is a hypothetical branch point metabolite, the genes for the linear pair of reactions '*R1*' and '*R3*', or the pair '*R2*' and '*R4*', are more likely to be co-expressed than '*R3*', '*R4*' and '*R5*', which are distinct branches. When decomposing a FD containing '*R1*' to '*R4*', two EFMs containing pair '*R1*'and '*R3*' and pair '*R2*' and '*R4*' are thus a more preferable choice than one EFM containing all '*R1*' to '*R4*', as there are probably two distinct pathways. This suggests the rationale of minimizing branching pathways to choose EFMs that are more likely to be biologically feasible. This rationale is also expected to allow clearer interpretation of the roles of the chosen EFMs because they are expected to contain fewer distinct pathways. We believed that such EFMs can have wide applicability. As the first attempt based on this rationale, in this article, a new optimization objective called minimal branching decomposition (MBD) is proposed to identify more biologically relevant EFMs to decompose FDs using stoichiometric information alone.

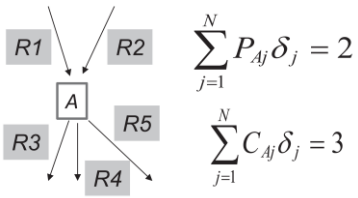

Figure A.1. The graphical meaning of NP_{ik}.
A is a metabolite in the network. If EFM 1 contains all five reactions, then $NP_{A1} = 2 \times 3 = 6$, equal to the number of all locally different paths passing through *A*.

A.3 Methods

A.3.1 Optimization objective

The goal is to derive an optimization objective for finding $\alpha_1 \cdots \alpha_K$ to compute an MBD composed of EFMs with as few branching pathways as possible. Given the set of all EFM contained in the matrix $\mathbf{E} = [\mathbf{e}_1 \cdots \mathbf{e}_K] = [e_{jk}] \in \mathbf{R}^{n \times K}$ and the stoichiometric matrix $\mathbf{S} = [S_{ij}] \in \mathbf{R}^{m \times n}$ in a metabolic network with *m* metabolites and *n* reactions, assume that the FD to be decomposed is $\mathbf{v} = [v_j] \in \mathbf{R}^n$.

First, define the consumption matrix $\mathbf{C} = [C_{ij}]$ and the production matrix $\mathbf{P} = [P_{ij}]$ for metabolites:

$$C_{ij} = \begin{cases} 1 & \text{if} \quad S_{ij} < 0 \\ 0 & \text{if} \quad S_{ij} \geq 0 \end{cases}, \; P_{ij} = \begin{cases} 1 & \text{if} \quad S_{ij} > 0 \\ 0 & \text{if} \quad S_{ij} \leq 0 \end{cases} \tag{2}$$

In other words, if $C_{ij} = 1$, then metabolite *i* is consumed by reaction *j* and if $P_{ij} = 1$, then metabolite *i* is produced by reaction *j*. Based on **C** and **P**, compute the number of paths $\mathbf{NP} = [NP_{ik}] \in \mathbf{R}^{m \times K}$ passing through metabolite *i* in EFM *k*:

$$NP_{ik} = \left(\sum_{j=1}^{n} C_{ij} \delta_{jk} \right) \left(\sum_{j=1}^{n} P_{ij} \delta_{jk} \right) \tag{3}$$

where $\delta_{jk} = 1$ if $e_{jk} \neq 0$ and $\delta_{jk} = 0$ if $e_{jk} = 0$. NP_{ik} is in fact the number of reactions consuming metabolite *i* multiplied by the number of reactions producing metabolite *i* in EFM *k*. It is thus the number of locally different paths passing through metabolite *i*. Figure A.1 illustrates an example. **NP** is used for distinguishing EFMs which deviate from linear flow through branch point metabolites. Perfectly linear EFMs would have $NP_{ik} = 1$ for all metabolites and EFMs with more branching flow would have higher NP_{ik}. The minimum use of EFMs with high NP_{ik} therefore defines the optimization objective to obtain an MBD. Hence, the objective coefficient c_k for EFM *k* is expressed as the following sum:

$$c_k = \sum_{i=1}^{m} w_i NP_{ik} \tag{4}$$

where w_i is the weight for metabolite *i*. It is manually assigned to account for the relative importance of a metabolite as a branch point metabolite. The simplest way for assigning weights to metabolites is to just assign 1 for all weights meaning that there is no bias toward the branching of any metabolite in an EFM. In practice, biological knowledge is required to choose suitable weights to obtain better decomposition. For example, for pyruvate which is a true branch point metabolite involved in different metabolic pathways, a decomposition by EFMs with different fates of pyruvate, for instance, one going into the anaerobic fermentation and the other going into the TCA cycle, is preferred to a decomposition by all EFMs involving both the fermentation and the TCA cycle. In this case, branching of pyruvate within an EFM is strongly undesired so the weight can be set to be much higher than 1. In contrast, cofactors like ATP/ADP are global cellular currencies and their distinct linear flow may not be biologically relevant. Low or zero weights can be assigned to them. The weighting also depends on the particular purpose of application. For example, if one focuses on comparing the glycolysis and the pentose phosphate pathway, a high weight can then be assigned to glucose 6-phosphate, which is a branch point of the two pathways.

A.3.2 Minimal branching decomposition

Having derived the objective, an MBD can be obtained by solving the following mixed integer linear programming problem (MILP):

$$\min \sum_{k=1}^{K} \sum_{i=1}^{m} w_i NP_{ik} \beta_k \tag{5}$$

$$\text{subject to } \sum_{k=1}^{K} e_{jk} \alpha_k = v_j \text{ for } j = 1, \ldots, N \tag{6}$$

$$0 \le \alpha_k \le \beta_k \text{ for } k = 1, \ldots, K \tag{7}$$

$$\beta_k \in \{0,1\} \text{ for } k = 1, \ldots, K \tag{8}$$

Objective (5) minimizes the use of EFMs with higher numbers of non-linear pathways being active at branch point metabolites. Equation (6) is the constraint for decomposition. Constraint (7) is the on/off switch for an EFM. If $\beta_k = 0$, EFM *k* is switched off. If $\beta_k = 1$, EFM *k* is switched on. In the problem stated here, two assumptions without loss of generality are made on the EFM matrix $\mathbf{E} = [e_{jk}]$ for simpler presentation. First, **E** is calculated from a stoichiometric matrix consisting of irreversible reactions only. It can be achieved by dividing each reversible reaction into two irreversible reactions with stoichiometry negative to each other. This avoids negative fluxes and additional constraints on reversible EFMs. Second, all EFMs are assumed to be scaled to have maximum weights not greater than 1 ($\alpha_k \le 1$). One way for scaling is to multiply each $\mathbf{e}_k$ by $r_k = \min_j \{v_j / e_{jk} \,|\, e_{jk} > 0\}$. Another method used in Wiback *et al*. (2003) is scaling to an uptake reaction by multiplying each $\mathbf{e}_k$ by $r_k = v_{\text{uptake}} / e_{\text{uptake},k}$.

It is noted that the 'no cancellation' property of decomposition by EFMs (Llaneras and Picó, 2010) ensures that if for a reaction *j*, $v_j = 0$, then all EFMs with $e_{jk} \neq 0$ must have $\alpha_k = 0$. It facilitates optimization by first selecting EFMs able to have non-zero weights for a FD, called 'contributable EFMs' and defined by $\mathbf{E}_{CONTRI} = \{\mathbf{e}_k \,|\, e_{jk} = 0 \text{ if } v_j = 0\}$, out of **E** which is usually intractable for larger networks (Klamt and Stelling, 2002; Trinh et al., 2009).

A.3.3 Enumeration of alternative optima

One of the major drawbacks of interpreting decomposition by EFMs is the non-uniqueness. Despite the use of certain optimization objectives, for instance, a minimum number of EFMs as in Wiback *et al*. (2003), the number of alternative optimal solutions can still be large. The performance of MBD regarding the uniqueness of decomposition was examined by enumerating alternative optima. The *R*-th alternative optimal MBD was calculated by adding the following constraint to the model:

$$\sum_{k=1}^{K} \beta_k^r \beta_k \le \left(\sum_{k=1}^{K} \beta_k^r \right) - 1 \text{ for } r = 1, \ldots, R-1 \tag{10}$$

where $\mathbf{b}_r = [\beta_1^r \quad \cdots \quad \beta_K^r]$ is the binary integer solution of the *r*-th alternative optimal MBD found. Suboptimal solutions can also be found.

A.3.4 Other decompositions for comparison

MBD was compared with decomposition by a minimum number of EFMs (MinEFMD) and random decomposition (RD). MinEFMD was calculated by replacing eq. (5) with for all k. RD was sampled as follows:

Initialization: $\mathbf{D} = \{\}$.

Step 1: find contributable EFMs $\mathbf{E}_{CONTRI} = \{\mathbf{e}_k \mid e_{jk} = 0 \text{ if } v_j = 0\}$.

Step 2: randomly choose an $\mathbf{e}_k$ from $\mathbf{D} \leftarrow \mathbf{D} \cup \{\mathbf{e}_k\}$.

Step 3: $\mathbf{v} \leftarrow \mathbf{v} - r\mathbf{e}_k$ where $r = \min_j \{v_j / e_{jk} \mid e_{jk} > 0\}$.

Step 4: if $\mathbf{v} = \mathbf{0}$, terminate and $\mathbf{D}$ is a decomposition. Else, go to step 1.

A.3.5 Implementations

EFMs were calculated using *efmtool* (Terzer and Stelling, 2008) and optimization models were solved by Gurobi 5.5® via the COBRA toolbox in MATLAB® in which all other calculations were performed. The MATLAB script file is available in the Supplementary Material (section A.8). The desktop computer used had a 3.1 GHz quad-core CPU and 16 GB of RAM.

A.4 Results

MBD was tested on randomly sampled FDs in the core *Escherichia coli* metabolic network as a validation of the method (Orth et al., 2010). It was then applied to a FD determined by isotopomer distributions reported previously for the cardiomyocyte in perfused mouse heart (Vo and Palsson, 2006) and to a FD estimated from a dataset of metabolite assimilation and excretion in the recently published genome-scale metabolic network of *Lactococcus lactis* (Flahaut et al., 2013). In the latter two cases, FDs were not sampled because they were estimated from experimental data.

A.4.1 Core *E. coli* metabolic network

The core *E. coli* metabolic network (Orth et al., 2010) with 95 reactions and 72 metabolites simplified from the *i*AF1260 genome-scale network of *E. coli* (Feist et al., 2007) includes glycolysis, TCA cycle, oxidative phosphorylation, pentose phosphate pathway and a biomass reaction, alongside with a set of transcriptional regulatory rules that can be readily implemented. Three different tests were performed to examine (i) the ability to separate fluxes at branch point metabolites; (ii) the performance in a

simulated case consistent with regulatory rules and (iii) the issue of multiple optimal decompositions. As the set of all possible FDs has infinitely many solutions, random sampling based on the hit-and-run method (Almaas et al., 2004) was applied to sample FDs for the tests. Table A.1 summarizes the results. More details can be found in Supplementary Material (section A.8).

Table A.1. Summary of test results in the core *E. coli* metabolic network.

Test	Result
1. Separation of combined fluxes at branch points. 83 cases in scenario 1 (Figure A.2a), 94 cases in scenario 2 (Figure A.2b)	Correct recovery rate Scenario 1 Scenario 2 MBD: 100% MBD: 94% RD: 7.5% RD: 1%
2. Coupling of glyoxylate cycle and acetate uptake implied by the regulatory rules in the presence of fructose and acetate (Figure A.2c).	No EFMs with simultaneous fructose uptake and glyoxylate cycle activity MBD: 100% MinEFMD : 0% RD: 1%
3. Uniqueness of decompositions. Enumeration of alternative MBDs and MinEFMDs	MBD: 2,000 FDs tested. 45% unique; 95% ≤ 8 optima. MinEFMD: 20 FDs tested. 100% ≥ 1,000 optima

RD: random decomposition.

Separation of fluxes at branch points

To check that the proposed method has the desired ability to choose EFMs of distinct branches at branch points, two scenarios were tested (Figure A.2a). First, two of the consuming reactions (*C1*, *C2*) of a branch point were chosen. Two sets of FDs, one with $v_{C1} \neq 0$, $v_{C2} = 0$ and vice versa, were sampled and summed up as the set of FDs being tested. The second scenario is more difficult in which metabolites have two producing reactions (*P1*, *P2*) individually and coupled to *C1* and *C2* respectively (Figure A.2b). FDs were sampled and summed up as complex FDs for testing. In both scenarios, FDs were decomposed into EFMs to check whether the distinct branches were correctly associated in the chosen EFMs. In this test, the available carbon sources were set to be fructose and acetate to allow more branch points while their simultaneous uptake does not conflict the given regulatory rules. As this test aimed to assess the basic ability of MBD, the weight w_i was set to 1 for the branch point being tested and 0 for the rest of metabolites. All metabolites were balanced during the calculation of EFMs. 19 500 EFMs were calculated.

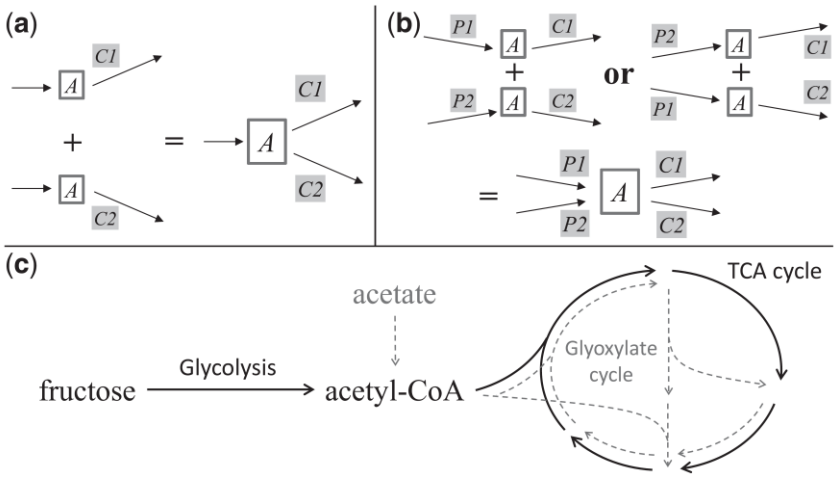

Figure A.2. Testing the ability of MBD to separate fluxes at branch points.

(a) Scenario 1 in test 1: separation of two individual consuming reactions. (b) Scenario 2 in test 1: correct separation of two pairs of coupled producing and consuming reactions. (c) Test 2: a simulated case of glyoxylate cycle coupled to acetate uptake implied by regulatory rules.

There are 11 branch points in the first scenario. In each case, 10 FDs were randomly sampled and then subjected to MBD. In all, 1000 RDs were obtained for each FD as comparison. In all cases, no EFMs in an MBD use two consuming reactions simultaneously whereas it is true for only 7.5% of the RDs overall. In scenario 2, six branch points with two or more producing and consuming reactions were identified and 94 combinations were tested. For each combination, 10 FDs for each of the four producing and consuming pairs were sampled and combined as shown in Figure A.2b. MBDs for the resultant FDs were then calculated. In 94% of the MBDs for near 2000 FDs, all EFMs involve the correct reaction pairs whereas only 1% of the RDs is correct. These results confirmed that the proposed MBD is capable of separating fluxes at branch point metabolites.

Coupling of glyoxylate cycle and acetate uptake

The given regulatory rules of the core *E. coli* network imply that the glyoxylate cycle is active only if acetate is being consumed. Thus, in the presence of fructose and acetate, the system can consume both substrates with the glyoxylate cycle used primarily for acetate metabolism. Similar experiments and results have been reported in yeast (dos Santos et al., 2003). To test whether MBD can distinguish the acetate-induced glyoxylate cycle from the TCA cycle, two sets of FDs were sampled, one without acetate uptake and glyoxylate cycle activity and the other without fructose uptake (**Figure A.3**c). One FD from each set was summed to form a complex FD which was subject to MBD. $w_i = 1$ for all metabolites except the obvious branch point Acetyl-CoA with $w_i = 1000$. MinEFMDs and RDs were also computed for comparison.

In all 200 FDs tested, no EFMs in any MBDs have simultaneous fructose uptake and glyoxylate cycle activity whereas all MinEFMDs do. Only 1.5% of MBDs use one EFM cometabolizing fructose and

acetate whereas all MinEFMDs do. For RDs, >99% have neither properties. This example demonstrated the unique capability of MBD to distinguish individually regulated pathways in a realistic system setting with underlying regulatory rules.

Uniqueness of MBDs

To investigate the uniqueness of MBDs, 2000 FDs with glucose as carbon source were sampled. Alternative optimal MBDs and MinEFMDs were enumerated. To obtain a smaller set of EFMs for easier optimization, several cofactors and small metabolites were unbalanced when calculating EFMs. It is noted that though EFMs resulting from unbalancing cofactors can still properly decompose any FDs, they cannot reflect the subtle interdependence between different metabolic pathways. More discussion can be found in the Supplementary Material (section A.8).

MBD has a satisfactory performance regarding uniqueness. There are 45% of FDs that have a unique MBD and 95% of the FDs have no more than eight multiple MBDs. To compare the results with MinEFMDs, we randomly picked 20 FDs and enumerated the alternative MinEFMDs. All FDs turned out to have ≥1000 different MinEFMDs. As the minimum number of EFMs required for decomposition is much smaller than the number of contributable EFMs, e.g. dozens out of hundreds or thousands, there are virtually countless MinEFMDs. The number of multiple MBDs is extremely small in this sense. The results suggested that MBD is effective in identifying a small subset of decompositions by EFMs with fewer branching pathways which are suitable for understanding the FDs.

A.4.2 Mouse myocardial metabolic network

To demonstrate that the proposed method indeed yield a more intuitive and biologically relevant decomposition, MBD was applied to a FD of mouse cardiomyocyte estimated from isotopomer labeling experiments performed in perfused mouse hearts (Vo and Palsson, 2006). The model and the FD are available as the supplementary information in that publication. The mouse myocardial metabolic network consists of 240 metabolites and 257 reactions compartmentalized into cytoplasm, mitochondrion and extracellular space. There are 99 active reactions in the FD (**Figure A.3**). Glucose and oleate (a fatty acid) were available as carbon sources. Lactate, pyruvate and the ketone bodies acetoacetate and 3-hydroxybutanoate were excreted. A small amount of citrate and succinate were also produced.

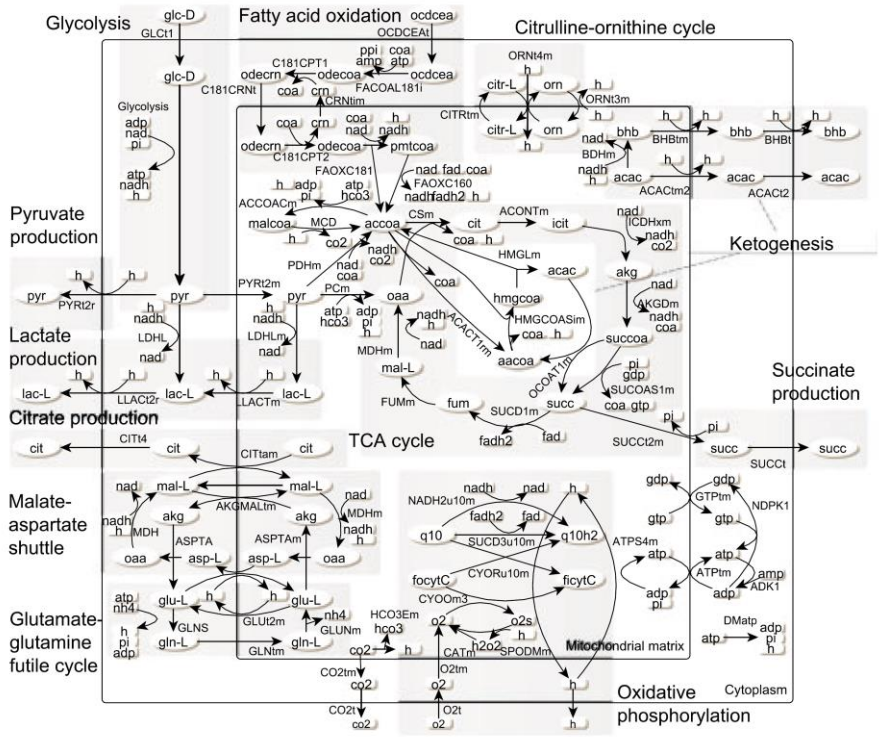

Figure A.3. Reactions with non-zero fluxes in the mouse myocardial metabolic network.

Intermediate steps of glycolysis are omitted. Water involved in reactions is not shown. All abbreviations of reactions and metabolites are the same as in the original network. Colored version is available in Supplementary Material.

The primary function of cardiomyocyte is energy production for heart contraction. It is represented by the reaction 'DMatp' hydrolyzing ATP in the network. By decomposing the FD into a set of EFMs, different pathways for energy production and other cellular activities can be revealed. All metabolites were balanced for EFM calculation. In all, 1236 EFMs were computed. Optimality could not be proved after 24 h in the initial trial to find an MBD using a uniform weight. We then attempted to put emphasis on the obvious branch point of glucose and fatty acid oxidation, acetyl-CoA, by giving a weight of 1000 to it and 1 to other metabolites. An optimal MBD comprising 14 EFMs was obtained and was proved to be unique. EFMs in the MBD can be divided into four types. The first is three EFMs of fatty acid oxidation that produce CO_2 and ketone bodies. The second is nine EFMs producing CO_2 and different organic acids from glucose. The third is an EFM consuming glucose and oleate and producing citrate, β-hydroxybutyrate (BHB) and CO_2. In this EFM, it is unambiguous that BHB is produced from oleate because pyruvate dehydrogenase, the only reaction in the FD converting pyruvate into acetyl-CoA, is not included in this EFM and acetyl-CoA is the precursor of BHB. The fourth type is an isolated cycle between citrulline and ornithine. The difference between EFMs lies in the products and the different cellular activities or pathways, including the malate-aspartate shuttle, pseudoketogenesis and an apparent glutamate-glutamine futile cycle.

We examined whether finding decomposition after removing EFMs with simultaneous oleate and glucose uptake is possible. No solution could be found, showing that at least one such EFM is required in any decomposition. To see whether this necessary interdependence of glucose and fatty acid oxidation originated from the balance of cofactors, we tried to find MBDs using sets of EFMs calculated from unbalancing some cofactors and small metabolites. When unbalancing NAD^+ and NADH, an MBD without any EFM using both carbon sources simultaneously was found, whereas unbalancing other metabolites such as ATP, ADP, H^+ or Pi did not give the desired result. This suggested that glucose and fatty acid oxidation interacted to have a balanced use of $NADH/NAD^+$. This kind of comparison between MBDs obtained from balanced and partially balanced EFMs can provide insights into the interdependence of pathways.

For comparison, MinEFMDs and RDs were computed. There were 35 optimal MinEFMDs, each with 13 EFMs. To have a fair comparison, nine suboptimal MBDs were enumerated. Comparing the three types of decomposition can distinguish several properties of an MBD (Table A.2). First, only one EFM in each MBD consumes glucose and oleate simultaneously. As one is hexose and the other is fatty acid, their uses lie in different pathways and thus a good decomposition should avoid using EFMs consuming both. In all MinEFMDs, however, at least five such EFMs were used.

Table A.2. Comparison of MBD, MinEFMD and random decomposition for the mouse myocardial flux distribution.

Property	MBD	MinEFMD	RD
1. Number of EFMs	14	13	14
2. Number of multiple optima	1 (unique)	35	--
3. Maximum number of products in EFMs	2	3 or 4	≥ 3 (88.8%)
4. Number of EFMs with simultaneous glucose and oleate uptake	1*	≥ 5	≥ 5 (99.5%)
5. No EFMs producing ketone bodies from glucose	True	True for 8.6%	True for 6.4%
6. No EFMs involving oleate uptake and malonyl-CoA simultaneously	True	None of the solutions	True for 0.1%

*Our results showed that at least one EFM consuming both carbon sources is required for decomposition. RD: random decomposition.

Second, most EFMs in the MBDs excrete at most one organic acid or ketone body except two EFMs that excrete two whereas all MinEFMDs use several EFMs producing three or four products simultaneously. Such decompositions are more difficult to interpret because the sole effect of producing a certain compound alone (e.g. role in ATP production) might not be observed by looking at individual EFMs. EFMs excreting more metabolites are also expectably longer which might be more difficult to visualize. Another relevant advantage of MBD is that because an MBD would in general use EFMs that produce as few compounds as possible, if coproduction is observed in an EFM in an MBD solution, it may suggest the possibility that the production of the compounds is coupled under the particular condition where the FD is measured.

Third, the EFMs used in the MBDs appear to be more consistent with the regulation of metabolic pathways. For instance, ketogenesis by which ketone bodies are produced is known to be associated with fatty acid oxidation rather than glycolysis. In MBDs, no EFMs producing ketone bodies from glucose are present but 19 of 35 MinEFMDs contain at least one of these EFMs. Another example is malonyl-CoA ('malcoa' in Fig. 3). Production of malonyl-CoA is a known mechanism leading to the repression of fatty acid oxidation by glucose by inhibiting the transfer of fatty acyl moieties into mitochondria in cardiac muscle (Depre et al., 1999). Use of EFMs that do not couple fatty acid oxidation and the cycle between malonyl-CoA and acetyl-CoA is thus a more rational choice. In the MBD, no EFMs simultaneously use oleate and involve malonyl-CoA whereas all MinEFMDs do. The same comparison was also performed between MBDs and MinEFMDs obtained from EFMs unbalancing NAD^+ and NADH. All properties still hold (see Supplementary Material in section A.8).

From the comparison, MBD is shown to have several properties of biological relevance that are possessed by only a tiny portion of MinEFMDs. We argue that the more biologically relevant decomposition by MBD does not occur by chance but rather by the minimization of the use of EFMs with branching pathways. The reasons are 2-fold. First, from the consideration of the network structure alone, naturally occurring metabolic pathways tend to prefer linearity to branching at branch point metabolites as suggested in Ihmels *et al*. (2004) based on their observation on data from ≥1000 experimental conditions. Second, the flux of a certain reaction is the sum of the fluxes of different pathways containing that particular reaction. As different pathways have different fluxes, minimizing the use of those 'hybrid' EFMs would force the use of EFMs representing the true pathways to fit the flux values rather than a combination of 'hybrid' EFMs which is also able to fit the values of fluxes with a similar number of EFMs.

A.4.3 *Lactococcus lactis* genome-scale metabolic network

Lactococcus lactis (*L. lactis*) is a model organism in the group of lactic acid bacteria and has an important role in cheese production. *L. lactis* is in general auxotrophic for several amino acids (AAs) (Jensen and Hammer, 1993) and grows on complex media. It also produces compounds involved in flavour formation (Ayad et al., 1999). From the recently published genome-scale metabolic network of *L. lactis* subsp. *cremoris* MG1363 which specifies many flavour-forming pathways (Flahaut et al., 2013), a FD with a complex profile of substrate consumption and production can be obtained and can thus test the applicability of MBD. The FD was simulated by FBA using the measured consumption/production rates of glucose, lactate, formate, acetate, ethanol and different AAs in a chemostat experiment at dilution rate 0.05 h^{-1} as constraints. The subnetwork spanned by the simulated FD contains 294 metabolites and 280 reactions, including 26 uptake and 13 excretion reactions. In all, 518 EFMs were computed when balancing all the metabolites.

A unique MBD of 11 EFMs was computed. Nine other suboptimal MBDs, 10 MinEFMDs and 10^4 RDs were obtained for comparison. First, we focused on two properties, the number of exchange reactions and the length of the EFMs. They can reflect the interpretability and visualizability of the EFMs. Figure A.4 shows their distribution in the three types of decompositions. MBD in general used shorter EFMs with lower numbers of uptake and excretion reactions whereas MinEFMD and RD performed similarly. This indicates that MBD is easier for interpretation and visualization.

Second, we looked into the organization of individual pathways. An interesting observation pertains to the fermentation mode. *L. lactis* has been well known for its shift between homolactic fermentation producing only lactate and mixed-acid fermentation that produces formate, acetate and ethanol in addition depending on the glucose uptake rate (Thomas et al., 1979). The two modes are regulated differently. The reactions responsible for lactate, formate, acetate and ethanol production are lactate dehydrogenase (LDH), pyruvate-formate lyase (PFL), acetate kinase (ACK) and alcohol dehydrogenase (ADH) respectively. No MBDs contain EFMs involving concurrent use of LDH and PFL, ACK or ADH, while 97% of RDs and all but 1 MinEFMDs do.

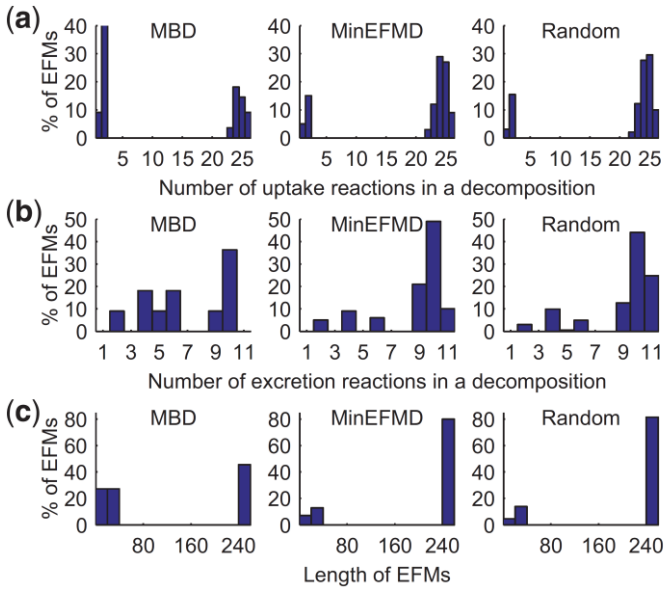

Figure A.4. (a) Number of uptake reactions, (b) number of excretion reactions and (c) length of EFMs in MBD, MinEFMD and random decomposition.

The *L. lactis* network also models detailed AA metabolism including pathways for AA interconversion and tRNA biosynthesis. According to a recently reconstructed transcriptional regulatory network of *L. lactis* (Ravcheev et al., 2013) available in RegPrecise database (Novichkov et al., 2010), they belong to different regulons and meanwhile they coincide at many metabolites. It is relevant to check how MBD performs regarding these branch points. In the current MBD, however,

the EFM matrix used to calculate MBD includes the biomass reaction, forcing many pathways to participate in one EFM to produce biomass. This is also the reason for the small size of the EFM set.

To cope with this, in a new round of MBD calculation, the biomass reaction was split into several reactions producing individual biomass components, including DNA, RNA, proteins, lipid, peptidoglycan, etc. This then resulted in 32 962 EFMs. A weight equal to 1000 was assigned to branch points in AA metabolism (Table A.3), and 1 to other metabolites. Most branch points are AAs acting as precursors for tRNA, other biomass components or flavour compounds. Cysteine and serine as an exception contribute to the pyruvate pool. Other branch points include 2-oxobutanoate (2OBUT), a precursor for a flavour compound where the fluxes from threonine and cystathionine meet; ribose 5-phosphate (R5P), synthesized from the pentose phosphate pathway or the ribose produced from methionine and phosphoribosyl pyrophosphate (PRPP), synthesized from R5P, used for producing either tryptophan or NAD^+.

Table A.3. AA branch points in the flux distribution in *L. lactis* network.

Branch point	Flow from	Flow towards	% with no EFM of >1 branches	
			MBD	RD
Ala	Ala[e], pyruvate	Ala-tRNA[a], D-alanine[a]	100%	13%
Cys	Cys[e]	Cys-tRNA[a], L-cysth, pyruvate, CoA[a]	80%	0
Met	Met[e]	Met-tRNA[a], L-cysth.	100%	1%
Gly	Gly[e]	Gly-tRNA[a], Thr	100%	0.1%
Thr	Thr[e], Gly	Thr-tRNA[a], 2OBUT	100%	0
Ser	Ser[e]	Ser-tRNA[a], pyruvate	0	0.8%
Val	Val[e]	Val-tRNA[a], 2H3MB[e][b]	100%	1.4%
Glu	Glu[e]	Glu-tRNA[a], D-glutamate[a]	100%	14%
Leu	Leu[e]	Leu-tRNA[a], 2HXIC[e][b]	0	0
Lys	Lys[e]	Lys-tRNA[a], uAGL[a]	100%	14%
2OBUT	Thr, L-cysth	2H3MP[e][b]	100%	50%
R5P	ribose, RU5P	PRPP	100%	0.4%
PRPP	R5P	Trp-tRNA[a], NAD^+ [a]	100%	6%

Notes. [e], extracellular; L-cysth, L-cystathionine; 2OBUT, 2-oxobutanoate; 2H3MB, 2-hydroxy-3-methylbutanoate; 2H3MP, 2-hydroxy-3-methylpentanoate; 2HXIC, L-2-hydroxyisocaproate; uAGL, UDP-N-acetylmuramoyl-L-alanyl-D-glutamyl-L-lysine; R5P, ribose 5-phosphate; RU5P, ribulose 5-phosphate; PRPP, phosphoribosyl pyrophosphate.

[a]biomass precursors.

[b]flavour compounds.

Convergence to optimality seemed impractical and five suboptimal MBDs were obtained. The best one has an optimality gap of 22% after 24 h of calculation. For MinEFMD, no solution using less EFMs than RD could be found so only RD was considered.

Comparing the original MBDs with the current ones, differences can be observed. First, the present MBDs consist of eight more EFMs than the original. Second, EFMs are shorter in the present MBDs. These changes are expectable because smaller parts of metabolism are sufficient for producing individual biomass components at steady state while more EFMs are required when each EFM covers a smaller part. We also looked into the ATP turnover: in the original MBDs, ATP consumption is perfectly distributed to growth requirement in five EFMs and non-growth-associated maintenance in the other six EFMs. In the current MBDs, however, only 70% of ATP maintenance is consumed in EFMs independent of synthesis of biomass components. This may be the result of suboptimality. Alternatively, this suggests that simultaneous clear roles in both ATP consumption and AA branch points are impossible. However, as an advantage of the current MBDs, the ATP consumption by synthesizing each biomass components can be reflected. tRNA and nucleotide synthesis consume >80% of the ATP.

Regarding AA branch points, MBD successfully chose separate EFMs representing the production of biomass components and flavour compounds. Table A.3 compares the five MBDs and 10^4 RDs. All tRNAs are produced in three EFMs and other amino-acid-consuming reactions are in other EFMs, except for the cases of serine and leucine. For example, beside tRNA charging in three EFMs, cysteine participates in the reaction of phosphopantothenate-cysteine ligase for biosynthesis of coenzyme A in another EFM, goes into the pyruvate pool by cysteine desulfhydrase in three other EFMs, and produces cystathionine (for producing a flavour compound) in one EFM. Taking glycine and threonine as another example, beside tRNA charging of the two AAs in three EFMs, threonine is converted into 2OBUT by threonine deaminase for flavour compound production in four other EFMs, of which threonine is taken up from the medium in three of the EFMs and is converted from glycine by threonine aldolase in the other one. In most cases, RD failed to have such properties. More details can be found in Supplementary Material (section A.8).

For leucine, we found that in all EFMs, tRNA charging was coupled to the production of a flavour compound, thus inseparable. For serine, if EFMs with only one serine-consuming reaction are used, EFMs branching at either threonine or cysteine must be used. It was observed that all three AAs had one consuming reaction producing NH_4. We thus suspected that branches were not separated due to NH_4 balance. When finding MBD from EFMs with NH_4 unbalanced, indeed the issue was resolved.

From this and the previous examples, an interesting observation is that the FDs can be represented by most EFMs of individual pathways together with a few necessary EFMs coupling the pathways. It may suggest that while a large part of the metabolism can be interpreted as the sum of individual pathways, at least a small part must be ascribed to cooperation between pathways.

A.5 Conclusion

MBD to decompose a FD into a set of EFMs was derived. The EFMs contain as few branching pathways as possible. MBD advances the analysis of FD by decomposition into EFMs in three aspects. First, it originates from the consideration of the branching structure in metabolic network based on experimental evidence which is a novel attempt. Second, MBD results in more biologically relevant EFMs leading to clearer interpretation. Third, MBD showed good performance regarding uniqueness. It diminishes the ambiguity of decomposition.

The minimal branching EFM concept underlying MBD can be useful in further applications, e.g. identifying metabolic pathways for engineering by acting as an estimate for biologically feasible EFMs. Scaling up the method to genome-scale networks is necessary for practical applicability. In conclusion, MBD is able to bring useful insights when analyzing FDs. Combining information from e.g. transcriptional regulation and thermodynamics, wider application of EFMs can be anticipated.

A.6 Acknowledgements

The authors would like to acknowledge the helpful comments made by the three anonymous reviewers.

A.7 References

Almaas,E. *et al.* (2004) Global organization of metabolic fluxes in the bacterium *Escherichia coli*. *Nature*, **427**, 839–43.

Ayad,E.H.E. *et al.* (1999) Flavour forming abilities and amino acid requirements of *Lactococcus lactis* strains isolated from artisanal and non-dairy origin. *Int. Dairy J.*, **9**, 725–735.

Chan,S.H.J. and Ji,P. (2011) Decomposing flux distributions into elementary flux modes in genome-scale metabolic networks. *Bioinformatics*, **27**, 2256–2262.

de Figueiredo,L.F. *et al.* (2009) Computing the shortest elementary flux modes in genome-scale metabolic networks. *Bioinformatics*, **25**, 3158–65.

dos Santos,M.M. *et al.* (2003) Identification of *in vivo* enzyme activities in the cometabolism of glucose and acetate by *Saccharomyces cerevisiae* by using ^{13}C-labeled substrates. *Eukaryot. Cell.*, **2**, 599-608.

Depre,C. *et al.* (1999) Glucose for the Heart. *Circulation*, **99**, 578–588.

Edwards,J.S. and Palsson,B.Ø. (1999) Systems properties of the *Haemophilus influenzae* Rd metabolic genotype. *J. Biol. Chem.*, **274**, 17410–6.

Feist,A.M. *et al.* (2007) A genome-scale metabolic reconstruction for *Escherichia coli* K-12 MG1655 that accounts for 1260 ORFs and thermodynamic information. *Mol. Syst. Biol.*, **3**, 121.

Flahaut,N. a L. *et al*. (2013) Genome-scale metabolic model for *Lactococcus lactis* MG1363 and its application to the analysis of flavour formation. *Appl. Microbiol. Biotechnol.*, **97**, 8729–39.

Ihmels,J. *et al.* (2004) Principles of transcriptional control in the metabolic network of Saccharomyces cerevisiae. *Nat Biotech*, **22**, 86–92.

Ip,K. *et al.* (2011) Analysis of complex metabolic behavior through pathway decomposition. *BMC Syst. Biol.*, **5**, 91.

Jensen,P.R. and Hammer,K. (1993) Minimal Requirements for Exponential Growth of *Lactococcus lactis*. *Appl. Environ. Microbiol.*, **59**, 4263–6.

Jol,S.J. *et al.* (2012) System-level insights into yeast metabolism by thermodynamic analysis of elementary flux modes. *PLoS Comput. Biol.*, **8**, e1002415.

Jungreuthmayer,C. *et al.* (2013) regEfmtool: Speeding up elementary flux mode calculation using transcriptional regulatory rules in the form of three-state logic. *Biosystems*, **113**, 37–39.

Klamt,S. and Stelling,J. (2002) Combinatorial complexity of pathway analysis in metabolic networks. *Mol. Biol. Rep.*, **29**, 233–6.

Lewis,N.E. *et al.* (2012) Constraining the metabolic genotype–phenotype relationship using a phylogeny of in silico methods. *Nat Rev Micro*, **10**, 291–305.

Llaneras,F. and Picó,J. (2010) Which metabolic pathways generate and characterize the flux space? A comparison among elementary modes, extreme pathways and minimal generators. *J. Biomed. Biotechnol.*, **2010**, 753904.

Machado,D. *et al.* (2012) Random sampling of elementary flux modes in large-scale metabolic networks. *Bioinformatics*, **28**, i515–i521.

Novichkov,P.S. *et al.* (2010) RegPrecise: a database of curated genomic inferences of transcriptional regulatory interactions in prokaryotes. *Nucleic Acids Res.*, **38**, D111–8.

Oberhardt,M.A. *et al.* (2009) Applications of genome-scale metabolic reconstructions. *Mol. Syst. Biol.*, **5**, 320.

Orth,J.D. *et al.* (2010) Reconstruction and use of microbial metabolic networks: the core *Escherichia coli* metabolic model as an educational guide. In, Karp,P.D. (ed), *EcoSal -- Escherichia coli and Salmonella Cellular and Molecular Biology*., p. 10.2.1. ASM Press, Washington DC.

Pey,J. and Planes,F.J. (2014) Direct calculation of elementary flux modes satisfying several biological constraints in genome-scale metabolic networks. *Bioinformatics*, in press. doi: 10.1093/bioinformatics/btu193.

Poolman,M.G. *et al*. (2004) A method for the determination of flux in elementary modes, and its application to *Lactobacillus rhamnosus*. *Biotechnol. Bioeng.*, **88**, 601-12.

Price,N.D. *et al.* (2004) Genome-scale models of microbial cells: evaluating the consequences of constraints. *Nat. Rev. Microbiol.*, **2**, 886-97.

Ravcheev,D. a *et al.* (2013) Genomic reconstruction of transcriptional regulatory networks in lactic acid bacteria. *BMC Genomics*, **14**, 94.

Rezola,A. *et al.* (2011) Exploring metabolic pathways in genome-scale networks via generating flux modes. *Bioinformatics*, **27**, 534–40.

Schuster,S. and Hilgetag C. (1994) On the elementary flux modes in biochemical reaction systems at steady state. *J. Biol. Syst.*, **2**,165-82.

Schwartz,J.M. and Kanehisa,M. (2005) A quadratic programming approach for decomposing steady-state metabolic flux distributions onto elementary modes. *Bioinformatics*, **21** (Suppl. 2), ii204–ii205.

Schwartz,J.M. and Kanehisa,M. (2006) Quantitative elementary mode analysis of metabolic pathways: the example of yeast glycolysis. *BMC Bioinformatics*, **7**, 186.

Tabe-Bordbar,S. and Marashi,S.-A. (2013) Finding elementary flux modes in metabolic networks based on flux balance analysis and flux coupling analysis: application to the analysis of *Escherichia coli* metabolism. *Biotechnol. Lett.*, **35**, 2039-44.

Terzer,M. and Stelling,J. (2008) Large-scale computation of elementary flux modes with bit pattern trees. *Bioinformatics*, **24**, 2229–35.

Thomas,T.D. *et al.* (1979) Change from homo- to heterolactic fermentation by *Streptococcus lactis* resulting from glucose limitation in anaerobic chemostat cultures. *J. Bacteriol.*, **138**, 109–17.

Trinh,C.T. *et al.* (2009) Elementary mode analysis: a useful metabolic pathway analysis tool for characterizing cellular metabolism. *Appl. Microbiol. Biotechnol.*, **81**, 813–26.

Vo,T.D. and Palsson,B.O. (2006) Isotopomer analysis of myocardial substrate metabolism: a systems biology approach. *Biotechnol. Bioeng.*, **95**, 972–83.

Wiback,S.J. *et al.* (2003) Reconstructing metabolic flux vectors from extreme pathways: defining the α-spectrum. *J. Theor. Biol.*, **224**, 313–324.

Zanghellini,J. *et al.* (2013) Elementary flux modes in a nutshell: Properties, calculation and applications. *Biotechnol. J.*, **8**, 1009–16.a

A.8 Supplementary Material

A.8.1 Contributable EFMs

The whole set of EFMs **E** or at least the subset called 'contributable EFMs' $\mathbf{E}_{\text{contri}}$ (EFMs able to have non-zero weights for a particular flux distribution) needs to be calculated before MBD or other optimization objectives can be applied to choose a particular subset of EFMs to reconstruct a flux distribution. In the article, contributable EFMs with respect to a flux distribution **v** is defined as:

$$\mathbf{E}_{CONTRI} = \{\mathbf{e}_k \mid \forall j \text{ s.t. } v_j = 0 \Rightarrow e_{jk} = 0 \}$$

EFMs in **E** but not in $\mathbf{E}_{\text{contri}}$ can have only zero weight to **v** whereas those in $\mathbf{E}_{\text{contri}}$ are always possible to have non-zero weight to **v** because of the 'no cancellation' property. Concretely, it means that because each reversible reaction is split into two irreversible reactions, fluxes in all EFMs must be positive ($e_{jk} > 0$) so from the equation of decomposition:

$$v_j = \sum_{k=1}^{K} \alpha_k e_{jk}$$

Thus $v_j = 0$ implies that $\alpha_k = 0$ whenever $e_{jk} > 0$. $\mathbf{E}_{\text{contri}}$ can also be found given the whole set **E** by deleting the columns with $e_{jk} \neq 0$ but $v_j = 0$ for each j. Or alternatively, let $\mathbf{S} = [\mathbf{S}_{v_j \neq 0} \mid \mathbf{S}_{v_j = 0}]$ where $\mathbf{S}_{v_j \neq 0}$ and $\mathbf{S}_{v_j = 0}$ contain the columns of reactions with non-zero and zero fluxes respectively. Then a more practical way is to calculate $\mathbf{E}_{\text{contri}}$ directly from the submatrix $\mathbf{S}_{v_j \neq 0}$. In summary:

- **E** can recover any flux distributions satisfying $\mathbf{S}\mathbf{v} = 0, \mathbf{v}_{ub} \geq \mathbf{v} \geq \mathbf{v}_{lb}$ but not always tractable
- $\mathbf{E}_{\text{contri}}$ is defined for a given flux distribution **v** and is more likely tractable or can be found from **E** if **E** is known.
- $\mathbf{E}_{\text{contri}}$ in general cannot recover all flux distributions in the network defined by **S** but can recover all flux distributions in the subnetwork defined by $\mathbf{S}_{v_j \neq 0}$

A.8.2 Decompositions by EFMs with unbalanced metabolites

EFMs resulting from unbalancing cofactors cannot reflect the subtle inter-dependence between different metabolic pathways but they can still properly decompose any FDs because of the following:

Let $\mathbf{S} = \begin{bmatrix} \mathbf{S}_{bal} \\ \mathbf{S}_{unbal} \end{bmatrix} \in \mathbf{R}^{m \times n}$ be the stoichiometric matrix where $\mathbf{S}_{bal} \in \mathbf{R}^{m_b \times n}$ and $\mathbf{S}_{unbal} \in \mathbf{R}^{(m-m_b) \times n}$ are the stoichiometric matrices of balanced and unbalanced metabolites respectively.

Denote the EFM matrix derived from $\mathbf{S}_{bal}$ by:

$$\mathbf{E}_{bal} = [\mathbf{e}_{bal,1} \quad \mathbf{e}_{bal,2} \quad \cdots \quad \mathbf{e}_{bal,K}] \in \mathbf{R}^{n \times K}.$$

Note that a flux distribution **v** satisfying $\mathbf{Sv}=\mathbf{0}$ also satisfies $\mathbf{S}_{bal}\mathbf{v}=\mathbf{0}$. This implies $\mathbf{v}=\mathbf{E}_{bal}\alpha$ where $\alpha=[\alpha_1 \quad \alpha_2 \quad \cdots \quad \alpha_K]$ is the weight vector of EFM.

The imbalance of unbalanced metabolites in the *k*-th EFM, mathematically equal to the vector $\mathbf{S}_{unbal}(\alpha_k\mathbf{e}_{bal,k})$ actually reflects the net production/ consumption of unbalanced metabolites of that EFM in the flux distribution which is always cancelled out by other EFMs in the decomposition. Occasionally, it can bring insights into the different roles of the pathways regarding the production/consumption of the unbalanced metabolites which are overall balanced in the flux distribution.

A.8.3 Test of uniqueness of MBDs

To obtain a smaller set of EFMs for easier optimization, several cofactors and small metabolites were not required to be balanced when calculating EFMs, including ATP and ADP, acetyl-coenzyme A and coenzyme A, NADH and NAD^+, NADPH and $NADP^+$, O_2, CO_2, H_2O, H^+, NH_4 and inorganic phosphate. In this setting, many branches balancing cofactors are excluded and not accounted by MBD. 10^5 EFMs were computed. For each flux distribution, contributable EFMs were selected by ruling out EFMs with $e_{jk}\neq 0$ but $v_j=0$. A summary about the tests on the two sets of flux distributions is shown in Table A.4. The number of alternative MBDs and the time required for computing the first MBD solution are plotted in Figure A.5.

Table A.4. Summary about the tests of uniqueness of MBDs.

Carbon source	Glucose
Samples decomposed	2000
Weight w_i	1 for all metabolites
Contributable EFMs in each flux distribution	159 (sd = 27)
EFMs in MBD for each flux distribution	36
Flux distributions with unique MBD	898 (45%)
Alternative MinEFMDs for 20 tested FDs	≥1000

sd, standard deviation.

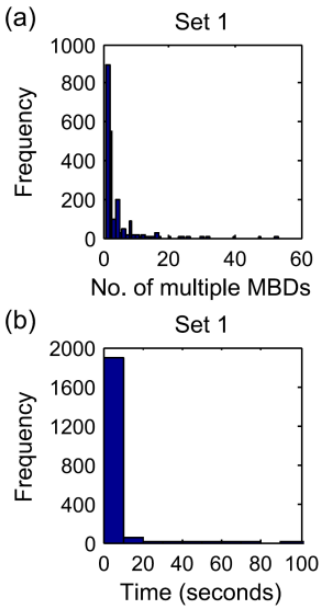

Figure A.5. (a) Number of multiple MBDs and (b) time required for computing the first MBD for FDs randomly sampled from the core *E. coli* metabolic network.

A.8.4 Mouse myocardial metabolic network

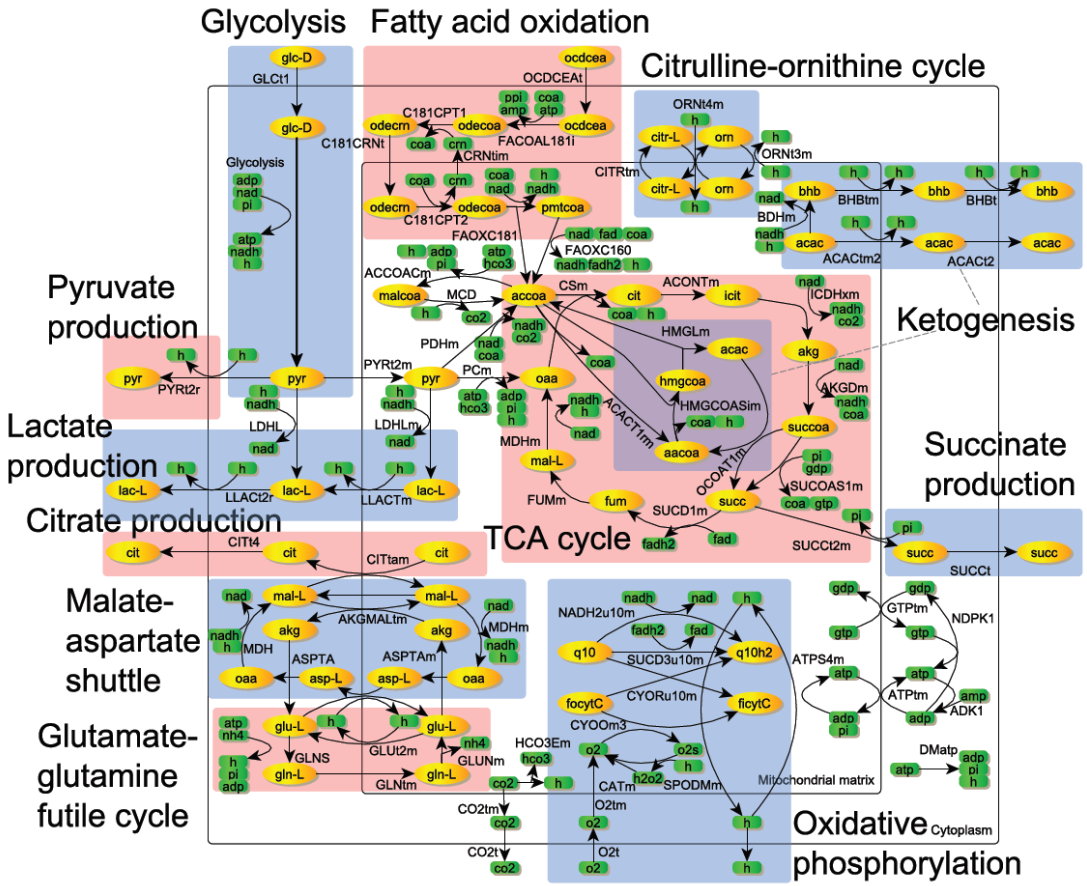

Figure A.6. Reactions with non-zero fluxes in the mouse myocardial metabolic network (color).
Intermediate steps of glycolysis are omitted. Water involved in reactions is not shown. All abbreviations of reactions and metabolites are the same as in the original network.

As described in the article, we also performed analysis of MBD and MinEFMD using the set of EFMs resulted from unbalancing NADH and NAD^+. Table A.5 summarizes the results. >20,000 alternative MinEFMDs were found whereas the MBD is unique. Figure A.7 shows the unique MBD and a randomly selected MinEFMD.

Table A.5. Comparison of the properties of MBD and MinEFMD for the mouse myocardial flux distribution calculated from the EFM matrix in which NADH and NAD^+ are left unbalanced.

	Property	MBD	MinEFMD
1.	Number of EFMs in the solution	16	16
2.	Number of multiple optima	1 (unique)	>20,000
3.	Number of products excreted in EFMs	All EFMs produce 1 product except one EFM producing 2	83% of solutions contain ≥ 2 EFMs producing 2 – 3
4.	No EFMs catabolizing glucose and oleate simultaneously	True	True for 0.005% of solutions
5.	No EFMs producing ketone bodies from glucose	True	True for 0.1% of the solutions
6.	No EFMs catabolizing oleate and involving malonyl-CoA simultaneously	True	True for 4.3% of the solutions
7.	Satisfying any two of the property 3 – 5	True	None of the solutions

(a) MBD

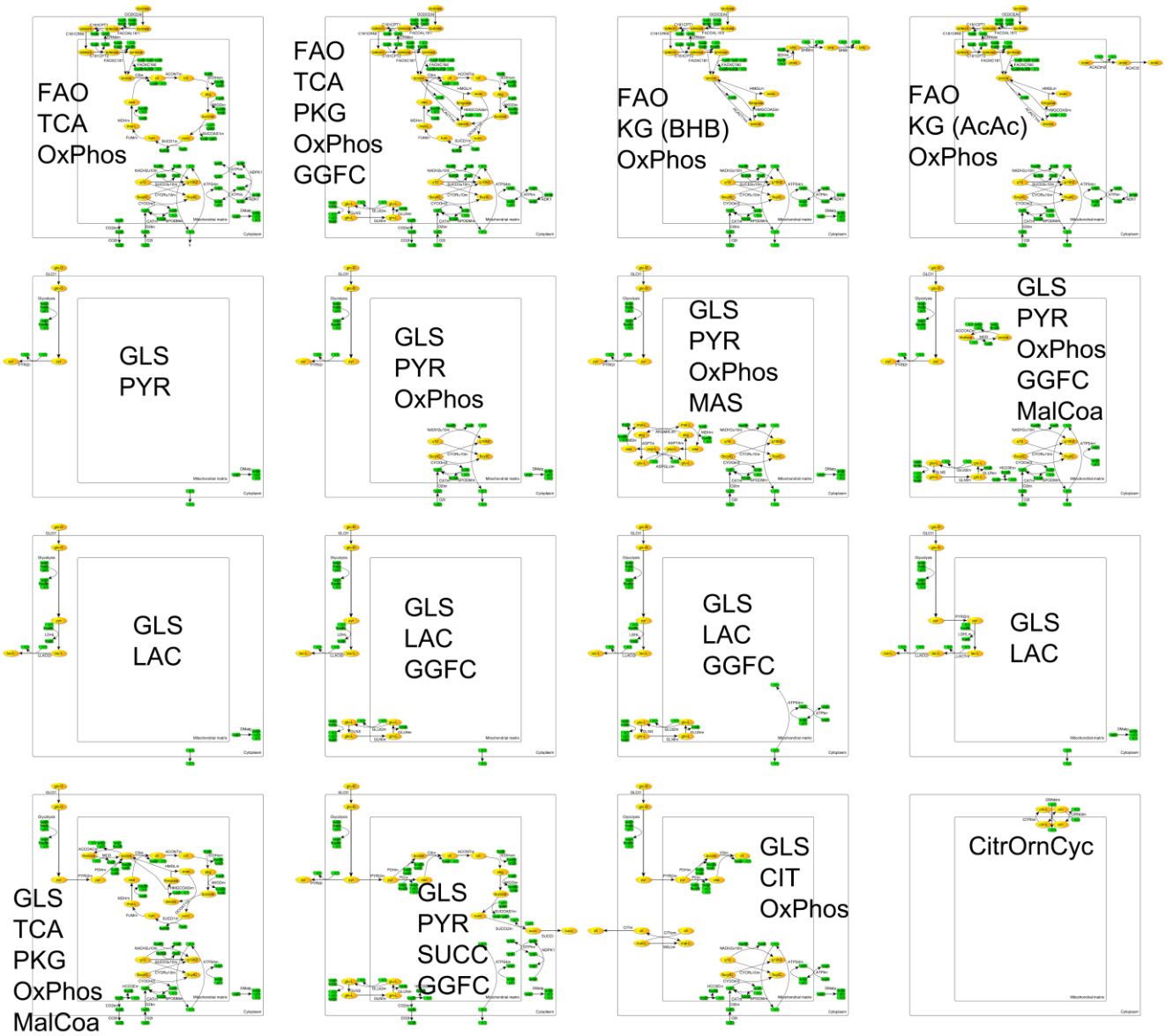
FAO
TCA
OxPhos
FAO
TCA
PKG
OxPhos
GGFC
FAO
KG (BHB)
OxPhos
FAO
KG (AcAc)
OxPhos
GLS
PYR
GLS
PYR
OxPhos
GLS
PYR
OxPhos
MAS
GLS
PYR
OxPhos
GGFC
MalCoa
GLS
LAC
GLS
LAC
GGFC
GLS
LAC
GGFC
GLS
LAC
GLS
TCA
PKG
OxPhos
MalCoa
GLS
PYR
SUCC
GGFC
GLS
CIT
OxPhos
CitrOrnCyc

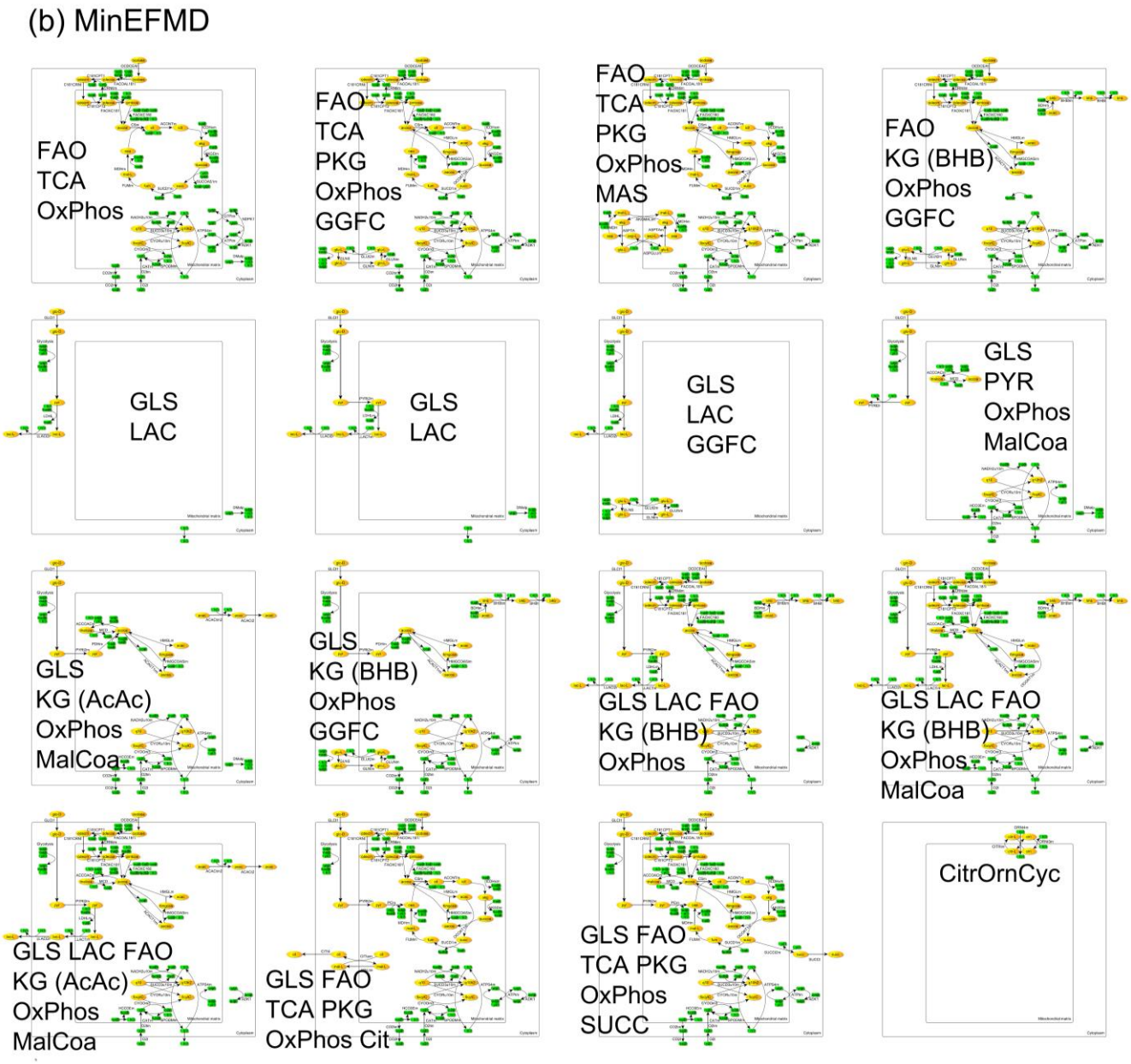

Figure A.7. Two sets of 16 EFMs composing (a) the unique MBD and (b) a randomly selected MinEFMD calculated from EFMs in which NADH and NAD^+ are left unbalanced.

Each thumbnail shows the reactions of an EFM. Two EFMs containing only the transport reactions for water are not shown. Abbreviations correspond to the pathways or compounds produced. FAO: fatty acid oxidation. GLS: glycolysis. TCA: tricarboxylic acid cycle. OxPhos: oxidative phosphorylation. MalCoa: involvement of malonyl-CoA. KG: ketogenesis. PKG: pesudoketogenesis. GGFC: glutamate-glutamine futile cycle. MAS: malate-aspartate shuttle. CitrOrnCyc: citrulline-ornithine cycle. LAC, PYR, SUCC, CIT, AcAc, BHB: production of lactate, pyruvate, succinate, citrate, acetoacetate and 3-hydroxybutanoate respectively.

A.8.5 *Lactococcus lactis*'s metabolic network

In the second round of MBD calculation to study the amino acid metabolism in *Lactococcus lactis*, the biomass reaction was separated several reactions producing individual components. They are listed in Table A.6 put at the end of this document.

Figure A.8 shows the branch points in the amino acid metabolism. Figure A.9 shows the best MBD obtained and Figure A.10 shows a randomly selected EFM from a randomly selected random decomposition. The most obvious difference is that in the MBD, all tRNA charging reactions do not mix with reactions in other branches except for leucine and serine. For leucine, tRNA charging is necessarily coupled to a flavour compound production and for serine branches are not separated due to NH_4 balance as explained in the article. In non-tRNA-charging EFMs, amino acids are further metabolized to produce other biomass components or flavour compounds. For example, in peptidoglycan synthesis, starting from fructose 6-phosphate, alanine, glutamate and lysine are involved in turn. For cysteine, it can participate in the reaction of phosphopantothenatecysteine ligase for biosynthesis of coenzyme A from pantothenate; go into the pyruvate pool by cysteine desulfhydrase; and produces cystathionine with another substrate O-acetyl-L-homoserine produced from methionine to finally produce a flavour compound. For glycine, it can be converted to threonine which is used to produce the same flavour compound. There are also three branch points which are not amino acids but are involved in the amino acid metabolism, including 2-oxobutanoate (2OBUT), a precursor for a flavour compound where the fluxes from threonine and cystathionine meet; ribose 5-phosphate (R5P), synthesized from the pentose phosphate pathway or the ribose produced from methionine; phosphoribosyl pyrophosphate (PRPP), synthesized from R5P and used for producing either tryptophan or NAD^+. From Figure A.9, it can be seen how different parts of the amino acid metabolism and the different branches of branch points were included in different EFMs whereas in a general random decomposition, many EFMs similar to Figure A.10 containing many branches of branch points co-exist.

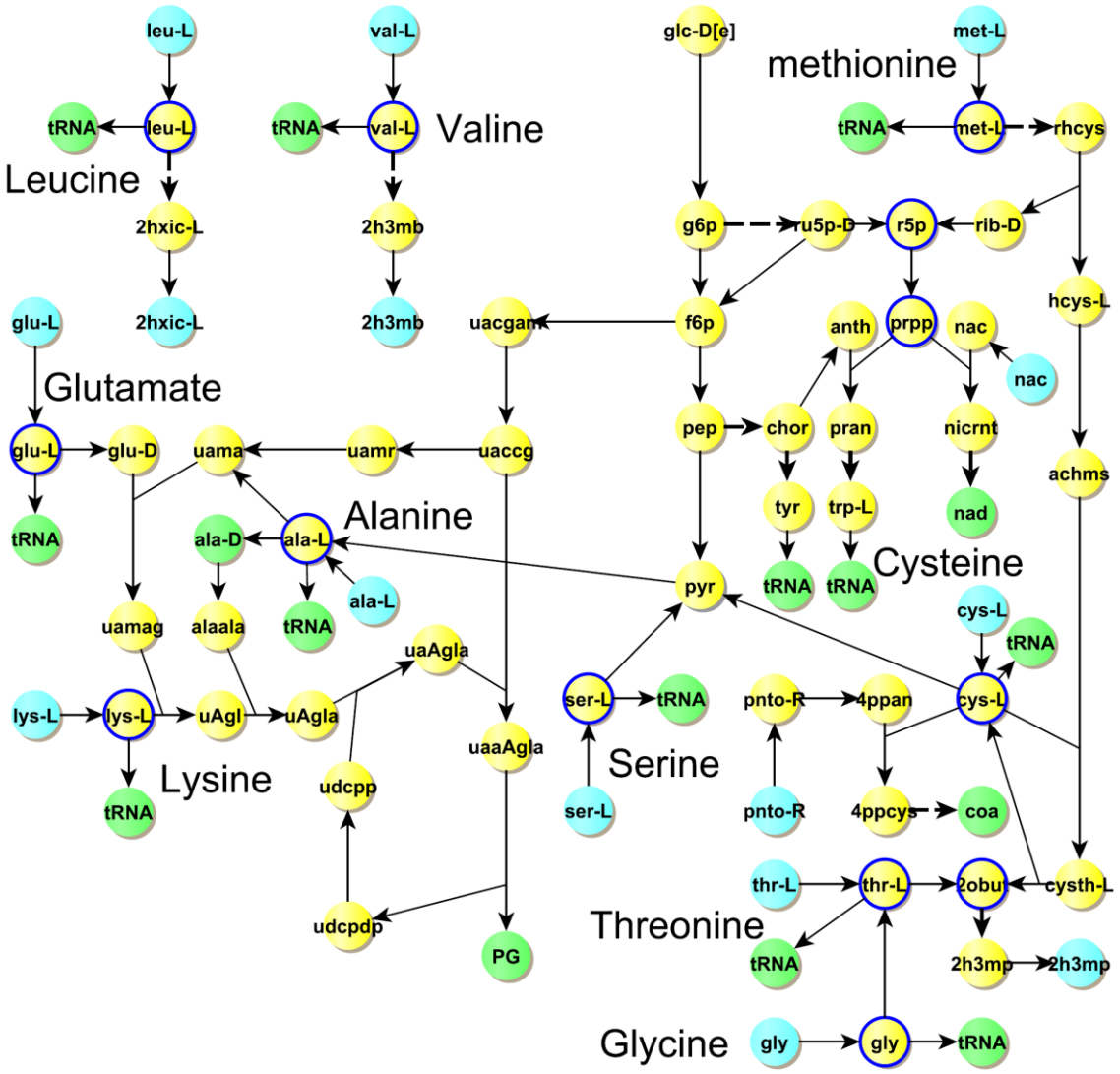

Figure A.8. Branch points in the amino acid metabolism in the flux distribution in the *L. lactis* metabolic network. Extracellular metabolites are in blue. Biomass components are in green. Circled metabolites are the branch points in the amino acid metabolism which were given a high weight for the calculation of MBD. Some reactions are lumped for simplicity. All abbreviations follow the original publication of the *L. lactis* metabolic network (Flahaut,N. a L. *et al.* (2013) Genome-scale metabolic model for *Lactococcus lactis* MG1363 and its application to the analysis of flavour formation. *Appl. Microbiol. Biotechnol.*, **97**, 8729–39).

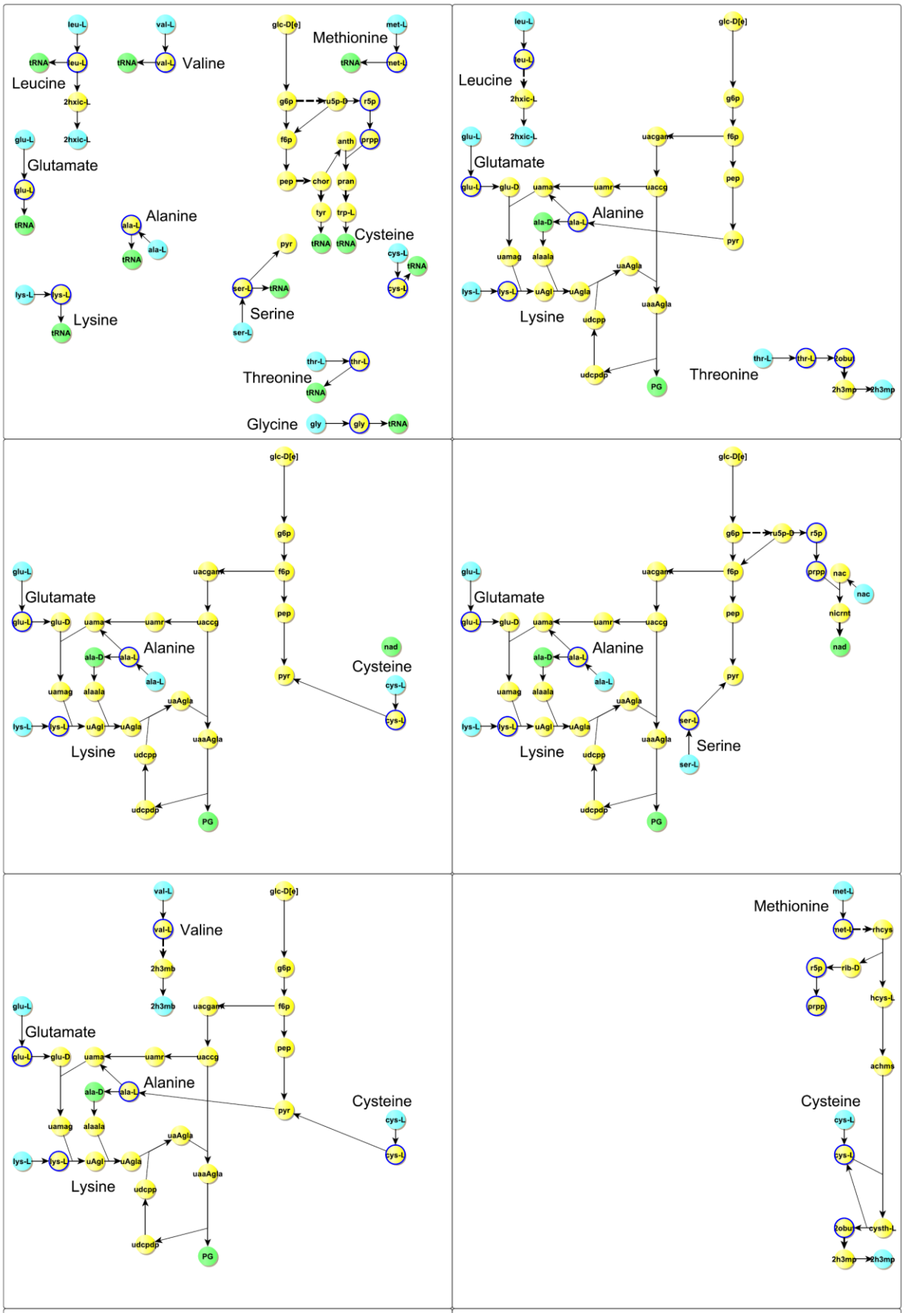
Leucine
Valine
Methionine
Glutamate
Alanine
Cysteine
Lysine
Serine
Threonine
Glycine
Leucine
Glutamate
Alanine
Lysine
Threonine
Glutamate
Alanine
Cysteine
Lysine
Glutamate
Alanine
Cysteine
Serine
Lysine
Valine
Glutamate
Alanine
Cysteine
Lysine
Methionine
Cysteine

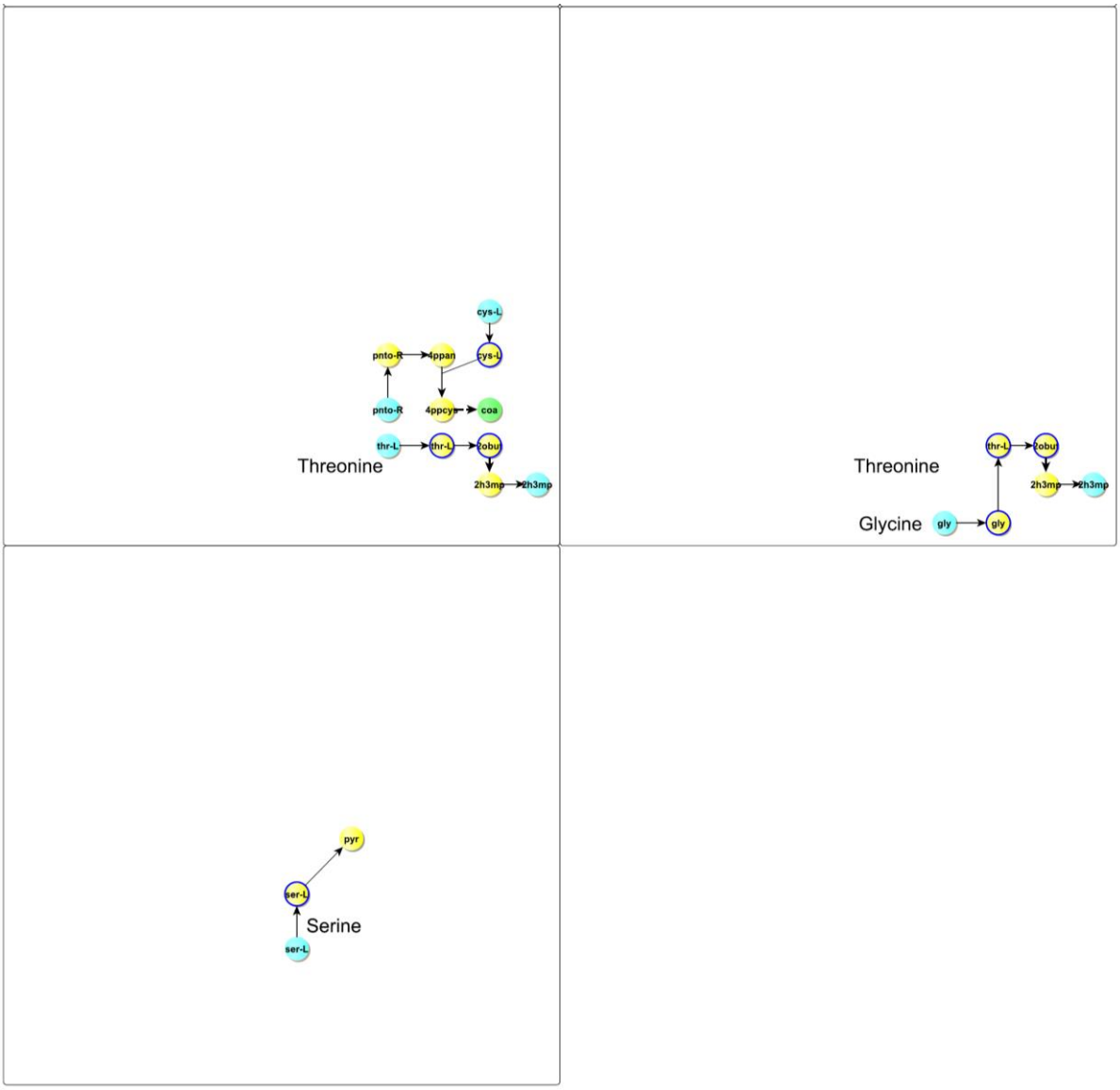

Figure A.9. MBD with high weights on amino acid branch point.

Each thumbnail shows the active reactions in the amino acid metabolism of an EFM. Only EFMs with distinct active reactions in the amino acid metabolism are shown.

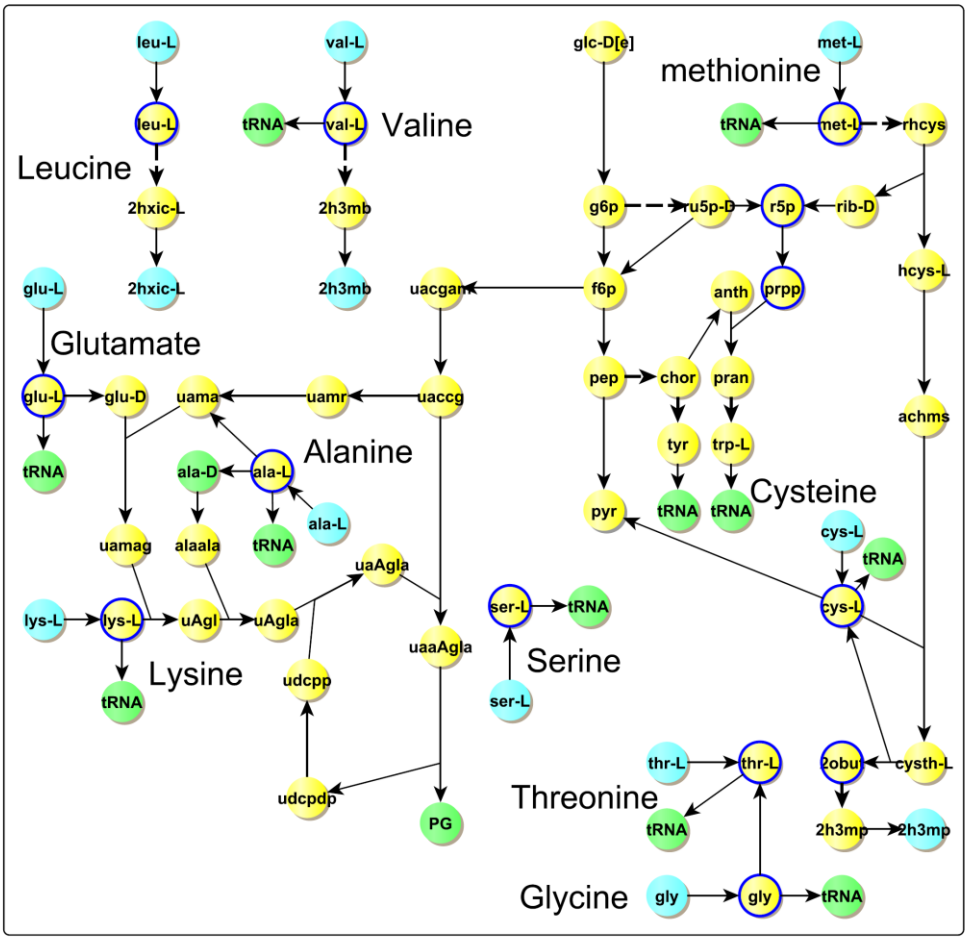

Figure A.10. A randomly selected EFM from a randomly selected random decomposition of the flux distribution in the *L. lactis* metabolic network.

Table A.6. Splitting the biomass reaction into groups of metabolites

metabolite	stoichiometry	group
2chdeacp[c]	-0.00365	phospholipid
2cocdacp[c]	-0.05359	phospholipid
2ctdeacp[c]	-0.00061	phospholipid
acp[c]	0.1218	phospholipid
cpocdacp[c]	-0.01583	phospholipid
hdeacp[c]	-0.03593	phospholipid
ocdacp[c]	-0.00122	phospholipid
tdeacp[c]	-0.01096	phospholipid
glyc3p[c]	-0.3359	phospholipid
glyc[c]	0.0138	phospholipid
alatrna[c]	-0.36549	tRNA
argtrna[c]	-0.17644	tRNA
asntrna[c]	-0.19745	tRNA
asptrna[c]	-0.19745	tRNA
cystrna[c]	-0.20585	tRNA
glntrna[c]	-0.23106	tRNA
glutrna[c]	-0.23106	tRNA
glytrna[c]	-0.24786	tRNA
histrna[c]	-0.07562	tRNA
iletrna[c]	-0.24366	tRNA
leutrna[c]	-0.36969	tRNA
lystrna[c]	-0.23656	tRNA
mettrna[c]	-0.08402	tRNA
phetrna[c]	-0.16804	tRNA
protrna[c]	-0.18064	tRNA
sertrna[c]	-0.24786	tRNA
thrtrna[c]	-0.27727	tRNA
trnaala[c]	0.365487	tRNA
trnaarg[c]	0.176442	tRNA
trnaasn[c]	0.197447	tRNA
trnaasp[c]	0.197447	tRNA
trnacys[c]	0.205849	tRNA
trnagln[c]	0.231055	tRNA
trnaglu[c]	0.231055	tRNA
trnagly[c]	0.247859	tRNA
trnahis[c]	0.075618	tRNA
trnaile[c]	0.243658	tRNA
trnaleu[c]	0.369688	tRNA
trnalys[c]	0.236556	tRNA

metabolite	stoichiometry	group
trnamet[c]	0.08402	tRNA
trnaphe[c]	0.16804	tRNA
trnapro[c]	0.180643	tRNA
trnaser[c]	0.247859	tRNA
trnathr[c]	0.277266	tRNA
trnatrp[c]	0.033608	tRNA
trnatyr[c]	0.12603	tRNA
trnaval[c]	0.306673	tRNA
trptrna[c]	-0.03361	tRNA
tyrtrna[c]	-0.12603	tRNA
valtrna[c]	-0.30667	tRNA
adp[c]	41.22259	nucleotide
atp[c]	-41.3081	nucleotide
cmp[c]	0.275	nucleotide
ctp[c]	-0.3408	nucleotide
datp[c]	-0.02368	nucleotide
dctp[c]	-0.01332	nucleotide
dgtp[c]	-0.01332	nucleotide
dttp[c]	-0.02368	nucleotide
gdp[c]	8.402	nucleotide
gtp[c]	-8.50728	nucleotide
h2o[c]	-49.6253	nucleotide
h[c]	49.76409	nucleotide
pi[c]	49.68549	nucleotide
ppi[c]	0.678	nucleotide
udp[c]	0.2103	nucleotide
ump[c]	0.0064	nucleotide
utp[c]	-0.07238	nucleotide
dtdp6dm[c]	-0.0064	nucleotide sugar 1
dtdp[c]	0.0064	nucleotide sugar 1
udcpdp[c]	-0.0002	nucleotide sugar 2
udpg[c]	-0.0633	nucleotide sugar 2
udpgal[c]	-0.1534	nucleotide sugar 2
PG[c]	-0.119	peptidoglycan
ala-D[c]	-0.09	D-alanine
coa[c]	-0.0002	coenzyme A
nad[c]	-0.002	NAD^+
thf[c]	-1.00E-05	tetrahydrofolate
thmpp[c]	-1.00E-05	Thiamine diphosphate

All abbreviations follow the original model. (Flahaut,N. a L. *et al*. (2013) Genome-scale metabolic model for *Lactococcus lactis* MG1363 and its application to the analysis of flavour formation. *Appl. Microbiol. Biotechnol.*, **97**, 8729–39.)

A.8.6 Matlab script

The matlab script for MBD together with a data file containing examples can be downloaded at Bioinformatics online:
http://bioinformatics.oxfordjournals.org/

or

https://github.com/shjchan/MinBranchDecomp

Appendix B Supplementary Material for Chapter 4

B.1. Supplementary tables

Table B.1. Primers used in the study in Chapter 4.

Primer	Restriction site	Amplified region/ Description	Sequence
DNA deletion			
56f	BamHI	*ackA1* core upstream	gacaggatccGGAGGATTTACTGACAAGTG
56r	PstI		tactgctgcagCAATGCCGGCAGCATTTG
57f	PstI	*ackA1* core downstream	tactgctgcagCACCTCTTGCTGGAGTG
57r	XhoI		gtttactcgagCTAACGTGTTCTTCGTTGTTG
59f	/	Verify *ackA1* core deletion with 57r	CAAATGCTGCCGGCATTG
60f	BamHI	*ackA2* core upstream	gacaggatccGATGTATGTTGACCGCATTC
60r	XhoI		gtttactcgagAAACGTTGGCCGGATTATG
61f	XhoI	*ackA2* core downstream	gtttactcgagGCGATTGAAGGTGGTAAATC
61r	KpnI		tagaggtaccCAACAGATCAATTTGCTCATG
63f	/	Verify *ackA2* core deletion with 61r	CTTTACATAATCCGGCCAAC
CSO834	XbaI	*pfl* upstream	ctagtctagaCAAGTGATGTACCAAATGAC
CSO835	BamHI		cgcggatccTTTGAAATCTCCTTTGTTCT
CSO836	BamHI	*pfl* downstream	cgcggatccTTCTTAGTATTAAAAAATATAAAG
CSO837	XhoI		ggtactcgagTGTGATTCACCCCTATTTCT
CSO852	/	Verify *pfl* deletion	CTTGAATTCTGTTTGCTATTATC
CSO853	/		CTTTGTCAGCATCAATTACTTG
His-tagging			
71f	BglII	*ackA1* gene for His-tagging	actgaagatctACCAAAACATTAGCAGTAAACGCTGGTTCATC
71r	SalI		actgagtcgacTTATTTTTTAAGTGCCTCAACGTC
62f	BamHI	*ackA2* gene for His-tagging	gacaggatccGAAAAAACGCTCGCTGTCAAT
62r	SalI		tacagtcgacTTATTTAGCCGCTTCGACATC
Construction of gusA reporter strains			
11f	XbaI	436-bp *ackA1* upstream and 36-bp CDS with a stop codon	atcgatctagaGAGGATTTACTGACAAGTG
11r	PstI		atcgactgcagttaTGATGAACCAGCGTTTAC
12f	XbaI	444-bp *ackA2* upstream and 45-bp CDS with a stop codon	atcgatctagaTGAGATGTATGTTGACCG
12r	PstI		atcgactgcagttaTAATGATGAGGAGCCTG
75r	SalI	Anti-sense to *ackA* genes; priming the predicted transcription terminator of *ackA1* and excluding the putative promoter of *ackA2*	actgagtcgacTTCCTACAACTTTGTATCTTGCTGTCAT
CSO50	BamHI	Verify chromosomal integration of pLB85	ggaaggatccCCCATAGTTCATCAGTTATC
CSO263	/		CGCGATCCAGACTGAATG
RACE			
72r	/	5'-RACE for *ackA1*	CCAGCAAGAGGTGTGAAGCCCAT
73r	/	5'-RACE for *ackA2*	CGAAAACAGCGACCGCAAGTGCAT

doi:10.1371/journal.pone.0092256.s001

Table B.2. Plasmid used in Chapter 4.

Plasmid	Description
pCS1966	Contain *oroP* for orotate transporter as counterselection tool for deletion; Erm^r [26]
pCS1966-*ackA1*core	pCS1966 containing the upstream and downstream regions of the core part of *ackA1* obtained with primer pairs 56-57; Erm^r
pCS1966-*ackA2*core	pCS1966 containing the upstream and downstream regions of the core part of *ackA2* obtained with primer pairs 60-61; Erm^r
pCS1966-*pfl*	pCS1966 containing the upstream and downstream regions of *pfl* obtained with primers CSO834-837; Erm^r
pLB65	Contain *orf1* expressing phage TP901-1 integrase; Cam^r [27]
pLB85	Reporter vector containing *gusA* reporter; Erm^r, Amp^r [27]
pLB85-*ackA1*	pLB85 containing fragment A obtained with primer pair 11 (including 36-bp CDS and 436-bp upstream region of *ackA1*); Erm^r, Amp^r
pLB85-*ackA12*	pLB85 containing fragment B obtained with primers 11f, 12r (including 36-bp CDS and the promoter region of *ackA2* as well as the CDS and 436-bp upstream region of *ackA1*); Erm^r, Amp^r
pLB85-*ackA2*	pLB85 containing fragment C obtained with primer pair 12 (45-bp CDS and 444-bp upstream region of *ackA2*); Erm^r, Amp^r
pLB85-*ackA1*term	pLB85 containing fragment D obtained with primers 11f, 75r (fragment B excluding the region immediately after the predicted transcription terminator of *ackA1*); Erm^r, Amp^r
pLB85-*ackA2*term	pLB85 containing fragment E obtained with primers 12f, 75r (fragment C excluding the region immediately after the predicted transcription terminator of *ackA1*); Erm^r, Amp^r
pQE30	Commercial vector (Qiagen) used for N-terminal His-tagging; Amp^r
pQE30-*ackA1*	pQE30 containing the gene *ackA1* amplified using primer pair 71; Amp^r
pQE30-*ackA2*	pQE30 containing the gene *ackA2* amplified using primer pair 62; Amp^r

Erm^r, Cam^r and Amp^r stand for erythromycin, chloramphenicol and ampicillin resistance respectively. CDS: coding sequence. doi:10.1371/journal.pone.0092256.s002

Table B.3. Strains used in Chapter 4.

Strain	Description
MG1363	A plasmid-free strain derived from *L. lactis subsp. cremoris* NCDO 712 [24]
MG1363Δ*pfl*	MG1363 with *pfl* deleted using pCS1966-*pfl*
MG1363Δ*ackA1*	MG1363 with the core part of *ackA1* deleted using pCS1966-*ackA1*core
MG1363Δ*ackA2*	MG1363 with the core part of *ackA2* deleted using pCS1966-*ackA2*core
MG1363Δ*ackA12*	MG1363Δ*ackA1* with the core parts of *ackA2* deleted using pCS1966-*ackA1*core
MG1363Δ*ackA1*Δ*pfl*	MG1363Δ*ackA1* with *pfl* deleted using pCS1966-*pfl*
MG1363Δ*ackA2*Δ*pfl*	MG1363Δ*ackA2* with *pfl* deleted using pCS1966-*pfl*
MG1363Δ*ackA12*Δ*pfl*	MG1363Δ*ackA12* with *pfl* deleted using pCS1966-*pfl*
LB436	MG1363 containing pLB65
LB436/blank	LB436 with pLB85 integrated into the TP901-1 attachment site
LB436/*ackA1*	LB436 with pLB85-*ackA1* integrated into the TP901-1 attachment site
LB436/*ackA12*	LB436 with pLB85-*ackA12* integrated into the TP901-1 attachment site
LB436/*ackA2*	LB436 with pLB85-*ackA2* integrated into the TP901-1 attachment site
LB436/*ackA1*term	LB436 with pLB85-*ackA1*term integrated into the TP901-1 attachment site
LB436/*ackA2*term	LB436 with pLB85-*ackA2*term integrated into the TP901-1 attachment site
M15 pREP4 *groESL*	An *E. coli* strain for protein overexpression [25]
SC136	M15 pREP4 groESL containing pQE30-*ackA1*
SC137	M15 pREP4 groESL containing pQE30-*ackA2*

doi:10.1371/journal.pone.0092256.s004

B.2. ACK entries in Uniprot

The data for counting the number of species with multiple ACKs from the 11,112 ACK entries in Uniprot is too large to be put in the thesis. Interested readers please download the .xlsx file from PLoS ONE website:

http://www.plosone.org/article/info%3Adoi%2F10.1371%2Fjournal.pone.0092256

B.3. Supplementary figures

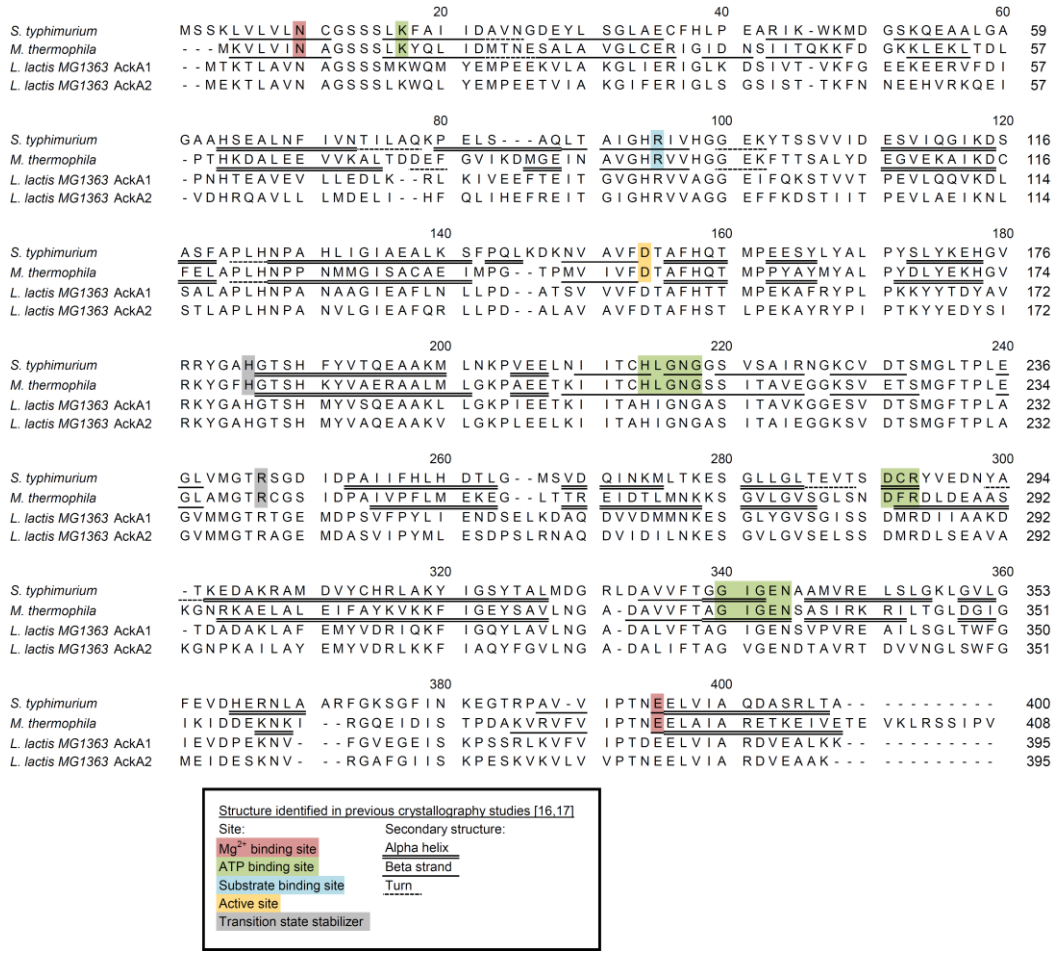

Figure B.1. Multiple alignment of AckA1, AckA2 and ACKs from *Salmonella typhimurium* and *Methanosarcina thermophila*.

Structures identified in previous crystallographic studies* are annotated. doi:10.1371/journal.pone.0092256.s005

*Buss KA, Ingram-Smith C, Ferry JG, Sanders DA, Hasson MS (1997) Crystallization of acetate kinase from *Methanosarcina thermophila* and prediction of its fold. *Protein Sci* 6: 2659–2662 doi:10.1002/pro.5560061222.

*Chittori S, Savithri HS, Murthy MRN (2012) Structural and mechanistic investigations on *Salmonella typhimurium* acetate kinase (AckA): identification of a putative ligand binding pocket at the dimeric interface. BMC Struct Biol 12: 24 doi:10.1186/1472-6807-12-24.

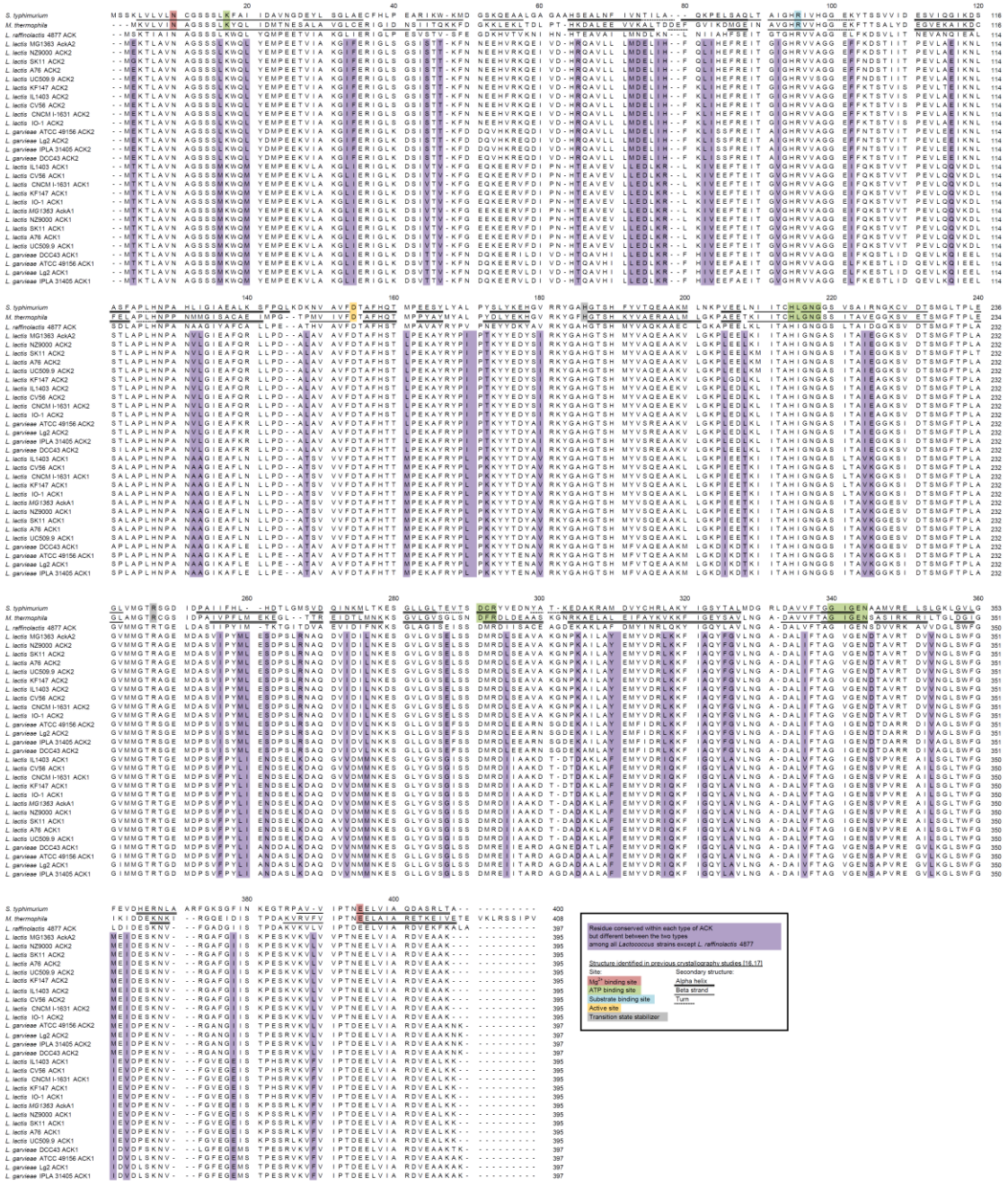

Figure B.2. Multiple alignment of all lactococcal ACKs.

Residues conserved with each type of ACK but different between the two types are annotated.

doi:10.1371/journal.pone.0092256.s006

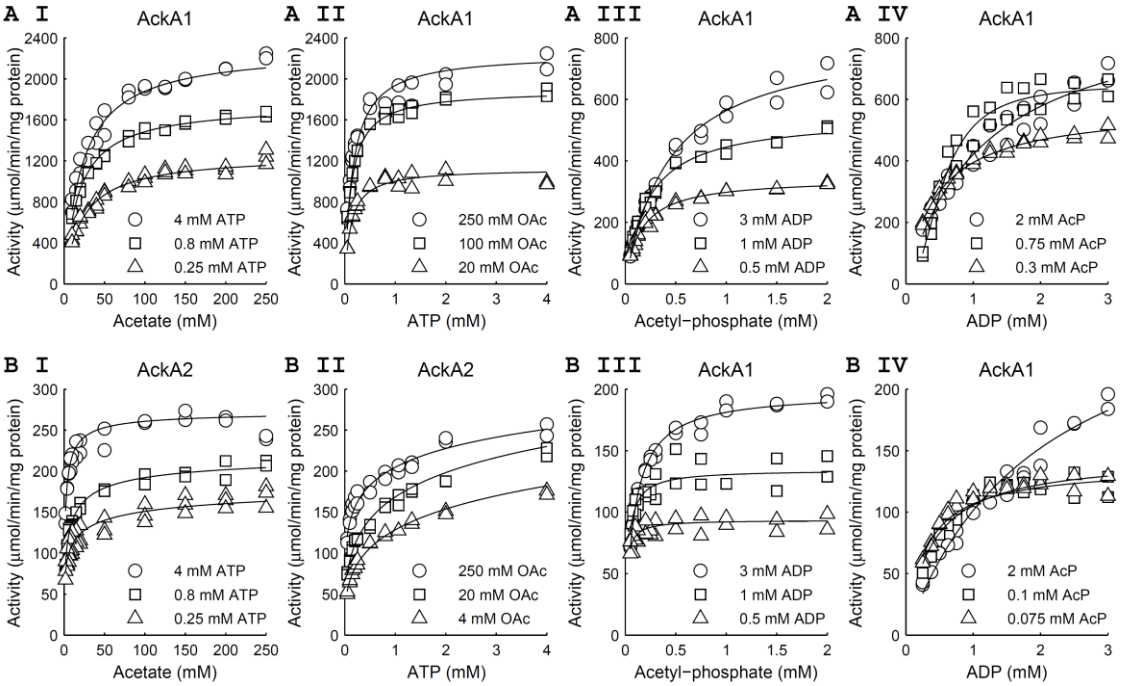

Figure B.3. Activities of purified acetate kinases.

(a) AckA1 and (b) AckA2 converting acetate (OAc) into acetyl-phosphate (Ac-P) at different levels of (i) acetate and (ii) ATP and, converting acetyl-phosphate into acetate at different levels of (iii) Ac-P and (iv) ADP, respectively.

doi:10.1371/journal.pone.0092256.s007

Appendix C Supplementary Material for Chapter 5

Table C.1. MG1363 and MG/SP1-*bdh* growing in MalSALN with or without acetoin.

Strain	Acetoin added	Growth rate (h^{-1})	Specific rate of sugar consumption and product formation (mmol $h^{-1}gdw^{-1}$)				
			Maltose	Lactate	Formate	Acetate	Ethanol
MG1363	0	0.60 ± 0.01	7.7 ± 0.1	11.7 ± 0.2	16.6 ± 0.4	9.6 ± 0.7	6.4 ± 0.7
	20 mM	0.54 ± 0.01	6.4 ± 0.4	17.0 ± 1.2	5.8 ± 0.2	4.9 ± 0.1	1.4 ± 0.1
MG/SP1-*bdh*	0	0.61 ± 0.01	7.0 ± 0.1	11.1 ± 0.2	15.9 ± 0.6	9.5 ± 0.1	5.9 ± 0.2
	5 mM	0.67 ± 0.01	7.5 ± 0.02	11.8 ± 0.3	16.5 ± 0.5	12.4 ± 0.3	4.0 ± 0.5
	20 mM	0.72 ± 0.01	6.9 ± 0.1	7.6 ± 0.1	5.5 ± 0.2	14.9 ± 0.1	-0.4 ± 0.6

Table C.2. Product yield, carbon recovery and biomass yield for growth in MalSALN.

Strain	Acetoin added	Product yield on sugar [a]				Carbon recovery[b]	Biomass yield (gdw / C6-mol)
		Lactate	Formate	Acetate	Ethanol		
MG1363	0	38% ± 0%	54% ± 1%	31% ± 2%	21% ± 2%	90% ± 4%	38.8 ± 0.7
	20 mM	23% ± 2%	23% ± 2%	19% ± 1%	6% ± 0%	91% ± 3%	42.0 ± 2.8
MG/SP1-*bdh*	0	57% ± 2%	57% ± 2%	34% ± 0%	21% ± 1%	95% ± 1%	43.7 ± 0.9
	5 mM	55% ± 2%	55% ± 2%	41% ± 1%	13% ± 2%	94% ± 4%	44.7 ± 0.5
	20 mM	20% ± 1%	20% ± 1%	54% ± 1%	-1% ± 2%	80% ± 1%	51.9 ± 1.4

[a] Yield was calculated in terms of C_3-mol (= product flux / maltose flux / 4).

[b] Carbon recovery was the sum of lactate, ethanol and acetate yield on sugar.

Table C.3. Product yield, carbon recovery and biomass yield for growth in MalSALN(BGP).

Acetoin added	Strain	Product yield on sugar [a]				Carbon recovery [b]	Biomass yield (gdw / C_6-mol)
		Lactate	Formate	Acetate	Ethanol		
0	MG1363	35%	60%	33%	23%	90.0%	31.3
	MG/SP2--*bdh*	38%	57%	32%	22%	90.0%	31.4
	MG/SP1-*bdh*	41%	58%	33%	20%	90.0%	31.4
5 mM	MG1363	55 ± 3 %	30 ± 2 %	22 ± 1 %	8 ± 1 %	84 ± 6 %	25.3 ± 0.7
	MG/SP2--*bdh*	47 ± 1 %	53 ± 3 %	37 ± 0.1 %	16 ± 0.3 %	99 ± 1 %	34.1 ± 0.8
	MG/SP1-*bdh*	36 ± 1 %	58 ± 2 %	42 ± 0.2 %	13 ± 1 %	90 ± 1 %	34.7 ± 0.7

[a] Yield was calculated in terms of C_3-mol (= product flux / maltose flux / 4).

[b] Carbon recovery was the sum of lactate, ethanol and acetate yield on sugar.

Table C.4. Product yield, carbon recovery and biomass yield for growth in GluSALN(BGP).

Acetoin added	Strain	Product yield on sugar [a]				Carbon recovery [b]	Biomass yield (gdw / C_6-mol)
		Lactate	Formate	Acetate	Ethanol		
0	MG1363	90.7%	4.2%	3.3%	0.0%	94%	39.8
	MG/SP2--*bdh*	98.2%	4.7%	4.2%	1.7%	104%	40.8
	MG/SP1-*bdh*	89.7%	4.2%	3.8%	0.0%	93%	38.0
5 mM	MG1363	95 ± 4 %	2.2 ± 0.3 %	2.1 ± 0.4 %	1.0 ± 1.3 %	98 ± 6 %	40.1 ± 1
	MG/SP2--*bdh*	85 ± 0 %	1.2 ± 0.2 %	6.5 ± 0.4 %	-0.6 ± 1.1 %	91 ± 2 %	40.4 ± 0.7
	MG/SP1-*bdh*	80 ± 2 %	1.0 ± 0.4 %	10.9 ± 0.4 %	0.3 ± 0.5 %	91 ± 3 %	40.7 ± 0.5

[a] Yield was calculated in terms of C_3-mol (= product flux / glucose flux / 2).

[b] Carbon recovery was the sum of lactate, ethanol and acetate yield on sugar.

Table C.5. 23BDH activities and rates of acetoin consumption and 23BD production in SALN(BGP).

Acetoin in medium	Strain	23BDH activity in MalSALN(BGP) (μmolmin^{-1}mg protein^{-1})	Specific rate (mmolh^{-1}gdw^{-1})[a]			
			MalSALN(BGP)		GluSALN(BGP)	
			Acetoin	23BD	Acetoin	23BD
0	MG1363	N.D.	0	0.3	0	0.0
	MG/SP2--*bdh*	N.D.	0	0.3	0	0.2
	MG/SP1-*bdh*	N.D.	0	0.3	0	0.5
5 mM	MG1363	0.07 ± 0.02	1.8 ± 0.2	1.9 ± 0.2	-0.7 ± 0.9	0.1 ± 0.1
	MG/SP2--*bdh*	0.50 ± 0.05	3.0 ± 0.6	2.8 ± 0.3	4.8 ± 0.1	3.2 ± 0.1
	MG/SP1-*bdh*	2.67 ± 0.08	4.1 ± 0.5	4.0 ± 0.3	8.8 ± 0.4	6.7 ± 0.9

N.D., not determined. 23BDH, 2,3-butanediol dehydrogenase; 23BD, 2,3-butanediol.

[a] positive values for acetoin and 23BD for consumption and production respectively.

National Food Institute
Technical University of Denmark
Mørkhøj Bygade 19
2860 Søborg

Tel. +45 35 88 70 00
Fax 35 88 70 01

www.food.dtu.dk